Vakgroep Analytische Scheikunde
Instituut voor Nucleaire Wetenschappen

Fractionation of indium and speciation of arsenic in body fluids and tissues after exposure

Marijn Van Hulle

Proefschrift voorgelegd tot het behalen van de graad van
Doctor in de Wetenschappen: Scheikunde

Promotor: Dr. Rita Cornelis

Academiejaar 2003-2004

Vakgroep Analytische Scheikunde
Instituut voor Nucleaire Wetenschappen

Fractionation of indium and speciation of arsenic in body fluids and tissues after exposure

Marijn Van Hulle

Proefschrift voorgelegd tot het behalen van de graad van
Doctor in de Wetenschappen: Scheikunde

Promotor: Dr. Rita Cornelis

Academiejaar 2003-2004

Namaste,

First of all I wish to thank Inge. You are my *moppietje* for almost seven years and the best mother Oona could ever have. Your continuous support during the years in which I worked, struggled, failed and succeeded, helped me enormously. In contrast to what I continuously try to say... I'm probably not the easiest man to live with.

Next I would like to thank my parents for their critical point of view about many aspects in life and for pulling me back to modesty whenever I put myself above it. It's definitely worth mentioning the rest of the family: Liesbeth & Stephanie, David, and Katrijn & David. They made a welcome change during the many verbally explosive family parties.

Dr. Rita Cornelis I am immensely grateful to for giving me the possibility to work under her wings. I know few supervisors who give their students that much freedom, independence and possibilities. It was a pleasure to be one of her students. Thanks a lot, Rita. And for once, I will shave properly!

In this research group I was lucky to have very fine colleagues. I will always remember Louis Mees as the problem solver of all things I was too clumsy and ignorant for. I would like to thank him for his conscientious technical assistance in 1001 things, his advice about 1002 things and the conversations... about even more things. Koen De Cremer has never hesitated to give me the necessary advice. He is the perfect example of a helpful, intelligent and dedicated researcher. It is not custom to have females in the group, but I was glad to have had the company of Emmie Dumont. I wish her a lot of success in the coming years. I had the opportunity to supervise Bart Schotte during his graduation. I wish him good luck with his bicycle carrier and his future work in electrochemistry, which will - unfortunately but logically - be less interesting than arsenic. Cyrille Cédric Chéry, although not an official member of this group, I'd like to thank here, not only for making tea every day, but also for his critical revisions and good advise.

I owe thanks to Prof. Em. Dr. Richard Dams, former director of the department for giving me the opportunity to work in this laboratory and for his interest in the research of all students. For the same reason I wish to thank the new director Prof. Dr. Karel Strijckmans, but also for his efforts in the production of radioisotopes. I am grateful to Prof. Dr. Raymond Vanholder for giving me the opportunity to work with laboratory animals and Tommy D'Huivaert for his technical assistance during these experiments. I acknowledge Prof. Dr. Frank Vanhaecke for giving me the ability to use the mass spectrometry equipment. Chantal Hufkens definitely earns my gratitude for being a superb secretary and a nice person. I also wish to thank the technical staff for their assistance.

I could enjoy the company of some fine colleagues. Syed Mohammod Hossain has always been a very friendly office-mate. I wish him all the best back home, and most of all... enough time to finally enjoy his wife and two sons. It is my pleasure to include Prof. Dr. Frans De Corte here and thank him for the interesting conversations we had about foreign cultures such as those from West-Vlaanderen. Dimitri Vandenberghe has nearly always shared the office with me. Being the opposite of a nine to fiver, he proved to be a nice colleague and a dedicated researcher. Jan Courtyn, study mate since my first year at university and a regular player in the institute's football team I ought to mention too. Also Jordy Vercauteren was a regular player in this brilliant team. I wish him a lot of astonishing moments on his world trip. I would like to add Ilse Gelaude, with whom I spent many hours in the same office and Veerle Vanlierde as she liked to knock a lot on our door.

With much respect I look back at the Chinese students I met in the frame of the bilateral scientific co-operation between Ghent University and Tsinghua University (Beijing, P.R. China). In particular I'd like to mention Chao Zhang, who was here for three months and made it back just in time to witness the birth of his daughter, and Prof. Dr. Xin Rong Zhang for his hospitality during my two visits at his department. Working in China was definitely an interesting experience.

Last but not least I would like to thank the Institute for the Promotion of Science and Technology in Flanders (IWT), the Fund for Scientific Research (FWO) and the Flemish Government for their financial support.

Dhanyabad

Table of contents

List of abbreviations

AB	arsenobetaine
AC	affinity chromatography
AC	arsenocholine
AEC	anion exchange chromatography
AFS	atomic fluorescence spectrometry
ALAD	δ-aminolevulinic acid dehydratase
ALAS	δ-aminolevulinic acid synthase
As^{III}	arsenous acid, arsenite
As^{V}	arsenic acid, arsenate
AsSug-254	5-deoxy-5(dimethylarsinoyl)-ß-D-ribofuranose (free arsenosugar)
AsSug-OH	3-[5'-deoxy-5'(dimethylarsinoyl)-ß-D-ribofuranosyloxy]-propylene glycol (arsenosugar OH)
AsSug-PO_4	3-[5'-deoxy-5'(dimethylarsinoyl)-ß-D-ribofuranosyloxy]-2-hydroxypropyl 2,3-hydroxypropylphosphate (arsenosugar PO_4)
AsSug-SO_3	3-[5'-deoxy-5'(dimethylarsinoyl)-ß-D-ribofuranosyloxy]-2-hydroxypropane-sulphonic acid (arsenosugar SO_3)
AsSug-SO_4	3-[5'-deoxy-5'(dimethylarsinoyl)-ß-D-ribofuranosyloxy]-2-hydroxypropyl hydrogensulphate (arsenosugar SO_4)
BALF	bronchoalveolar lavage fluid
CAD	collision activated dissociation
CEC	cation exchange chromatography
DC	direct current
DMA	dimethylarsinic acid
DMAA	dimethylarsinoyl acetic acid
DMAE	dimethylarsinoyl ethanol
DMA^{III}	dimethylarsinous acid
DTPA	diethylenetriaminepenta acetate
EDTA	ethylenediaminetetra acetate

ES-MS(/MS)	electrospray (tandem) mass spectrometry
FPLC	fast protein liquid chromatography
FWHM	full width at half maximum
Ge(Li)	germanium-lithium semiconductor detector
GF-AAS	graphite furnace atomic absorption spectrometry
GI	gastro intestinal
GLS	gas liquid separator
HETP	height equivalent to a theoretical plate
HG	hydride generation
HMM	high molecular mass
HPLC	high performance liquid chromatography
i.m.	intramuscular
i.p.	intraperitoneal
i.t.	intratracheal
i.v.	intravenous
ICP-MS	inductively coupled plasma mass spectrometry
LD_{50}	LD_{50} is the amount of a material, given all at once, which causes the death of 50% of a group of test animals.
LD_{100}	LD_{100} is the amount of a material, given all at once, which causes the death of 100% of a group of test animals.
LMM	low molecular mass
MA	metylarsonic acid
MA^{III}	methylarsonous acid
MM	molecular mass
MRM	multiple reaction monitoring
NAA	neutron activation analysis
NaI(Tl)	sodium iodide-thalium scintillation detector
Oac	acetate
PBS	phosphate buffered saline
p.o.	per oral
RES	reticuloendothelial system
RF	radio frequent
RPC	reversed phase chromatography
rpm	rounds per minute
SAM	S-adenosyl methionine

s.c.	subcutaneous
SEC	size exclusion chromatography
SGF	simulated gastric fluid
SIF	simulated intestinal fluid
SIR	single ion recording
S/N	signal to noise ratio
$t_{½}$	half-life
TETRA	tetramethylarsonium ion
TMA	trimethylarsine
TMAO	trimethylarsine oxide
UV	ultraviolet

Chapter 1. Introduction

The keywords describing this work are *fractionation* and *speciation,* the elements *indium* and *arsenic* and the terms *body fluids*, *tissues* and *exposure*. The terms *fractionation* and *speciation* will be discussed in the next paragraph. Indium and arsenic are two elements having completely different physical and chemical properties. They only touch common ground when incorporated as indium arsenide (InAs) in semiconductors.

The two elements will be discussed in chapters two and three. In the workgroup led by Dr. Rita Cornelis, the field of interest has since long been chemical speciation in clinical samples. Clinical samples include body fluids such as urine, blood, serum, packed cells, but also organ tissues, hair, nails *etc*. The term *exposure* is to be interpreted in the most comprehensive way. In the case of indium, laboratory animals have been exposed to background levels of an indium compound. In the case of arsenic, healthy human volunteers have been exposed to arsenosugar-containing foodstuffs. As will be discussed later, arsenosugars are believed to cause no harm to human health.

1.1. Chemical speciation

[Templeton *et al.*, 2000]

There was a lot of debate before the international community achieved unanimity about the nomenclature and definition of the word *speciation*. According to the International Union for Pure and Applied Chemistry (IUPAC), chemical speciation of an element is defined as *the distribution of an element amongst defined chemical species in a system*. Chemical species are *specific forms of an element defined as to isotopic composition, electronic or oxidation state, and/or complex or molecular structure*. Speciation analysis is at last defined as *analytical activities of identifying and/or measuring the quantities of one or more individual chemical species in a sample*. When elemental speciation is not feasible, the term

fractionation is used, *i.e.*, *the process of classification of an analyte or a group of analytes from a certain sample according to physical (e.g., size, solubility) or chemical (e.g., bonding, reactivity) properties.*

Speciation analysis is carried out in the field of environmental, geological, nuclear, biological, clinical chemistry, in food, occupational health and hygiene, medicine *etc*.

It is noteworthy to differentiate between fractionation and speciation. The analytical techniques used for separation of indium containing complexes are not able to ensure that one single species is detected. In the case of arsenic single species can be isolated using high performance liquid chromatography (HPLC) techniques.

In relation to the nomenclature and definitions about elemental chemical speciation, it is worth citing from a lecture held at the last International Conference on Biological and Environmental Aspects of Main-group Organometallics (ICEBAMO) in Pau, December 3-5th, 2003: *"For years, people have been doing speciation analysis without knowing, while other people think they are doing speciation analysis but are not"*.

1.2. Timeframe and scope of this work

This manuscript consists of two parts: indium and arsenic. The original concept of this PhD was to study the metabolism of two elements, indium and gallium, in body fluids and tissues. Indium and gallium have numerous applications in industry, the most important ones being their incorporation in the so-called, III-V semiconductors. Examples are GaAs and InAs. The unique properties of these binary compounds make them ideal for advanced applications in electronics. Along with their growing use, there is an increasing interest in the effects of both elements on human health. During the production and processing as well as during maintenance procedures, workers are exposed to dust and fumes of these particles and their derivatives. A series of experiments have revealed various adverse systemic and toxic effects on laboratory animals. Most of these studies used a toxicological and biochemical approach. My intention was to carry out speciation analyses in order to find out how indium and gallium are taken up, distributed, metabolised and excreted, and what the chemical forms of indium and gallium are in the different body fluids and tissues. I chose to use radioisotopes of both elements. Radiotracers have many advantages in the field of *in vitro* and *in vivo* studies. From a practical point of view, indium was selected to

be studied first. Speciation analysis imply the use of separation techniques. Because the primary interest was analysis of blood and body fluids, consisting of hundreds of proteins, fast protein liquid chromatography methods were optimised. Afterwards three sets of *in vivo* experiments with laboratory animals were carried out, the last one dealing with the speciation of indium after oral administration of [^{114m}In]InAs to rats.

At about the same time, a bilateral scientific co-operation with the Tsinghua University of Beijing, P.R. China, as well as the funding for an electrospray triple quadrupole mass spectrometer (ES-MS/MS) were approved within the research group. The area of interest of this bilateral co-operation was the speciation of arsenic in humans who are exposed to arsenosugar containing food, such as edible algae, crustaceans and molluscs. The identity of most of the metabolites of these arsenosugars in urine is still unknown. Electrospray mass spectrometry lends itself as a powerful technique to deal with structure confirmation and elucidation. As will be clearly mentioned in chapter three, the toxicity of arsenic is highly dependent on the chemical form. Inorganic arsenic is very toxic, whereas 'seafood arsenicals' are assumed to be innocuous. Measuring the total amount of arsenic in foodstuffs, water, *etc.* does therefore not give the necessary information on health hazards. Likewise, the analysis of the total amount of arsenic in clinical samples, such as urine and blood does not provide the necessary information on possible exposure to toxic substances. Therefore chemical speciation analysis is again the key answer to the study of the metabolism of arsenosugars by humans.

As the results of the last *in vivo* experiment of indium showed that absorption of orally administered InAs is negligible and does not lead to accumulation of indium in the body, and in order to make good use of the ES-MS/MS, it was decided to leave the field of indium speciation and replace gallium with arsenic. Arsenic speciation in environmental and clinical samples implied thorough method development and optimisation.

Both studies will be described in detail. The theoretical part of this script will focus on both elements, but from a different point of view. The starting point for the speciation of indium in body fluids and tissues was the toxicity of indium in compounds such as III-V semiconductors. Therefore the theoretical aspects dealing with toxicity of indium will be highlighted in chapter 2. Arsenic speciation in body fluids after ingestion of arsenosugar containing food focuses on the transformations of arsenic in the environment and in the human body. Therefore these metabolic aspects will be thoroughly described in chapter 3.

An overview of the applied separation and detection methods will be given in chapter 4. Chapters 5 and 6 deal with *in vitro* and *in vivo* experiments, respectively, of indium in body fluids and tissues. Chapter 7 copes with the optimisation of the techniques for the determination of arsenic. The measurement of arsenic metabolites from arsenosugars is described in chapter 8.

References

[Templeton *et al.*, 2000]

Templeton DM, Ariese F, Cornelis R, Danielsson LG, Muntau H, Van Leeuwen HP and Lobinski R (2000). *Pure Appl. Chem.*, **72**, 1453-1470.

Chapter 2. Indium: chemistry and biology

2.1. Introduction

2.1.1. History and occurrence

[Downs, 1993]

The German scientists Ferdinand Reich and Theodor Richter were the first to identify indium in 1863. Spectrographic examination of a crude zinc chloride liquid derived from samples of zinc blendes (sphalerite) disclosed a brilliant indigo blue line. Reich and Richter were able to isolate the oxide of the new element and reduce it to the metal by heating it in a stream of hydrogen or coal gas. They were responsible too for coining the name indium in token of the element distinctive flame colouration (Latin *indicum*, indigo).

Table 2.1. Abundance of indium in different environmental compartments.

environmental compartment	concentration	reference
sun	45 atoms per 10^{12} of H	[Downs, 1993]
earth	4 ng/g	[Downs, 1993]
continental crust	50 ng/g	[Downs, 1993]
Atlantic ocean	0.1 ng/L	[Matthews and Riley, 1970]
air (England)	0.3 ng/m^3	[Peirson *et al.*, 1973]

Indium belongs to group 13 of the periodic table. All the members of this group have odd atomic numbers and their nuclei are therefore less stable than those of the adjacent members of the carbon group. Indium does not form any minerals of its own. Instead it is

widely distributed in minute amounts in many zinc (sphalerite), copper, lead and tin minerals, usually but not exclusively being concentrated in sulphide deposits. Zinc, which it also resembles in size and other properties, is an important carrier, and zinc blendes are the principal commercial source of the metal. With a terrestrial abundance of 4 ng/g, indium is a rare element. It is about as rare as silver. Few minerals contain more than 0.1%, although pegmatite dikes in western Utah (USA) are reported to contain up to 2.8% indium. Germanite ($Cu_3(Fe,Ge)S_4$) and cylindrite ($Pb_3Sn_4FeSb_2S_4$) contain relatively large amounts of indium (0.1 to 1% In). The abundance of indium in different environmental compartments is shown in table 2.1.

2.1.2. Physical, chemical and nuclear properties

[Downs, 1993]

Indium is a soft, semiprecious non-ferrous metal with a silvery-white colour and a brilliant lustre. It is very malleable and ductile and can undergo almost limitless deformation. The atomic number is 49; it has an atomic weight of 114.82. The electronic configuration is $[Kr]5s^2 4d^{10} 5p^1$. The melting point is 156.6°C, the boiling point is 2080°C, and the specific gravity is 7.31 (20°C). Indium metal is unaffected by air at ordinary temperatures, but at red heat it burns with a blue-violet flame to form the yellow oxide In_2O_3. The metal dissolves in mineral acids but is unaffected by potassium hydroxide or boiling water. When heated in the presence of halogens or sulphur, direct combination takes place. Though a few authentic indium(I) compounds have been prepared (*e.g.*, halides), indium is commonly trivalent in its compounds.

The solution chemistry of indium is characterised by extensive hydrolysis, described by the following general equation:

$$xIn^{3+} + yH_2O \xleftrightarrow{Q_{xy}} \left[In_x(OH)_y\right]^{(3x-y)+} + yH^+$$

with Q_{xy} the stepwise stoichiometric constants, y = 1 to 4 for the 4 successive hydrolysis steps and x = 1 for mononuclear species. The indium cation in non-complexing aqueous solutions is $[In(OH_2)_6]^{3+}$. In perchlorate solutions, hydrolysis first becomes detectable above pH 2 and, at ordinary concentrations, hydroxyl numbers from 0.6 to 0.8 can be reached

before precipitation of the hydroxide occurs. Hydrolysis leads to $In(OH)^{2+}$ and $In(OH)_2^{+}$ species, as well as several polynuclear complexes $In_{n+1}(OH)_{2n}^{(n+3)+}$, such as $In_2(OH)_2^{4+}$ and $In_3(OH)_4^{5+}$. Base induced hydrolysis of trivalent indium solutions causes precipitation well before the OH/In ratio reaches 3.0. The outcome depends on the nature of the counter-anion and on the particular base and is influenced by temperature and ageing of the precipitate. If halide ions are present, they are likely to be incorporated in the precipitate, but in their absence, $In(OH)_3$ is the eventual product. In the presence of chloride, hydrolysis is retarded and at high concentrations of chloride does not become appreciable until the pH exceeds 4. $In(OH)_3$ is in essence a basic hydroxide. A slight solubility in concentrated NaOH has been ascribed to four coordinate $[In(OH)_4]^-$ or six-coordinate $[In(OH)_4(OH_2)_2]^-$. The successive hydrolysis steps are described by the following equations:

$$In^{3+} + H_2O \xleftrightarrow{Q_{11}} InOH^{2+} + H^+$$

$$In^{3+} + 2H_2O \xleftrightarrow{Q_{12}} In(OH)_2^{+} + 2H^+$$

$$In^{3+} + 3H_2O \xleftrightarrow{Q_{13}} In(OH)_3 + 3H^+$$

$$In^{3+} + 4H_2O \xleftrightarrow{Q_{14}} In(OH)_4^{-} + 4H^+$$

Table 2.2. Hydrolysis constants of indium.

	[Martell and Smith, 1984]	[Baes and Mesmer, 1976]
-log Q_{11}	4.3	4.4
-log Q_{12}	9.4	8.8
-log Q_{13}	13.9	12.4
-log Q_{14}	23.4	22.1

Stepwise stoichiometric constants have been determined and compiled by several researchers. The stoichiometric constants Q_{xy} of these four hydroxides as described in two references are shown in table 2.2.

Natural indium consists of two isotopes: ^{113}In (stable, 4.33%) and ^{115}In (half-life 4.4 x 10^{14} y, 95.67%). A list of the most common radioisotopes can be found in table 2.3 [Sunderman and Townley, 1960].

Table 2.3. Characteristics of the most common radioisotopes of indium.

isotope	production	half-life	mode of decay	main g-rays [keV]
^{111}In	^{109}Ag(α,2n)^{111}In, ^{111}Cd(p,n)^{111}In	2.805 d	ε to ^{111}Cd	245.4, 171.3
^{113m}In	^{112}Sn(n,γ)^{113}Sn and ε to ^{113m}In	1.658 h	IT to ^{113}In	391.7
^{114m}In	^{113}In(n,γ)^{114m}In, ^{114}Cd(p,n)^{114m}In	49.51 d	IT to ^{114}In; ε to ^{114}Cd	190.3, 558.4, 725.2
^{116m}In	^{115}In(n,γ)^{116m}In	54.1 min	β^- to ^{116}Sn	1293.6, 1097.3

n: neutron; p: proton; α: alpha decay; ε: electron capture; β^-: negatron decay
γ: gamma decay; IT: internal transition

2.1.3. Production and uses

Because of the widespread but low abundance of indium in minerals, commercial production of the element arises almost exclusively from metal residues, slags and flue dusts during the smelting of zinc ores.

In 1982, the world year production of indium was 50 tons. This amounted to 200 tons in 1996. In 1988, 40% of the indium was used in the electronics industry, another 40% was used in solders and alloys and 20% in research and others.

The first reported commercial application of indium was as a minor addition to gold-based dental alloys in which indium served as a scavenger for oxygen. Hardness and ductility were also improved, as was resistance to discoloration. Indium is still added to some of these alloys.

Major uses in 1993 were as follows [Polmear, 1993]:

Semiconductors. Indium combines with Group 15 elements such as arsenic, antimony and phosphorus to produce compounds that exhibit semiconductor characteristics. The so-called III-V compounds form the material systems for solid-state opto-electronic devices and are used extensively in high-speed, high frequency applications. Components made in these materials include infrared and visible light-emitting diodes and detectors, lasers and

high-speed and microwave integrated circuits. Developments arise along similar lines as the main representative of the III-V group, namely GaAs. Optical fibre telecommunications have driven the development of InP-based lasers and detectors for transmission in the optimum wavelength band. Modern telephone trunk networks rely on InP devices. The optical properties are a result of the electronic energy band structure. The band gap between conduction and valence band allows optical transitions. The high-speed applications are a consequence of the higher electron mobility. InP and $CuInSe_2$ are relatively efficient at converting sunlight into electricity and are therefore used in solar cells.

Fusible alloys. Indium is a component of a number of alloys that have very low melting points, *e.g.*, Bi(22%)Pb(18%)In(11%)Sn(8.5%) melts at 48°C. These alloys are used in temperature overload devices such as fuses and plugs for sprinkler systems.

Speciality solders. A number of solders based on indium are available with melting points as low as 93°C. Indium is incorporated in solders based on lead, bismuth, tin and cadmium.

Speciality bearings. Indium may be applied as an electroplated or sprayer layer to lead-based bearings and then allowed to diffuse into the surface by heating. This leads to improved hardness, corrosion-resistance and anti-seizure properties. These bearings are used in high performance engines.

Nuclear control rods. Rods composed of Ag, In and Cd have high capture cross-section for neutrons and are therefore widely applied in the majority of pressurised water nuclear reactors.

Conductive films. Because of the high transparency of films of the compounds In_2O_3 and $(In,Sn)_2O_3$ to visible light, they are used on glass as conductive patterns for liquid crystal displays and as demister strips on motorcar windscreens.

Sodium vapour lamps. Indium is applied on the inside of the glass cylinder of low-pressure sodium vapour lamps that are commonly used for outdoor lightning. The indium coating reflects infrared waves emitted by the lamp while, at the same time, transmitting the visible light, which permits the lamp to operate at a higher temperature, thereby raising its efficiency.

Jewellery. Indium is used in alloys with gold and one composition comprising 5% In has a distinctive colour referred to as 'green gold'.

Radiopharmaceuticals. Because of the favourable decay characteristics of ^{111}In and to a lesser degree ^{113m}In, both radioisotopes have numerous applications in nuclear medicine as radiopharmaceuticals. ^{111}In decays by electron capture and has no ß emission. The half-life of 67 hours allows *in vivo* studies to be carried out for several days without having to administer excessively large quantities of radioactivity. Moreover the energy of the gamma photo emission of ^{111}In (171.3 keV and 245.4 keV) is in the optimum detectable range and the abundance is high (89% and 94%, respectively). Radiopharmaceuticals can be grouped into two groups: pharmaceuticals for dynamic functional studies of certain organs and pharmaceuticals for localisation of abnormalities in the body (*e.g.*, tumours, infarcts, abnormal organs). Reports mention the use of several indium compounds such as ^{113m}In-$Fe(OH)_3$ for lung scanning [Stern *et al.*, 1966; Goodwin, 1971]; $^{113m}In(OH)_3$ above pH 4 for liver scanning [Goodwin *et al.*, 1966]; $^{113m}InCl_3$ for blood-pool (heart, placenta) scanning [Stern *et al.*, 1967; Olkkonen *et al.*, 1977]; ^{111}In-colloid for lymphatic scintigraphy after 24 hours [Goodwin *et al.*, 1969]; $^{111}InCl_3$ for localisation in soft tissue tumours [Hunter and De Kock, 1969; Hunter and Riccobono, 1970], in tumours of head and neck [Farrer *et al.*, 1972] and in abscesses [Sayle *et al.*, 1983]; $^{113m}InCl_3$ to estimate plasma volume [Wochner *et al.*, 1970] and for labelling of red blood cells [Adatepe *et al.*, 1971]; $^{111}InCl_3$ for haematopoietic bone marrow scanning after 24h [Rayudu *et al.*, 1973; Reske, 1991]; $^{111}InCl_3$ [Lilien *et al.*, 1973; Farrer *et al.*, 1973] and ^{111}In-citrate [Glaubitt *et al.*, 1975] for bone marrow scanning; ^{111}In-colloid for leucocyte labelling [Zimmer and Spies, 1983]. All these applications make use of the chemical properties of the indium compounds. Moreover ^{111}In and to a lesser degree ^{113m}In have been complexed with several ligands. Here indium isotopes are chosen because of their favourable radiochemical properties and the application is based on the type of ligand. Examples are ^{113m}In-Fe-DTPA (diethylenetriaminepenta acetate) for brain scanning [Stern *et al.*, 1967] and for renal imaging (Reba *et al.*, 1968; Farrer and Saha, 1973); ^{111}In labelled bleomycin for tumour scanning and ^{111}In-oxine for labelling of leukocytes [Thakur, 1977]; ^{111}In-DTPA labelled to antibodies for localisation in inflammatory lesions and tumours [Saccavini *et al.*, 1984; Weiner and Thakur, 1995]; ^{111}In labelled to neutrophils for accumulation in abscesses [Bitar *et al.*, 1986]; ^{111}In-leukocytes for bone scintigraphy [Outwater *et al.*, 1988]; ^{111}In-DTPA to determine the distribution of cerebrospinal fluid [Weiner and Thakur, 1995]; ^{111}In-oxine labelled to leukocytes for imaging arthritis inflammation [Chinol *et al.*, 1996].

2.2. Indium in the body

[Fowler and Goering, 1991; Fowler, 1986; Fowler, 1988; Fowler, 1995; Hayes, 1988]

2.2.1. Food, daily intake and absorption

The indium content in plants and animal tissues consumed as food ranges from below detection to 0.01 mg/kg (beef muscle and ham). However, algae, fish and shellfish collected near smelter outfalls have been reported to contain concentrations ranging from 0.4-7 mg/kg (for algae) up to 10-15 mg/kg (for fish and shellfish). The daily intake for humans of indium has been estimated at about 8-10 μg.

Indium is poorly absorbed by inhalation. Smith *et al.* [1960] have evaluated the absorption, distribution and excretion of $^{114m}In(OH)_3$ or ^{114m}In-citrate following intratracheal (i.t.) instillation in rats and found that most of the administered dose was taken up by the tracheobronchial lymph nodes. Leach *et al.* [1961] reported similar findings in rats exposed to In_2O_3 via inhalation. The absorption of inhaled ^{114m}In sesquioxide particles by rats has been estimated to be between 3% and 6% of the total dose after a single one-hour exposure and about 18% for sequential one-hour exposures on 4 successive days. Isitman *et al.* [1974] administered $^{111}InCl_3$ or ^{111}In-DTPA to adult humans by ultrasonic nebulisation and found deposition in the major airways with little (1.3% to 4.4%) alveolar deposition.

Absorption of indium by ingestion is reported to be very low. The intestinal absorption of indium in rats has been reported to be about 0.5% of the administered dose (0.4 or 0.8 g In/kg body mass) given as either $In(OH)_3$ or indium citrate. The intestinal absorption of indium in volunteers was less than 2% of a 200 μCi dose of ^{113}In as a DTPA complex. Coates *et al.* [1973] reported no detectable absorption of a 500 μCi dose of $[^{113}In]InCl_3$ to human adults. More recently, Zheng *et al.* [1994] showed that InP was poorly absorbed from the GI tract following oral (p.o.) administration to rats in both single- and multiple-dose studies. Only 0.67% of a single dose and 0.27% of the last dose in the multiple-dose study were retained in the tissues and excreted in the urine 24 hours following the administration.

2.2.2. Distribution and excretion

The metabolism of indium after administration of a single i.t., subcutaneous (s.c.), intramuscular (i.m.) and p.o. dose to rats was investigated by Smith *et al.* [1960]. Kidney, spleen, liver and salivary glands were target organs, but pelt, skeleton and muscle contained the largest absolute amounts. The transport and distribution of indium in body fluids and tissues is determined by the chemical form [Castronovo and Wagner, 1971a; Castronovo and Wagner, 1971b, Castronovo and Wagner, 1973]. Ionic indium (at pH 3.0) is transported in the blood bound to transferrin and was found to be cleared within 3 days from the blood of mice given an intravenous (i.v.) injection. On the other hand colloidal hydrated indium oxide (at pH 7.2) injected i.v. was immediately cleared from the blood. Distribution of indium is also dependent on its chemical form. The kidney extensively accumulates ionic indium. Three days after a single i.v. injection, about 20% of a tracer dose and 30% of an LD_{100} dose of ionic $^{114m}InCl_3$ was found in the kidneys of mice. In contrast colloidal indium oxide is accumulated by the liver (64% of a tracer dose and 40% of an LD_{100} dose), spleen and the reticulo-endothelial system (RES). The chemical form administered determines the primary route of indium excretion from the body. Ionic indium is mainly excreted in the urine while colloidal indium complexes are primarily excreted in faeces. Mice have been found to excrete 52% of an administered dose of ionic indium via urine and 53% of a dose of colloidal indium via faeces. InAs s.c. administered to hamsters dissolves slowly over time and is concentrated in kidney, liver, lung and spleen [Yamauchi *et al.*, 1992]. Zheng *et al.* [1994] studied the tissue distribution of InP in rats after i.t. and p.o. administration. Upon oral absorption indium was relatively evenly distributed among the major organs such as liver, kidney, lung, spleen and testes. The majority, however, was recovered from the GI tract. Faecal excretion served as the major route for indium elimination. After i.t. instillation, the lungs concentrated virtually all indium. Hoyes *et al.* [1995] intraperitoneally (i.p.) injected adult and neonatal rats with $^{114m}In[InCl_3]$ and looked at the tissue distribution at 2 and 63 days post injection. At each time point, the highest accumulation of ^{114m}In was observed in liver, spleen and kidneys in both adult and neonatal rats.

2.2.3. Health effects and biological monitoring

Human exposure to indium compounds may occur in the semiconductor industry during the manufacture (sawing, grinding, or polishing) of semiconductor wafers or during maintenance of the production equipment, and as a result of indium isotope utilisation for organ scanning and treatment of tumours. The impact of waste disposal of electronic equipment on human health has not yet been taken into account. A series of animal experiments has shown that indium is toxic to mammals. Liver, kidneys, blood, haem biosynthetic pathway, lungs, reproductive and developmental systems and the immune system are adversely affected by indium compounds.

Liver. Castronovo and Wagner [1971b] investigated the hepatoxicity of lethal doses of $InCl_3$ and $In(OH)_3$ in mice. Administration resulted in inflammation and multiple small areas of necrosis. The effects of $InCl_3$ on hepatocyte structure and function were studied in male rats injected i.p. with doses of 10-40 mg/kg [Fowler *et al.*, 1983]. The primary intracellular target was the endoplasmic reticulum (fragmentation and degranulation, increase of surface density) and its associated microsomal enzymatic activities. Volume density increased in the lysosome compartment, but decreased in the vacuole compartment. The effects of indium compounds on the hepatic haem biosynthetic pathway are described below.

Kidneys. Administration of LD_{50} and LD_{100} levels of $InCl_3$ and $In(OH)_3$ to mice showed necrosis of the cells lining the proximal portion of the convoluted tubules [Castronovo and Wagner, 1971b]. In a dose finding pilot study by Chapin *et al.* [1995] male and female mice were administered $InCl_3$ at doses of 50-350 mg In /kg/day by gavage during 22 days. In males, urinary N-acetyl glucosaminidase decreased, which is an indicator for proximal tubular damage. For both sexes there was a trend toward reduction in overall white blood cells and increased kidney weight. The effects on the renal haem biosynthesis are described below.

Haem biosynthesis. Indium is capable of altering the haem biosynthetic pathway in liver, kidney and erythrocytes. Haem is a red pigment comprised of four subunits joined together as a single large tetrapyrrole (porphyrin) ring structure and at the centre a transition metal (*e.g.*, Fe, Cu, Co) is chelated. In physiological systems it is bound to proteins, and these proteins bind oxygen at the site of the metal (*e.g.*, haemoglobin, catalase) or they function

as components of membrane-bound electron transport chains (*i.e.*, cytochromes). Cellular respiration, energy respiration and chemical oxidations are dependent on these haem proteins. The haem biosynthetic/degradative pathway is sensitive to alteration by metals. The inhibition of haem synthesis for example compromises the production of the microsomal haemoprotein cytochrome P-450, resulting in a reduced capacity to biotransform xenobiotics as well as endogenous compounds. The haem biosynthesis takes place in the mitochondrion and cytosol. The pathway starts with the formation of δ-aminolevulinic acid and the condensation of two δ-aminolevulinic acid units to porphobilinogen. These two steps are catalysed by the enzymes δ-aminolevulinic acid synthase (ALAS) and δ-aminolevulinic acid dehydratase (ALAD), respectively. [Maines and Kappas, 1977]

Woods *et al.* [1979] administered $InCl_3$ i.p. at doses of 5-40 mg/kg to rats and studied the hepatic influences. There was a dose dependent decrease of ALAS activity and a dose dependent increase of haem oxygenase in the liver. Both enzymes are the rate-limiting enzymes in the production and breakdown of haem. These changes were accompanied by a marked reduction in microsomal haem concentrations and a decrease in microsomal haem dependent oxidative functions in the liver such as cytochrome P-450. Woods *et al.* further investigated the effects of $InCl_3$ (i.p. injection of 10-40 mg/kg $InCl_3$) to kidney rats. $InCl_3$ exerts a dose dependent inhibition of ALAD owing to selective localisation of indium within the cytosolic fraction of the proximal tubule cells. Zn^{2+}, a nutritional cofactor of ALAD could prevent inhibition by $InCl_3$. Conner *et al.* [1995] investigated the effects of subcutaneously administered $InCl_3$ (1.5 mg/kg 3 times per week for 4 weeks) and InAs (single injection of 1000 mg/kg) in hamsters and reported reduced ALAD activities in erythrocytes, but not in liver. *In vitro* studies showed that hepatic ALAD activity was primarily influenced by the indium moiety.

Pulmonary toxicity. Tanaka *et al.* [1994] examined the pulmonary toxicity of i.t. instilled InAs (0.82 mg In, once a week for 15 weeks) in hamsters. They reported reduced body weight gain, histopathological findings (proteinosis-like lesions, pneumonia, alveolar or bronchiolar cell hyperplasia), but the incidence of tumours was not significantly higher than the control group. Another experiment by Tanaka *et al.* [1996] included InP, administered in analogy to the protocol mentioned above. Although InP administration did not reduce the increase in body weight, it also resulted in histopathological findings that were similar to that in the InAs treated group. In a study by Blazka *et al.* [1994a] a single i.t. dose of

1.3 mg/kg $InCl_3$ was given to rats. Their study showed that $InCl_3$ is capable of producing severe pulmonary responses that are present 56 days after dosing, even though most of the administered dose had left the lungs. These include inflammatory response, increased lung weight, increased number of cells in the bronchoalveolar lavage fluid (BALF), biochemical changes and development of fibrosis. Blazka *et al.* [1994b] extended their research to inhalation experiments with rats exposed to varying doses (up to 20 mg $InCl_3/m^3$). Low doses of $InCl_3$ in air initiated an inflammatory response. Higher doses induced biochemical changes on the longer term. The acute pulmonary toxicity of Copper Indium diselenide ($CuInSe_2$) was studied by Morgan *et al.* [1995]. Female rats were administered 12-100 mg/kg $CuInSe_2$ intratracheally once. It was found to be responsible for increased lung weight, reduced body weight gain, and increased number of cells in the BALF. $CuInSe_2$ also caused intra-alveolar inflammation and cell hyperplasia. The long-term health effects of $CuInSe_2$ to rats were also examined by Morgan *et al.* [1997]. Female rats were administered i.t. with 24 mg/kg $CuInSe_2$ and euthanised up to 28 days after exposure. Relative lung weights and BALF cell numbers were increased. Inflammatory lesions, biochemical changes and hyperplasia were observed. Oda [1997] examined the toxicity of low level (1.2 - 62.0 μg/kg) InP in rats after i.t. instillation. Biochemical changes were observed in the BALF in all groups after 1 day. After 8 days BALF parameters were changed only in the highest exposure group. Uemura *et al.* [1997] studied the effects of i.t. administered InP (1-10 mg/kg) on rats. There was a dose dependent increase in BALF parameters. Indium was detected in liver and spleen in a dose dependent manner with phagocytosis of macrophages probably being responsible for the disposal and distribution from the lungs to these organs. Yamazaki *et al.* [2000] investigated the long-term (2 years) toxicity of InAs and InP (2.4 mg In /kg twice a week for 8 weeks), instilled i.t. in hamsters. Weight gain was suppressed in both groups. Serum indium levels were increased, more drastically in the case of InAs, an indication of *in vivo* dissociation. Severe pulmonary inflammation and localised lesions were present in both groups. Gottschling *et al.* [2001] observed dose-dependent incidences of alveolar adenomas and carcinomas after two years in both male and female rats that were chronically exposed to an aerosol of InP (6 h/day, 5 days/week for 21 weeks at levels of 0.1 and 0.3 mg/m^3 or 105 weeks at levels of 0.03 mg/m^3). Three-month exposure resulted in severe pulmonary inflammation and alveolar proteinosis. Tanaka *et al.* [2002] further investigated the pulmonary toxicity of indium-tin oxide after i.t. instillation into hamsters (4.5 mg In /kg, once a week for 16 weeks). Lung weight significantly increased, but there was no reduced weight gain. In general the inflammatory response was weaker than in the case of an equal amount of InP. The report

from Homma *et al.* [2003] is the first case history describing a man with interstitial pneumonia consistent with the inhalation of indium-tin oxide particles. Numerous fine particles were scattered throughout the lungs and an extremely high indium serum level (290 ng/mL) was found. The high blood levels had also caused chronic adverse health effects in liver and spleen.

Reproductive and developmental system and testicular toxicity. Ferm and Carpenter [1970] reported the teratogenic and embryopathic effects of a single dose of indium nitrate i.v. injected in increasing amounts into pregnant hamsters on day 8 of gestation. Indium caused a high incidence of malformations of the digits. At doses above 1 mg/kg it was completely embryopathic, killing all embryos *in utero*. The study of Chapin *et al.* [1995] is an extension of the previous report. The conclusion of a series of experiments was that doses of 50, 150 and 250 mg In kg/day $InCl_3$ given orally by gavage during 20 days did not affect the ability of male mice to impregnate females or the ability of those females to become pregnant, but did adversely affect foetal survival. Also a decreased body weight gain for females and body weight loss for males was observed. An *in vitro* test showed that indium was embryotoxic at levels consistent with the amount of indium found in the foetuses from the indium-treated dams. Hoyes *et al.* [1995] i.p. injected 37 MBq/kg [^{114m}In]$InCl_3$ into adult and neonatal male rats. The treated rats had reduced sperm head counts and abnormal testicular histology, adults being more prone than neonates. Ungvary *et al.* [2000] administered several oral doses (50-400 mg/kg) of $InCl_3$ to rats on days 6-15 of gestation. They also administered several doses (50-20 mg/kg) of $InCl_3$ to rabbits on days 6-20 of gestation. In rats, $InCl_3$ produced dose-dependent maternal toxic effects and was embryotoxic and teratogenic up to 200 mg/kg and embryolethal at the highest level. The teratogenic effects were highest on days 11 and 12 of gestation. The teratogenic effects result from indium crossing the placental barrier. In rabbits the highest dose was lethal for the dams and lethal and teratogenic for the embryos. Nakajima *et al.* [1998, 1999 and 2000] examined the developmental toxicity of $InCl_3$ by i.v. and oral administration in rats, of $InCl_3$ in cultured rat embryos and of $InCl_3$ in both rats and mice. A single dose of 0.4 mg In /kg given to rats i.v. on day 9 of gestation was teratogenic (malformation of the tail and digits) and embryolethal. No significant changes were observed in the group receiving p.o. doses up to 300 mg In /kg. Also here the *in vitro* test showed that indium was embryotoxic at levels comparable to the serum levels in the i.v. treated rats. It was concluded from this study that both rats and mice were susceptible to the embryotoxicity of indium at similar developmental stages in the early organogenetic period, but that mice

were less susceptible than rats in terms of malformations. Omura *et al.* administered 7.7 mg/kg InAs i.t. 14 times in 8 weeks to male hamsters [1996a] and rats [1996b]. In case of the hamster InAs did not show any testicular toxicity, but body weight decreased after the 8th instillation and weight of testes and epididymes significantly increased. Epididymal sperm count did not decrease. Rats receiving the same doses, 16 times in total, showed a sperm count decrease in the epididymes, but a change in weight was not observed. Because of the emaciation of the hamsters and the fact that high concentrations of indium and arsenic were still detected in the serum of the hamsters, Omura *et al.* [2000] extended their research on testicular toxicity of InAs and InP in hamsters during a two-year period after repeated i.t. instillations (twice weekly for 8 weeks) of 4 mg/kg/day InAs and 3 mg/kg/day InP. This was half of the amount of indium compared to the previous study. After 88 weeks InAs caused reduced body weight and sperm count; and both materials decreased testes and epididymis weight. Severe histopathological changes were observed in the testes for both InAs and InP. InAs is more toxic than InP; this could be explained by the difference in internal exposure to indium (higher serum levels at all times). Omura *et al.* [2002] further examined the testicular toxicity of indium-tin oxide and InP after repeated (once weekly for 16 weeks) i.t. instillation of 6 mg/kg indium-tin oxide and InP. Similar results as in their study were observed for InP. In the indium-tin oxide group body, testes and epididymis weight did not alter. Sperm count did not change and only few histopathological changes were observed in the indium-tin oxide group.

Immunotoxicity. $InCl_3$ induces a dose dependent apoptosis in rat thymocytes at low doses (1 μM) and causes necrosis at higher doses (1 mM) *in vitro* [Bustamente *et al.*, 1997].

Conner *et al.* [1995] suggest, on the basis of *in vivo* studies on hamster, that the altered urinary excretion patterns and erythrocyte ALAD activity may be appropriate biological markers for evaluating exposure to InAs. Miyaki *et al.* [2003] analysed blood and urine of occupationally exposed workers and reported that blood, serum and creatinine adjusted urinary indium concentrations are useful indices of indium exposure.

In summary, indium compounds cause adverse effects on the haem biosynthetic pathway in liver, kidney and erythrocytes. The enzymatic activity of ALAD and ALAS is altered. At higher doses $InCl_3$ and $In(OH)_3$ are nephrotoxic (necrosis of cells lining the proximal portion of the convoluted tubes) and hepatoxic (damage to endoplasmic reticulum and associated enzymatic activities). The pulmonary toxicity of several indium-containing III-V

semiconductor compounds as well as $InCl_3$ has been recognised. Inflammatory response, increased lung weight, reduced body weight gain and several histopathological findings were reported. Indium compounds are embryotoxic, but do not affect the ability of males to impregnate females and of females to become pregnant. $InCl_3$, InAs and InP cause decreased sperm count and reduced testes and epididymis weight.

References

[Adatepe *et al.*, 1971]

Adatepe MH, Penkoske P, Van Amberg A, Wharton T, Evens RG and Potchen EJ (1971). *Int. J. Appl. Rad. Isot.*, **22**, 498-501.

[Baes and Mesmer, 1976]

Baes CF and Mesmer RE (1976). *The Hydrolysis of Cations*, John Wiley and Sons, New York, pp 319-327.

[Bitar *et al.*, 1986]

Bitar RA, Scheffel U, Murphy PA and Bartlett JG (1986). *J. Nucl. Med.*, **27**, 1883-1889.

[Blazka *et al.*, 1994a]

Blazka ME, Dixon D, Haskins E and Rosenthal GJ (1994). *Fund. Appl. Toxicol.*, **22**, 231-239.

[Blazka *et al.*, 1994b]

Blazka ME, Tepper JS, Dixon D, Winsett DW, Oconnor RW and Luster MI (1994). *Environm. Res.*, **67**, 68-83.

[Bustamente *et al.*, 1997]

Bustamente J, Dock L, Vahter M, Fowler BA and Orrenius S (1997). *Toxicology*, **118**, 129-136.

[Castronovo and Wagner, 1971a]

Castronovo FP and Wagner HN Jr (1971). *J. Nucl. Med.*, **11**, 307.

[Castronovo and Wagner, 1971b]

Castronovo FP and Wagner HN Jr (1971). *Br. J. Exp. Path.*, **52**, 543-559.

[Castronovo and Wagner, 1973]

Castronovo FP and Wagner HN Jr (1973). *J. Nucl. Med.*, **14**, 677-682.

[Chapin *et al.*, 1995]

Chapin RE, Harris MW, Hunter ES, Davis BJ, Collins BJ and Lockhart AC (1995). *Fund. Appl. Toxicol.*, **27**, 140-148.

[Chinol *et al.*, 1996]

Chinol, M, Vallabhajosula S, Goldsmith SJ, Paganelli G and Palestro CJ (1996). *Ann. Nucl. Med.*, **10**, 287-291.

[Coates *et al.*, 1973]

Coates G, Gilday DL, Cradduck TD and Wood DE (1973). *Can. Med. Assoc. J.*, **108**, 180-183.

[Conner *et al.*, 1995]

Conner EA, Yamauchi H and Fowler BA (1995). *Chem. Biol. Interactions*, **96**, 273-285.

[Downs, 1993]

Downs AJ (1993). In *Chemistry of Aluminium, Gallium, Indium and Thallium* (ed. Downs AJ), Chapman and Hall, London, pp 1-80.

[Farrer and Saha, 1973]

Farrer PA and Saha GB (1973). *J. Nucl. Med.*, **14**, 394.

[Farrrer *et al.*, 1972]

Farrer PA, Saha GB and Shibata HN (1972). *J. Nucl. Med.*, **13**, 429.

[Farrer *et al.*, 1973]

Farrer PA, Saha GB and Katz M (1973). *J. Nucl. Med.*, **14**, 394-395.

[Ferm and Carpenter, 1970]

Ferm VH and Carpenter SJ (1970). *Toxicol. Appl. Pharmacol.*, **16**, 166-170.

[Fowler, 1986]

Fowler BA (1986). In *Handbook on the Toxicology of Metals* (ed. Friberg L, Nordberg GF and Vouk V), Elsevier, Amsterdam, pp 267-275.

[Fowler, 1988]

Fowler BA (1988). In *Biological Monitoring of Toxic Metals* (ed. Clarkson TW, Friberg L, Nordberg G and Sager P), Plenum Press, New York, pp 469-478.

[Fowler, 1995]

Fowler BA (1995). In *Metal Toxicology* (ed. Goyer RA, Klaassen CD and Waalkes MP), Academic Press, San Diego, pp 187-196.

[Folwer and Goering, 1991]

Fowler BA and Goering PL (1991). In *Metals and their Compounds in the Environment* (ed. Merian E), VCH, Weinheim, pp 939-944.

[Folwer *et al.*, 1983]

Fowler BA, Kardish RM and Woods JS (1983). *Lab. Invest.*, **48**, 471-478.

[Glaubitt *et al.*, 1975]

Glaubitt DM, Schlüter IH and Haberland KU (1975). *J. Nucl. Med.*, **16**, 769-774.

[Goering *et al.*, 1987]

Goering PL, Mistry P and Fowler BA (1987). In *Handbook of Toxicology* (ed. Haley TJ and Berndt WO), Hemisphere Publishing, Washington DC, pp 384-425.

[Goodwin, 1971]

Goodwin DA (1971). *J. Nucl. Med.*, **12**, 580-582.

[Goodwin *et al.*, 1966]

Goodwin DA, Stern HS, Wagner HN Jr and Kramer HH (1966). *Nucleonics*, **24**, 65&68.

[Goodwin *et al.*, 1969]

Goodwin DA, Finston RA, Colombetti LG, Beaver JE and Hupf H (1969). *J. Nucl. Med.*, **10**, 337.

[Gottschling *et al.*, 2001]

Gottschling BC, Maronpot RR, Hailey JR, Peddada S, Moomaw CR, Klaunig JE and Nyska A (2001). *Toxicol. Sci.*, **64**, 28-40.

[Hayes, 1988]

Hayes RL (1988). In *Handbook on the Toxicity of Inorganic Compounds* (ed. Seiler HG and Sigel H), Marcel Dekker, New York, pp 323-326.

[Homma *et al.*, 2003]

Homma T, Ueno T, Sekizawa K, Tanaka A and Hirata M (2003). *J. Occup. Health*, **45**, 137-139.

[Hoyes *et al.*, 1995]

Hoyes KP, Johnson C, Johnston RE, Lendon RG, Hendry JH, Sharma HL and Morris IA (1995). *Reprod. Toxicol.*, **9**, 297-305.

[Hunter and De Kock, 1969]

Hunter WW and De Kock HW (1969). *J. Nucl. Med.*, **10**, 343.

[Hunter and Riccobono, 1970]

Hunter WW and Riccobono XJ (1970). *J. Nucl. Med.*, **11**, 329.

[Isitman *et al.*, 1974]

Isitman AT, Manoli R, Schmidt GH and Holmes RA (1974). *Am. J. Roentgenol. Radium Ther. Nucl. Med.*, **120**, 776-781.

[Leach *et al.*, 1961]

Leach LJ, Scott JK, Armstrong RD and Steadman LT (1961). *The inhalation Toxicity of Indium Sesquioxide in the Rat*. The University of Rochester Atomic Energy Project Report No. UR590. University of Rochester, Rochester, New York.

[Lilien *et al.*, 1973]

Lilien DL, Berger HG, Anderson DP and Bennett LR (1973). *J. Nucl. Med.*, **14**, 184-186.

[Maines and Kappas, 1977]

Maines MD and Kappas A (1977). *Science*, **198**, 1215-1221.

[Martell and Smith, 1984]

Martell AE and Smith RM (1984). *Critical Stability Constants*, Plenum Press, New York.

[Matthews and Riley, 1970]

Matthews AD and Riley JP (1970). *Anal. Chim. Acta*, **51**, 287-294.

[Miyaki *et al.*, 2003]

Miyaki K, Hosoda K, Hirata M, Tanaka A, Nishiwaki Y, Takebayashi T, Inoue N and Omae Kazuyuki (2003). *J. Occup. Health*, **45**, 228-230.

[Morgan *et al.*, 1995]

Morgan DL, Shines CJ, Jeter SP, Wilson RE, Elwell MP, Price HC and Moskowitz PD (1995). *Environ. Res.*, **71**, 16-24.

[Morgan *et al.*, 1997]

Morgan DL, Shines CJ, Jeter SP, Blazka ME, Elwell MP, Wilson RE, Ward SM, Price HC and Moskowitz PD (1997). *Toxicol. Appl. Pharmacol.*, **147**, 399-410.

[Nakajima *et al.*, 1999]

Nakajima M, Sasaki M, Kobayashi Y, Ohno Y and Usami M (1999). *Teratogen. Carcin. Mut.*, **19**, 205-209.

[Nakajima *et al.*, 1998]

Nakajima M, Takahashi H, Sasaki M, Kobayashi Y, Awano T, Irie D, Sakemi K, Ohno K and Usami M (1998). *Teratogen. Carcin. Mut.*, **18**, 231-238.

[Nakajima *et al.*, 2000]

Nakajima M, Takahashi H, Sasaki M, Kobayashi Y, Ohno K and Usami M (2000). *Teratogen. Carcin. Mut.*, **20**, 219-227.

[Oda, 1997]

Oda K (1997). *Industr. Health*, **35**, 61-68.

[Olkkonen *et al.*, 1977]

Olkkonen H, Lahtinen ST and Penttilä IM (1977). *Int. J. Nucl. Med. Biol.*, **4**, 179-183.

[Omura *et al.*, 1996a]

Omura M, Hirata M, Tanaka A, Zhao M, Makita Y, Inoue N, Gotoh K and Ishinishi N (1996). *Toxicol. Lett.*, **89**, 123-129.

[Omura *et al.*, 1996b]

Omura M, Tanaka A, Hirata M, Zhao M, Makita Y, Inoue N, Gotoh K and Ishinishi N (1996). *Fund. Appl. Toxicol.*, **32**, 72-78.

[Omura *et al.*, 2000]

Omura M, Yamazaki K, Tanaka A, Hirata M, Makita Y and Inoue N (2000). *J. Occup. Health*, **42**, 196-204.

[Omura *et al.*, 2002]

Omura M, Tanaka A, Hirata M, Inoue N, Ueno T, Homma T and Sekizawa K (2002). *J. Occup. Health*, **44**, 105-107.

[Outwater *et al.*, 1988]

Outwater E, Oates E and Sarno RC (1988). *J. Nucl. Med.*, **29**, 1871-1874.

[Peirson *et al.*, 1973]

Peirson DH, Cawse PA, Salmon L and Cambray RS (1973). *Nature*, **241**, 252-256.

[Polmear, 1993]

Polmear AJ (1993). In *Chemistry of Alumnium, Gallium, Indium and Thallium* (ed. Downs AJ), Chapman and Hall, London, pp 81-110.

[Rayudu *et al.*, 1973]

Rayudu VS, Shirazi PH, Friedman A and Fordham EW (1973). *J. Nucl. Med.*, **14**, 397.

[Reba *et al.*, 1968]

Reba RC, Hosain F and Wagner HN Jr (1968). *Radiology*, **90**, 147-149

[Reske, 1991]

Reske SN (1991). *Eur. J. Nucl. Med.*, **18**, 203-221.

[Saccavini *et al.*, 1984]

Saccavini, Bruneau J, Grzyb J, Bourdoiseau M and Chatal JF (1984). *Radiopharmaceuticals and labelled compounds, conference proceedings*, pp 153-158.

[Sayle *et al.*, 1983]

Sayle BA, Balachandran S and Rogers CA (1983). *J. Nucl. Med.*, **24**, 1114-1118.

[Smith *et al.*, 1960]

Smith GA, Thomas RG and Scott JK (1960). *Health Phys.*, **4**, 101-108.

[Stern *et al.*, 1966]

Stern HS, Goodwin DA, Wagner HN Jr and Kramer HH (1966). *Nucleonics*, **24**, 57-59.

[Stern *et al.*, 1967]

Stern HS, Goodwin DA, Scheffel U, Wagner HN Jr and Kramer HH (1967). *Nucleonics*, **25**, 62-65&68.

[Sunderman and Townley, 1960]

Sunderman DN and Townley CW (1960). *The Radiochemistry of Indium*. National Academy of Sciences, Washington.

[Tanaka *et al.*, 1994]

Tanaka A, Hisanaga A, Hirata M, Omura M, Inoue, N and Ishinishi N (1994). *Appl. Organomet. Chem.*, **8**, 265-271.

[Tanaka *et al.*, 1996]

Tanaka A, Hisanaga A, Hirata M, Omura M, Makita Y, Inoue N and Ishinishi N (1996). *Fukuoka Acta Medica*, **87**, 108-115.

[Tanaka *et al.*, 2002]

Tanaka A, Hirata M, Omura M, Inoue N, Ueno T, Homma T and Sekizawa K (2002). *J. Occup. Health*, **44**, 99-102.

[Thakur, 1977]

Thakur ML (1977). *Int. J. Appl. Rad. Isot.*, **28**, 183-201.

[Uemura *et al.*, 1997]

Uemura T, Oda K, Omae K, Takebeyashi T, Nomiyama T, Ishizuka C, Hosoda K, Sakurai H, Yamazaki K and Kabe I (1997). *J. Occup. Health*, **39**, 205-210.

[Ungvary *et al.*, 2000]

Ungvary G, Szakmary E, Tatrai E, Hudak A, Naray M and Morvai V (2000). *J. Toxicol Environm. Health A*, **59**, 27-42.

[Weiner and Thakur, 1995]

Weiner RE and Thakur ML (1995). *Radiochim. Acta*, **70/71**, 273-287.

[Wochner *et al.*, 1970]

Wochner RD, Adatepe MH, Van Amburg A and Potchen EJ (1970). *J. Lab. Clin. Med.*, **75**, 711-720.

[Woods and Fowler, 1982]

Woods JS and Fowler BA (1982). *Exp. Mol. Pathol.*, **36**, 306-315.

[Woods *et al.*, 1979]

Woods JS, Carver GT and Fowler BA (1979). *Toxicol. Appl. Pharmacol.*, **49**, 455-461.

[Yamauchi *et al.*, 1992]

Yamauchi H, Takahashi K, Yamamura Y and Fowler BA (1992). *Toxicol. Appl. Pharmacol.*, **116**, 66-70.

[Yamazaki and Kabi, 1997]

Yamazaki K and Kabi I (1997). *J. Occup. Health*, **39**, 205-210.

[Yamazaki *et al.*, 2000]

Yamazaki k, Tanaka A, Hirata M, Omura M, Makita Y, Inoue N, Sugio K and Sugimachi K (2000). *J. Occup. Health*, **42**, 169-178.

[Zheng *et al.*, 1994]

Zheng W, Winter SM, Kattnig MJ, Carter DE and Sipes IG (1994). *J. Toxicol Environ. Health*, **43**, 483-494.

[Zimmer and Spies, 1983]

Zimmer AM and Spies SM (1983). *Int. J. Appl. Radiat. Isot.*, **34**, 1541-1544.

Chapter 3. Arsenic: chemistry and biology

3.1. Introduction

3.1.1. History

Arsenic is named after the yellow coloured ore orpiment (As_2S_3) in which arsenic is found [Nriagu, 2002]. The Greek name *arsenikon* means bold, valiant or masculine and it refers to the reactivity of the sulphide ores with other metals. Although many an alchemist claims to be the real discoverer of the metalloid arsenic, the discovery of elemental arsenic is generally credited to the German chemist Albertus Magnus (1193-1280).

3.1.2. Physical, chemical and nuclear properties

[Ishinishi *et al.*, 1986; Adriano, 1986]

Arsenic belongs to group 15 in the periodic table. The atomic number is 33 and it has an atomic weight of 74.92. Several allotropic forms of arsenic are known, but at 20°C only the grey form is stable. The metastable yellow form rapidly changes to the grey, semi-metallic form at low temperatures, and instantaneously in sunlight at room temperature. Brown and black amorphous forms are also known. The grey form is a crystalline solid with a brilliant cluster. It is a good conductor of heat but a poor electrical conductor. Arsenic melts in the absence of oxygen at 814°C (36 atm) and sublimes at 615°C. Naturally occurring arsenic consists of one isotope ^{75}As, which is stable. The principle oxidation states of arsenic are +V (in arsenates) or +III (in arsenites), and to a lesser extent +II (in realgar) and -III (in arsenides). The oxidation state of arsenic in arsines is not fully understood. The

electronegativity of As and H are 2.18 and 2.20, respectively, on the Pauling scale, and 2.20 each according to the Allred-Rochow scale. In some books, the oxidation state of As in arsines is denoted as -III, although +III can be found in other references. In this work the arsenic will be assumed to be +III. Other important properties are compiled in table 3.1. A list of the arsenic species, mentioned throughout this script, is given in table 3.2.

Table 3.1. Physical, chemical and nuclear properties of arsenic.

first ionisation energy [kJ/mol]		947		
redox potential As^{V} ® As^{III} [V]		$H_3AsO_4 + 3H^+ + 2e^- \rightarrow H_3AsO_3 + H_2O$ $E°$ = 0.559		
electronic configuration		$[Ar]3d^{10}4s^24p^3$		
electronegativity (Pauling scale)				
As	H	C	O	S
2.18	2.20	2.55	3.44	2.55
bond enthalpies in gaseous diatomic species [kJ/mol]				
As-As	As-H	As-C	As-O	As-S
348	245	200	477	379
isotope	**production**	**half-life**	**mode of decay**	**main γ-rays [keV]**
^{74}As	$^{74}Ge(p,n)^{74}As$	17.78 d	ε and β^+ to ^{74}Ge	595.9
			β^- to ^{74}Se	634.8
^{76}As	$^{75}As(n,\gamma)^{76}As$	26.3 h	β^- to ^{76}Se	559.1

p: proton; n: neutron; ε: electron capture; β^-: negatron decay; β^+: positron decay; γ: gamma decay

Table 3.2. Name, chemical formula and structure and pKa of arsenic species.

	name & formula	**chemical structure**	**pKa**
As^{III}	arsenous acid H_3AsO_3	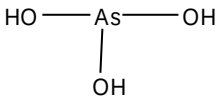	pKa_1: 9.2 pKa_2: 13.5 pKa_3: 14.0
	arsine AsH_3	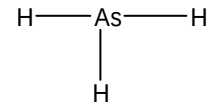	none
MA^{III}	methylarsonous acid $CH_3As(OH)_2$	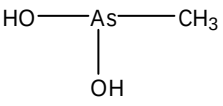	*~9
DMA^{III}	dimethylarsinous acid $(CH_3)_2AsOH$	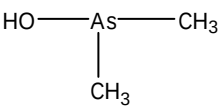	*?
TMA	trimethylarsine $(CH_3)_3As$	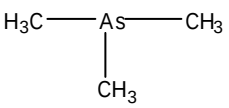	none

As^{V}	arsenic acid H_3AsO_4	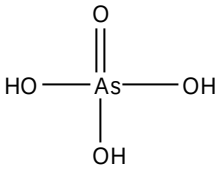	pKa_1: 2.3 pKa_2: 6.7 pKa_3: 11.6
MA	methylarsonic acid $CH_3AsO(OH)_2$	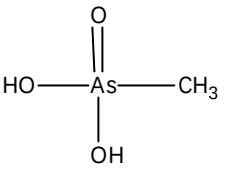	pKa_1: 3.6 pKa_2: 8.2
DMA	dimethylarsinic acid $(CH_3)_2AsO(OH)$	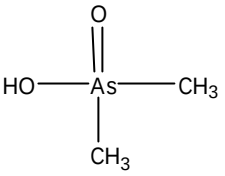	**pKa_1: 1.3 pKa_2: 6.2
TMAO	trimethylarsine oxide $(CH_3)_3AsO$	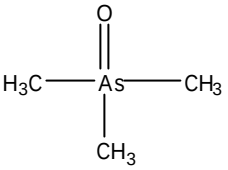	***pKa_1: 3.6
TETRA	tetramethylarsonium ion $(CH_3)_4As^+$	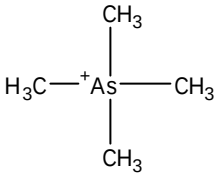	none
DMAE	dimethylarsinoyl ethanol $(CH_3)_2AsOCH_2CH_2OH$	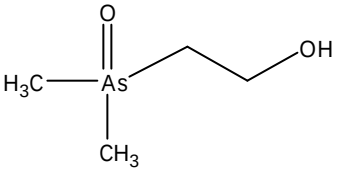	?
DMAA	dimethylarsinoyl acetic acid $(CH_3)_2AsOCH_2COOH$	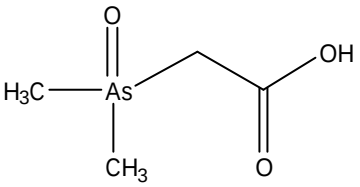	?
AB	arsenobetaine $(CH_3)_3As^+CH_2COOH$	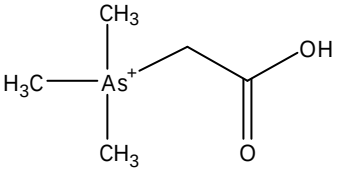	pKa_1: 2.2
AC	arsenocholine $(CH_3)_3As^+CH_2CH_2OH$	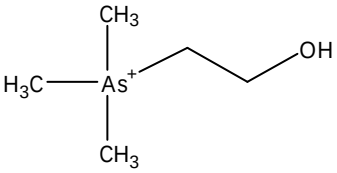	none

* estimate for MA^{III} and unknown for DMA^{III} [Gailer *et al.*, 1999]

** pKa_1: 1.3 for the reaction: $(CH_3)_2As^+(OH)_2 \leftrightarrow (CH_3)_2AsO(OH) + H^+$

*** pKa: 3.6 for the reaction $(CH_3)_3As^+OH \leftrightarrow (CH_3)_3AsO + H^+$

3.1.3. Production and uses

[Azcue and Nriagu, 1994; Ishinishi *et al.*, 1986; Adriano, 1986]

Arsenic is produced commercially by reduction of As_2O_3 with charcoal. As_2O_3 is produced as a by-product of metal-smelting operations. It is present in flue dust from the roasting of ores, especially those produced in copper smelting. The world year production of As_2O_3 in recent years has lowered to 20000 tons, but amounted up to 47000 tons in 1973.

Historical uses. Arsenic has a rich history of uses and abuses. Throughout the ages arsenic has been used in metallurgy (bronze), as a pigment, to produce a silvery shine on mirrors and statues, and as a homicidal poison. Fowler's solution (1% potassium arsenite solution) was used as a medication. Over 8000 arsenic based compounds were used to treat asthma, malaria, tuberculosis, diabetes, and skin diseases. Also, it is stated that arsenic based compounds were used until the mid 1980s for treating sleeping sickness. During these centuries arsenic has killed millions of people, be it by occupational exposure, by iatrogenic effects, or in cases of homicide and suicide.

Agriculture. One of the main uses of arsenic is in agriculture, namely as different kinds of pesticides. In 1983, arsenical insecticides were one of the largest classes of biocontrol agents in the USA. From the 1970s there has been a shift from inorganic compounds (including lead and calcium arsenate and copper acetoarsenite) to inorganic and organic compounds (arsenic acid, sodium arsenate, mono- and disodium methanearsonate, and DMA). Both inorganic arsenicals, primarily, sodium arsenite and organic arsenicals, are widely used since about 1890 as weed killers, particularly as non-selective soil sterilants. Arsenic acid is used extensively as a cotton desiccant to facilitate harvesting. Complexes of arsenic, such as fluor-chrome-arsenic-phenol, chromated copper arsenate, ammonical copper arsenate are used as wood preservatives.

Feed additives. Many arsenic compounds are used as feed additives. In 1946 it was shown that 3-nitro-4-hydroxyphenylarsonic acid (roxarsone, 3-NHPAA) was capable of controlling coccidiosis in poultry. While investigating the therapeutic performance of this compound, it was also discovered that it acted as a growth promoter, improved feed conversion, provided better feathering, increased egg production and pigmentation. Other arsenic compounds were shown to have similar properties: p-arsanilic acid (p-ASA), 4-nitro-

phenylarsonic acid (4-NPAA) and p-ureidophenylarsonic acid (p-UPAA). Nowadays 3-NHPAA and p-ASA are approved as animal feed additives for both poultry and swine, whereas 4-NPAA and p-UPAA are approved only for controlling blackhead disease in turkey.

Industrial. Arsenic pentoxide and As_2O_3 are used as additives in alloys, particularly with lead and copper; arsenic and As_2O_3 are used in the manufacturing of low-melting glasses. Arsenic trioxide is used in decolourising and fining agent (reduction in bubbles) in the production of glass. Manufacturing of ceramics utilizes arsenic. High-purity arsenic metal, gallium arsenide and indium arsenide are also used in semiconductor products.

3.2. Arsenic in the environment

3.2.1. Arsenic compounds in the marine environment

3.2.1.1. Arsenic in seawater and marine sediments

Arsenic concentrations in seawater are quite uniform at around 2 µg/L with slightly higher values in deep-water compared to surface water. $HAsO_4^{2-}$ is the predominant form in seawater (pH 7.5-8.3). As^{V}/As^{III} ratios of 10^{15}-10^{26} have been calculated for seawater, depending on the choice of p*E* (8.0 or 12.5, respectively). However, arsenite occurs at concentrations greater than those expected from purely thermodynamic considerations. The reason for this is that arsenate is partly reduced by marine bacteria and marine phytoplankton. Seawater also contains small amounts of MA and DMA. The concentrations of As^{III}, MA and DMA are higher in the photic zone of marine waters, suggesting that algae play an important role in the production of these species from As^{V}. Other organisms were also shown to transform arsenate into arsenite, MA and DMA.

The average level of arsenic in marine sediments of the world oceans is about 40 mg/kg. Information on the chemical form of the arsenicals in marine sediments is difficult to obtain, because extraction procedures are needed to gain knowledge of the way arsenic is bound within the sediments. These chemical extraction techniques may change the form of arsenic originally present. Sediments from coastal regions and estuaries contain rather lower concentrations of arsenic than deep-sea sediments. Alternatively sediment pore

waters (interstitial water) can be examined, because they provide information about the bio-available arsenic. According to a study of Andreae [1979] both forms of inorganic arsenic are present, but contrary to thermodynamic considerations, arsenate is the major form. MA, DMA and TMAO were also found in interstitual water.

3.2.1.2. Arsenic in marine algae

Algae are very simple chlorophyll-containing organisms. Members of this group are pond scums, terrestrial algae, snow algae, seaweeds, and freshwater and marine phytoplankton. Algae are simple organisms composed of one cell, or grouped together in colonies, or as multicellular organisms, sometimes collaborating together as simple tissues. Algae are found in seas, rivers and lakes, on soils and walls, in animals and plants (as symbionts - partners collaborating together). Algae can differ greatly in size: from unicellular (3-10 μm) to giant kelps up to 70 meters long and growing at up to 50 cm per day. Algae are found in the fossil record dating back to approximately 3 billion years in the Precambrian. They exhibit a wide range of reproductive strategies, from simple, asexual cell division to complex forms of sexual reproduction. A detailed classification is beyond the scope of this work. In general algae are divided in *bacillariophyta* (diatoms), *charophyta* (stoneworts), *dinophyta* (dinoflagellates), *chlorophyta* (green algae), *chrysophyta* (golden algae), *cyanobacteria* (blue-green algae), *phaeophyta* (brown algae) and *rhodophyta* (red algae) [http 1; http 2; http 3].

Most reports on arsenic in algae deal with macroalgae, commonly called seaweeds. The most important macroalgae are the rhodophyta such as *Phorphyra*, phaeophyta such as *Laminaria*, *Sargassum*, *Fucus* and *Undaria*, and the chlorophyta such as *Codium*. Seaweeds do not have roots and shoots like higher plants but they generally have root-like attachment structures and leaf-like fronds that act like shoots. Most seaweeds are made up of cells that are relatively unspecialised but there are seaweeds that transport material internally (kelps). Seaweeds grow mostly on rocky areas or on coral reefs. Seaweeds are used as a source of food, for industrial applications and as a fertiliser. Industrial utilisation is at present largely confined to extraction for gums and chemicals. The major utilisation of these plants as food is in Asia, where seaweed cultivation has become a major industry. Most important food species are *Porphyra* (*nori* in Japanese, *zicai* in Chinese), *Laminaria* (*kombu* in Japanese, *haidai* in Chinese) and *Undaria Pinnatifida* (*wakame* in Japanese,

qundaicai in Chinese). In most western countries food and animal consumption is restricted.

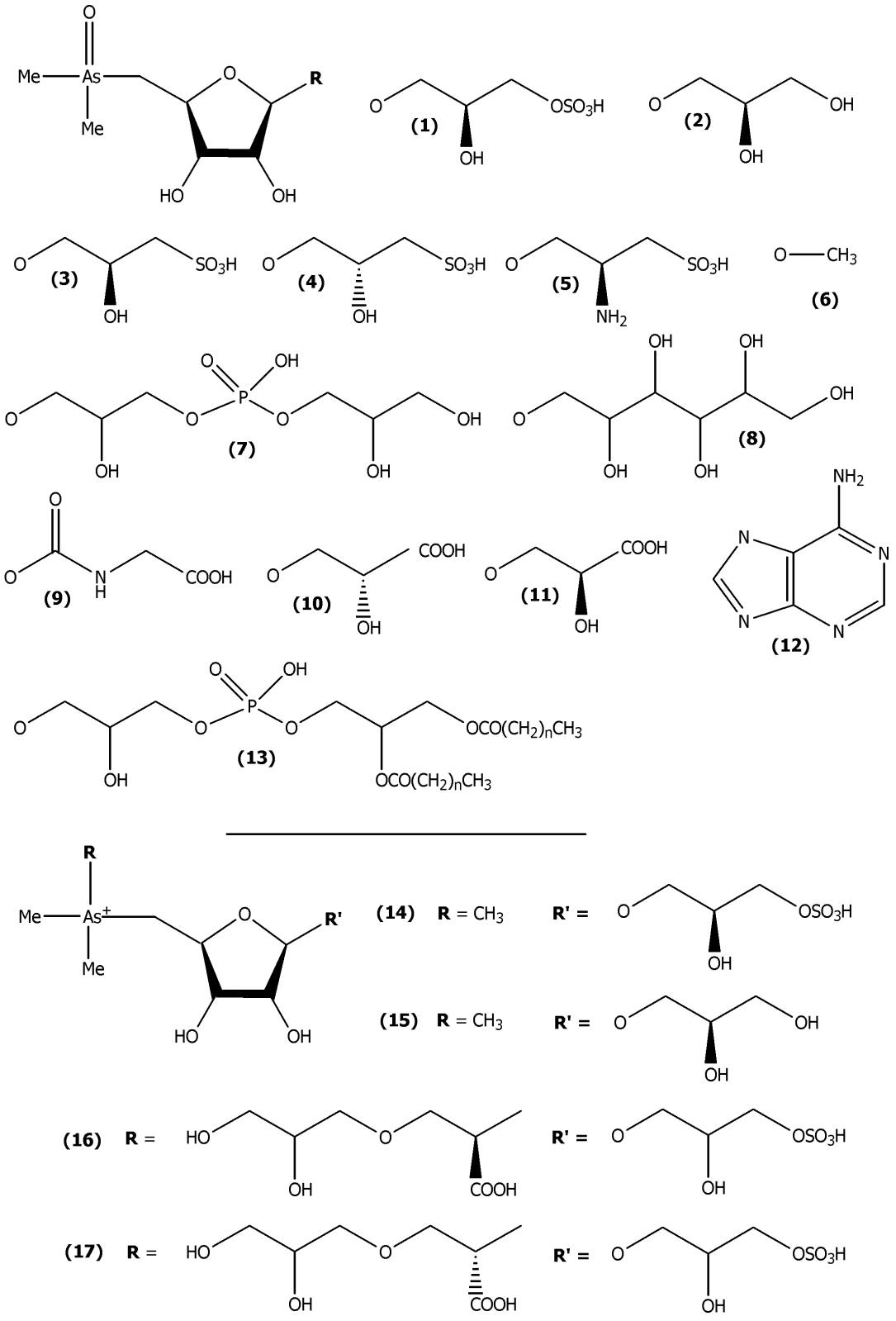

Figure 3.1. Chemical structure of 17 naturally occurring arsenosugars.

Algae contain high levels of arsenic (up to 230 mg/kg dry mass). Reports of arsenic in the sea and in its organisms first appeared at the beginning of the 20th century but it was not until the 1920 that the application of improved analytical techniques led to the acceptance that marine organisms naturally contain high levels of arsenic. Jones [1922] was one of the first to give concentration levels of arsenic in different algae. It soon became apparent that the form of arsenicals present in algae was different from those in marine animals. A report by Lunde [1973] showed that marine unicellular algae incorporated radiolabeled (^{74}As) arsenite and arsenate into various water-soluble and lipid-soluble fractions, the latter being relatively unstable and easily convertible into a water-soluble compound already present in the algae. Other researchers confirmed these findings [Irgolic *et al.*, 1977; Cooney *et al.*, 1978]. Edmonds and Francesconi [1981] analysed the brown alga *Ecklonia radiata* and were the first to report the presence of what now is commonly denoted as arsenosugars. During the following years these two, among other authors, frequently reported new arsenosugars found in several biological species such as the giant clam *Tridacna maxima* [Edmonds *et al.*, 1982a] and the brown algae *Ecklonia radiata* [Edmonds and Francesconi, 1983], *Hizikia fusiforme* [Edmonds *et al.*, 1987] and *Sargassum lacerifolium* [Francesconi *et al.*, 1991a]. X-ray crystal structure analysis and NMR were used for identification.

Arsenosugars comprise a dimethylarsinoyl or a trialkylarsonium derivative bound to a ribofuranoside sugar. A total of 17 different arsenosugars have been isolated from natural sources so far: 13 species are dimethylarsinoyl derivatives, 4 species are quaternary arsonio analogues. Compounds **1**-**12** and **14**-**17** are water-soluble, whereas compound **13** is lipid-soluble. A complete list of all naturally occurring arsenosugars is shown in figure 3.1. Next to the naturally occurring arsenosugars, other analogues have been synthesised. Although the diversity of arsenosugars is outspoken, four arsenosugars predominate. The four readily available arsenosugars, shown in figure 3.2, received several denotations so far, which are often misleading. The full names of these arsenosugars are 3-[5'-deoxy-5'(dimethylarsinoyl)-ß-D-ribofuranosyloxy]-propylene glycol (arsenosugar OH), 3-[5'-deoxy-5'-(dimethylarsinoyl)-ß-D-ribofuranosyloxy]-2-hydroxypropyl 2,3 dihydroxypropyl phosphate (arsenosugar PO_4), 3-[5'-deoxy-5'(dimethylarsinoyl)-ß-D-ribofuranosyloxy]-2-hydroxy-propanesulphonic acid (arsenosugar SO_3) and 3-[5'-deoxy-5'-(dimethylarsinoyl)-ß-D-ribofuranosyloxy]-2-hydroxypropyl hydrogen sulphate (arsenosugar SO_4) The notation for the sugars in figure 3.2 refers to a part of the functional group of the side chain. In some cases in the text, and also in the tables and chromatograms shown later, the abbreviations AsSug-OH, AsSug-PO_4, AsSug-SO_3 and AsSug-SO_4 will be used.

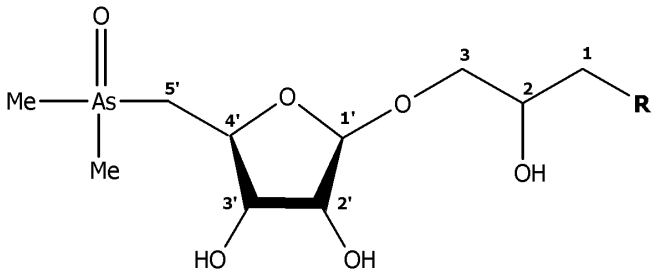

arsenosugar OH (AsSug-OH): **R** = OH
arsenosugar PO_4 (AsSug-PO_4): **R** = $OP(O)(OH)OCH_2CH(OH)CH_2OH$
arsenosugar SO_3 (AsSug-SO_3): **R** = SO_3H
arsenosugar SO_4 (AsSug-SO_4): **R** = OSO_3H

Figure 3.2. Structure and denotation of the four most common arsenosugars.

Arsenosugar OH and arsenosugar PO_4 are common arsenicals in green and red macroalgae. Arsenosugar SO_3 is the dominant form in brown macroalgae of the class *Laminariales*. In brown seaweed of the class *Fucales* all four common arsenosugars are found. In general the concentrations of arsenosugars in brown algae (<1-230 mg/kg dry mass) are higher than those found in red (0.4-45 mg/kg dry mass) and green (0.1-23 mg/kg dry mass) species. A minor though commonly found constituent in macroalgae is DMA. As^{III}, As^{V} and MA appear at trace level but are often not detected at all. A notable exception is the brown alga *Hizikia fusiforme*, which contains approximately half of its arsenic content as inorganic arsenate. Studies on the lipid-soluble fraction of the brown alga *Undaria pinnatifida*, carried out using NMR and GC mass spectrometric analysis, revealed the presence of a phosphatidylarsenosugar (compund **13** in figure 3.1). This compound comprises up to 25% of the total content. The identification of lipid-type arsenicals is, however, hampered by their instability and ease towards hydrolysis [Morita and Shibata, 1988].

The arsenic pattern in unicellular algae became clear after the analysis of the kidney of the giant clam *Tridacna maxima* [Edmonds *et al.*, 1982a]. Clams host the unicellular algae in their mantle edges. The algae serve as food to the clam. They remain intact in the mantle before being carried to the visceral mass for digestion. The compounds found in unicellular algae are essentially the same as those formed by macroalgae.

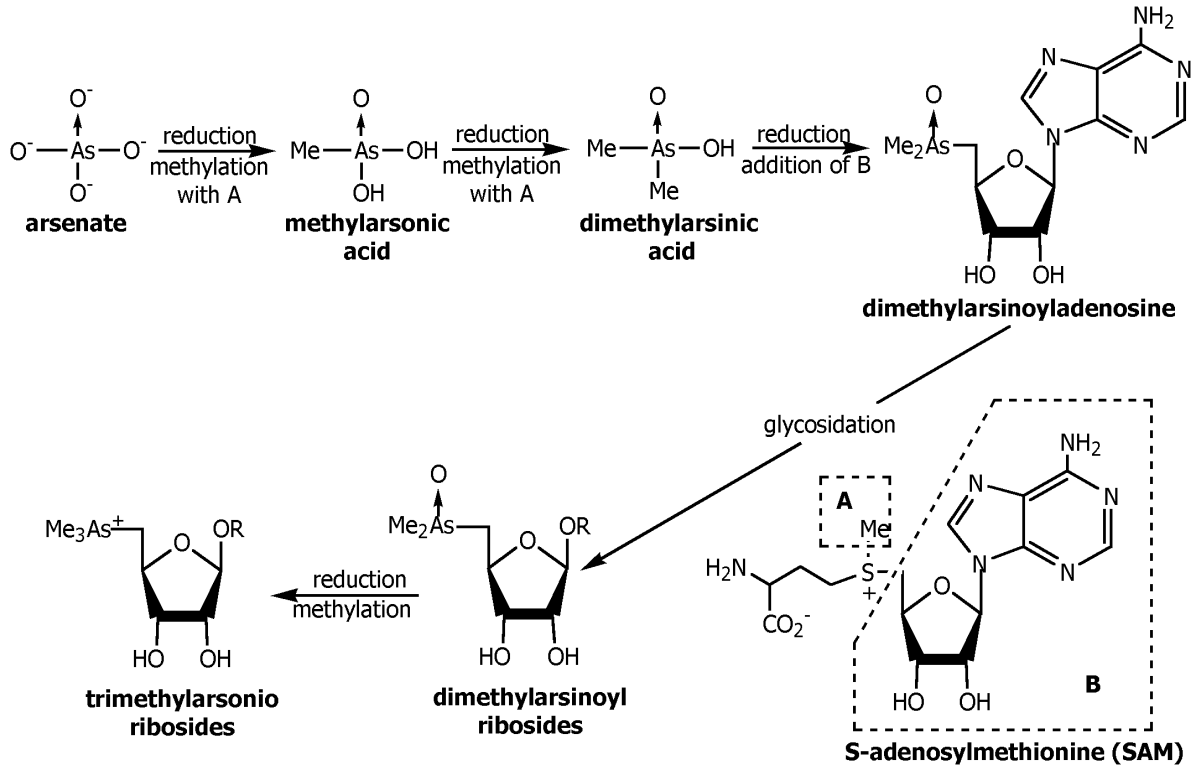

Figure 3.3. Pathway for the formation of arsenosugars from arsenate.

Marine algae are exposed to arsenate originating from the ambient seawater. They absorb this arsenate, possibly because of an inability to distinguish it from phosphate. Although the exact mechanism of this uptake is not yet clear, once within the cell the arsenate is transformed into the range of arsenic compounds discussed above. With the exception of DMA, MA, As^{V}, As^{III} and a taurine derivative [$(CH_3)_2As(O)CH_2CH_2CH_2C(O)NHCH_2CH_2SO_3H$], all these compounds contain a riboside moiety. One fundamentally supported mechanism was proposed by Edmonds *et al.* [1982] and Edmonds and Francesconi [1987b]. It is based on the work of Challenger [1945] and Cantoni [1952 and 1953]. Arsenate is transformed into DMA by sequential reduction and oxidative methylation, followed by adenosylation, with SAM being both the methyl and adenosine donor. Considerable support for this pathway was provided by isolation of the key intermediate dimethylarsinoyladenosine [Francesconi *et al.*, 1991b; Francesconi *et al.*, 1992a]. This intermediate, upon glycosidation with available algal metabolites, yields the range of arsenosugars that have been identified from algal sources. A schematic overview of the pathway is given in figure 3.3. This pathway may also form trimethylarsonioribosides, although the stage at which the third methyl group is transferred to arsenic is more speculative.

3.2.1.3. Arsenic in marine animals

Marine animals can be divided into three main groups: fish (such as mackerel, cod, plaice, tuna), crustaceans (*e.g.*, lobster, shrimp, crab, krill, prawn, amphipod) and molluscs (*e.g.*, mussel, oyster, scallop, cockle, clam, whelk).

One of the first reports on arsenic in marine organisms was published by Chapman [1926]. He found that molluscs and crustaceans contained much higher concentrations of arsenic than did fish. Although he was not able to reveal the chemical form of the arsenicals, he already saw the importance of speciation and stated that the arsenicals in marine organisms could not be present as arsenic trioxide or in any form having a similar toxicity. He postulated that the main arsenic compound present in lobster is a more or less complex organic substance, soluble in both water and alcohol and sufficiently stable to resist the action of hot dilute HCl or 5% NaOH. Further research showed that the level of arsenic in a particular organism did not appear to be related to its position in the food chain and to the size of the animal. First Edmonds and Francesconi [1977a] postulated that the trimethylated arsenic compound found in the rock bbster *Panulirus Cygnus* was most likely TMAO, but soon afterwards this compound was identified as AB. The identity was confirmed with X-ray analysis [Edmonds and Francesconi, 1977b]. In the following years, AB was found to be the major arsenical in many more marine animals [Edmonds and Francesconi, 1981b; Edmonds and Francesconi, 1981c; Francesconi and Edmonds, 1987a]. AB is now generally accepted as non-toxic. AC was the second arsenical to be identified in marine animals. However it appears only at trace amounts [Norin and Christakopoulos, 1982]. The discovery of TETRA was important as it appeared in many crustacean and mollusc species at considerable concentrations [Shiomi *et al.*, 1987; Morita and Shibata, 1987]. TMAO was found as a minor natural component in marine animals [Edmonds and Francesconi, 1987a]. TMAO and AC are considered as a breakdown product and a precursor of AB, respectively. Also arsenosugars have been identified in marine animals, more exactly in tissues of the giant clam *Tridacna maxima* [Edmonds *et al.*, 1982a; Francesconi *et al.*, 1992a;] and in species of gastropod [Francesconi *et al.*, 1998]. Marine algae are the source of arsenosugars in these animals. Next to arsenosugars, lipid-soluble arsenic compounds were found in the yelloweye mullet *Aldrichetta forsteri* following oral administration of AC. It was seen that AC was incorporated in phosphatidylarsenocholine and glycerylphosphorylarsenocholine, the latter being found as a minor water-soluble compound and as an alkaline hydrolysis product of the lipid-soluble phosphatidyl-

arsenocholine [Francesconi *et al.*, 1990]. Later Edmonds *et al.* [1992] found phosphatidylarsenocholine and a lipid-soluble arsenosugar (compound **13** in figure 3.1) in the digestive gland of the Western rock lobster *Panulirius cygnus*.

Although marine animals contain many arsenic compounds, most animals contain AB as the major arsenical. Fish tend to have a simple pattern of arsenic compounds dominated by AB. Crustaceans also generally contain AB as a high percentage of their total arsenic. Gastropods often contain very high arsenic concentrations (up to 340 mg/kg wet mass), most of which is usually AB. Bivalve molluscs, in addition to AB, can contain large quantities of TETRA. High arsenosugar levels have been reported in some scallop species. Marine mammals contain only low levels of arsenic. In all cases AB predominates. Lipid arsenic compounds also occur in marine animals. MA, DMA, inorganic As and some unknown species appear at trace or minor levels in marine animals as well. The origin of AB in marine animals remains a matter of debate. Possible sources are water and food.

It seems that marine animals are unable to convert inorganic arsenic from the ambient seawater into AB. Lunde [1972] showed that fish absorb inorganic arsenic, but that no organo arsenicals are formed. Klumpp and Peterson [1981] exposed fish to ^{74}As-arsenate but were not able to detect neither a radioactive AB nor any precursor of AB. In another study it was shown that the mussel *Mytilus edulis* did not accumulate appreciable amounts of arsenite and arsenate [Gailer *et al.*, 1995]. The same type of mussels was maintained in seawater containing different levels of AB. The mussels accumulated the AB readily, in a dose and time dependent way. The mussels were unable to regulate their rate of uptake. The AB was not further metabolised (Francesconi and Edmonds, 1987b). Similar experiments were carried out with the lobster *Panulirus Cygnus*. The lobsters accumulated the AB less efficiently and during a depuration period the levels decreased more rapidly compared to the mussels. From both experiments, however, it could be concluded that AB in seawater was not a significant contributor to the body burden of AB. Moreover, AB has by now not been found at detectable levels in seawater. A reason for the apparent absence of AB from seawater is that this compound is rapidly degraded into DMAA and DMA, obviously by microbial demethylation [Khokiattiwong *et al.*, 2001]. Hunter *et al.* [1998] examined the uptake of As^{V}, TMAO and AB by the shrimp *Crangon crangon*. These arsenic species do not significantly contribute to the high AB levels. By now, it can be concluded that AB is not synthesized *de novo* by marine animals from ingested arsenic.

Likewise marine animals seem unable to convert AB directly from arsenic containing food. Several experiments have been carried out in which different arsenicals were administered through food. Edmonds and Francesconi [1987a] showed that the catfish *Cnidoglanis macrocephalus* and the school whiting *Sillago bassensis* accumulated less than 1% of arsenate as TMAO. The methylation was probably achieved by the gut microflora. These authors also conducted a similar experiment [Francesconi *et al.*, 1989]. Of a set of organo-arsenicals, only AB and AC were accumulated by the yelloweye mullet *Aldrichetta forsteri*. Dimethylarsinoyl ethanol (DMAE), dimethylarsinoyl acetate (DMAA) and dimethyl-arsinothioyl ethanol were not retained by the fish, suggesting that no methylation occurred. An important finding was that the AC was rapidly and quantitatively transformed into AB (see below). Experiments on radiolabeled arsenosugars, originating from algae exposed to ^{74}As-arsenate in seawater, fed to the lobster *Homarus americanus*, revealed no new radioactive compounds and ^{74}As-arsenobetaine was not detected [Cooney and Benson, 1980]. In a recent study by Francesconi *et al.* [1999a] the shrimp *Crangon crangon* was fed a synthetic dimethylated and a trimethylated arsenosugar. The dimethylated compound was poorly absorbed and found mostly unchanged. The trimethylated sugar was slightly absorbed and half of this was transformed into AB. Goessler *et al.* [1997] found large amounts of AB in the herbivorous gastropod *Austrocochlea constricta*, which fed on the seaweed *Hormosira banksii* but they were unable to prove whether the AB was originating from the arsenosugar present in the alga rather than from other sources. The arsenic profile in the next step of the food chain, the carnivorous gastropod *Morula marginalba*, was not much different. Edmonds *et al.* [1997] studied another five food chains but were unable to conclude whether AB is originating from the ambient water, food or through direct conversion from arsenosugars. The identification of TMAO, which might be a precursor of AB, might reveal new insights. As in the case of seawater, marine animals seem unable to biotransform AB from food.

However, marine animals, directly or indirectly, feed on algae. Despite the apparent lack of AB in algae, the arsenosugars - because of their high levels in algae - remain the most plausible precursors of AB. When considering the chemical structure of arsenosugars, it can easily be seen that conversion of dimethylarsinoyl ribosides to AB requires cleavage of the C_3-C_4 bond of the sugar ring with subsequent oxidation at C_4, and reduction and further methylation on arsenic. These changes could be microbially mediated and may take place in sediments. This hypothesis was supported by experimental evidence. When the brown alga *Ecklonia radiata* was allowed to decompose with marine sediment and associated

microflora under controlled anaerobic conditions, the dimethylated arsenosugars were quantitatively transformed into DMAE [Edmonds *et al.*, 1982b]. Only a limited number of experiments have been carried out, on benthic-feeding organisms. TMAO in estuary catfish is believed to originate from methylation of arsenate in surface sediments [Edmonds and Francesconi, 1987a]. In another experiment the polychaete *Tharyx marioni* was found to contain extremely high amounts of arsenic and radiotracer experiments showed that sediments were the source of this. However, the chemical identity of this arsenic remained unknown [Gibbs *et al.*, 1983]. The formation of DMAE from arsenosugars might also occur in the gut tract of the marine animals.

DMAE requires only methylation and oxidation (or vice versa) via arsenocholine or DMAA, respectively, for conversion to AB. Unfortunately this hypothesis could not yet be confirmed by experimental evidence. As already described, Francesconi *et al.* [1989] carried out feeding experiments with yelloweye mullet (*Aldrichetta forsteri*) but found that fish receiving DMAE or DMAA showed no increase in arsenic concentration compared to the control group. It is yet to be established at what stage in the food chain (bacteria < detritovores < AB-containing animals of higher trophic levels) the final conversion of DMAE to AB occurs.

In analogy, anaerobic microbial degradation of a trimethylarsonioriboside leads to AC [Francesconi et al., 1992b]. No further methylation outside the algae is required in this case. It can easily be shown that AC is a precursor of AB. AC fed to fish is immediately transformed into AB [Francesconi *et al.*, 1989].

Both proposed pathways are illustrated in figure 3.4. The two steps in the transformation of trimethyl derivatives into AB occur readily under laboratory conditions. The proposed pathway based on dimethyl derivatives, however, requires an extra methylation step, which has yet to be achieved from laboratory experiments. Still the large amounts of dimethylarsinoyl sugars seem to be the only source of AB. The biogenesis of AB is still under investigation. Recently a new arsenobetaine has been isolated from marine organisms [Francesconi *et al.*, 2000] and new findings about the uptake of several arsenic-betaines [Francesconi *et al.*, 1999b] have been published. Moreover an alternative mechanism for the formation of AB, based on the chemical structure of a trialkylarsonioriboside has been suggested [Edmonds, 2000].

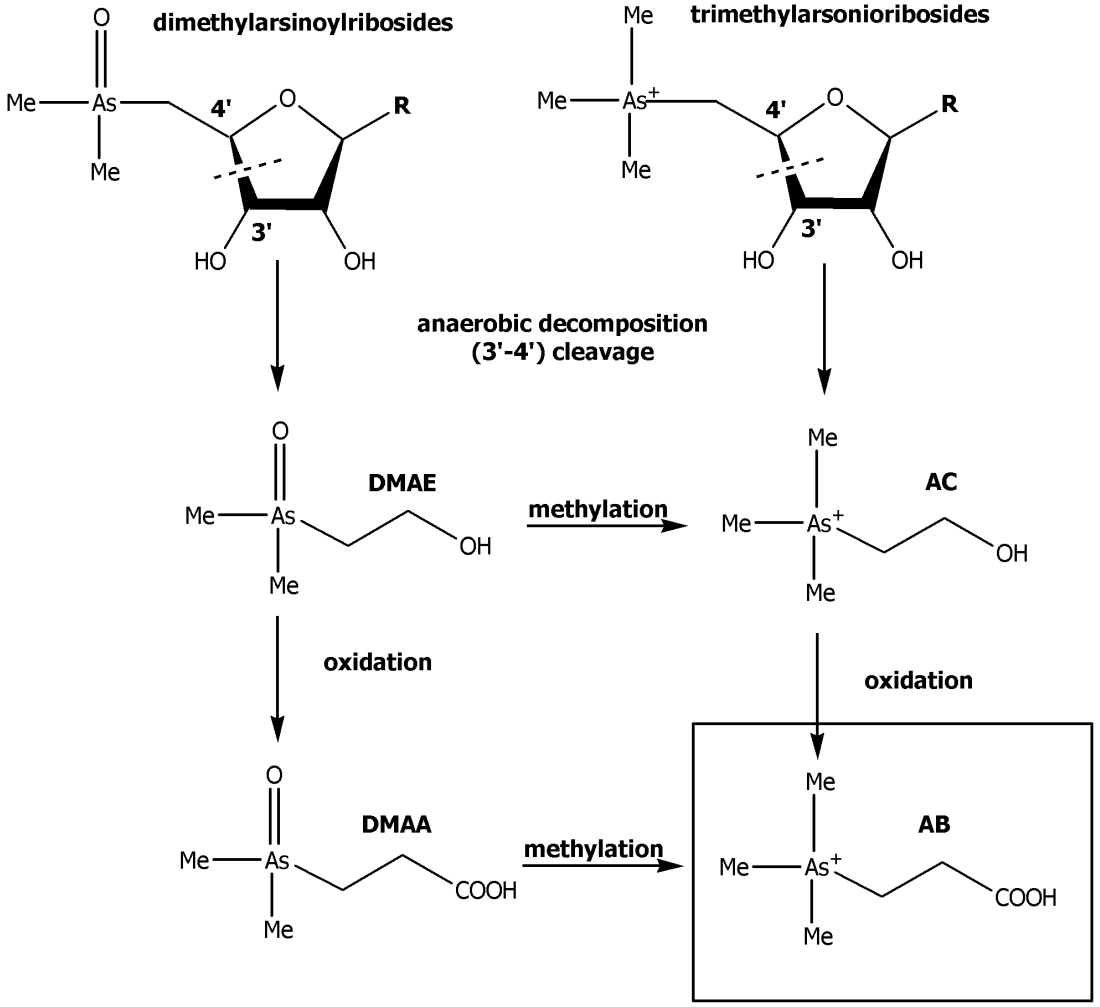

Figure 3.4. Pathway for the formation of arsenobetaine from dimethylarsinoylribosides and trimethylarsonioribosides.

3.2.2. Arsenic compounds in the atmospheric and terrestrial environment

[Cullen and Reimer, 1989; Mandal and Suzuki, 2002]

3.2.2.1. Arsenic in the earth's crust

The terrestrial abundance of arsenic is around 1.5-3 mg/kg, being the 20th most abundant element in the earth's crust. There is, however, a large variability depending on rock type, with sedimentary rock generally containing higher levels than igneous rock. It has been estimated that of the total arsenic contained in the various reservoirs (rocks, oceans, soils, biota, atmosphere), more than 99% is associated with rocks and minerals. Arsenic naturally

occurs in over 200 different mineral forms, of which 60% are arsenates, 20% sulphides and sulphosalts and the remaining 20% include arsenides, arsenites, oxides, silicates and elemental arsenic. Arsenopyrite (FeAsS) is the most abundant arsenic-containing mineral. Pure arsenic ores are realgar (As_4S_4), orpiment (As_2S_3) and arsenolite (As_2O_3). Other important minerals are olivenite (Cu_2OHAsO_4), cobaltite (CoAsS) and proustite (Ag_3AsS_3).

3.2.2.2. Arsenic in soils and terrestrial sediments

Arsenic concentration in soil and shales is considerably higher than in earth's crust, because of its accumulation during weathering and translocation in colloid fractions. Background concentrations of arsenic in soil range from 0.1-50 mg/kg with a mean of about 6 mg/kg. Many factors may influence the arsenic content in soils. The natural sources of arsenic in soil are mainly the parent (or rock) materials from which it is derived. Arsenic may also accumulate in soil through anthropogenic sources such as pesticides, herbicides, fungicides, fertilisers, irrigation water from mines, dust from fossil fuel combustion and disposal of industrial and animal wastes. Arsenic occurs mainly as inorganic species, with depending on the pH and the redox conditions of the soil, arsenates and arsenites being the stable arsenic species. Inorganic arsenic compounds can be methylated to MA, DMA and TMAO by microorganisms. Further reduction can lead to volatile trivalent methylarsines.

The natural level of arsenic in sediments is usually below 10 mg/kg (dry mass). As^{V}, As^{III}, MA and DMA are the predominant species.

3.2.2.3. Arsenic in the atmosphere

Arsenic enters the atmosphere from natural sources that include volcanic activity, wind erosion, sea spray, forest fires, microbial reduction and low temperature volatilisation (mainly biological formation of volatile arsenicals). Smelting operations and fossil fuel combustion contribute to anthropogenic sources of arsenic. The ratio of natural to anthropogenic sources is 60:40. Particulate arsenic trioxide is the main form of arsenic released by these processes. Arsine and methylated arsines ($MeAsH_2$, Me_2AsH, Me_3As) have been reported over sites where biological activity is high. These species then partly oxidate to the pentavalent state. Typical background levels for arsenic are 0.2-1.5 ng/m^3 for rural areas, 0.5-3 ng/m^3 for urban areas and < 50 ng/m^3 for industrial sites.

3.2.2.4. Arsenic in freshwater and groundwater

Arsenic is found at low concentration in natural surface water. The concentration of arsenic in unpolluted fresh waters ranges from 1-10 µg/L. In 2001, the US Environmental Protection Agency adopted a new standard for arsenic in drinking water at 10 µg/L, replacing the old standard of 50 µg/L. The date by which systems must comply with the new 10 µg/L standard is January, 2006 [http 4]. The World Health Organisation has established a provisional guideline value of 10 µg/L [http 5].

Arsenic levels in groundwater average about 1-2 µg/L, except in areas with volcanic rock and sulphide mineral deposits where arsenic levels can range up to 3.4 mg/L.

3.2.2.5. Arsenic in terrestrial and freshwater plants

Arsenic levels in terrestrial plants are generally lower than those found in marine plants. The concentrations seldom exceed levels higher than 1 mg/kg dry mass. Inorganic arsenic predominates (arsenite, or more usually arsenate) and MA and DMA can be found as well. TMAO, TETRA, AB and presumably also AC have been detected as well. AsSug-OH and AsSug-SO_3 have been detected in some plant species. Plants that serve as foodstuff for humans do not cause a substantial increase in the arsenic burden. Values for total arsenic in lettuce, beans, carrots etc. range between 0.1 and 10 µg/kg (wet mass). Notable exceptions are mushrooms. Although not classified as plants they will be described here. Arsenic levels in fungi vary between <1-2000 mg/kg (dry mass). DMA predominates in fungi although the amount of MA can be up to 50%. Inorganic arsenate is also a common constituent. AB can be the major arsenical and TETRA and/or AC can be found as well. TMAO and arsenosugars have been detected in some species.

In freshwater plants arsenite and arsenate predominate and low levels of MA and DMA are also detectable. Arsenosugars are only occasionally detected. TETRA and an appreciable amount of lipid-soluble arsenic can be seen as well.

3.2.2.6. Arsenic in terrestrial animals

Arsenic levels in terrestrial animals are low. Arsenite and arsenate predominate. Median levels in pork, poultry and beef are around 5 µg/kg (wet mass). Also here animals served as food for humans do not give rise to high uptake of arsenic.

3.3. Arsenic in the human body

3.3.1. Arsenic in humans after intake of inorganic arsenic

3.3.1.1. Exposure, uptake, storage and excretion

[Ishinishi *et al.*, 1986]

Because of its widespread use and occurrence, humans may be exposed to various arsenic species from many different sources, both natural and anthropogenic. Anthropogenic sources are more important than natural sources. The main routes of exposure are inhalation (dust and fumes) and ingestion (water, beverages, soil and food), although skin absorption of trivalent arsenic has been reported. Inhalation of airborne arsenic is commonly associated with smelting and mining activities and from coal fly ash due to the burning of high arsenic containing coals. Exposure by the general population occurs mainly through ingestion of arsenic in drinking water (high arsenic levels in groundwater in regions of India, Bangladesh, Mongolia...) and food (contaminated with arsenic pesticides, grown on arsenic rich soils or with arsenic contaminated water). Short or long-time exposure to inorganic arsenic leads to different adverse health effects. Exposure to arsenicals present in food such as fish, crustaceans, molluscs and algae was not shown to cause any danger for human health. The metabolism and kinetics of excretion is, however, highly dependent on the chemical form of the ingested arsenical. Because this aspect is of prime interest for the scope of this work, it will be discussed in a separate paragraph. This paragraph will focus mainly on inorganic arsenic.

Once ingested, the gastrointestinal tract easily takes up (over 90%) dissolved inorganic arsenic. In blood arsenic is preferentially found in the packed cell fraction. Whole blood levels for unexposed people vary between 2-7 µg/L. Serum and packed cell levels amount

around 0.1-5.5 µg/L and 0.4-20 µg/L As, respectively [Versieck and Vanballenberghe, 1985]. Absorbed arsenite and arsenate are initially bound to haemoglobin, yet they leave the intravascular space within 24 hours and are concentrated in the liver, kidneys, spleen, lungs and gastrointestinal tract. Within a day, residual arsenic is found in nails, hair and skin and this due to the high thiol content of keratin. Inorganic arsenic is mainly excreted through urine.

3.3.1.2. Metabolism and mechanisms of toxicity of inorganic arsenic

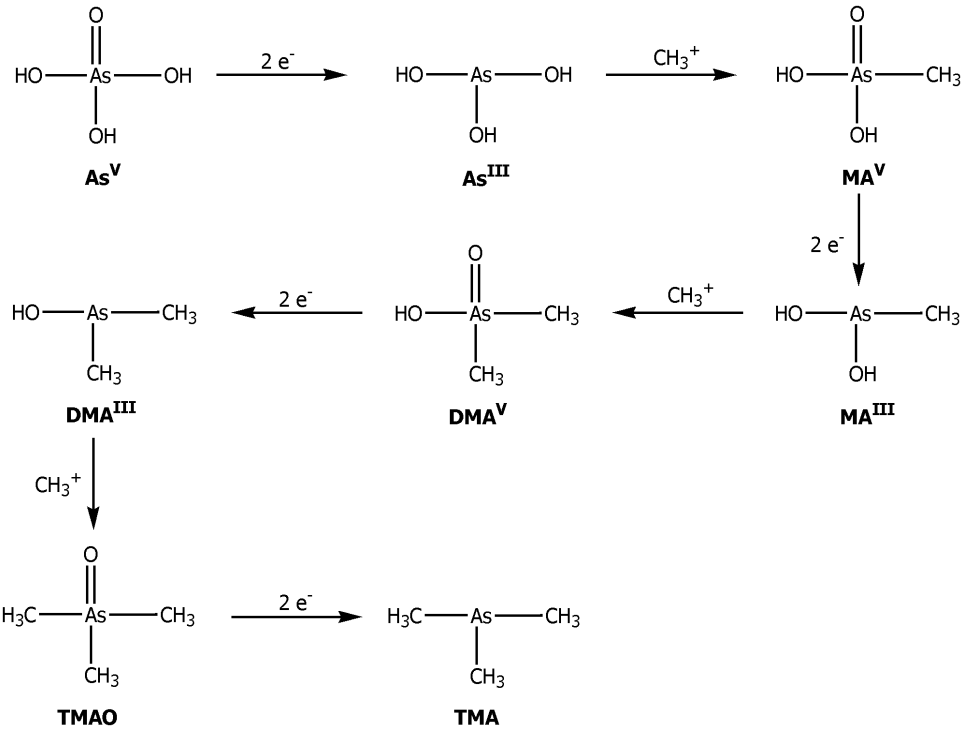

Figure 3.5. Biomethylation of inorganic arsenic.

Several studies have shown that mammals metabolise inorganic arsenic to MA and DMA [Crecelius, 1977; Buchet *et al.*, 1981]. These methylated species are a result of biomethylation, which involves a stepwise reduction of pentavalent arsenical to a trivalent arsenical followed by oxidative addition of a methyl group. In humans DMA is the end metabolite. Gluthathione (GSH) [Buchet and Lauwerys, 1987] and S-adenosylmethionine (SAM) [Marafante and Vahter, 1984; Buchet and Lauwerys, 1985] serve as the reducing agent and methyl donor, respectively. The liver is the main site for this methylation. The methylating capability is, however, very much dependent on the biological species. Marmoset monkeys, *e.g.*, have a very poor methylating efficiency [Vahter *et al.*, 1982]. The process of (bio)methylation was first described by Challenger [1945]. A schematic overview

is given in figure 3.5. Challenger developed his findings in analogy with other methyl-forming metals such as selenium and tellurium. The identification of Gosio gas as trimethylarsine (TMA), a gas having a garlic odour and formed by interaction of moulds with arsenicals present as pigments in wallpaper, led Challenger to put forward this mechanism, which is now generally accepted. According to Challenger, arsenate is transformed to TMA by the mould *Scopulariopsis brevicaulis* by sequential reduction and oxidative methylation through several intermediates such as arsenite, MA, DMA and TMAO. Although he could not isolate these intermediates at that time, addition of MA, DMA and TMAO to a culture of *S. brevicaulis* always yielded TMA. He also postulated that SAM was the likely source of Me^+. This has been confirmed later on. Methylation of inorganic occurs in bacteria, fungi, yeasts, anaerobic microorganisms and mammals... The methylation pathway in these organisms is identical, but reducing agents and methyl donors might be different.

It has long been assumed that this methylation is a detoxification process. Indeed the methylated species have much higher LD_{50} values compared to inorganic species (see table 3.3). However, during the last years work has focussed on the trivalent methylated intermediates MA^{III} and DMA^{III}. Animal experiments and *in vitro* studies have shown that these species are at least as toxic as the inorganic arsenicals and maybe even more. Because these reduced species have been reported to be very unstable [Gong *et al.*, 2001], their toxicity is still a matter of debate.

When highlighting the mechanism by which arsenic poses a threat for human health, it is important to distinguish between arsenite and arsenate. It is generally thought that the overall toxicity of arsenite is due to the inhibition of critical sulphhydryl-containing enzymes by trivalent arsenic. Many enzymes are susceptible to deactivation by arsenic. The deactivation is believed to be reversible because adding an excess of a monothiol such as GSH restores the enzymatic activity. Moreover GSH depletion has been shown to be more susceptible to arsenic intoxication. Some pentavalent compounds are partly reduced *in vivo* to the more toxic trivalent forms, but the redox equilibrium *in vivo* favours the pentavalent state. Pentavalent arsenic does not appear to lead to enzyme inhibition. It is, however, capable of uncoupling the oxidative phosphorylation in the mitochondria by a process called arsenolysis. The oxidative phosphorylation is the process in which adenosine triphosphate (ATP) is formed. The mechanism of toxicity for arsenate is thought to be related to the competitive substitution of arsenate for phosphate, with which it is isoelectric and isosteric,

and to the subsequent formation of an unstable arsenate ester of ADP, which is rapidly hydrolysed. In this regard, it can be concluded that arsenic has a doubled toxic impact on the cellular respiration: the trivalent arsenic inhibits the reduction of nicotinamide adenine dinucleotide (NADPH) by deactivating critical enzymes, and the pentavalent arsenic uncouples the oxidative phosphorylation.

Table 3.3. LD_{50} values of different arsenic species in mammals.

LD_{50} in humans (mg/kg)			
As_2O_3	1.4	oral	[Fairchild *et al.*, 1977]
MA	50	oral	[Fairchild *et al.*, 1977]
DMA	500	oral	[Fairchild *et al.*, 1977]
LD_{50} values in animals (mg/kg)			
As_2O_3	34.5	mouse, oral	[Kaise *et al.*, 1985]
arsenite	4.5	rat, ip	[Frank and Moxon, 1936]
arsenate	14-18	rat, ip	[Frank and Moxon, 1936]
MA	1800	mouse, oral	[Kaise *et al.*, 1989]
DMA	1200	mouse, oral	[Kaise *et al.*, 1989]
TMAO	10600	mouse, oral	[Kaise *et al.*, 1989]
AB	>10000	mouse, oral	[Kaise *et al.*, 1985]

The toxicity of arsenic is highly dependent on its chemical form. Inorganic arsenicals (arsine, arsenite and arsenate) are highly toxic, whereas MA and DMA are much less toxic. Trimethyl and tetra-alkylarsonium compounds (TMAO, TETRA, AC, AB, and arsenosugars) are considered innocuous. MA^{III} and DMA^{III} are at least as toxic as inorganic arsenic. In general, soluble inorganic arsenicals are more toxic than the organic ones, and As^{III} is more toxic than As^{V}. A table with LD_{50} values of some arsenic species is given in table 3.3.

Biomarkers of inorganic arsenic exposure are to be found in urine in short-term (up to one week) and in hair or in nails for long-term (several weeks to several months) exposure. Blood levels are generally low, because of the fast clearance into tissues. Only in the case of continued arsenic exposure is the blood arsenic level likely to be a useful indicator.

3.3.2. Arsenic in humans after intake of marine food

Arsenic is present in seafood at concentration as high as several 100 mg/kg. Speciation studies show that AB is the major component in fish and crustaceans, with arsenosugars,

AC, TMAO, TETRA, MA, DMA and inorganic arsenic present as minor species. Both AB and arsenosugars are present in molluscs. Arsenosugars are the primary arsenic constituents of algae, the residual arsenicals being DMA and inorganic arsenic.

3.3.2.1. Arsenic in humans after exposure to arsenobetaine

Cox [1925] reported high values of arsenic found in patients, often leading to the conclusion that they were chronically poisoned by arsenic. As he was aware of the fact that fish contains high amounts of arsenic, he made a link between the arsenic in fish and in urine. Chapman [1926] found that when two people ate lobster, the arsenic levels in the urine drastically increased and only a small proportion of this could be directly detected, *i.e.*, without mineralisation of the organic matter by nitric and sulphuric acids. Although it was impossible to conclude whether the compound found in the urine was identical to the one in the lobster, he concluded that after passage of this compound through the body it had not changed into a compound that could directly be analysed by reduction with hydrogen. Coulson *et al.* [1935] carried out experiments with both humans and rats to compare the rate and completeness of excretion of shrimp-arsenic. They found that this arsenic compound was excreted rapidly and unchanged by the kidneys. Crecelius [1977] found no marked increase in urinary levels of As^{III}, As^{V}, DMA and MA after a volunteer had ingested crab. However, after hot basic digestion with 2 M NaOH, high levels of DMA were detected in the samples. Measurements were carried out with a hydride generation (HG) technique. Using HG, only directly hydride-forming elements are detected, whereas organo-arsenicals are insensitive towards this technique (see paragraph 4.4). This shows again that the arsenical present in the urine after ingestion of crab-arsenic was organic. Crecelius also reported that the crab-arsenical was excreted within 1-2 days after ingestion. In 1977 Edmonds and Francesconi [1977b] identified this compounds as AB. Buchet *et al.* [1980] reported a mean arsenic biological half-life of 18 hours after 4 volunteers ate crab. This half-life was significantly shorter than that reported for inorganic arsenic (30 hours). A mass balance was determined and it was found that 56% of the ingested arsenic was recovered from the urine within 4 days. Cannon *et al.* [1981] found that AB was excreted unchanged in the urine of a volunteer who had a meal of the Western Rock lobster *Panulirus Cygnus*, which contains AB as the sole constituent. They therefore concluded that AB represents no toxic hazard for humans. Kaise *et al.* [1985] determined an LD_{50} value of AB in male mice. No deaths were observed with oral administration of 10 g/kg, so the LD_{50}

value was set to this amount (see table 3.3). They recovered the arsenical in urine in the non-metabolised form. Yamauchi *et al.* [1992] determined the content of inorganic and mono-, di- and trimethylated species in several diets as well as in blood and urine of a Japanese population. The mean total arsenic intake was 195 µg per day, composed of 76% trimethylated arsenic. An average of 64.6% of a total mean of 129 µg/L arsenic in urine was also trimethylated. The mean blood total arsenic level was 7.3 µg/ L arsenic of which 73% was trimethylated. The trimethylated levels in urine correlated well with the trimethylated levels in blood. After the ingestion of 500 g crab, a 10-fold increase of total urinary arsenic was observed, with a maximum recovered between 4 and 17 hours after intake. The ingestion of crab, shrimp and salmon showed no effect on the urinary excretion of MA and DMA [Le *et al.*, 1993]. Later Le *et al.* [1994] conducted a study in which several volunteers ingested a portion of crab and shrimp. The AB was excreted unchanged and for two volunteers 66% and 73% of the ingested arsenic was recovered within 37 hours after ingestion. A maximum amount was recovered from urine 8 hours after intake.

In general it can be concluded that AB is excreted fast and unchanged in the urine and therefore is not believed to pose any threat on human health. Regarding this latter remark, Buchet *et al.* [1994; 1996] followed the assessment of inorganic arsenic after seafood consumption. They found that consumption of ray, cod or plaice did not result in an increase of urinary arsenite, but that consumption of mussels led to an amount of DMA excreted in urine, which is significantly higher than that expected on the basis of the amount of inorganic arsenic and its methylated derivatives already present in the shellfish. This is due to the arsenosugar content in the mussels.

3.3.2.2. Arsenic in humans after exposure to arsenosugars

The ingestion of arsenosugar containing food shows a totally different urinary excretion pattern.

Le *et al.* [1994] carried out several experiments on different kinds of algae samples. In one study two male volunteers consumed a portion of kelp. The total arsenic and hydride-forming arsenic was followed in function of time relative to the ingestion of kelp. Both results show the same time dependent response and only small amounts of arsenic are non-hydride forming arsenicals. A considerable concentration of arsenic is found between 17 and 37 hours after ingestion. Speciation analysis shows that the kelp consists of

arsenosugars OH and PO_4 and an unidentified species comprising about 40% of the total extractable arsenic. On the other hand speciation analysis of selected urine samples before and after ingestion led to the conclusion that in the first case only DMA and arsenate were found, whereas 23 hours after eating, 3 unknown species were detected besides increased amounts of DMA and As^V. In the urine of the other volunteer two identical and one different unidentified arsenic species were found. Because of these findings they suggested that the metabolism of arsenosugars is dependent on the individual and they extended their study to 9 people ingesting a portion of nori, an algae containing only one arsenosugar. Urinary arsenic levels peaked between 10 and 60 hours after ingestion for 7 volunteers. Two volunteers showed no response. Selected urine samples were again subjected to speciation analysis with HPLC-ICP-MS. Up to 6 unknown arsenicals in addition to increased amounts of DMA and As^V were present in the urine samples. Because of the mutual differences between the nine subjects, they concluded again that the metabolism of arsenosugars differs from individual to individual. Finally they suggested that arsenosugars were not simply decomposed by the acid present in the stomach as an extraction of nori in water and in 10 mM HCl showed no significant difference. Ma and Le [1998] subsequently reported similar findings. Again they showed the presence of unknown metabolites and an increased amount of DMA. Spiking of the urine samples with the algae extract moreover showed that the unknown peaks could not be attributed to the arsenosugars originally present in the consumed seaweed. Time dependent plots of urinary excretion were similar to those presented earlier.

Francesconi *et al.* [2002] carried out a thorough study. A male volunteer ingested a synthetic arsenosugar (1.22 mg in As). Determination of total arsenic versus time showed that 81% is excreted within 94 hours after ingestion. The highest amount was found 27 hours after eating. Both anion and cation exchange HPLC-ICP-MS was used to elucidate the identity of the different metabolites present in the urine. Four major peaks were present in the urine after separation on the anion exchange column. One of them was assigned to as DMA. Another eluted in the void volume and is a mixture of neutral and cationic compounds. Cation exchange chromatography revealed two major peaks, eluting closely together. The largest peak was assigned to as DMAE, by matching retention times and by recording the molecular ion with electrospray mass spectrometry (ES-MS). It was postulated that the DMAE was formed by microbial breakdown of the arsenosugar by the gut microflora. The small peak was postulated to be TMAO. Evidence was found by spiking the urine sample with a calibrant. More evidence for the presence of DMAE and TMAO was

found by eluting the urine sample under different chromatographic conditions. For both species, the change in retention time matched that of a pure standard. The authors also found that the different arsenic species were excreted at different rates. The two unknown compounds from the anion exchange chromatogram peaked at 22 h, whereas DMA and DMAE reached a maximum after 27 hours. Finally they postulated that one significant metabolite was possibly dimethylarsinous acid (DMA^{III}).

Three more studies conducted by Feldmann *et al.* [2000] and Hansen *et al.* [2003a; 2003b] are worth mentioning. Instead of humans they carried out experiments on sheep from Northern Scotland. These sheep feed on seaweed and ingest enormous amounts (3-5 kg per day). Besides urine, also tissue, wool, faeces and blood were analysed. Urine, blood and wool levels of arsenic were significantly higher than those of control sheep that fed on grass. Especially the arsenic concentration in wool was astounding as it reached a 100-fold increase compared to the control sheep. Arsenic in wool was measured because it is one of the primary sites for long-term storage of arsenic. Speciation experiments of urine showed that almost all arsenic was found as DMA. Minor metabolites were MA, TETRA and arsenosugar OH. In a similar second study, sheep were again submitted to a feeding experiment [Hansen *et al.*, 2003a]. 13% of the ingested arsenic was excreted in the faeces, with the remainder estimated to be excreted in the urine. DMA (60%) and MA, TETRA, As^{V} and DMAE were recovered from the urine of the sheep. The excretion rate peaked between 4 and 28 hours after seaweed intake. In Hansen *et al.* [2003b] no mention of MA is made, but DMAA was identified as the second most abundant metabolite.

There are no reports on the acute toxicity of arsenosugars. Sakurai *et al.* [1997] investigated the *in vitro* cytotoxicity of arsenosugar OH and reported that it was not cytotoxic to both peritoneal macrophages and to alveolar macrophages at the µM concentration level, although it was able to induce several cellular responses in both macrophages at high concentrations (1-10 mM). In a review written by Sakurai [2002], an experiment is mentioned in which the *in vivo* acute toxicity was tested (unpublished results). An indicative LD_{50} value of > 6 g/kg was given for oral administration to mice. He concluded that one-time consumption is not very toxic to the human health. However, the fact that arsenosugars are partly transformed into DMA raises questions about the possible toxicity of arsenosugars. DMA has been said to be a potent co-carcinogen.

References

[Adriano, 1986]

Adriano DC (1986). In *Trace Elements in the Terrestrial Environment*, Springer, New York, pp 47-72.

[Andreae, 1979]

Andreae MO (1994). *Limnol. Oceanogr.*, **24**, 440-452.

[Azcue and Nriagu, 1994]

Azcue JM and Nriagu JO (1994). In *Arsenic in the environment, part I: cycling and characterization* (ed. Nriagu JO), John Wiley & Sons, New York, pp 1-15.

[Buchet and Lauwerys, 1985]

Buchet JP and Lauwerys R (1985). *Arch. Toxicol.*, **57**, 125-129.

[Buchet and Lauwerys, 1987]

Buchet JP and Lauwerys R (1987). *Toxicol. Appl. Pharmacol.*, **91**, 65-74.

[Buchet *et al.*, 1980]

Buchet JP, Lauwerys R and Roels H (1980). *Int. Arch. Occup. Environm. Health*, **46**, 11-29.

[Buchet *et al.*, 1981]

Buchet JP, Lauwerys R and Roels H (1981). *Int. Arch. Occup. Environ. Health*, **48**, 71-79.

[Buchet *et al.*, 1994]

Buchet JP, Pauwels J and Lauwerys R (1994). *Environ. Res.*, **66**, 44-51.

[Buchet *et al.*, 1996]

Buchet JP, Lison D, Ruggeri M, Foa V and Elia G (1996). *Arch Toxicol.*, **70**, 773-778.

[Cannon *et al.*, 1981]

Cannon JR, Edmonds JS, Francesconi KA, Raston CL, Saunders JB, Skelton BW and White AH (1981). *Aust. J. Chem.*, **34**, 787-798.

[Cantoni, 1952]

Cantoni GL (1952). *J. Am. Chem. Soc.*, **74**, 2942-2943.

[Cantoni, 1953]

Cantoni GL (1953). *J. Biol. Chem.*, **204**, 403-416.

[Challenger, 1945]

Challenger F (1945). *Chem. Rev.*, **36**, 315-361.

[Chapman, 1926]

Chapman AC (1926). *Analyst*, **51**, 548-563.

[Cooney and Benson, 1980]

Cooney RV and Benson AA (1980). *Chemosphere*, **9**, 335-341.

[Cooney *et al.*, 1978]

Cooney RV, Mumma RO and Benson AA (1978). *Proc. Natl. Acad. Sci. USA*, **75**, 4262-4264.

[Coulson *et al.*, 1935]

Coulson EJ, Remington RE and Lynch KM (1935). *J. Nutr.*, **10**, 255-270.

[Cox, 1925]

Cox HE (1925). *Analyst*, **50**, 3-13.

[Crecelius, 1977]

Crecelius EA (1977). *Environ. Health Persp.*, **19**, 147-150.

[Cullen and Reimer, 1989]

Cullen WR and Reimer KJ (1989). *Chem. Rev.*, **89**, 713-764.

[Edmonds and Francesconi, 1977a]

Edmonds JS and Francesconi KA (1977). *Tetrah. Letters*, **18**, 1543-1546.

[Edmonds and Francesconi, 1977b]

Edmonds JS and Francesconi KA (1977). *Nature*, **265**, 436.

[Edmonds and Francesconi, 1981a]

Edmonds JS and Francesconi KA (1981). *Nature*, **289**, 602-604.

[Edmonds and Francesconi, 1981b]

Edmonds JS and Francesconi KA (1981). *Mar. Poll. Bull.*, **12**, 92-96.

[Edmonds and Francesconi, 1981c]

Edmonds JS and Francesconi KA (1981). *Chemosphere*, **10**, 1041-1044.

[Edmonds and Francesconi, 1983]

Edmonds JS and Francesconi KA (1983). *J. Chem. Soc. Perkin Trans. I*, 2375-2382.

[Edmonds and Francesconi, 1987a]

Edmonds JS and Francesconi KA (1987). *Sci. Tot. Environ.*, **64**, 317-323.

[Edmonds and Francesconi, 1987b]

Edmonds JS and Francesconi KA (1987). *Experientia*, **43**, 553-557.

[Edmonds *et al.*, 1982a]

Edmonds JS, Francesconi KA, Healy PC and White AH (1982). *J. Chem. Soc. Perkin Trans. I*, 2989-2993.

[Edmonds *et al.*, 1982b]

Edmonds JS, Francesconi KA and Hansen JA (1982). *Experientia*, **38**, 643-644.

[Edmonds *et al.*, 1987]

Edmonds JS, Morita M and Shibata Y (1987). *J. Chem. Soc. Perkin Trans. I*, 577-580.

[Edmonds *et al.*, 1992]

Edmonds JS, Shibata Y, Francesconi KA, Yoshinaga J and Morita M (1992). *Sci. Tot. Environ.*, **122**, 321-335.

[Edmonds *et al.*, 1997]

Edmonds JS, Shibata Y, Francesconi KA Rippingale RJ and Morita M (1997). *Appl. Organomet. Chem.*, **11**, 281-287.

[Edmonds, 2000]

Edmonds JS (2000). *Bioorg. Med. Chem. Lett.*, **10**, 1105-1108.

[Fairchild *et al.*, 1977]

Fairchild EJ, Lewis RJ and Tatken RL (1977). *Registry of toxic effects of chemical substances, US Department of Health, Education, and Welfare*. National Institute for Occupational Safety and Health, Cincinnati.

[Feldmann *et al.*, 2000]

Feldmann J, John K and Pengprecha P (2000). *Fres. J. Anal. Chem.*, **368**, 116-121.

[Francesconi and Edmonds, 1987a]

Francesconi KA and Edmonds JS (1987). *Comp. Biochem. Physiol.*, **87C**, 345-347.

[Francesconi and Edmonds, 1987b]

Francesconi KA and Edmonds JS (1987). In *Heavy metals in the environment, volume 2* (ed. Lindberg SE and Hutchinson TC), CEP consultants, Edinburgh, pp 71-73.

[Francesconi *et al.*, 1989]

Francesconi KA, Edmonds JS and Stick RV (1989). *Sci. Tot. Environ.*, **79**, 59-67.

[Francesconi *et al.*, 1990]

Francesconi KA, Stick RV and Edmonds JS (1990). *Experientia*, **46**, 464-466.

[Francesconi *et al.*, 1991a]

Francesconi KA, Edmonds JS, Stick RV, Skelton BW and White AH (1991). *J. Chem. Soc. Perkin Trans. I*, 2707-2716.

[Francesconi *et al.*, 1991b]

Francesconi KA, Stick RV and Edmonds JS (1991). *J. Chem. Soc. Chem. Commun.*, 928-929.

[Francesconi *et al.*, 1992a]

Francesconi KA, Edmonds JS and Stick RV (1992). *J. Chem. Soc. Perkin Trans. I*, 1349-1357.

[Francesconi *et al.*, 1992b]

Francesconi KA, Edmonds JS and Stick RV (1992). *Appl. Organomet. Chem.*, **6**, 247-249.

[Francesconi *et al.*, 1998]

Francesconi KA, Goessler W, Panutrakul S and Irgolic KJ (1998). *Sci. Tot. Environ.*, **221**, 139-148.

[Francesconi *et al.*, 1999a]

Francesconi KA, Hunter DA, Bachmann B, Raber G and Goessler W (1999). *Appl. Organomet. Chem.*, **13**, 669-679.

[Francesconi *et al.*, 1999b]

Francesconi KA, Gailer J, Edmonds JS, Goessler W and Irgolic KJ (1999). *Comp. Biochem. Physiol. C*, **122**, 131-137.

[Francesconi *et al.*, 2000]

Francesconi KA, Khokiattiwong S, Goessler W, Pedersen SN and Pavkov M (2000). *Chem. Comm.*, 1083-1084.

[Francesconi *et al.*, 2002a]

Francesconi KA, Tanggaard R, McKenzie CJ and Goessler W (2002). *Clin. Chem.*, **48**, 92-101.

[Franke and Moxon, 1936]

Franke KW and Moxon AL (1936). *J. Pharmacol. Exp. Ther.*, **58**, 454-459.

[Gailer *et al.*, 1995]

Gailer J, Francesconi KA, Edmonds JS and Irgolic KJ (1995). *Appl. Organomet. Chem.*, **9**, 341-355.

[Gailer *et al.*, 1999]

Gailer J, Madden S, Cullen WR and Denton MB (1999). *Appl. Organomet. Chem.*, **13**, 837-843.

[Gibbs *et al.*, 1983]

Gibbs PE, Langston WJ, Burt GR and Pascoe PL (1983). *J. Mar. Biol. Assoc. U.K.*, **63**, 313-325.

[Goessler *et al.*, 1997]

Goessler W, Maher W, Irgolic KJ, Kuehnelt D, Schlagenhaufen C and Kaise T (1997). *Fres. J. Anal. Chem.*, **359**, 434-437.

[Gong *et al.*, 2001]

Gong Z, Lu, X, Cullen WR and Le XC (2001). *J. Anal. At. Spectrom.*, **16**, 1409-1413.

[Hansen *et al.*, 2003a]

Hansen HR, Raab A, Francesconi KA and Feldmann J (2003). *Environ. Sci. Technol.*, **37**, 845-851.

[Hansen *et al.*, 2003b]

Hansen HR, Raab A and Feldmann J (2003). *J. Anal. At. Spectrom.*, **18**, 474-479.

[http 1]

http://seaweed.ucg.ie.

[http 2]

http://botany.ubc.ca/algae.

[http 3]

http://www.nmnh.si.edu/botany/projects/algae/AlgIntro.htm

[http 4]

http://www.epa.gov/safewater/ars/implement.html

[http 5]

http://www.who.int/mediacentre/factsheets/fs210/en

[Hunter *et al.*, 1998]

Hunter DA, Goessler W and Francesconi KA (1998). *Mar. Biol.*, **131**, 543-552.

[Irgolic *et al.*, 1977]

Irgolic KJ, Woolson EA, Stockton RA, Newman RD, Bottino NR, Zingaro RA, Kearney PC, Pyles RA, Maeda S, Mcshane WJ and Cox ER (1977). *Environ. Health Persp.*, **19**, 61-66.

[Ishinishi *et al.*, 1986]

Ishinishi N, Tsuchiya K, Vahter M and Fowler BA (1986). In *Handbook on the Toxicology of Metals, volume II: Specific Metals* (ed. Friberg L, Nordberg GF and Vouk VB), Elsevier, Amsterdam, pp 43-83.

[Jones, 1922]

Jones AJ (1922). *Year book of Pharmacy*, J&A Churchill, London, pp 388-395.

[Kaise *et al.*, 1985]

Kaise T, Watanabe S and Itoh K (1985). *Chemosphere*, **14**, 1327-1332.

[Kaise *et al.*, 1989]

Kaise T, Yamauchi H, Horiguchi Y, Tani T, Watanabe S, Hirayama T and Fukui S (1989). *Appl. Organomet. Chem.*, **3**, 237-277.

[Khokiattiwong *et al.*, 2001]

Khokiattiwong S, Goessler W, Pedersen SN, Cox R and Francesconi KA (2001). *Appl. Organomet. Chem.*, **15**, 481-489.

[Klumpp and Peterson, 1981]

Klumpp DW and Peterson PJ (1981). *Mar. Biol. (Berlin)*, **62**, 297-305.

[Le *et al.*, 1993]

Le XC, Cullen WR and Reimer KJ (1993). *Talanta*, **40**, 185-193.

[Le *et al.*, 1994]

Le XC, Cullen WR and Reimer KJ (1994). *Clin. Chem.*, **40**, 617-624.

[Lunde, 1972]

Lunde G (1972). *Fiskeridir. Skr., Ser. Teknol. Unders.*, **5**, 1-16.

[Lunde, 1973]

Lunde G (1973). *Acta Chem. Scand.*, **27**, 1586-1594.

[Ma and Le, 1998]

Ma M and Le XC (1998). *Clin. Chem.*, **44**, 539-550.

[Mandal and Suzuki, 2002]

Mandal BK and Suzuki KT (2002). *Talanta*, **58**, 201-235.

[Marafante and Vahter, 1984]

Marafante E and Vahter M (1984). *Chem. Biol. Interact.*, **50**, 49-57.

[Morita and Shibata, 1987]

Morita M and Shibata Y (1987). *Anal. Sci.*, **3**, 575-577.

[Morita and Shibata, 1988]

Morita M and Shibata Y (1988). *Chemosphere*, **17**, 1147-1152.

[Morton and Dunnette, 1994]

Morton WE and Dunnette DA (1994). In *Arsenic in the Environment, part II: Human Health and Ecosystem Effects* (ed. Nriagu JO), John Wiley, New York, pp 17-34.

[Norin and Christakopoulos, 1982]

Norin H and Christakopoulos A (1982). *Chemosphere*, **11**, 287-298.

[Nriagu, 2002]

Nriagu JO (2002). In *Environmental Chemistry of Arsenic* (ed. Frankenberger WT Jr.), Marcel Dekker, New York, pp 1-26.

[Sakurai *et al.*, 1997]

Sakurai T, Kaise T, Ochi T, Saitoh T and Matsubaru C (1997). *Toxicology*, **122**, 205-212.

[Sakurai, 2002]

Sakurai T (2002). *Appl. Organomet. Chem.*, **15**, 401-405.

[Shiomi *et al.*, 1987]

Shiomi K, Kakehashi Y, Yamanaka H and Kikuchi T (1987). *Appl. Organomet. Chem.*, **1**, 177-183.

[Vahter *et al.*, 1982]

Vahter M, Marafante E, Lindgren A and Dencker L (1982). *Arch. Toxicol.*, **51**, 65-77.

[Versieck and Vanballenberghe, 1985]

Versieck J and Vanballenberghe (1985). In *Trace elements in Man and Animals, Volume 5* (ed. Mills CF, Bremner I and Chesters JK), Farnham, Commonwealth Agricultural Bureau UK, pp 650-655.

[Yamauchi *et al.*, 1992]

Yamauchi H, Takahashi K, Mashiko M, Saitoh J and Yamamura Y (1992). *Appl. Organomet. Chem.*, **6**, 383-388.

Chapter 4. Analytical techniques

4.1. Production and measurement of radiotracers

4.1.1. Choice and production of a suitable radiotracer for indium

Although a radioisotope exists for almost every element in the periodic table, only a few are suitable for *in vitro* and *in vivo* studies. Firstly, the half-life ($t_{½}$) of the isotope must be adequate for the duration of the experiment. Half-lives of the order of days are preferable. The second prerequisite is that the radiation should be measurable under the experimental conditions. Gamma-emitters are the most suitable because the self-absorption of the radiation is negligible and the samples are easy to prepare. Any liquid or solid form is convenient for measurement with a scintillation or semiconductor detector. The use of carrier-free radioisotopes is very important. Preferably no stable indium isotopes are added as toxic levels can easily be reached. Low-level exposure is more representative for *in vivo* studies [Cornelis, 1992]. In the case of indium, four isotopes have the potential for being used in further research [Firestone, 1996]. They are shown in table 4.1.

Table 4.1. Characteristics of indium radioisotopes.

isotope	$t_{½}$	main γ-rays [keV] & decay probability	production
^{111}In	2.80 d	245.4 (94.5%), 171.3 (90.7%)	^{111}Cd(p,n)^{111}In
^{113m}In	1.658 h	391.7 (100.0%)	^{112}Sn(n,γ)^{113}Sn and ε to ^{113m}In
^{114m}In	49.51 d	190.3 (15.4%), 558.4 (4.4%), 725.2 (4.4%)	^{113}In(n,γ)^{114m}In; ^{114}Cd(p,n)^{114m}In
^{116m}In	54.2 min	1293.6 (84.4%), 1097.3 (56.2%)	^{115}In(n,γ)^{116m}In

Because of the long term *in vivo* experiments that were planned, ^{114m}In with a half-life of 49.51 days was selected. ^{116m}In was used for the optimisation of the ^{114m}In tracer purification procedure.

Using charged particle activation, the production of carrier free radioisotopes is guaranteed. In charged particle activation a nucleus is bombarded with charged particles, thereby inducing a nuclear reaction. Nuclear reactions with charged particles can vary from simple (p,n) reactions to complex (p, ^{3}He2n) reactions, depending on the identity and energy of the charged particles and target nucleus [Vandecasteele, 1988].

The *Q*-value of a nuclear reaction *A*(a,b)B is the energy associated with each reaction event. When *Q* is positive, the reaction is exoergic and energy is released. When *Q* is negative, the reaction is endoergic and the charged particle must exceed a given energy, called the threshold energy E_T. This threshold energy is the minimum energy needed by a projectile to make the reaction energetically possible. When a positively charged particle approaches a nucleus, it is repelled by the electrostatic field. At a 'short' distance (*i.e.*, the sum of the radius of projectile and target nucleus) the strong attractive nuclear forces are more important. At a certain distance both effects will compensate. The loss in kinetic energy caused by this barrier is called the Coulomb energy. If a nuclear reaction is energetically possible, it can take place only if the energy of the incident particle exceeds the Coulomb energy. The loss in kinetic energy necessary to overcome the Coulomb barrier is released again after the nuclear reaction took place.

The probability of a nuclear reaction is expressed by means of the cross section $s(E)$, which has the dimensions of a surface. The barn (10^{-24} cm^2) is often used. The cross section is dependent on the energy of the incident particle; their relation is given in an excitation function. $s(E)$ changes with depth in the sample, as the energy of the projectile changes with depth. The total cross section is the sum of the cross sections of several reactions: (p,n), (p,2n), (p,pn)... The cross section is zero for an energy lower than the threshold energy, very low for an energy lower than the Coulomb barrier, increases with increasing particle energy because the probability for penetration of the Coulomb barrier increases. At increasing energy, the excitation energy is sufficient to allow the emission of 2 neutrons and competition between the (p,n) and (p,2n) occurs, resulting in a decreasing cross section for the (p,n) reaction. The excitation function therefore shows a maximum. The total amount of activity induced by the nuclear reaction is called thick target yield.

On their path through matter, charged particles lose energy mainly by interaction with electrons. This eventually leads to excitation or ionisation of atoms and molecules or to dissociation of molecules. Charged particles have a range: when a mono-energetic beam of charged particles loses energy on its path through matter, the number of particles in the beam does not change, and eventually all the particles are stopped after roughly the same path length. The range *R* is the mean path length for a large number of particles. Because of the large mass of the projectile relative to the electron mass, the fractional loss per collision is small. The stopping power *S(E)* of a material for a particle with energy *E* is a measure of the ability of materials to absorb all the energy of the projectile. The stopping power is inversely proportional to the particle energy.

4.1.2. Neutron activation analysis

[Ehmann and Vance, 1991]

Neutron activation analysis (NAA) is a radiometric method for the determination of trace amounts of elements. By irradiation of stable nuclei with thermal neutrons, *i.e.*, neutrons having an energy of ± 0.0025 eV, (n,γ) reactions are induced, giving rise to an excited intermediate, also called compound nucleus. This nucleus emits prompt gamma rays. The neutrons are provided by a nuclear reactor. Further decay by a, b and/or g-rays of the induced radioisotope offers a suitable means of radiometric detection.

The rate at which radioactive nuclei are formed by neutron bombardment is given by:

$$\frac{dN^*}{dt} = N \cdot s \cdot f - l \cdot N^*$$

with N^* the number of radioactive nuclei, N the number of stable nuclei, s the absorption cross-section for thermal neutrons [barn = 10^{-24}cm^2], f the neutron flux [neutrons.cm^{-2}.s^{-1}] and λ the decay constant (0.693 / $t_{½}$) [s^{-1}]. The total amount of activity produced within the irradiation time t_i is therefore:

$$A_{t_i} = l \cdot N^* = N \cdot s \cdot f \cdot \left(1 - e^{-l t_i}\right)$$

The term between brackets is called the saturation factor *S*. *S* becomes 1 when the irradiation time t_i ® ¥. The activity at a waiting period t_w after irradiation is described by:

$$A_{t_w} = A_{t_i} \cdot e^{-l \cdot t_w} = N \cdot s \cdot f \cdot \left(1 - e^{-l \cdot t_i}\right) \cdot e^{-l \cdot t_w}$$

Accurate quantification can be done by relative calibration. The relation between *N* and *m* can be described as follows:

$$m = \frac{N \cdot A_M}{q \cdot N_A}$$

with *m* the mass [g], A_M the atom mass [g.mol^{-1}], N_A the Avogadro constant [mol^{-1}] and *q* the isotopic abundance (100% = 1). When a standard (*s*) and a sample (*x*) are irradiated and measured simultaneously, the equation

$$m_x / m_s = A_x / A_s$$

holds true. A_x and A_s are the activity of the radioisotope in sample and standard at the start of the measurement [Bq] and m_x and m_s the mass of sample and standard [g]. To eliminate errors due to a different geometrical position of standards and samples, so called flux monitors, *i.e.*, discs of Fe, Al or Au are also irradiated. Relative changes in the induced activity during irradiation in the different discs is a measure of the change in neutron flux and thus for the fluctuations in induced activity of the radioisotope in the different samples and standards (differences among samples in space or time). Most detectors measure only a part of the absolute activity. The detection efficiency is the ratio of the measured activity [counts per seconds] and the absolute activity [Bq]. The measured activity *A* will not be recorded, but rather an amount of counts *C* is registered during a measuring time t_m:

$$C = \int_0^{t_m} A \cdot dt$$

The measured activity A_{tw} at the beginning of the measurement can thus be calculated as:

$$A_{t_w} = \frac{C \cdot l}{\left(1 - e^{-l \cdot t_m}\right)}$$

From the above mentioned equations it can be stated that:

$$m_x = m_s \cdot \frac{C_x \cdot \left(1 - e^{-l \cdot t_{i_s}}\right) \cdot e^{-l \cdot t_{w_s}} \cdot \left(1 - e^{-l \cdot t_{m_s}}\right) \cdot f_s}{C_s \cdot \left(1 - e^{-l \cdot t_{i_x}}\right) \cdot e^{-l \cdot t_{w_x}} \cdot \left(1 - e^{-l \cdot t_{m_x}}\right) \cdot f_x}$$

with f_s/f_x the neutron flux ratio for standard to sample, that can be gauged form the measurement of the induced radioactivity in de flux monitors.

4.1.3. Gamma-ray spectrometry

[Ehmann and Vance, 1991]

The activity can be measured with different instruments depending on the type of irradiation emitted. Gamma-ray detection depends on the transfer of the g-ray energy to electrons within the detector material. Depending on the energy loss, the interaction is attributed to photoelectric absorption (PE), Compton scattering (CS) or pair production (PP). Depending on the size and geometry of the detector, a characteristic spectrum can be obtained for each radioactive nuclide. The bigger the detector the more efficient is the interaction of the gamma rays and the more gamma ray energy is recovered within the full energy peak. For a small detector the contribution of Compton scattering is more outspoken and single and double escape peaks (in case of pair production) can be seen. Both a NaI(Tl) scintillation detector and a Ge(Li) semiconductor detector were used.

Scintillation detectors are based on the emission of light induced by incoming radiation. The incoming radiation interacts with the scintillation material by PE, CS and PP, producing ionisation and excitation. The excited electrons undergo de-excitation by emission of light photons. This light is directed towards a photomultiplier tube (PMT), which converts the light into an electrical signal. The scintillation material should be optically transparent at the wavelength of light generated and light emission should be fast. The most widely used gamma-ray detectors are alkali halide crystal such as NaI. These crystals have a structure of valence and conduction bands. Absorption of energy from incident radiation can excite an electron from the valence band into the conduction band. As the excited electrons return to their ground state, they emit photons. In a pure NaI crystal the energy gap between valence and conduction band is very large, so that electron transitions are not

highly probable. If electron transitions do occur, the emitted photons have an energy that is too high for efficient amplification in a PMT. By doping the crystal with an impurity (*e.g.*, Tl) new energy levels are created within the band gap. Electron transitions to these new levels do not require as much energy, so that they are more likely to occur and the emitted light will be primarily in the UV or visible region where the PMT has a higher efficiency.

Semiconductor detectors are usually made of Ge or Si. A similar band structure as in a NaI crystal exists here too. However, the band gap is much smaller so that the passage of radiation may inject enough energy to raise an electron from the valence band to the conduction band, creating an electron-hole pair. Under normal circumstances the excited electrons in the conduction band might be expected to eventually de-excite and return to the valence band. In the presence of an applied electric field they will instead migrate and can produce an electric signal. The number of electron-hole pairs is directly proportional to the gamma-ray energy absorbed. Impurities in the crystal such as B or Ga produce p-type or acceptor-type Ge. As and P will cause an n-type or donor-type semiconductor. When a p-type and n-type semiconductor are brought into contact, forming a p-n junction, the semiconductor can be used as a radiation detector. In the immediate vicinity of the p-n junction electrons will migrate toward the p-zone and holes toward the n-zone. This will create an area where there are neither excess holes nor excess electrons. This depletion region resists the passage of electric current. When a reverse bias is applied to the p-n junction, the depletion region is increased because of the movement of electrons and holes away from the junction in the n-type and p-type semiconductor, respectively. In practice all Ge and Si detectors turn out to be p-type. When the purity of Ge is questioned, it is often doped with lithium. The lithium atoms act as n-type and cancel the p-type acceptor impurities, which are found in excess in Ge. A compensated region is formed which acts identical to a depletion region. Because of the high mobility of Li in the crystal, the detector must be cooled at all times. Nowadays Ge(Li) detectors are largely replaced by intrinsic Ge detectors. These Ge detectors without Li are sufficiently pure to approach the properties of the theoretical true intrinsic semiconductor material. Intrinsic Ge detectors are similar to Ge(Li) detectors in their efficiency and resolution characteristics, but are in some case even better. Another advantage is that no cooling is required when they are not in use. The intrinsic Ge detector has not been used throughout this work.

The biggest disadvantage of NaI(Tl) crystals is their poor energy resolution in comparison to Ge(Li) detectors (NaI(Tl): 6% for the 662 keV γ-ray of ^{137}Cs, Ge(Li): 0.1% for the 1332

keV γ-ray of ^{60}Co). On the other hand scintillation detectors offer a superior detection efficiency. When a mixture of different isotopes (*e.g.*, after NAA) is measured or in case of a high dose rate, a Ge(Li) detector was used. In the case of *in vitro* and *in vivo* incubation experiments with pure tracer, detection was mostly realised with a NaI(Tl) detector.

4.2. Liquid chromatography

4.2.1. Principle

[Meyer, 1998]

Liquid chromatography involves a sample being dissolved in a liquid mobile phase. The mobile phase is then forced through an immobile, immiscible stationary phase. The phases are chosen such that components of the sample have different selectivity for each phase. A component, which shows a higher affinity for the stationary phase, will take longer to travel through it than a component that does not. As a result of these differences in mobility, sample components will become separated from each other as they travel through the stationary phase. The sample is transported through the column by continuous addition of mobile phase.

The distribution of analytes between phases can often be described quite simply. An analyte is in equilibrium between the two phases. An equilibrium constant K_D termed the distribution coefficient, is defined as the molar concentration of analyte in the stationary phase divided by the molar concentration of the analyte in the mobile phase. Phase preference can also be expressed by the retention factor *k*.

$$K_D = \frac{c_S}{c_M} \qquad \text{and} \qquad k = \frac{n_S}{n_M} = \frac{c_S \cdot V_S}{c_M \cdot V_M} = K_D \cdot \frac{V_S}{V_M}$$

with c_S and n_S the molar concentration and number of moles of an analyte in the stationary phase, respectively, V_S the volume of the stationary phase, c_M and n_M the molar concentration and number of moles of an analyte in the mobile phase, respectively, and V_M the volume of the mobile phase.

The time between sample injection and an analyte peak reaching a detector at the end of the column is called the *retention time* (t_R). Each analyte in a sample will have a different retention time. The linear velocity of the mobile phase u_M flowing through a column of length L can be calculated as

$$u_M = \frac{L}{t_M}$$

with t_M the time taken for the mobile phase or a non-retained compound to pass through the column. The retention time is function of mobile phase flow velocity and column length. If the mobile phase is moving slowly or if the column is long, then t_M and t_R are both large. Therefore retention time is not suitable for characterising a compound. Instead the retention factor k is preferred, which is also defined as

$$k = \frac{t_R - t_M}{t_M}$$

k is independent of the column length and mobile phase flow rate and represents the molar ratio of the compound in the stationary and the mobile phase, as mentioned earlier. Two components A and B in a mixture cannot be separated unless they have different k values, the means of assessment being provided by the *selectivity factor*, α. α is the ratio of the k values of two compounds.

To obtain optimal separations, sharp, narrow, symmetrical chromatographic peaks must be obtained. This means that band broadening must be limited. Band broadening is defined by the column efficiency. A theoretical model is therefore proposed. The plate model supposes that the chromatographic column contains a large number of separate layers (theoretical plates). Separate equilibrations of the sample between the stationary and mobile phase occur in these plates. The analyte moves down the column by transfer of equilibrated mobile phase from one plate to the next. The efficiency of a certain column can then be described by either the number of theoretical plates N in a column, or by stating the plate height or the *Height Equivalent to a Theoretical Plate* (*HETP*).

$$HETP = H = \frac{L}{N} = \frac{s^2}{L}$$

with *L* the length of the column. Because of the Gaussian character of a chromatographic peak, it is possible to express the column efficiency in terms of the variance s^2 per unit of column length. The variance is the sum of all peak-broadening factors, originating from the column and extra column contributions. The number of theoretical plates that a real column possesses can be found experimentally by examining a chromatographic peak after elution:

$$N = \frac{L}{H} = \frac{L^2}{s^2} = \frac{t_R^2}{s_t^2} = 5.54 \frac{t_R^2}{w_{1/2}^2}$$

where $w_{1/2}$ is the peak width at half-height (see figure 4.1). A non-gaussian peak can show tailing or fronting. The tailing factor is defined as the ratio of b to a in figure 4.1. Fronting is the opposite. The factors a and b are measured at 10% of the peak height.

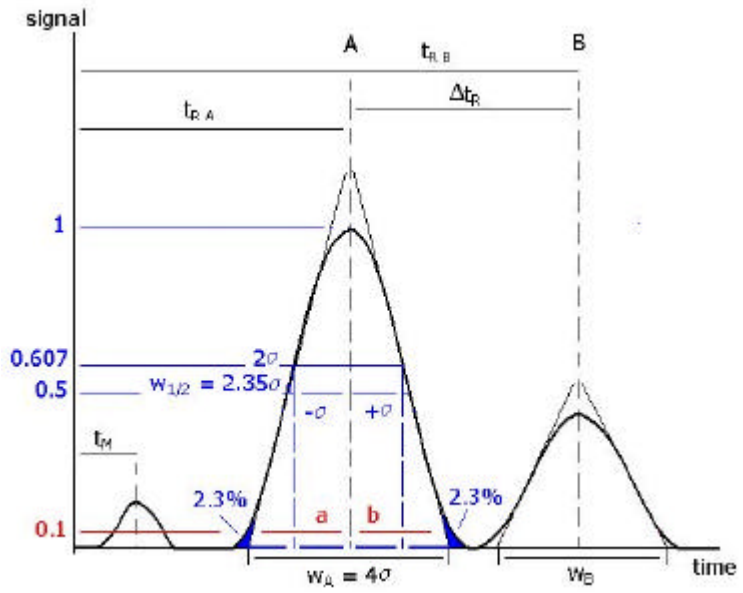

Figure 4.1. Characteristic features of a chromatographic peak.

There are many reasons for band broadening during a chromatographic elution. Different processes contribute to the overall column variance s^2.

A-term. The mobile phase moves through the column that is packed with stationary phase. Solute molecules will take different paths through the stationary phase at random. This will cause broadening of the solute band, because different paths are of different lengths. The mobile phase passes in a laminar flow between the stationary phase particles. The flow is

faster in the centre than it is near a particle. This leads to band broadening as well. Packing the column with evenly sized particles may reduce Eddy diffusion and flow distribution. The broadening due to Eddy diffusion and flow distribution is little affected, if at all, by the mobile phase flow velocity.

B-term. Sample molecules spread out in the solvent without any external influence. This longitudinal diffusion has a disadvantageous effect on column efficiency. If the velocity of the mobile phase is high then the analyte spends less time on the column, which decreases the effects of longitudinal diffusion.

C-term. The analyte takes a certain amount of time to equilibrate between the stationary and mobile phase. If the velocity of the mobile phase is high, and the analyte has a strong affinity for the stationary phase, then the analyte in the mobile phase will move ahead of the analyte in the stationary phase. Slow interactions at the surface will hold back the molecules more than expected from the distribution constant. Non-uniform stationary phase particles cause the analytes to traverse different distances before they reach the contact surface. The deeper the pores of the particles (size exclusion chromatography), or the thickness of the stationary phase (ion exchange, reversed phase) the longer the migration time and the greater the spreading will be. The higher the velocity of the mobile phase, the worse the broadening becomes.

The contribution of these factors leads to the overall column variance. This column efficiency is described by the Van Deemter equation:

$$H = 2\,l\,d_p + \frac{2\,l\,D_M}{u} + \left[w \cdot \frac{d_p^2}{D_M} + \frac{k}{(1+k)^2} \cdot \frac{d_f^2}{D_S} \right] \cdot u = A + \frac{B}{u} + C \cdot u$$

with l and w packing factors, d_p the particle size, D_M and D_S the diffusion coefficient of the analyte in the mobile and stationary phase respectively and d_f is the diffusion distance in the stationary phase. A plot of plate height versus linear velocity of mobile phase, which is called a Van Deemter plot, is of considerable use in determining the optimum mobile phase flow rate.

A measure of how well species have been separated is provided by measurement of the resolution. The resolution of two species, A and B, is defined as

$$R = 2 \cdot \frac{[(t_R)_B - (t_R)_A]}{w_A + w_B}$$

Baseline resolution is achieved when R = 1.5 It is useful to relate the resolution to the number of plates in the column, the selectivity factor and the retention factors of the two solutes

$$R = \frac{\sqrt{N}}{4} \cdot \frac{(a-1)}{a} \cdot \frac{1+k_B}{\bar{k}}$$

with $\bar{k}$ the average retention factor of compounds A and B.

To obtain high resolution, the three terms must be maximised. An increase in *N* by lengthening the column leads to an increase in retention time and increased band broadening - which may not be desirable. Instead, to increase the number of plates, the *HETP* can be reduced by reducing the size of the stationary phase particles. It is often found that by controlling the capacity factor, separations can be greatly improved. This can be achieved by changing the composition of the mobile phase. Gradient elution is an efficient way of doing so. The selectivity factor a can also be manipulated to improve separations. When a is close to unity, optimising *k* and increasing *N* is not sufficient to give good separation in a reasonable time. In these cases, *k* and a are increased by changing mobile or stationary phase composition or the column temperature.

4.2.2. Chromatography in practice

[Amersham Pharmacia, 1987; 1998; 1999; 2001]

Different kinds of chromatographic separation modes have been used throughout this work. Size exclusion chromatography (SEC) was applied for the separation of indium bound to proteins and low molecular mass compounds in serum, packed cell lysate, urine and the cytosolic fraction of liver, kidney and spleen cells. Reverse phase chromatography (RPC) was utilised for the separation of creatinine in urine. Anion (AEC) and cation (CEC)

exchange chromatography were used extensively for the separation of indium compounds in serum and for the separation of arsenic species in marine sample extracts, serum, urine and other kinds of samples. Affinity chromatography (AC) has been used to study the binding of indium to albumin. AEC, CEC, RPC and AC are based on the adsorption of analytes on the stationary phase according to a chemical interaction. In SEC a simple molecule size classification process forms the basis of the separation.

Reverse phase chromatography is the term used to describe the state in which the stationary phase is less polar than the mobile phase. Chemically bonded octadecylsilane (ODS), an *n*-alkane with 18 carbon atoms, is the most frequently used stationary phase. The less water-soluble the sample compounds are, the better they are retained by the stationary phase. Also the retention time increases as the number of carbon atoms increases. The mobile phase generally consists of mixtures of water or aqueous buffer solution with various water-miscible solvents such as methanol and acetonitrile. Separation in RPC is due to the different binding properties of the solutes present in the sample as a result of the differences in their hydrophobic properties.

In ion exchange chromatography, the stationary phase has electric charges on its surface. Ionic groups such as HSO_3^-, COO^-, NH_3^+, NR_3^+ are incorporated in the resin or gel of the stationary phase. These charges are neutralised by mobile counter ions. The ions in the mobile phase and ionic sample molecules compete for a place on the surface on the stationary phase. Strong anion and cation exchange refer to the fact that the functional group is charged over the whole pH range. Sulphonic and quaternary amine groups are strong cation and anion exchangers respectively. Carboxy and tertiary amine groups can be categorised as weak. Type, pH and concentration of the mobile phase determine the elution behaviour of analytes.

Affinity chromatography is the most specific chromatographic method. The interaction is biochemical in nature, *e.g.*, antigen $\leftrightarrow$ antibody, enzyme $\leftrightarrow$ inhibitor or hormone $\leftrightarrow$ carrier. The highly specific nature of these interactions is due to the fact that the two participating compounds are ideally suited to each other spatially and electrostatically. One component (ligand) is bound to a support and the other (sample) is adsorbed from solution, the process being reversible.

Size exclusion chromatography is based on the sieving effect of the stationary phase, which consists of inert porous particles of a well-defined size. The pores of the gel are comparable in size to the molecules that are to be separated. In theory the elution will be in the order of large to small molecular masses. Molecules larger than the largest pores are completely excluded from the stationary phase and will have a retention volume V_R that is identical to the void volume V_0 (*i.e.*, the volume of the mobile phase outside the particles). Small molecules are delayed in their passage through the column compared with the large molecules. Molecules smaller than the smallest pores on the other hand are completely accessible for the stationary phase

$$V_R = V_S + V_0$$

With V_S the volume of the stationary phase particles. The diffusion of intermediary sized molecules can be described by the distribution coefficient K_D

$$V_R = K_D \cdot V_S + V_0 \qquad \text{or} \qquad K_D = \frac{V_R - V_0}{V_S}$$

Residual charges on the particles can lead to ionic interactions with the analytes in solution and hence a non-ideal elution is obtained. As a consequence some molecules have a retention time, which is different from that obtained from the distribution coefficient. Because V_S is difficult to calculate, the equilibrium can be described by K_{SEC}

$$K_{SEC} = \frac{V_R - V_0}{V_t - V_0}$$

with V_t the sum of the volume of stationary phase and stagnant mobile phase, *i.e.*, the mobile phase within the pores of the particles.

Depending on the type of samples analysed we can distinguish between High Performance Liquid Chromatography (HPLC) and Fast Protein Liquid Chromatography (FPLC). FPLC is a commercial name, which involves the separation of biological macromolecules such as proteins. Special stationary phases have been developed to allow the separation of these biomolecules with good resolution, recovery and selectivity.

Different HPLC systems were used throughout this work. In combination with ICP-MS an Alltech Model 526 (Alltech, Deerfield, USA) metal free isocratic HPLC pump fitted with a 6-port valve and injection loop (Rheodyne, Cotata, USA) was used. For ES-MS/MS and/or UV-HG-AFS measurements an Alliance 2690 HPLC system (Waters, Milford, USA) with quaternary pump, built-in on-line vacuum degassing unit, cooled autosampler and thermostated column compartment was used. For FPLC separations an Äkta Purifier 10 (Amersham Biosciences, Uppsala, Sweden) integrated system with binary pump, pH and conductivity monitor, variable wavelength UV monitor and fraction collector was used. This unit was also used for the preparative HPLC separations of the urine samples (see chapter 8). Urinary creatinine was determined by reversed phase HPLC with UV detection on a Waters 600 pump and a Waters 486 UV detector (Waters, Milford, USA).

4.3. Mass spectrometry

Mass spectrometry is an instrumental approach that allows the mass measurement of atoms and molecules. The basic parts of any mass spectrometer are a sample introduction device, an ionisation source, a mass analyser, a vacuum system and an ion detector. A mass spectrometer determines the atomic or molecular mass by ionising, separating, and measuring atomic or molecular ions according to their mass-to-charge ratio (*m/z*). Positive ions are generated in the ionisation source by inducing either a loss of an electron, or addition of a proton or an ionic adduct. Negative ions can be generated by loss of a proton. Once the ions are formed in the gas phase they can be electrostatically directed into a mass analyser, separated according to *m/z* and finally detected. Two techniques with a different ionisation source that allow detection of either atoms or molecules have been used: inductively coupled plasma for elemental analysis and electrospray for molecular analysis.

4.3.1. Electrospray mass spectrometry

[Blades *et al.*, 1991; Kebarle and Tang, 1993; Kebarle and Ho, 1997; Kebarle and Peschke, 2000; Gaskell, 1997; Watson, 1997]

Electrospray mass spectrometry (ES-MS) provides molecular and structural information about an analyte. By applying a strong electrical charge to the eluent as it emerges from a nebuliser, an aerosol of charged droplets is produced. Solvent evaporation reduces the size

of the droplets until a sufficient charge density makes the ejection of sample ions from the surface of the droplets possible. Characteristically, ions are singly or multiply charged and the mass analyser sorts them by mass-to-charge (*m/z*) ratio. ES-MS allows rapid, accurate and sensitive analysis of a wide range of analytes from low molecular mass (less than 200 Da) polar compounds to biopolymers larger than 100 kDa. Generally, compounds less than 1 kDa produce singly charged positive or negative ions. High mass biopolymers, for example peptides, proteins and oligonucleotides, produce a series of multiply charged ions. The acquired data can be transformed by the data system to give a molecular mass profile of the biopolymer.

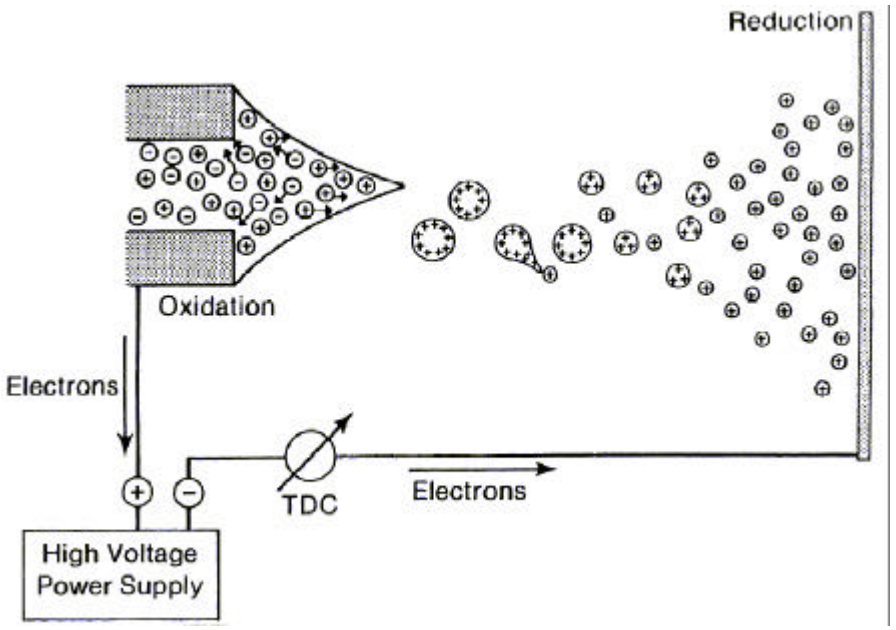

Figure 4.2. Schematic representation of the major processes occurring in the source.

Liquid containing the analyte of interest is pumped through a metal capillary, which is surrounded by a nitrogen flow. The tip of this capillary is connected to a voltage supply (around 3 kV). The end of the tip faces a counter-electrode plate held at 0 V. The electric field, when turned on, will penetrate the solution at the capillary tip and the positive and negative electrolyte ions in the solution will move under the influence of the field until a charge distribution results which counteracts the imposed field and leads to essentially field free conditions inside the solution. When the capillary is the positive electrode (in positive ion mode), positive ions will have drifted downfield in the solution, *i.e.*, towards the meniscus of the liquid. Negative ions will have drifted away from the surface. The repulsion between the positive ions on the surface overcomes the surface tension of the liquid and the surface begins to expand allowing the positive charges and liquid to move downfield. A

cone forms, the Taylor cone, and if the applied field is sufficiently high, a fine jet emerges from the cone tip which breaks up into small charged droplets (figure 4.2).

The droplets are positively charged due to the excess of positive electrolyte ions on the surface of the liquid cone and the cone jet. The charged droplets drift downfield through the air towards the counter electrode. Solvent evaporation at constant charge leads to droplet shrinkage and an increase in the electric field normal to the surface of the droplets. This solvent evaporation is controlled by a gas flow, by heating or a combination of both. At some given radius R and charge q, the force due to the repulsion of the surface charges becomes equal to the surface tension force of the liquid. This condition is expressed by Rayleigh's stability limit q_{Ry}:

$$q_{Ry} = 8\pi(\varepsilon_0 \gamma R_{Ry}^3)^{1/2}$$

where ε_0 is the permitivity of vacuum and γ is the surface tension of the solvent. Further evaporation leading to a decrease in the radius below the Rayleigh value results in droplet fission. A schematic representation of the development of the droplet fission and evaporation is shown in figure 4.3.

A sequence of repeated droplet fission and evaporation leads ultimately to gas phase ions. Two alternative models have been described: the Charged Residue Model (CRM) and the Ion Evaporation Model (IEM). Both theories assume that gas phase ions are formed only from very small droplets. The CRM proposes that gas phase ions result from the evaporation of solvent from very small droplets, which contain only one analyte molecule and one ion. Such droplets are assumed to have been formed by a succession of Rayleigh desintegrations. The type of droplets needed, can be found in the second generation of offspring droplets, leading to sizes with R < 3 nm (see bottom right in figure 4.3). The IEM theory assumes that gas phase ions solvated by several solvent molecules can be emitted into the gas phase from charged droplets which are much larger (R = 10 nm) and which carry some hundreds of charges. Such droplets can be found in the first offspring droplets. Ion evaporation from such droplets is predicted to be faster than the Rayleigh fission of the droplet.

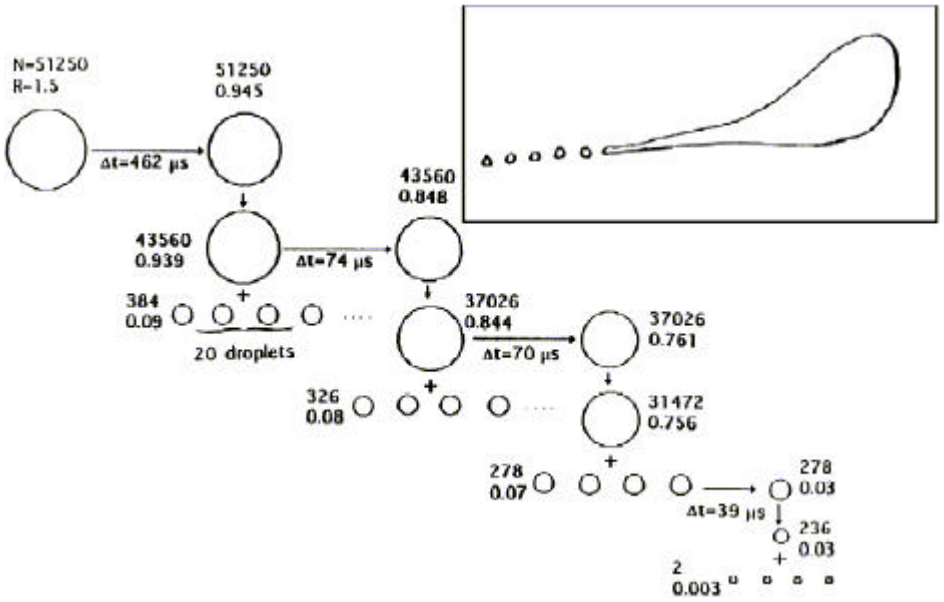

Figure 4.3. Schematic representation of droplet fission and evaporation. *N* is the number of elementary charges on the droplet, *R* is the radius (μm).

Most of the ions produced by electrospray tend to be very similar to those formed by straightforward chemical ionisation with a lot of protonated ($[M+H]^+$) or cationated ($[M+Na]^+$, $[M+NH_4]^+$) positive ions, or negative ions lacking a hydrogen ($[M-H]^-$). Briefly, chemical ionisation works by collision between sample molecules and specially produced reagent gas ions such that ions are formed from sample molecules by various processes, one of the most important of which is the transfer of a proton.

It is assumed that the charging of the unipolar droplet spray is due to electrophoretic charging, *i.e.*, the separation of positive from negative electrolyte ions present in the solution. Thus at a steady operation of the ES, positive droplet emission will continuously carry off positive ions (in positive ion mode). The requirement for charge balance in such a continuous-electric-current device, together with the fact that only electrons can flow through the metal wire supplying the electric potential to the electrodes, leads to the supposition that the ES process must include an electrochemical conversion of ions to electrons. In this sense the electrospray source can be regarded as a special type of electrolytic cell. It is special because the ion transport does not solely occur through an uninterrupted solution, but also through the gas phase, where unipolar charged droplets and gas-phase ions are the charge carriers. A conventional electrochemical oxidation reaction should be occurring at the positive electrode, which either converts atoms from the capillary metal M to positive ions in solution (1) or which removes negative ions present

in the solution (2, 3). The net effect of the oxidation reaction at the capillary tip is the creation of an excess of positive ions over negative ions in the solution. In this regard, reaction 4 could also be a process producing positive ions. All reactions result in the formation of electrons that will be used for the reduction reactions at the counter electrode.

$M\ (s) \rightarrow M^{n+}\ (aq) + ne^-$	$E°_{red}$ = -0.76 (Zn^{2+}/Zn)	(1)
$4OH^-\ (aq) \rightarrow O_2\ (g) + 2H_2O + 4e^-$	$E°_{red}$ = 0.40	(2)
$2Cl^-\ (aq) \rightarrow Cl_2\ (g) + 2e^-$	$E°_{red}$ = 1.36	(3)
$2H_2O \rightarrow O_2\ (g) + 4H^+\ (aq) + 4e^-$	$E°_{red}$ = 0.68	(4)

When a Zn or stainless steel capillary tip was used, release of Zn^{2+} and Fe^{2+}, respectively to the solution could be detected. Furthermore, the amount of Zn^{2+} and Fe^{2+} released to the solution per unit time when converted to coulombs per second was found to be equal to the measured electrospray current.

The ES interface consists of a Z-spray source fitted with an electrospray probe [Micromass 1; Micromass 2]. Mobile phase from an HPLC column or infusion pump enters through the probe and is pneumatically converted to an electrostatically charged aerosol spray. At very low flow rate (a few μL/min), the difference in potential is sufficient to create the spray. At higher flow rate, a nebuliser gas (nitrogen) is necessary to maintain a stable spray. Efficient solvent evaporation is provided by a heated nitrogen flow close to the probe (desolvation gas) and by the cone (cone gas). The source block is also heated, for final desolvation. The resulting analyte and solvent ions are drawn through the sample cone aperture into the ion block, from where they are then extracted into the analyser. A schematic representation is shown in figure 4.4. In the first stage the Z-spray source the spray is directed perpendicularly past the sampling cone, which is displaced from the central axis of the instrument. Ions are extracted orthogonally from the spray into the sampling cone aperture leaving large droplets, involatile materials, particulates and other unwanted components behind. The second orthogonal step enables the volume of gas (and ions) sampled from the atmosphere to be increased. Gas at atmospheric pressure sampled through an aperture into a partial vacuum forms a freely expanding jet, which represents a region of high pressure compared to the surrounding vacuum. If this jet is directed on-axis into the second aperture of the interface it increases the flow of gas through the second aperture. Maintaining a suitable vacuum in the MS analyser therefore places a restriction on the maximum diameter of the aperture. However, if the jet passes orthogonal to the second

aperture the flow into it is significantly decreased. Consequently in the Z-spray interface the diameter of the sampling cone aperture may be increased to allow more gas (and ions) to be sampled from the atmospheric spray without degrading the analyser vacuum or increasing the pumping speed of the system. Ions in the partial vacuum of the ion block are extracted electrostatically into the hexapole ion bridge, which efficiently transports ions to the analyser. Additionally background or 'neutral' noise is significantly reduced by orthogonal sampling.

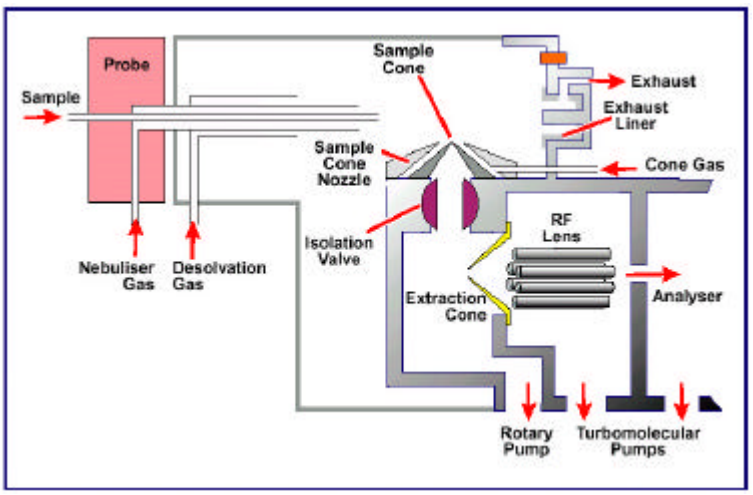

Figure 4.4. Schematic representation of electrospray probe and ion source block.

A 50:50 mixture of acetonitrile or methanol and water is a suitable mobile phase for the syringe pump system. This is appropriate for positive and negative ion operation. Positive ion operation may be enhanced by 0.1 to 1% formic acid in the sample solution. Negative ion operation may be enhanced by 0.1 to 1% ammonia in the sample solution. Although the electrospray can accommodate flow rates up to 1 mL/min, it is recommended that the flow is split post-column to approximately 200 µL/min. Also even at lower flow rates, a split may be required for saving valuable samples. The post-column split consists of a zero dead-volume tee piece. The mass spectrometer in itself is a mass-flow sensitive detector, which means that the response is directly proportional to the mass-flow (change of mass per unit of time). However, when an electrospray source is coupled to the MS, it often behaves more like a concentration sensitive detection technique due to the opposing effects of increased mass-flow and reduced droplet charging at higher flow rates. Once the ions have been produced, they need to be separated according to the masses to be determined. For this purpose electrospray can be coupled to a wide range of mass analysers including quadrupole, time-of-flight, quadrupole ion-trap, Fourier transform ion

cyclotron resonance and magnetic-sector or a combination of the above mentioned instruments. The instrument used throughout this study consists of a triple quadrupole mass spectrometer (figure 4.5).

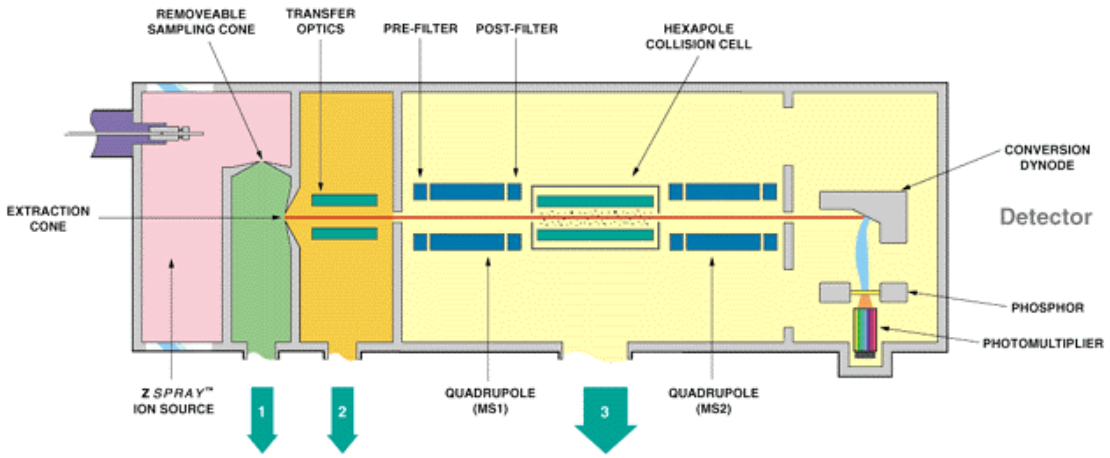

Figure 4.5. Schematic representation of a triple quadrupole mass spectrometer.

The triple quadrupole mass spectrometer is a tandem arrangement, in which the first (Q_1) and third (Q_2) quadrupoles are mass selective, whereas the second quadrupole (q) operating in RF-only mode serves as an ion guide in a collision cell. The collision cell, which in fact is a hexapole, is a small chamber mounted in the ion path of the mass spectrometer. It has two small openings, one to let the precursor ion *i.e.*, any ion selected for analysis by collision activated dissociation (CAD) in and the second to let the product ions out. The chamber can be pressurised with a collision gas that collides with the precursor ions, thereby activating their decomposition or fragmentation into product ions. Triple quadrupole mass spectrometry allows the use of several single MS and MS/MS scan and static analysing modes. In the full scan mode, in which Q_1 is used as the mass filter, the instrument detects signals over a mass range during a short period of time. In single ion recording mode (SIR), the first quadrupole is set to only monitor a few known *m/z* ratios. As a result the quadrupole is able to spend more time sampling each of the *m/z* values, with a concomitant and large increase in sensitivity. The product ion scan is the most used MS/MS scan mode. Precursor ions are selected in Q_1 for CAD in the collision cell. The resulting fragments can be scanned using Q_2. It is used for structural elucidation and for method development studies. Precursor ion scanning is the reverse of product ion scanning. Q_1 scans the precursor ions of the CAD products ions that are selected by Q_2. Precursor ion scanning provides complementary or confirmatory information for production

ion scan data. Neutral loss scanning is interesting when the mass of a certain CAD is known (*e.g.*, in sugar analysis). The scans of Q_1 and Q_2 are synchronised, *i.e.*, both quadrupoles scan at a certain *m/z* difference. Multiple reaction monitoring (MRM) is the MS/MS equivalent of SIR. Q_1 and Q_2 are fixed on a precursor and product ion respectively. As both quadrupoles are static, this allows a greater dwell time on the ions of interest and therefore a better sensitivity (~100x) compared to scanning MS/MS. Moreover as only one *m/z* ratio is allowed to pass each quadrupole, the noise is very low, resulting in a better signal to noise. An overview of all MS and MS/MS modes is given in table 4.2. A Quattro Micro triple quadrupole mass spectrometer (Micromass, Manchester, UK) with Z-spray dual orthogonal electrospray source and hexapole collision cell was used in this work.

Table 4.2. Overview of MS and MS/MS modes.

<table>
<tr><th>analysis mode</th><th>Q_1</th><th>q</th><th>Q_2</th></tr>
<tr><td>full scanning</td><td>scanning</td><td colspan="2">RF only (pass all masses)</td></tr>
<tr><td>selected ion recording</td><td>static</td><td colspan="2">RF only (pass all masses)</td></tr>
<tr><td>product ion scanning</td><td>static
(precursor mass selection)</td><td rowspan="4">RF only (pass all masses)</td><td>scanning</td></tr>
<tr><td>precursor ion scanning</td><td>scanning</td><td>static
(product mass selection)</td></tr>
<tr><td>multiple reaction monitoring</td><td>static
(precursor mass selection)</td><td>static
(product mass selection)</td></tr>
<tr><td>constant neutral loss scanning</td><td>scanning
(synchronised with Q_2)</td><td>scanning
(synchronised with Q_1)</td></tr>
</table>

4.3.2. Inductively coupled plasma mass spectrometry

[Ebdon *et al.*, 1998a; Montaser *et al.*, 1998; Vandecasteele and Block, 1993a]

Inductively coupled plasma mass spectrometry (ICP-MS) allows elemental analysis with excellent sensitivity and high sample throughput. The ICP-MS instrument employs a plasma as the ionisation source and a mass spectrometer analyser to detect the ions. It can measure most elements in the periodic table within the same run and determine analyte concentration down to the sub ng/L level.

Liquid supplied via a peristaltic pump (total analysis) or via a column effluent (speciation analysis) is introduced into a pneumatic nebuliser where it is converted into the sample aerosol. A spray chamber ensures that only the smallest droplets (diameter <10 μm) are introduced into the plasma. The plasma is formed in a stream of argon gas flowing through an assembly of three concentric quartz tubes, known as the plasma torch. The torch is encircled at the top by a water-cooled induction coil, connected to an RF generator. The magnetic field generated by the RF current through the coil induces a current in the argon gas stream. A plasma is formed almost instantaneously when the argon gas is seeded with electrons. These electrons are produced by a high voltage Tesla discharge. Once in the ICP, the aerosol droplets are desolvated, the molecules are atomised and the atoms thus formed are ionised by the high temperature of the plasma (6000-10000 K). If an electron acquires sufficient energy, equal to the first ionisation energy of the element, it escapes from the influence of the attraction of the atomic nucleus and an ion is formed. The major mechanism by which this ionisation occurs are electron impact ($M + e^- \rightarrow M^+ + 2e^-$) and Penning ionisation ($M + Ar^* \rightarrow M^+ + Ar + e^-$). The degree of ionisation of an element can be estimated from the Saha equation (for a system in thermal equilibrium):

$$\frac{n_i n_e}{n_a} = 2\frac{Z_i}{Z_a}\left(2\pi mk\frac{T}{h^2}\right)^{3/2} exp(-E_i/kT)$$

where n_i and n_e are the number densities of the ions and free electrons, respectively, n_a is the number density of the atoms, Z_i and Z_a are the ionic and atomic partition functions, respectively, m the electron mass, k the Boltzmann constant, T the temperature, h Planck's constant and E_i is the first ionisation energy. The degree of ionisation is dependent on the electron number density, the temperature and the ionisation energy of the element in question. Taking the average electron number for an argon ICP to be 10^{15} cm^{-3} and the ionisation temperature to be 7500 K, then the degree of ionisation for arsenic is about 52% [Houk, 1986]. This is much lower than the >90% efficiency, which is obtained for most metals in the periodic table. The reason for the low ionisation efficiency is the high first ionisation energy of arsenic: 947 kJ/mol. However, addition of carbon in the plasma enhances the signal intensity for arsenic, because of an alternative chemical ionisation mechanism:

$$C^+ + As \rightarrow As^{+*} + C$$

It is suggested that the introduction of carbon-containing components into the central part of the plasma via the sample aerosol leads to a strongly increased population of C^+ (1^{st} E_i = 1086 kJ/mol) and/or carbon-containing polyatomic ions. In order for the proposed reaction to take place, the first ionisation energy of carbon must be close to the energy of excited arsenic ions. The energy to generate excited As^+ ions, which corresponds to an electron shift between the ground state of $4p^2\ ^3P$ and $4p^2\ ^1D$, requires an energy of 1062 kJ/mol. This is very close to the 1^{st} E_i of carbon [Abou-Shakra *et al.*, 1997]. Larsen and Stürup [1994] found that the combined use of a high RF power and the addition of 3% methanol to the analyte solution (total analysis) or the elution buffer (speciation analysis) gives rise to a more than two-fold increase of the arsenic signal intensity.

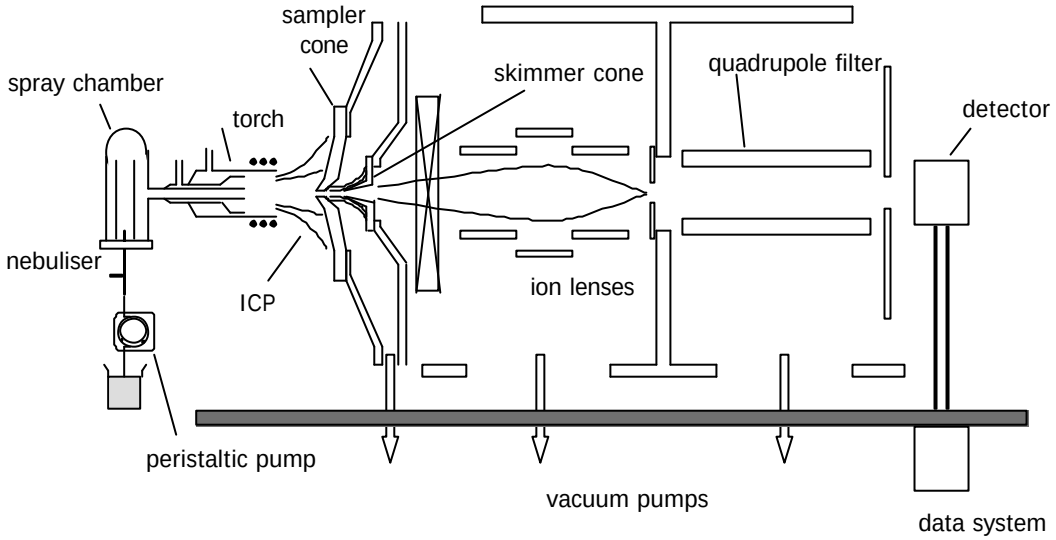

Figure 4.6. Schematic representation of an ICP-MS instrument.

Since the ICP operates at atmospheric pressure and since for its operation the mass spectrometer generally requires a vacuum better the 10^{-5} mbar, the ions must be extracted into a vacuum system. This is accomplished by making use of a series of differentially pumped vacuum chambers held at consecutively lower pressures. The ICP is aligned so that the central channel is on-axis with the tip of a water-cooled sampling cone, which has an orifice of approximately 1 mm in diameter. The pressure behind the sampling cone is about 1 mbar. As a result the plasma gases containing the analyte ions are extracted into the first chamber and expand. This supersonic expansion takes the form of a cone with a shock-wave structure at its base, called a Mach disc. The region within the expansion cone is called the 'zone of silence'. The 0.7 mm orifice of a second cone (skimmer cone) is

placed within this zone. The ions pass through the skimmer cone orifice into a second intermediate vacuum chamber held at $<10^{-4}$ mbar. The analyte ions are then focused by a series of ion lenses into a quadrupole mass analyser, which separates the ions according to their *m/z* ratio. Finally, the ions are detected using an electron multiplier. A schematic overview of an ICP-MS instrument is shown in figure 4.6. The ICP-MS instruments used in this work were an Elan 5000 (Ghent) or an Elan 6000 (Beijing, China) from Perkin-Elmer Sciex (Concord, Canada). For both systems, the sample introduction system consists of a cross flow nebuliser and a Ryton Scott-type double-pass spray chamber.

4.3.3. Quadrupole mass spectrometry

[De Hoffmann *et al.*, 1996; Watson, 1997]

In inductively coupled plasma mass spectrometry and electrospray mass spectrometry, the mass analyser consists of one and three quadrupoles, respectively. The quadrupole is a device, which uses the stability of the trajectories to separate ions according to their *m/z* ratio. It employs a combination of direct-current (DC) and radiofrequent (RF) fields as a mass filter. As illustrated in figure 4.7a, quadrupole analysers are made up of four rods with a hyperbolic cross section. Diagonally opposed rods are connected together electrically and to RF and DC voltage sources. They form electrode pairs exerting the same magnitude, but opposite potential. Ions entering the mass analyser and travelling along the z-axis are subjected to the influence of an electric field made up of the RF field superposed on the DC field. The potential Φ at each point in the quadrupole filter at any time will be described by:

$$F = \left[U + V\cos(wt)\right] \cdot \frac{x^2 - y^2}{2r_0^2}$$

where *U* is the magnitude of the DC potential, *Vcos(wt)* represents a radiofrequent field of amplitude V and angular frequency *w*, *x* and *y* are the distances along both axes and r_0 is the distance from the *z*-axis to either of the quadrupole rod surfaces. Along the central axis (x and y = 0) and when x = y (dashed lines in figure 4.7a), the potential is zero. Assume an ion has a zero velocity component along the y-axis: its trajectory will be in the x-z plane (positive U). Heavy ions with a high inertia will not substantially respond to the variation of the field: on average, they will sense the positive potential U and are focused on the

central axis. However, ions with lower mass, having a lower inertia, will oscillate with the change in voltage and as they gain amplitude will be discharged and thus lost on one of the electrodes. Thus the two positive electrodes constitute a high-mass filter. Consider now an ion that has a zero velocity component along the x-axis: it will remain in the y-z plane (negative U). Under these circumstances, heavy ions with a high inertia will eventually be attracted by the negative electrodes. Lighter ions that can rapidly react to the influence of the RF field will be transmitted. Thus the z-y plane constitutes a low-mass *filter*. In order for a certain ion to exhibit a stable path through the quadrupole filter, its trajectory should be stable in both planes. Only ions having an *m/z* above (x-z plane) and below (y-z plane) a critical mass will pass through the quadrupole. As a result, only ions within a small window will be transmitted. The width of the window is dependent on the ratio *U/V*, while the *m/z* ratio is given by the magnitude of both the DC and the RF voltage. An a and q term have been defined allowing to simplify the Mathieu equations, which give a quantitative description of the equation of motion for an ion within the quadrupole:

$$a_u = \frac{4zeU}{m^2 r_0^2 w^2} \qquad and \qquad q_u = \frac{2zeV}{m^2 r_0^2 w^2} \qquad and \qquad \frac{a_u}{q_u} = \frac{2U}{V}$$

with *z* the valence of the ion, *e* the electronic charge and *m* the mass of the ion. In an a_u-q_u diagram, the stability areas can be represented. In these areas, the values of *U* and *V* are such that *x* and *y* do not reach values above or equal to r_0. Figure 4.7b represents one of these stability areas. Although a whole series of stability regions exist, each corresponding to stable solutions to the Mathieu equations, only the regions near the origin in the a_u-q_u diagram are chosen for the operation of the quadrupole mass filter in commercial instrumentation. A line representing the ratio *a/q = 2U/V* can be drawn on the stability diagram. This line represents the situation where the ratio of the amplitudes of the RF and DC components is held constant while their absolute values are increased. Such a line is known as a scan line. The line passes from the origin through a region of *x* stability and *y* instability before crossing into a region of both *x* and *y* stability. As *a* and *q* further increase, the scan line passes into a region of *x* instability and *y* stability before finally reaching an area where both *x* and *y* are unstable. If *q* lies in the range q_1 to q_2, ion trajectories exist that will allow particles to pass the full length of the mass filter. By scanning the values of *U* and *V* while holding their ratio constant, it is possible to bring ions of different masses successively into the stability region for transmission. This is illustrated in figure 4.7c. As long as the scan line keeps going through stability areas, the higher the

slope of the scan line (slope of scan line 2 is higher than of scan line 1), the better will be the resolution.

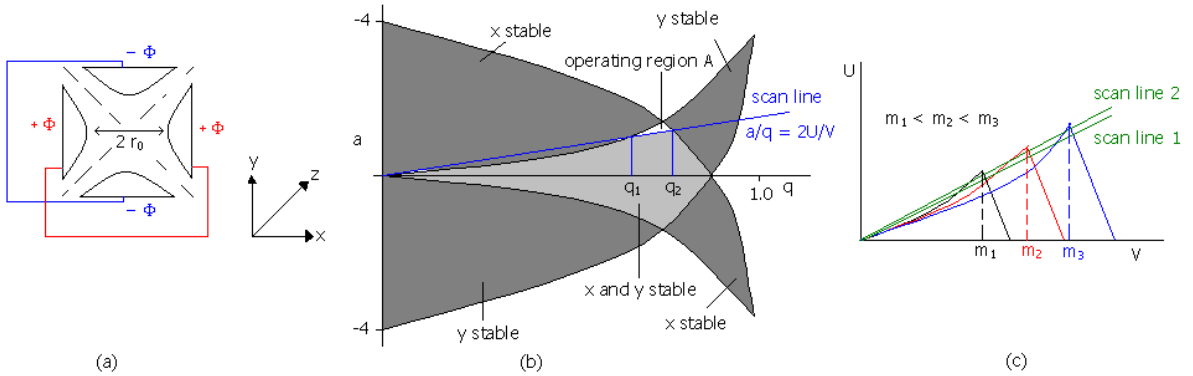

Figure 4.7. Schematic representation of the cross section of a quadrupole (a), of a stability area for an ion with certain *m/z* (b) and of a scan of three ions with mass m_1, m_2 and m_3 (c).

In RF-only mode (*e.g.*, in the collision cell of the triple quadrupole mass spectrometer), there is no DC voltage; thus *a* equals zero. Therefore the operating line lies horizontally along the abscissa, indicating theoretically that ions of all *m/z* values have stable trajectories and are transmitted through the quadrupole.

4.4. Hydride generation atomic fluorescence spectrometry

[Ebdon *et al.*, 1998b; Howard, 1997; Vandecasteele and Block, 1993b]

Atomic fluorescence spectrometry (AFS) uses radiation from a line source to excite atoms to a higher electronic state. The fluorescence emitted as the excited atoms return to the ground state is measured. The instrument used throughout this work utilises resonance fluorescence [Corns *et al.*, 1993; PS Analytical]. In this type, the fluorescence radiation is of the same wavelength as the absorbed radiation. For arsenic the fluorescence signal is obtained at the three resonance lines 189.04, 193.76, 197.26 nm. A set of lenses will collect and focus the useful radiation and a multi-reflectance filter is inserted to achieve wavelength isolation and reduce flame emissions. Illumination from the excitation source is at right angles to the detection axis to suppress detection of radiation from the excitation source. The intensity of AFS is proportional to the intensity of the absorbed radiation and to the concentration of the analyte atoms. Detection limits can thus be improved if an intense excitation source is used. A boosted discharge hollow cathode lamp (BDHCL), providing a more intense line spectrum compared to conventional hollow cathode lamps is therefore

used. A BDHCL uses a secondary discharge between the cathode and a high efficiency electron emitter, which passes through the atom cloud generated by the normal discharge.

Arsenic, among other elements of groups 14, 15 and 16 of the periodic table, forms hydrides with nascent hydrogen. A suitable reagent for reduction and hydride formation is sodium borohydride ($NaBH_4$). In the case of arsenic $NaBH_4$ can be thought of as acting as both a reductant and as a hydride generation (HG) source. In its reaction with pentavalent arsenicals, the first step is a reduction of the arsenic to the +III state:

$$R_nAs(O)(OH)_{3-n} + H^+ + BH_4^- \rightarrow R_nAs(OH)_{3-n} + H_2O + BH_3$$

where *R* is mostly a methyl group and *n* ranges from 0 to 3. Subsequent reaction with $NaBH_4$ takes the arsenic compound through to the corresponding arsine. The borane generated by these reactions hydrolyses giving boric acid and hydrogen.

$$R_nAs(OH)_{3-n} + (3-n)BH_4^- + (3-n)H^+ \rightarrow R_nAsH_{3-n} + (3-n)BH_3 + (3-n)H_2O$$
$$BH_3 + 3H_2O \rightarrow H_3BO_3 + 3H_2$$

Arsenite, arsenate, MA, DMA and TMAO can be converted into AsH_3, AsH_3, $MeAsH_2$, Me_2AsH and Me_3As, respectively. For As^V, it was found that the reaction was much slower than for As^{III} and that this species continued to be reduced in the reaction loop. This is explained by the fact that $NaBH_4$ is not converted directly into H_3BO_3 but into an intermediate product that is still able to produce AsH_3 from As^V. The difference between the trivalent and pentavalent oxidation states depends strongly on the system used and the experimental conditions. In batch systems and at pH <1 arsine is formed more slowly from As^V than from As^{III}, but the peak areas are more or less the same. In flow systems, the situation is significantly different. The slower reduction of the pentavalent oxidation state leads to greater differences in sensitivity due to kinetic discrimination. Pre-reduction of As^V to As^{III}, which is usually done in batch experiments using a solution of KI, KI + ascorbic acid or L-cysteine, is not advised for flow injection systems. The low kinetics and high temperatures needed prevent the technique of being used routinely without the loss of sensitivity. It is therefore better to use a longer reaction coil. An advantage of HG-AFS is that the element can be separated from almost all other accompanying materials, avoiding a lot of interference.

Organic arsenicals such as TETRA, AB and AC are insensitive towards hydride formation. In order to overcome this drawback, the organic arsenicals can be mixed with an oxidising solution of potassium persulphate ($K_2S_2O_8$) in combination with UV irradiation [Howard and Hunt, 1993; Rubio *et al.*, 1993 and 1995; Zhang *et al.*, 1996; van Elteren and Slejkovec, 1997, Slejkovec *et al.*, 1997 and 1999; Gomez-Ariza *et al.*, 1998; Dagnac *et al.*, 1999; Sur *et al.*, 1999; He *et al.*, 2000; Tsalev *et al.*, 1998 and 2000; Vilano and Rubio, 2001; Sanchez-Rodas *et al.*, 2002), microwave irradiation [Le *et al.*, 1993; Welz *et al.*, 1993; Lopez-Gonzalez *et al.*, 1995; Lamble and Hill, 1996; Sur *et al.*, 1999) or with heating [Suner *et al.*, 2001]. This process transforms the organoarsenicals into simpler arsenic forms. Attalah and Kalman [1991] have identified inorganic arsenic, MA, DMA and TETRA as photo-oxidation products of AB. In the ideal case, all organic arsenicals are transformed into arsenate. The persulphate ion is one of the strongest oxidising agents in aqueous solution [Golimowski and Golimowska, 1996]. The standard redox potential for the reduction of persulphate to sulphate equals 1.96 V. The first stage of the decomposition of $S_2O_8^{2-}$ is the formation of radicals:

$$S_2O_8^{2-} \rightarrow 2\,SO_4^{-\bullet}$$

In the second stage the sulphate radicals react with water to form hydroxyl radicals:

$$SO_4^{-\bullet} + H_2O \rightarrow HSO_4^- + OH^\bullet$$

The next stages of chain reaction of the $S_2O_8^{2-}$ decomposition are:

$$S_2O_8^{2-} + OH^\bullet \rightarrow HSO_4^- + SO_4^{-\bullet} + 1/2\,O_2$$

$$SO_4^{-\bullet} + OH^\bullet \rightarrow HSO_4^- + 1/2\,O_2$$

The hydroxyl radicals are capable of disrupting the arsenic-carbon bond. The best photo-oxidation of AB is obtained in neutral or basic solutions [Attalah and Kalman, 1991]. Photo-oxidation should occur on-line in order to do speciation analysis. The arsenicals in the mobile phase are mixed with a solution of $S_2O_8^{2-}$ in NaOH and directed to a reaction coil wrapped around a low-pressure mercury lamp. If a suitable reaction time is respected, the organoarsenicals will be transformed completely into arsenate. To prevent band broadening, which is inevitable when a photo-oxidation pretreatment is involved, the mobile phase can first be segmented with a flow of ambient air [Zhang *et al.*, 1996]. The air bubbles prevent the mobile phase of diffusing and thus the peak broadening is kept minimal. After conversion into arsenate, the flow is first mixed with HCl and then with a solution of $NaBH_4$ for production of the hydrides. This $NaBH_4$ is dissolved in alkaline media for stability reasons. The hydrides and the excess hydrogen are swept out of the liquid in a gas-liquid separator (GLS) using a stream of argon. The gaseous flow passes a drying

cassette, consisting of a set of coaxial membranes [Branch *et al.*, 1991; Corns *et al.*, 1992]. As the wet gas passes through the inner membrane, the moisture is removed and transferred to the outer tube, where a dryer gas in counter flow removes the moisture. Finally the hydrides are sent to an argon-hydrogen diffusion flame for atomisation. Atomisation is probably realised via a free radical mechanism within the flame. The resulting atoms are detected by AFS. The configuration is shown in figure 4.8. Only very recently, Schmeisser *et al.* [2004] have reported the hydride-forming capabilities of arsenosugars without prior decomposition. The HG efficiency depends on the type of GLS and is influenced by the concentration of $NaBH_4$ and HCl.

HG-AFS has also been used for the analysis of total arsenic in clinical samples. Prior to analysis with HG-AFS the samples need to be digested. Urine, serum, packed blood cells and blood were mineralised in open vessels with a mixture of $HNO_3/HClO_4/H_2SO_4$ in a ratio of 7:2:1 under the influence of a temperature-controlled programme [Zhang *et al.* 1995, Cornelis *et al.* 1998]. For total element analysis, the instrumental set-up is slightly different from that needed to carry out speciation analysis. In a flow injection mode, the sample is dissolved in HCl to which potassium iodide (1%) and ascorbic acid (0.2%) is added. This solution is then mixed with the hydride-forming reagent and sent immediately to the GLS. The remainder of the process is identical to the one described above. Potassium iodide and ascorbic acid is added to all blank solutions, samples and standards to ensure that all arsenic is in the trivalent form.

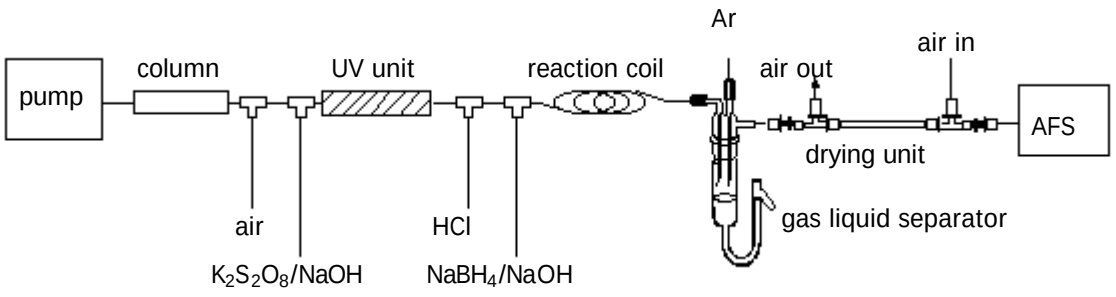

Figure 4.8. Schematic overview of the HPLC-UV-HG-AFS instrument.

The HG-AFS equipment was purchased from PS Analytical (Orpington, UK). The PSA 10.055 Millennium Excalibur system uses a boosted discharge hollow cathode lamp (Photron, Narre Warren, Australia) and can be employed in flow injection mode for measurement of total arsenic and for speciation analysis.

4.5. Nephelometry

[Behring]

Nephelometry is a technique used for the measurement of proteins. Quantification is based on the specific reaction of proteins with antisera. Proteins present in the sample react with the specific antiserum to form insoluble complexes. When light passes through this suspension, a portion of the light is scattered forward by the complexes and focused onto a photodiode by an optical lens system. An infrared light emitting diode (840 nm) serves as the light source. Because the particle diameter of the complexes is generally much larger than the incident IR light wavelength, Mie-scattering dominates over Rayleigh-scattering. The scattered light is collected on a photodiode from an angle ranging between 13° and 24°. Nephelometry has been used for semi-quantitative purposes. Fractions obtained after chromatographic separation of serum were analysed for the presence of transferrin, albumin and IgG in order to assess the retention behaviour of the proteins. Nephelometry is a more reliable and specific detection method compared with UV detection. The instrument was obtained from Behring (Hoechst, Charleroi, Belgium).

References

[Abou-Shakra *et al.*, 1997]

Abou-Shakra FR, Rayman MP, Ward NI, Hotton V and Bastian G (1997). *J. Anal. At. Spectrom.*, **12**, 429-433.

[Amersham Pharmacia, 1987]

Ion Exchange Chromatography, Principles and Methods (1987). Amersham Pharmacia, Sweden, pp 9-20.

[Amersham Pharmacia, 1998]

Gel Filtration, Principles and Methods (1998). Amersham Pharmacia, Sweden, pp 4-42.

[Amersham Pharmacia, 1999]

Reversed Phase Chromatography, Principles and Methods (1999). Amersham Pharmacia, Sweden, pp 5-28.

[Amersham Pharmacia, 2001]

Affinity Chromatography, Principles and Methods (2001). Amersham Pharmacia, Sweden, pp 7-24.

[Attalah and Kalman, 1991]

Atallah RH and Kalman DA (1991). *Talanta*, **38**, 167-173.

[Behring]

Behring Nephelometer 100 instruction manual, Behring.

[Blades *et al.*, 1991]

Blades AT, Ikonomou MG and Kebarle P (1991). *Anal. Chem.*, **63**, 2109-2114.

[Branch *et al.*, 1991]

Branch S, Corns WT, Ebdon L, Hill S and O'Neill P (1991). *J. Anal. At. Spectrom.*, **6**, 155-158.

[Cornelis *et al.*, 1998]

Cornelis R, Zhang XR, Mees L, Christensen JM, Byrialsen K and Dyrschel C (1998). *Analyst*, **123**, 2883-2886.

[Cornelis, 1992]

Cornelis R (1992). *Analyst*, **117**, 583-588.

[Corns *et al.*, 1992]

Corns WT, Ebdon L, Hill SJ and Stockwell PB (1992). *Analyst*, **117**, 717-720.

[Corns *et al.*, 1993]

Corns WT, Stockwell PB, Ebdon L and Hill SJ (1993). *J. Anal. At. Spectrom.*, **8**, 71-77.

[Dagnac *et al.*, 1999]

Dagnac T, Padro A, Rubio R and Rauret G (1999). *Talanta*, **48**, 763-772.

[De Hoffmann *et al.*, 1996]

De Hoffmann E, Charette J and Stroobant V (1996). *Mass Spectrometry, Principles and Applications*, John Wiley, Chichester, pp 41-51.

[Ebdon *et al.*, 1998a]

Ebdon L, Evans EH, Fisher AS and Hill SJ (1998). In *An Introduction to Analytical Atomic Spectrometry* (ed. Evans EH), Wiley, Chichester, pp 115-135.

[Ebdon *et al.*, 1998b]

Ebdon L, Evans EH, Fisher AS and Hill SJ (1998). In *An Introduction to Analytical Atomic Spectrometry* (ed. Evans EH), Wiley, Chichester, pp 137-144.

[Ehmann and Vance, 1991]

Ehmann WD and Vance DE (1991). In *Radiochemistry and Nuclear Methods of Analysis*, John Wiley, New York, pp 205-311.

[Firestone, 1996]

Firestone RB (1996). In *Table of Isotopes, Eigth Edition, Volume 1* (ed. Shirley VS), John Wiley, New York, pp 869-926.

[Gaskell, 1997]

Gaskell SJ (1997). *J. Mass Spectrom.*, **32**, 677-688.

[Golimowski and Golimowska, 1996]

Golimowski J and Golimowska K (1996). *Anal. Chim. Acta*, **325**, 111-133.

[Gomez-Ariza *et al.*, 1998]

Gomez-Ariza JL, Sanchez-Rodas D, Beltran R, Corns W and Stockwel P (1998). *Appl. Organomet. Chem.*, **12**, 439-447.

[He *et al.*, 2000]

He B, Jiang GB and Xu XB (2000). *Fres. J. Anal. Chem.*, **368**, 803-808.

[Houk, 1986]

Houk RS (1986). *Anal. Chem.*, **58**, 97A.

[Howard and Hunt, 1993]

Howard AG and Hunt LE (1993). *Anal. Chem.*, **65**, 2995-2998.

[Howard, 1997]

Howard AG (1997). *J. Anal. At. Spectrom.*, **12**, 267-272.

[Kebarle and Ho, 1997]

Kebarle P and Ho Y (1997). In *Electrospray Ionization Mass Spectrometry, Fundamentals, Instrumentation and Applications* (ed. Cole RB), John Wiley, New York, pp 3-63.

[Kebarle and Peschke, 2000]

Kebarle P and Peschke M (2000). *Anal. Chim. Acta*, **406**, 11-35

[Kebarle and Tang, 1993]

Kebarle P and Tang L (1993). *Anal. Chem.*, **65**, 972A-986A.

[Lamble and Hill, 1996]

Lamble KJ and Hill SJ (1996). *Anal. Chim. Acta*, **334**, 261-270.

[Larsen and Stürup, 1994]

Larsen EH and Stürup S (1994). *J. Anal. At. Spectrom.*, **9**, 1099-1105.

[Le *et al.*, 1993]

Le XC, Cullen WR and Reimer JR (1993). *Talanta*, **40**, 185-193.

[Lopez-Gonzales *et al.*, 1995]

Lopez-Gonzales MA, Gomez MM, Camara C and Palacios MA (1995). *Mikrochim. Acta*, **120**, 301-308.

[Meyer, 1998]

Meyer VR (1998). *Practical High-Performance Liquid Chromatography,* Wiley, Chichester, pp 14-51.

[Micromass 1]

Z-spray API Source, User's Guide, Micromass.

[Micromass 2]

Quattro Micro, User's Guide, Micromass.

[Montaser *et al.*, 1998]

Montaser A, McLean JA, Liu H and Mermet JM (1998). In *Inductively Coupled plasma Mass Spectrometry* (ed. Montaser A), Wiley, New York, pp 1-31.

[PS Analytical]

Excalibur User Manual, PS Analytical.

[Rubio *et al.*, 1993]

Rubio R, Padro A, Alberti J and Rauret G (1993). *Anal. Chim. Acta*, **283**, 160-166.

[Rubio *et al.*, 1995]

Rubio R, Alberti J, Padro A and Rauret G (1995). *Trends Anal. Chem.*, **14**, 274-279.

[Sanchez-Rodas *et al.*, 2002]

Sanchez-Rodas D, Geiszinger A, Gomez-Ariza JL and Francesconi KA (2002). *Analyst*, **127**, 60-65.

[Schmeisser et al., 2004]

Schmeisser E, Goessler W, Kienzl N and Francesconi KA (2004). *Anal. Chem.*, **76**, 418-423.

[Slejkovec *et al.*, 1997]

Slejkovec Z, van Elteren JT and Byrne AR (1997). *Acta Chim. Slov.*, **44**, 225-235.

[Slejkovec *et al.*, 1999]

Slejkovec Z, van Elteren JT and Byrne AR (1999). *Talanta*, **49**, 619-627.

[Suner *et al.*, 2001]

Suner MA, Devese V, Munoz O, Velez D and Montora R (2001). *J. Anal. At. Spectrom.*, **16**, 390-397.

[Sur *et al.*, 1999]

Sur R, Begerow J and Dunemann L (1999). *Fres. J. Anal. Chem.*, **363**, 526-530.

[Tsalev *et al.*, 1998]

Tsalev DL, Sperling M and Welz B (1998). *Analyst*, **123**, 1703-1710.

[Tsalev *et al.*, 2000]

Tsalev DL, Sperling M and Welz B (2000). *Spectrochim. Acta B*, **55**, 339-353.

[van Elteren and Slejkovec, 1997]

van Elteren JT and Slejkovec Z (1997). *J. Chrom.*, **789**, 339-348.

[Vandecasteele and Block, 1993a]

Vandecasteele C and Block CB (1993). In *Modern Methods for Trace Element Determination*, John Wiley, Chichester, pp 174-260.

[Vandecasteele and Block, 1993b]

Vandecasteele C and Block CB (1993). In *Modern Methods for Trace Element Determination*, John Wiley, Chichester, pp 159-167.

[Vandecasteele, 1988]

Vandecasteele C (1988). *Activation Analysis with Charged Particles*, Ellis Horwood Ltd., Chichester, UK, pp 13-50.

[Vilano and Rubio, 2001]

Vilano M and Rubio R (2001). *Appl. Organomet. Chem.*, **15**, 658-666.

[Watson, 1997]

Watson JT (1997). In *Introduction to Mass Spectrometry*, Lippincott-Raven, Philadelphia, pp 73-80.

[Welz *et al.*, 1993]

Welz B, He Y and Sperling M (1993). *Talanta*, **40**, 1917-1926.

[Zhang *et al.*, 1995]

Zhang X, Cornelis R, De Kimpe J, Mees L, Vanderbiesen V and Vanholder R (1995). *Fres. J. Anal. Chem.*, **353**, 143-147.

[Zhang *et al.*, 1996]

Zhang X, Cornelis R, De Kimpe J and Mees L (1996). *Anal. Chim. Acta*, **319**, 177-185.

Chapter 5. Indium: *in vitro* experiments

5.1. Preparation of [^{114m}In]$InCl_3$ radiotracer

^{114m}In can be produced from various nuclei. The most convenient way, however, is by irradiation of a cadmium target with protons, according to the following nuclear reaction:

$$^{114}Cd\ (p,n)\ ^{114m}In$$

^{114}Cd is the most abundant cadmium isotope (28.73%) and bombardment with protons of suitable energy could easily be done in the cyclotron of the institute. Naturally occurring cadmium consists of 8 stable isotopes, which will all undergo a (p,n) reaction. Moreover (p,2n) reactions are common interfering reactions. Table 5.1 lists the possible (p,n) and (p,2n) reactions.

Table 5.1. List of indium radioisotopes produced by proton bombardment of a Cd target.

isotope and abundance	(p,n) and $t_{½}$	(p,2n) and $t_{½}$
^{106}Cd (1.25%)	^{106m}In (5.3 min), ^{106}In (6.2 min)	^{105m}In (43 s), ^{105}In (5.1 min)
^{108}Cd (0.89%)	^{108m}In (40 min), ^{108}In (57 min)	^{107m}In (51 s), ^{107}In (32.4 min)
^{110}Cd (12.49%)	^{110m}In (1.15 h), ^{110}In (4.9 h)	^{109m}In (1.3 min), ^{109}In (4.2 h)
^{111}Cd (12.80%)	^{111m}In (7.7 min), **^{111}In (2.8049 d)**	^{110m}In (1.15 h), ^{110}In (4.9 h)
^{112}Cd (24.13)	^{112m}In (20.8 min), ^{112}In (14.4 min)	^{111m}In (7.7 min), ^{111}In (2.8049 d)
^{113}Cd (12.22%)	^{113m}In (1.658 h), **^{113}In (stable)**	^{112m}In (20.8 min), ^{112}In (14.4 min)
^{114}Cd (28.73%)	**^{114m}In (49.51 d)**, ^{114}In (1.198 min)	^{113m}In (1.658 h), ^{113}In (stable)
^{116}Cd (7.49%)	^{116n}In (2.16 s), ^{116m}In (54.2 min), ^{116}In (14.1 s)	^{115m}In (4.486 h), ^{115}In (stable)

Only ^{111}In has a half-life, which is sufficiently long to interfere with ^{114m}In. All other isotopes have half-lives in the order of seconds to a few hours and will decay within minutes to 4 days. The characteristics of both isotopes are listed in table 5.2. The measured induced activity of the nuclear reaction is proportional to e_γ x I_γ x ? / $t_{½}$, with e_γ the detection efficiency of the detector for a gamma ray, I_γ the decay probability and ? the isotopic abundance. From the last column in table 5.2 it can be seen that a gamma-ray spectrum taken immediately after production of the indium tracer would be dominated by the ^{111}In γ-rays. The measured radioactivity of the 171.28 keV γ-ray of ^{111}In is 50 times higher than the 190.27 keV γ-ray of ^{114m}In. After a cooling period of 36.5 or 46.4 days, the activity of ^{111}In is reduced to 1% and 0.1% of the ^{114m}In activity, respectively. At this time the remaining ^{114m}In is still 61% and 53% of the original activity, respectively.

Table 5.2. Characteristics of ^{111}In and ^{114m}In radioisotopes.

isotope	main γ-energy [keV]	I_γ [%]	rel. e_γ	? Cd [%]	$t_{½}$ [d]	rel. act.
^{111}In	171.28	90.7	2.8	12.80	2.80	50.0
	245.35	94.5	2.3			42.8
^{114m}In	190.27	15.4	2.6	28.73	49.51	1.0
	558.43	4.4	1.2			0.1
	725.24	4.4	1			0.1

The optimum parameters for proton bombardment of the Cd target were derived from literature values. The threshold energy is 2.2 MeV and the Coulomb energy is 8.5 MeV. Therefore the proton energy must exceed 8.5 MeV [Skakun *et al.*, 1975]. A proton energy of 18 MeV was chosen. At higher energies, interfering (p,2n) reactions are more likely to occur. Higher values do not significantly increase the total yield. For 18 MeV protons the stopping power is 14.82 MeV/g/cm^2. This corresponds to a range of 0.7206 g/cm^2 or 0.833 mm, taking into account a density of 8.65 g/cm^3 Cd. As only foils of 0.5, 0.75 and 1 mm are commercially available, the 1 mm thick foil was chosen. The advantage is that the protons are completely stopped by the foil. A disadvantage might be that more Cd has to be separated from the indium afterwards. The total amount of ^{114m}In activity depends on the irradiation time and the intensity of the proton current. A current of 1 μA was chosen in order not to overheat the sample. The Cd foil was placed in a double cooled sampler. A double cooled sampler was preferred because of the low melting temperature of cadmium

(320.9 °C). In theory interfering (p,α) reactions might produce Ag isotopes. However, these were not observed in the final product.

Afterwards a suitable separation procedure was developed to isolate the indium from the cadmium matrix (purity 99.999%). Notice in table 5.1 the formation of stable ^{113}In and ^{115}In isotopes. Together with the ultra-low levels of indium impurity present in the cadmium foil and in the reagents needed for the separation of indium from the foil, this will contribute to the total amount of indium carrier in the tracer. The separation method was done using solvent extraction [Lawson and Kahn, 1957; Schweitzer and Coe, 1961; Stary, 1963] and liquid chromatography [Chattopadhyay *et al.*, 1997]. Indium forms a stable complex with 8-hydroxyquinoline (oxine). The log K for $InOx_3$ is 0.89, while for $CdOx_2.2HOx$ this value amounts to –5.29. Moreover, the extraction into oxine is dependent on the initial pH of the aqueous solution. At pH 2.13 half of the indium is extracted with 0.01 M oxine while for Cd this value is reached at a pH of 6.65. A quantitative extraction of indium is realised from a solution having a pH between 3.4 and 6.4. At this pH Cd cannot yet be extracted with a solution of oxine. The indium can be back extracted with an acid solution. The whole method was optimised using reactor-produced radioisotopes of indium (^{116m}In) and cadmium (^{115}Cd). The following steps were carried out:

- ✓ dissolve the cadmium foil in a minimum amount of 14 M HNO_3.
- ✓ buffer the solution at pH 3.4 with NH_4OAc.
- ✓ extract twice with an equal volume of 10 mM oxine in chloroform.
- ✓ wash the organic phase twice with NH_4OAc.
- ✓ extract the organic phase back into the aqueous phase twice with 1 M HBr.

The yield proved to be nearly quantitative. An additional ion exchange purification step was necessary to remove remaining trace amounts of Cd. After extraction it could be calculated that about 360 µg Cd (0.07% of the original mass) was still present. Therefore the solution was evaporated to nearly dry, dissolved in concentrated HBr and brought onto a Dowex 50Wx4 ion exchange column (diameter: 7 mm, length: 70 mm). Rinsing with 9 M HBr leads to the elution of the remaining cadmium, while washing with 12 M HCl results in the selective elution of indium. Again the indium yield reached nearly 100%. The final product was radiochemically pure (only ^{114m}In). The ion exchange method is based on the formation of $[InBr_4]^-$ and $[CdBr_4]^{2-}$ in concentrated HBr and can be explained by the Donnan potential [Diamond and Whitney, 1966]. The origin of the Donnan potential will be outlined in the

case of a cation exchange resin composed of fixed SO_3^- groups, H^+ counter ions and a mobile phase containing HCl. The resin phase is usually more concentrated than the mobile phase, so the resin counter ions of the cation exchanger (*e.g.*, H^+) tend to diffuse into the mobile phase. Similarly, the aqueous-phase co-ions (co-ions are mobile phase ions in the resin phase carrying the same sign as that of the resin-fixed ions, *e.g.*, Cl^-) tend to diffuse into the resin phase. This distribution leads to a violation of the electro neutrality and as such a potential difference is established at the interface. In practice the cation exchange resin becomes negative with respect to the external solution. This potential prevents the uptake of non-exchangeable electrolyte such as $[InBr_4]^-$. The higher the valence of the non-exchangeable electrolyte, the more efficiently it is excluded from the resin phase. The importance of the phenomenon of Donnan exclusion for the present work, however, is the feature that the exclusion becomes poorer as the external solution concentration is increased. As a result, resins in contact with concentrated electrolyte solutions no longer only show equivalent exchange but also non-exchangeable electrolyte absorption or resin invasion, and the latter can become an important process. Using concentrated HBr, the indium $[InBr_4]^-$ is absorbed by the resin phase whereas cadmium $[CdBr_4]^{2-}$ is efficiently excluded. When changing the mobile phase composition into concentrated HCl, indium will form complexes with chlorine with a charge more negative than -1. As a result the indium can be eluted from the column.

5.2. Ultrafiltration experiments of indium species

The suitability of a chromatographic buffer is of major importance, especially in the case of weakly bound and kinetically not inert species, such as electrostatically bound metal-ligand complexes [Sanz-Medel, 1995]. The composition of this buffer should be chosen such that it does not disrupt the binding between the metal and the ligand. This metal ligand bond can be broken by changing the chemical properties of the medium, such as pH, ionic strength, temperature, addition of chemicals, *etc.* Ionic strength and pH of the buffer were always adapted to the type of sample to be analysed: serum, packed cell lysate, urine, homogenised tissue. Therefore only the type of buffer had to be tested for its suitability as a chromatographic eluent. Ultrafiltration is a convenient means of studying the behaviour of trace elements in clinical samples and the influence of different parameters on this behaviour. Ultrafiltration experiments were conducted in which serum, packed cells and solutions of transferrin, albumin and haemoglobin were incubated with $[^{114m}In]InCl_3$ and ultrafiltered on a 10 kDa cut-off filter. The activity in the ultrafiltrate was measured and

compared with a reference sample of the same incubated mixture. Thus a value of the amount of radio indium bound to the high molecular mass (HMM) and low molecular mass (LMM) fraction could be determined.

5.2.1. Ultrafiltration of indium species in serum

In a first stage 6 solutions were incubated with ionic [^{114m}In]$InCl_3$ for 2 h at 37°C:

- ✓ undiluted serum (A)
- ✓ serum 1+9 diluted in 25 mM $NaHCO_3$ + 0.15 M NaCl, pH 7.4 (B)
- ✓ serum 1+9 diluted in 20 mM tris:HCl + 10 mM $NaHCO_3$, pH 7.4 (C)
- ✓ serum 1+9 diluted in 20 mM tris:HCl + 10 mM $NaHCO_3$ + 0.32 M NaCl, pH 7.4 (D)
- ✓ serum 1+9 diluted in 10 mM hepes + 5 mM $NaHCO_3$ +0.15 M NaCl, pH 7.4 (E)
- ✓ serum 1+9 diluted in 10 mM hepes + 5 mM $NaHCO_3$ + 1 M NaCl, pH 7.4 (F)

Then 3 x 250 µL was transferred into an ultrafiltration cup and centrifuged during 20 min at 3000 rpm and 4°C in order to separate the LMM fraction from the HMM fraction. The activity in the filtrate was measured with a NaI(Tl) scintillation detector. The percentage protein bound indium was measured through comparison with a reference (a non-ultrafiltered solution of equal volume of the same mixture). Weighing the vessels before and after ultrafiltration allowed correction for the differences in sample throughput by the filter membranes. This was necessary since the sample was never centrifuged till dry. The results in table 5.3 indicate that 93% of the indium is associated with the protein fraction. This result is in good agreement with that of Kulprathipanja and Hnatowich [1978], who found that 96% of a [^{113m}In]$InCl_3$ activity was found in the protein fraction after both *in vitro* and *in vivo* incubation of dog serum with ^{113m}In. Their results were obtained with gel filtration. Hosain *et al.* [1969] found that ^{113m}In is bound to the protein transferrin. Their findings were based on experiments with starch gel electrophoresis and gel filtration. In a study on ^{113m}In for blood pool and brain scanning Stern *et al.* [1967] were the first to predict that indium is presumably bound to transferrin in serum. However, their hypothesis was not confirmed by experimental evidence. Hultkvist *et al.* [1987] demonstrated that the binding between indium and transferrin is dependent on the pH of the medium. They chromatographed rat blood plasma that was *in vivo* incubated with [^{113m}In]$InCl_3$ by gel filtration using buffers at different pH values and found that at pH values below 6, the indium was no longer found in the protein fraction. This clearly illustrates the carefulness one should take when doing chromatographic analyses on metal-protein complexes.

Table 5.3. Distribution of ^{114m}In in serum.

amount of $^{114m}In^{3+}$ in HMM fraction (n = 3) [%]		amount of $^{114m}In^{3+}$ in LMM fraction (n = 3) [%]	
A: undiluted serum/$^{114m}In^{3+}$	93	G: $^{114m}In^{3+}$ in HCl	96
B: serum/$^{114m}In^{3+}$ in $NaHCO_3$	94	H: $^{114m}In^{3+}$ in physiological buffer	95
C: serum/$^{114m}In^{3+}$ in tris:HCl + $NaHCO_3$	98	I: $^{114m}In^{3+}$ + In^{3+} carrier in physiological buffer	98
D: serum/$^{114m}In^{3+}$ in tris:HCl + $NaHCO_3$ + NaCl	95		
E: serum/$^{114m}In^{3+}$ in hepes + $NaHCO_3$	95		
F: serum/$^{114m}In^{3+}$ in hepes + $NaHCO_3$ + NaCl	95		

Compared to the amount of In^{3+} bound to the HMM fraction of the undiluted serum sample (93%), dilution in the different buffer systems does not drastically alter the binding characteristics of indium. Tris:HCl and hepes are two widely used biological buffers with low metal content and pKa values of 7.77 and 7.31, respectively. Buffers B and E can be used for gel filtration chromatography, whereas buffers C, D and F are used in anion exchange and affinity chromatography. Depending on the pH of the solution, indium undergoes hydrolysis, resulting in In^{3+} being present as $[In(OH)_n(H_2O)_{6-n}]^{3-n}$ (n = 0 to 4). At pH 7.4 indium forms insoluble $In[(OH)_3(H_2O)_3]$. To be sure that the high activity of ^{114m}In in the HMM fraction was a result of the protein binding affinity of In^{3+} and not due to precipitation of In^{3+} at physiological pH three more solution were also ultrafiltered:

- ✓ a solution of $[^{114m}In]InCl_3$ in 0.01 M HCl (G)
- ✓ a solution of $[^{114m}In]InCl_3$ in 25 mM $NaHCO_3$ + 1.6 mM phosphate + 0.1 mM citric acid + 0.15 M NaCl, pH 7.4 (H)
- ✓ a solution of $[^{114m}In]InCl_3$ and 150 µM $InCl_3$ carrier in 25 mM $NaHCO_3$ + 1.6 mM phosphate + 0.1 mM citric acid + 0.15 M NaCl, pH 7.4 (I)

In all three cases more than 95% of the $^{114m}In^{3+}$ activity was found in the ultrafiltrate, indicating that hydrolysis is not responsible for the high amount of indium in the HMM fraction.

Transferrin is the protein responsible for the transport of iron in serum. Since transferrin is only 30% saturated with Fe^{3+}, the protein is capable of complexing other metals, preferably trivalent metals such as In^{3+}. Albumin is the most abundant protein in serum, its primary function being the non-specific binding and transport of small molecules, metals, drugs and hormones in blood. In order to study the binding of In^{3+} with transferrin and albumin, a physiological solution of

- ✓ 2 g/L transferrin in 25 mM $NaHCO_3$ + 0.15 M NaCl, pH 7.4
- ✓ 2 g/L transferrin in 25 mM KH_2PO_4 + Na_2HPO_4 + 0.15 M NaCl, pH 7.4
- ✓ 2 g/L transferrin in 10 mM hepes + 0.15 M NaCl, pH 7.4.
- ✓ 40 g/L albumin in 25 mM $NaHCO_3$ + 1.6 mM phosphate + 0.1 mM citric acid + 0.15 M NaCl, pH 7.4
- ✓ 10 g/L albumin in 15 mM tris:HCl + 0.15 M NaCl, pH 7.3
- ✓ 10 g/L albumin in 25 mM $NaHCO_3$ + 0.15 M NaCl, pH 7.3
- ✓ 10 g/L albumin in 15 mM hepes + 0.15 M NaCl; pH 7.3

were incubated with [^{114m}In]$InCl_3$ at 37°C. After several time intervals an aliquot of 1 mL was taken from the reaction mixture. Ultrafiltration was done as described above. The binding of In^{3+} with transferrin is complete in case of the bicarbonate buffer but only moderate in case of the hepes buffer (maximum 16%) and in case of the phosphate buffer (maximum 23%). In case of the bicarbonate buffer, the binding shows no time dependency within the time interval of 1-8 h. Binding of In^{3+} with albumin is also rapidly established (within one hour). The percentage of ^{114m}In bound to albumin amounts to 91% when albumin is dissolved in the physiological buffer of bicarbonate, phosphate and citrate. Also the binding of In^{3+} to albumin seems to be influenced by the reaction medium. The percentage of In^{3+} bound to albumin amounted to maximum 65%, 70% and 67% in the case of tris:HCl, $NaHCO_3$ and hepes, respectively. These values are lower than the 91% found in the case of the physiological buffer of bicarbonate, phosphate and citrate.

These findings indicate that In^{3+} is capable of forming a metal-protein complex with both transferrin and albumin *in vitro*. A buffer containing HCO_3^- was chosen for the preparation of the transferrin solution because it is the main buffering substance in serum. Moreover, a synergistic carbonate anion is necessary for the binding of metals to transferrin. The low binding affinity of In^{3+} for transferrin in case of the hepes and phosphate buffer is in agreement with the findings of Harris *et al.* [1998], who postulated that the binding of non-synergistic anions to apotransferrin interferes with metal binding by competing directly with the binding of the synergistic bicarbonate anion. The strongest interfering non-synergistic anion is HPO_4^{2-}. In the above mentioned report it is also stated that previous studies had suggested that the sulphonic acid moiety in hepes may also act as a competitor to the synergistic bicarbonate anion. The binding constants for phosphate, bicarbonate and hepes to the two binding sites of transferrin are given in table 5.4.

Table 5.4. Binding constants for different ligands to transferrin.

	hepes	bicarbonate	phosphate
log K1	1.36	3.06	4.34
log K2	0.76	2.44	3.54

5.2.2. Ultrafiltration of indium species in packed cells

Similar ultrafiltration experiments have been carried out on the packed cell fraction. In order to do this, the cell content has to be lysed. Packed cells were washed with ice-cold phosphate buffered saline (PBS) and 1 mL of cells was lysed in a Potter-Elvehjem type homogeniser with 10 mL water and 0.1 mL toluene. The cell membranes were removed by centrifugation at 10000 rpm during 30 min. This solution was incubated with [^{114m}In]$InCl_3$ at 37°C. After 1, 2, 4, 8, 12 and 24 hours 3 x 300 µL was transferred into an ultrafiltration cup and centrifuged during 20 min at 3000 rpm and 4°C in order to separate the LMM fraction from the HMM fraction. The activity in the filtrate was measured with the NaI(Tl) scintillation detector. The percentage protein bound In^{3+} was measured by comparing with a reference (3 x 50 µL of a non-ultrafiltered solution). Weighing the vessels before and after ultrafiltration allowed correction for the differences in sample throughput by the filter membranes. Binding to the HMM fraction was realised within 1 hour and nearly complete (between 93% and 95%). Afterwards a more convenient lysis method was chosen in which 1 mL washed packed cells was lysed with 1 mL 200 g/L glucose and 3 mL water in a Potter-Elvehjem type homogeniser. An identical ultrafiltration experiment was done and 93% of the ^{114m}In activity was found in the HMM fraction.

Similar to serum, the effect of different buffers on the binding between [^{114m}In]$InCl_3$ and packed cell proteins was tested. Yet another lysis technique was chosen: packed cells were alternately thawed and frozen 4 times. Although less quantitative, this method does not require chemicals. Afterwards undiluted cell lysate and cell lysate 1:10 diluted in:

- ✓ 0.15 M NaCl
- ✓ 50 mM NH_4HCO_3
- ✓ 15 mM tris:HCl + 0.15 M NaCl
- ✓ 15 mM hepes + 0.15 M NaCl

(pH of all media was between 7.1 and 7.2) were incubated with [^{114m}In]$InCl_3$ for 2 hours at 37°C. All samples were filtered through a 0.22 µm PVDF syringe filter to remove residual intact cells. The undiluted fraction could not be filtered and had to be discarded. Therefore the 0.15 M NaCl was chosen as the reference value as it is expected that dilution in a physiological solution with identical ionic strength and pH as the media will not alter the binding behaviour of indium. Ultrafiltration was carried out as described above. There is no difference in % HMM bound ^{114m}In in case of 0.15 M NaCl, tris:HCl and hepes buffer. NH_4NO_3, selected because it is used for speciation of lead compounds in packed cell lysate [Bergdahl *et al.*, 1996], leads to a decrease in the % HMM amount and will not be used.

A solution of 10 g/L haemoglobin in 15 mM hepes + 0.15 M NaCl (pH 7.1) was also incubated with [^{114m}In]$InCl_3$ and ultrafiltered. However, only 40% was found in the haemoglobin fraction. It can thus be expected that other ligands of the erythrocytes are capable of forming a complex with In^{3+}.

5.3. Chromatography experiments of indium species

Different chromatographic columns were tested for their suitability for indium speciation. Of utmost importance is the chromatographic recovery of ^{114m}In. Therefore a mass balance was made: an equal amount of sample to be chromatographed, was diluted to the same extent and measured for its ^{114m}In content. The suitability of the chromatographic procedure was tested with *in vitro* experiments. *In vitro* incubation experiments were carried out with human serum and packed cells, which were incubated with [^{114m}In]$InCl_3$.

5.3.1. Chromatography of indium species in serum

Figure 5.1 shows the chromatogram of human serum incubated with [^{114m}In]$InCl_3$ and separated using size exclusion on Asahipak GS 520 7G. The Asahipak column separates molecules on the basis of their molecular mass (exclusion limit 300 kDa), but shows also an affinity for albumin. As a result albumin is separated from the high molecular mass fraction. The Asahipak column has been successfully applied for metal speciation in serum [Raab and Brätter, 1998]. Serum, 1+2 diluted in starting buffer was incubated with [^{114m}In]$InCl_3$ for 2 h. 100 µL was brought onto the column. Elution was done with 10 mM hepes + 5 mM $NaHCO_3$ + 0.15 M NaCl, pH 7.4. Fractions of 1 mL were collected and the activity was measured by means of NaI(Tl) scintillation counting. It can be seen that most of the

activity is found within the elution volume of 12-14 mL. This fraction also contains transferrin. Some activity is spread out over the fraction containing albumin and a third peak containing 9.3% of all ^{114m}In is found within the elution volume of 16-17 mL. Recovery for ^{114m}In was 100%, measured by comparison with the reference. The results of the chromatographic separations of serum incubated with indium tracer were similar to those of the ultrafiltration experiments.

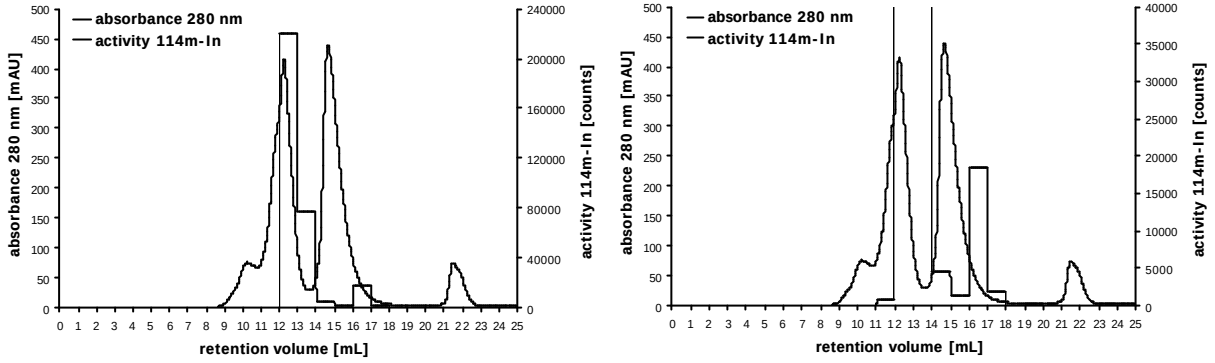

Figure 5.1. Chromatogram of serum + ^{114m}In separated on Asahipak GS 520 7G size exclusion column (left). Same chromatogram with enlarged scale for the ^{114m}In activity (right).

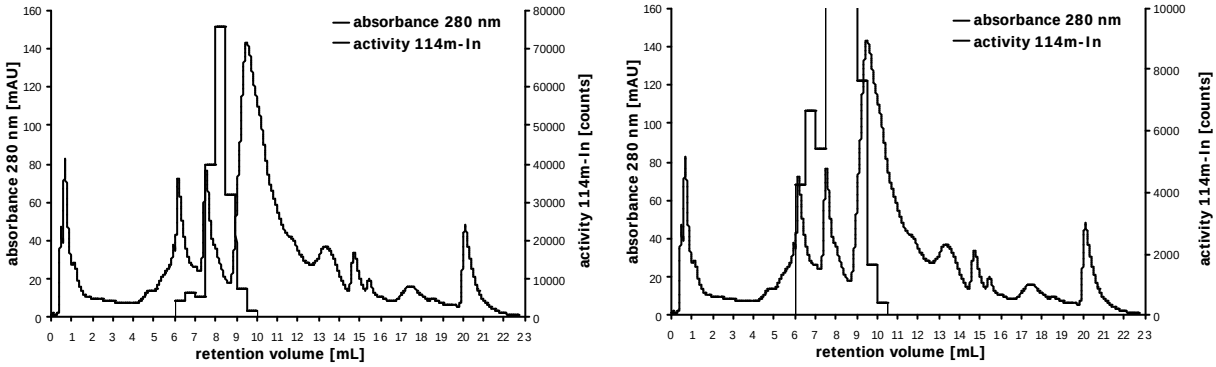

Figure 5.2. Chromatogram of serum + ^{114m}In separated on Mini Q anion exchange column (left). Same chromatogram with enlarged scale for the ^{114m}In activity (right).

The results of the anion exchange chromatography experiment are shown in Fig. 5.2. 1+10 diluted (in starting buffer) serum was incubated with [^{114m}In]$InCl_3$ for 2 h. 100 µL was brought onto a Mini Q PE anion exchange column. The starting buffer was 10 mM hepes + 5 mM $NaHCO_3$, pH 7.4. Gradient elution was performed with 10 mM hepes + 5 mM $NaHCO_3$ + 1 M NaCl, pH 7.4. Fractions of 500 µL were collected and the activity was measured by means of NaI(Tl) scintillation counting. The recovery of the ^{114m}In was 100%. Via

nephelometry, one could deduce that transferrin is found within mL-fraction 7.5-9, albumin within mL-fraction 9-14 and IgG within mL-fraction 0.5-1.5 and 5.5-7. It is clearly shown that In^{3+} is associated with transferrin, and to a lesser degree with albumin. A considerable amount (7.9%) of ^{114m}In is found around 6-7 mL.

The distribution of In^{3+} over transferrin and the LMM fraction, however, depends upon the pH of the indium tracer. The In^{3+} tracer incubated in serum in the latter example had a pH of 2. At pH 1, indium appears as the trivalent cation In^{3+}, whereas at pH 3 hydrolysis to $InOH^{2+}$ occurs. Serum was incubated with In^{3+} and $InOH^{2+}$ and analysed using gel filtration and anion exchange chromatography. The results are shown in figures 5.3 and 5.4.

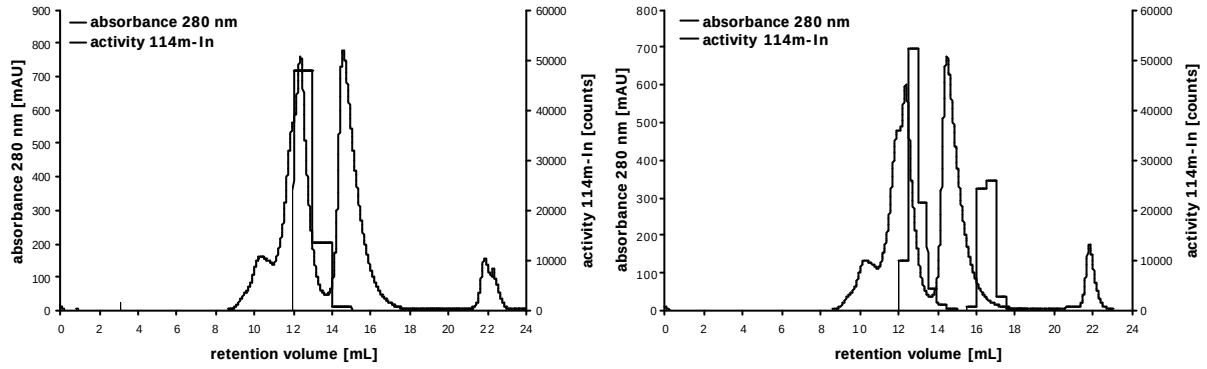

Figure 5.3 Chromatogram of serum + [^{114m}In]$InCl_3$ with tracer at pH 1 (left) and at pH 3 (right) separated on Asahipak GS 520 7G size exclusion column.

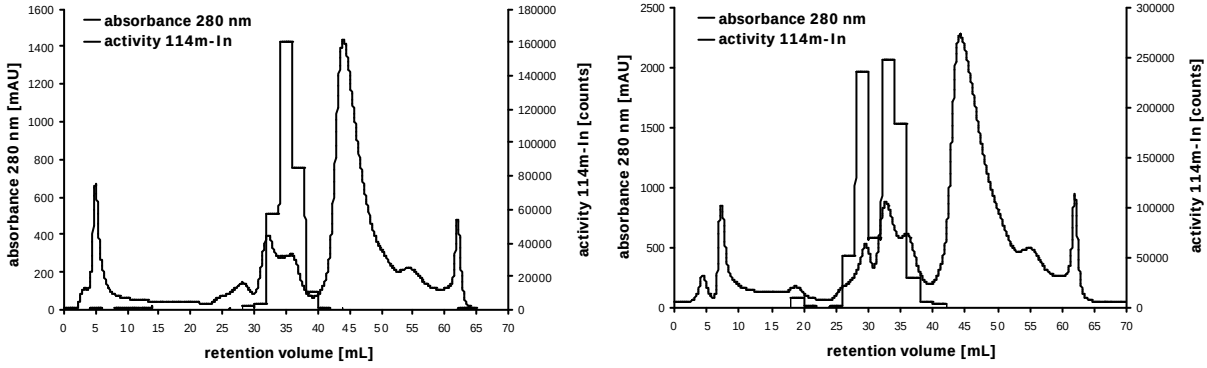

Figure 5.4 Chromatogram of serum + [^{114m}In]$InCl_3$ with tracer at pH 1 (left) and at pH 3 (right) separated on Hi Trap Q anion exchange column.

In the gel filtration experiment the procedure was identical to the one described above. For the anion exchange chromatography, undiluted serum was incubated with indium tracer for

2 hours and 500 µL was separated on a Hi Trap Q column. This column has a higher loading capacity compared to Mini Q, but the functional groups are identical. Fractions of 2 mL were taken and analysed for their ^{114m}In content using a NaI(Tl) detector. As can be seen from the chromatograms, at pH 1 of the tracer virtually all ^{114m}In appears in the transferrin region. When the pH of ^{114m}In[$InCl_3$] is increased to 3, 62.3% (gel filtration) and 60.2% of the indium tracer (anion exchange) is located with the transferrin fraction. Nephelometry has been used for semi quantification of transferrin in case of the anion exchange chromatography experiment. Between 28 and 30 mL where a first peak maximum of ^{114m}In can be seen, transferrin appears just above detection limits. Transferrin reaches a maximum in the range 32-36 mL. This matches perfectly well with the second peak in the chromatogram.

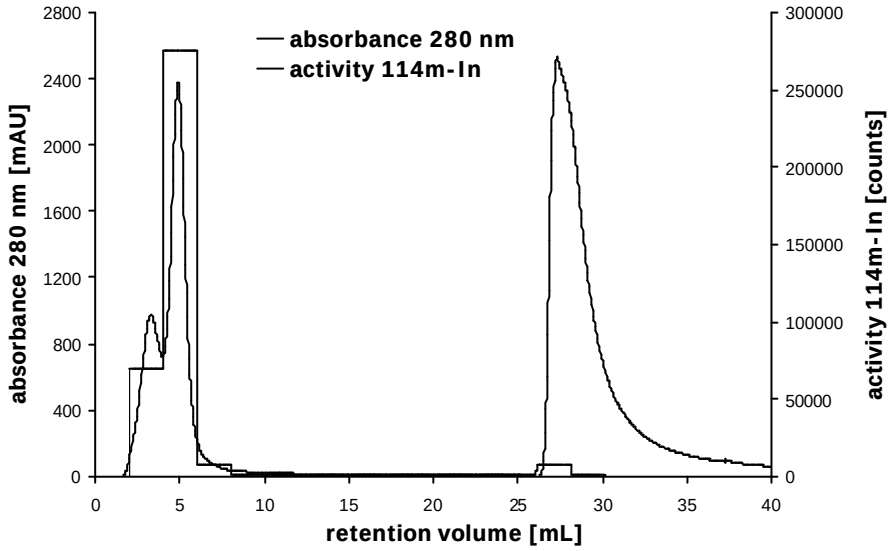

Figure 5.5. Chromatogram of serum + ^{114m}In separated on Hi Trap Blue affinity column.

Affinity chromatography has been tested to unambiguously prove the association between In^{3+} and albumin. 1+1 diluted serum in starting buffer was incubated with [^{114m}In]$InCl_3$ for 2 h and filtered through a 0.22 µm filter. 500 µL was brought onto a Hi Trap Blue affinity column. This cross-linked agarose column, substituted with Cibacron Blue F3G-A has an affinity for albumin, NAD^+, $NADP^+$, coagulation factors and interferons. The starting buffer was 20 mM tris:HCl + 10 mM $NaHCO_3$, pH 7.4. Albumin was eluted with 20 mM tris:HCl + 10 mM $NaHCO_3$ + 1.5 M NaCl, pH 7.4. Fractions of 2 mL were collected and the activity was measured with a NaI(Tl) scintillation detector. The chromatogram is shown in figure 5.5. It can be deduced that the fraction in which albumin is eluted, contains 8% of the ^{114m}In activity. Also here, recovery reached 100%. This amount seems to be much more

than the value obtained using gel filtration and anion exchange chromatography. Possibly flushing the column with the starting buffer did not elute all In^{3+} (bound to transferrin and a LMM compound) from the column. Changing the buffer ionic strength from 0 to 1.5 M NaCl could then result in the elution of the residual fraction. Consequently both the residual ^{114m}In and the albumin-bound ^{114m}In co-elute. Another possibility might be that indium is bound to NAD^+, $NADP^+$, coagulation factors and interferons, although this seems unlikely. Part of the ^{114m}In detected in the range 25-30 mL is probably the result of incomplete removal by buffer A. The ^{114m}In activity does not return to zero during flushing of the column, although a long flushing time (3 column volumes) was respected. Two albumin solutions (one in buffer A, one in buffer B) have been incubated with $[^{114m}In]InCl_3$ and ultrafiltered as described in section 5.2.1. An equal amount of ^{114m}In was found in he HMM fraction for both media, indicating that buffer B does not disrupt In^{3+} from albumin.

5.3.2. Chromatography of indium species in the LMM fraction in serum

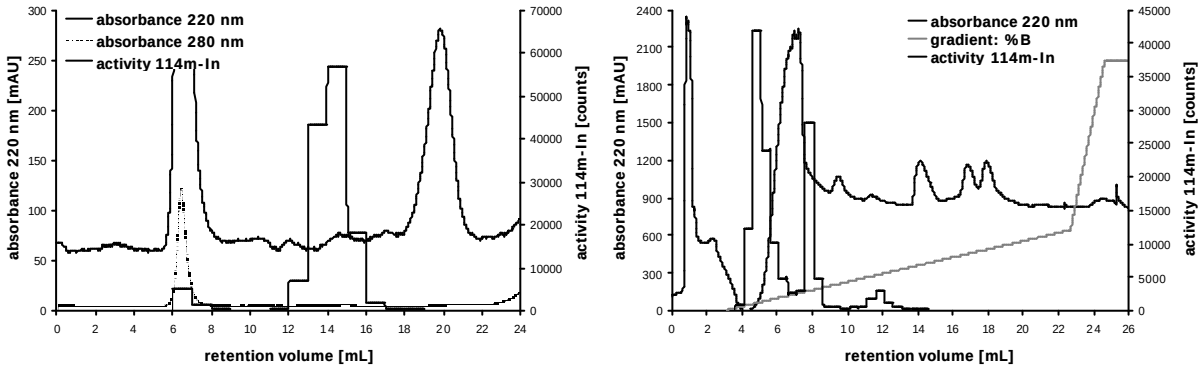

Figure 5.6. Chromatogram of ultrafiltrate of serum + ^{114m}In separated on Bio-Gel P2 size exclusion column (left) and on Mono Q anion exchange column (right).

Efforts were made to find out the identity of the LMM compound(s) that are able to complex indium *in vitro*. In order to obtain a substantial amount of the indium bound to the LMM fraction, serum was incubated with $[^{114m}In]InCl_3$ during 2 hours and ultrafiltered on a preparative 30 kDa filter. The ultrafiltrate was chromatographed on a Bio-Gel P2 size exclusion column (range 0.1-1.8 kDa). The result is shown in figure 5.6. The major share of the ^{114m}In appears in the range 13-15 mL. A small portion of indium is recovered from the void volume, indicating that some transferrin might have been ultrafiltered as well. The same sample was also separated using anion exchange chromatography on a Mono Q

column. Two major peaks appear now accompanied with a small peak around 11-12 mL which is due to residual transferrin present in the ultrafiltrate. Therefore it can be concluded that indium exists as at least two LMM compounds in serum *in vitro*.

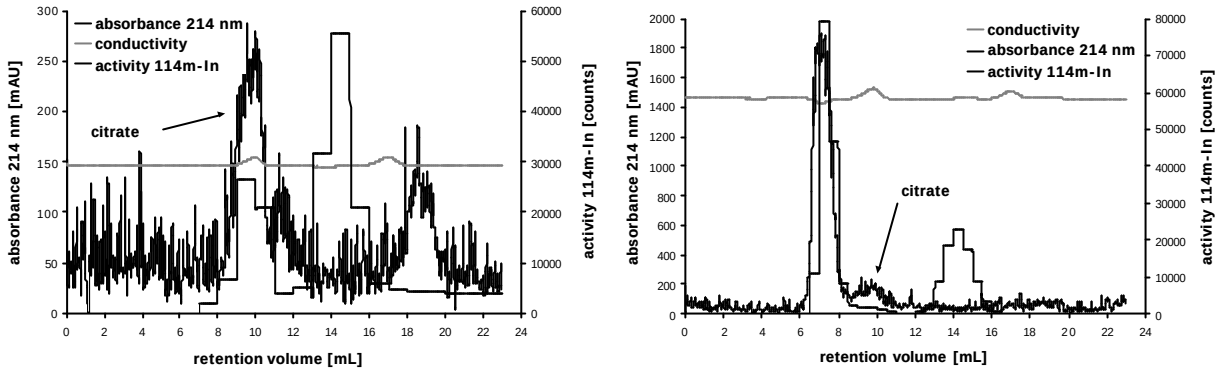

Figure 5.7. Chromatogram of citrate + ^{114m}In (left) and serum supplemented with citrate + ^{114m}In (right) separated on Bio-Gel P2 size exclusion column.

Citrate is known to complex Al^{3+} in serum [Bantan and Milacic, 1998]. Therefore it was checked whether citrate also binds to In^{3+}. A pure citrate solution (17 g/L) and a 1+1 mixture of serum + citrate (17 g/L) were incubated with [^{114m}In]$InCl_3$ and separated on a Bio-Gel P2 size exclusion chromatography column (figure 5.7). 29% of the ^{114m}In is found in the citrate fraction in case of the pure citrate solution, whereas in serum supplemented with citrate only 3% is associated with citrate.

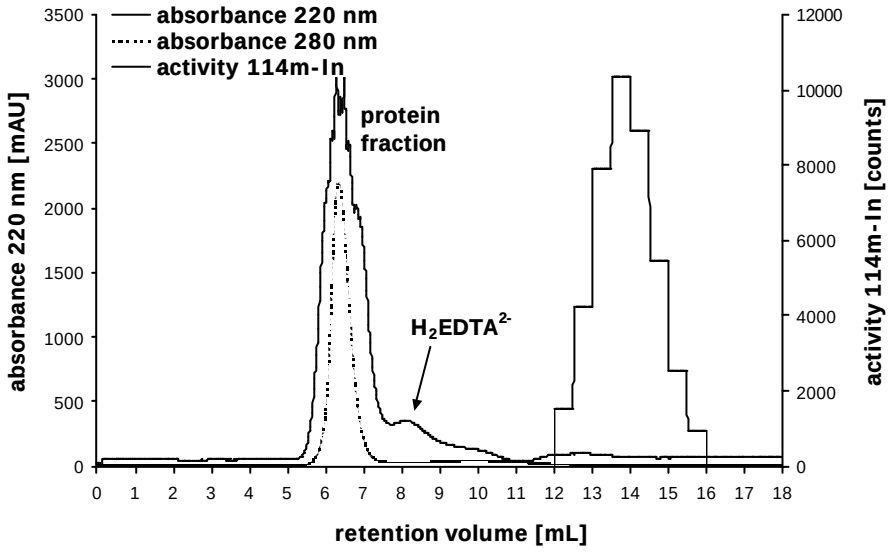

Figure 5.8. Chromatogram of plasma + ^{114m}In separated on Bio-Gel P2 size exclusion column after collection of blood in EDTA vacuum tubes.

The choice for a suitable medium in which to collect the blood is very important. To demonstrate this, blood was collected in an EDTA, a heparin containing tube and in an empty tube. Afterwards this blood was incubated with [^{114m}In]$InCl_3$ for 1 to 12 hours and centrifuged to obtain plasma and packed cells. An amount of 0.8 mL plasma, 0.2 mL packed cells and 1 mL original whole blood were measured for their ^{114m}In content by Ge(Li) detection. The results were normalised to 1 mL volumes. For both EDTA and heparin tubes, between 93.7% - 95.5% and 95.7% - 96.8%, respectively, of ^{114m}In was found in the plasma fraction. As can be seen in figure 5.8, the indium activity in the plasma that is obtained from EDTA tubes and separated on a Bio-Gel P2 size exclusion column, is completely eluted in the LMM fraction and is not bound to transferrin. In fact, each 4 mL collection tube contains 3.67 mM H_2EDTA^{2-}. The serum Tf concentration is around 25 µM. Given the fact that log K for EDTA-indium is 24.95 [Nitsch *et al.*, 1990] and log K for both Tf-indium binding sites are 18.52 and 16.64 [Harris *et al.*, 1994], respectively, it seems logical that an excess of EDTA will disrupt the binding between indium and transferrin. ^{114m}In elutes at another retention time than the H_2EDTA^{2-}. In^{3+} forms a complex with H_2EDTA^{2-} according to:

$$In^{3+} + H_2EDTA^{2-} \leftrightarrow InEDTA^{-} + 2H^{+}$$

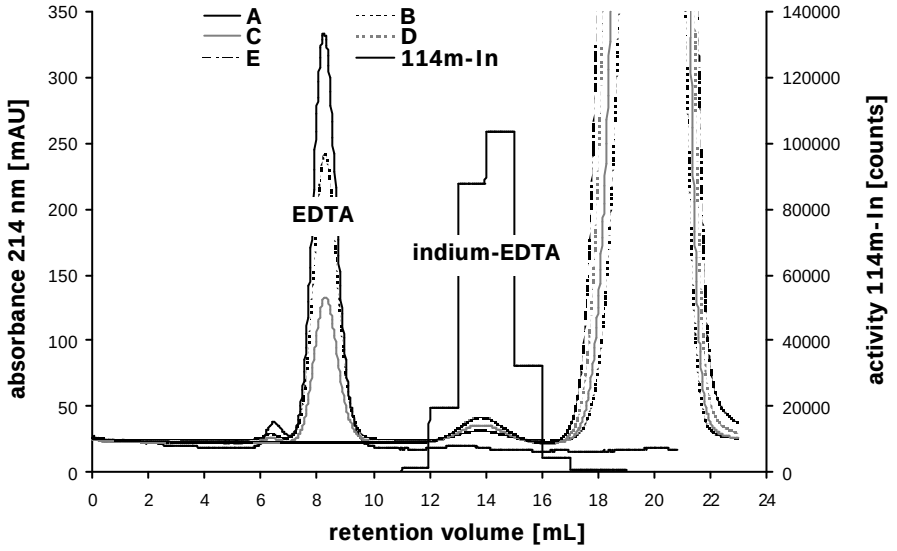

Figure 5.9. Chromatograms of EDTA + varying concentrations of [^{114m}In]$InCl_3$-$In(NO_3)_3$ separated on Bio-Gel P2 size exclusion column. The ^{114m}In activity was found as a single peak in all cases (A to E).

This indium-EDTA complex elutes separately from the non-complexed EDTA. Different amounts of $In(NO_3)_3$ (A: 0, B: 3.35 µmol, C: 6.7 µmol, D: 13.4 µmol and E: 26.8 µmol)

were mixed with equal amounts of $[^{114m}In]InCl_3$ and incubated with a solution of 26.1 µmol EDTA in 0.9% NaCl in order to obtain solutions with different concentrations of In^{3+} (equal amounts of radiolabeled indium but different amounts of 'carrier' indium) in equal concentrations of EDTA. All samples were chromatographed on the Bio-Gel P2 size exclusion column with 0.9% NaCl. The results are shown in figure 5.9. Non-complexed H_2EDTA^{2-} elutes at 8.4 mL. This peak decreases in function of an increasing indium (A → E) concentration and reaches zero when equimolar amounts of indium are reached (E). Correspondingly the peak at retention volume 13.9 mL increases, identified as the radiolabeled indium-EDTA complex.

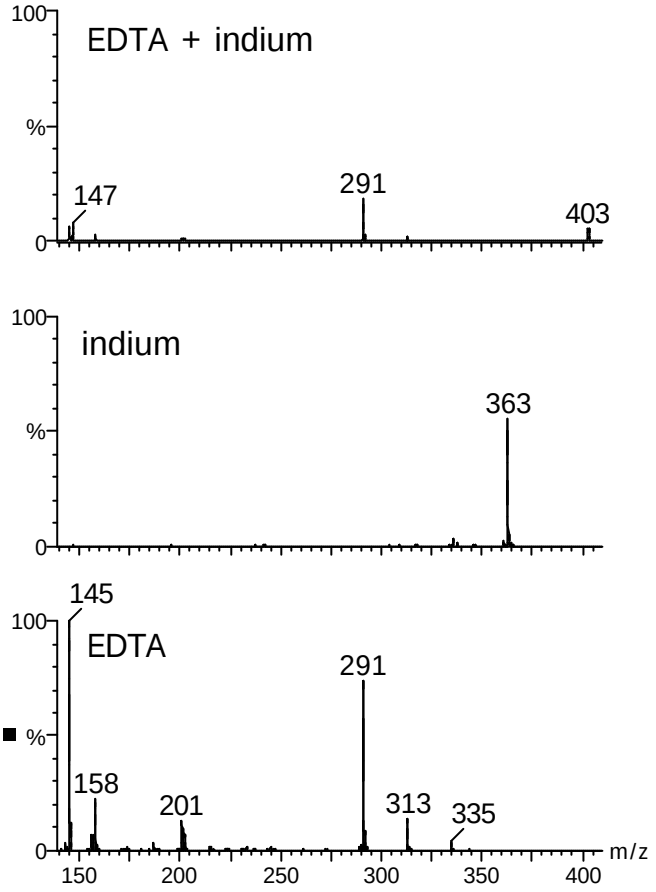

Figure 5.10. ES-MS spectra of H_2EDTA^{2-} + $In(NO_3)_3$ (top), $In(NO_3)_3$ (middle) and H_2EDTA^{2-} (bottom) using infusion full scan MS in negative ion mode. Sample cone voltage was set to 20 V. Intensity axes are linked.

The $InEDTA^-$ complex was further studied by infusion electrospray mass spectrometry. Individual solutions of 3.67 mM H_2EDTA^{2-}, 1 mM $In(NO_3)_3$ and 1 M $In(NO_3)_3$ + 3.67 mM

H_2EDTA^{2-} were analysed in positive and negative full scan mode. Mass scans between *m/z* 100 and 800 were recorded during 1 minute with a scan speed of 2 seconds. The indium stock solution initially contained 10.09 g/L indium in 2-5% HNO_3. To obtain a 1 mM indium solution, the stock solution was diluted 94 times, creating a pH between 2.1 and 2.5.Figure 5.10 shows the ES-MS of the three solutions, recorded in negative ion mode. In the EDTA spectrum, the following peaks can be observed (MM Na_2H_2EDTA = 336 Da):

145	$[H_2EDTA]^{2-}$	291	$[H_3EDTA]^-$
158	?	313	$[NaH_2EDTA]^-$
201	?	335	$[Na_2HEDTA]^-$

In the $In(NO_3)_3$ spectrum a single peak at *m/z* 363 appears, because of the presence of $In(NO_3)_4^-$. The top chromatogram shows that binding of $In(NO_3)_3$ to H_2EDTA^{2-} leads to a decrease of excess EDTA and formation of a peak at *m/z* 403, corresponding to the molecular ion $[InEDTA]^-$.

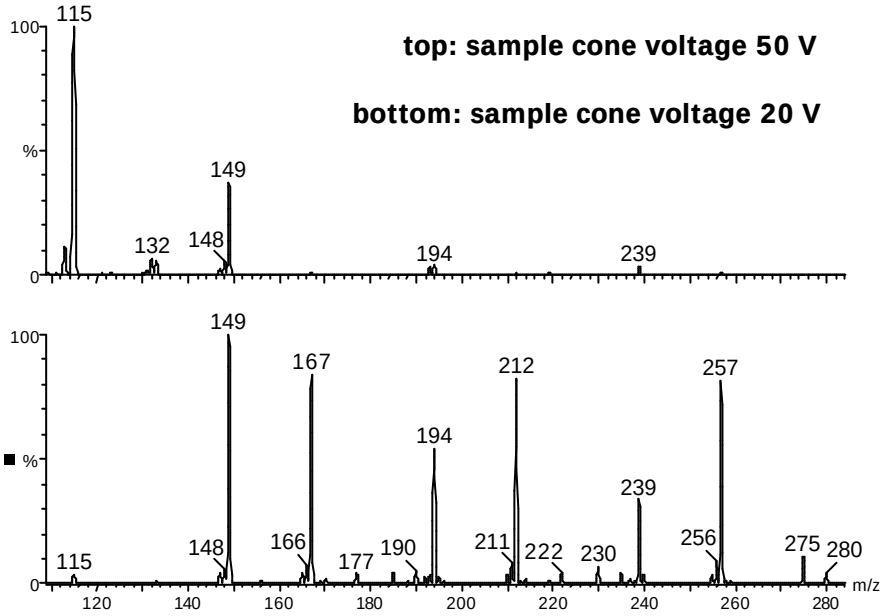

Figure 5.11. ES-MS spectra of $In(NO_3)_3$ using infusion full scan MS in positive ion mode. Sample cone voltage was set to 50 V (top) and 20 V (bottom). Intensity axes are linked.

Figure 5.11 shows two spectra of $In(NO_3)_3$ recorded in positive ion mode at different sample cone values. At the pH of 2.1-2.5, a wide range of indium complexes can be seen:

115	$[In]^+$	194	$[In(OH)(NO_3)]^+$	257	$[In(H_2O)(NO_3)_2]^+$
132	$[In(OH)]^+$	212	$[In(OH)(H_2O)(NO_3)]^+$	275	$[In(H_2O)_2(NO_3)_2]^+$
149	$[In(OH)_2]^+$	230	$[In(OH)(H_2O)_2(NO_3)]^+$		
167	$[In(OH)_2(H_2O)]^+$	239	$[In(NO_3)_2]^+$		

The relative abundance of these complexes is dependent on the sample cone voltage. A higher sample cone voltage leads to more in source fragmentation of the labile indium complexes and results in a higher relative abundance of the smaller indium complexes. It can thus not be stated that the spectra in figure 5.11 give a real image of the complexes in the solution.

Figure 5.12 shows the spectra of H_2EDTA^{2-} and H_2EDTA^{2-} + $In(NO_3)_3$ in positive ion mode using a sample cone voltage of 20 V. In the spectrum of EDTA, peaks at *m/z* 315 and 359 predominate, due to the presence of $[NaH_4EDTA]^+$ and $[Na_3H_2EDTA]^+$, respectively. In between these peaks, a small peak at *m/z* 337 can be seen, owing to the presence of $[Na_2H_3EDTA]^+$. In the spectrum of EDTA + indium, the peaks due to the presence of EDTA decrease and peaks at *m/z* 449 ($[InNa_2EDTA]^+$) and *m/z* 427 ($[InNaHEDTA]^+$) appear. The fact that no more peaks can be observed in the range m/z 110 to 280 (see figure 5.11) indicates that the indium is completely complexed by EDTA.

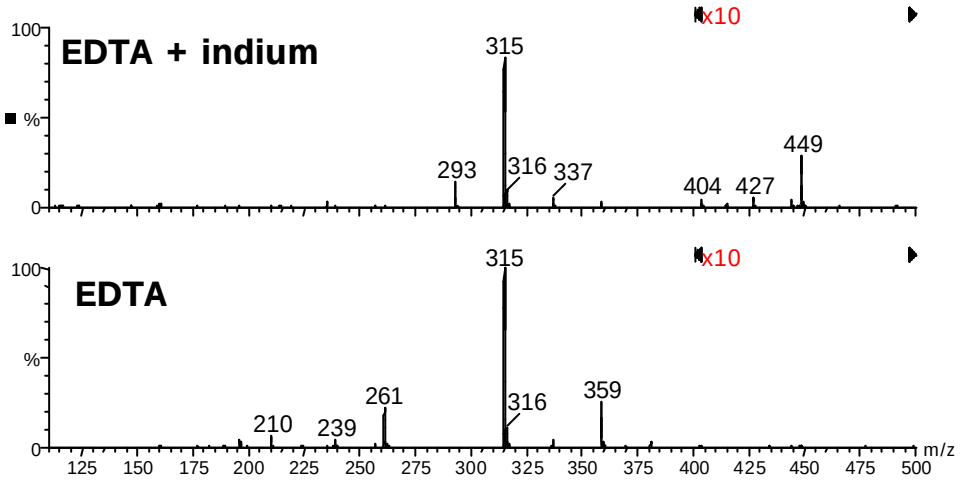

Figure 5.12. ES-MS spectra of H_2EDTA^{2-} + $In(NO_3)_3$ (top) and H_2EDTA^{2-} (bottom) using infusion full scan MS in positive ion mode. Sample cone voltage was set to 20 V. Intensity axes are linked. The area between *m/z* 400 and 500 is enhanced 10-fold.

The behaviour of pure $[^{114m}In]InCl_3$ tracer on Bio-Gel P2 (figure 5.13) and Mono Q (figure 5.14) was studied. When pure tracer is chromatographed with hepes buffer it elutes as a single peak at the same retention volume as in figure 5.6 (left) and 5.7. However, when the same tracer is separated in the presence of 0.9% NaCl, it elutes in the total volume (indicated by the increase in conductivity) of the column. Recovery is quantitative in case of a hepes elution, but only 42% in 0.9% NaCl.

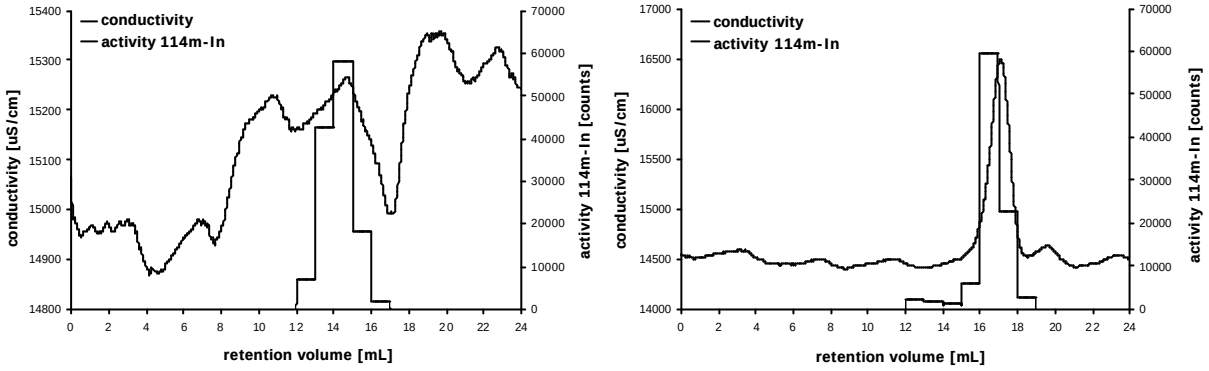

Figure 5.13. Chromatograms of pure [^{114m}In]$InCl_3$ separated on Bio-Gel P2 size exclusion column and eluted with hepes (left) and 0.9% NaCl (right).

The same conclusion can be drawn when indium tracer is eluted with tris:HCl buffer (figure not shown). The ^{114m}In activity appears at the same retention time as in the case of hepes. It is thought that indium is bound to the buffer and elutes as an In-hepes complex. This kind of behaviour has been reported in the past for soluble Fe^{3+} solutions complexed to tris:HCl buffer [Taillefert *et al.*, 2000]. When pure tracer is chromatographed with hepes on a Mono Q anion exchange column, again the same peaks appear as in figure 5.6 (right), indicating that there seems to be no difference between a pure solution of [^{114m}In]$InCl_3$ tracer and [^{114m}In]$InCl_3$ tracer in the LMM fraction of serum.

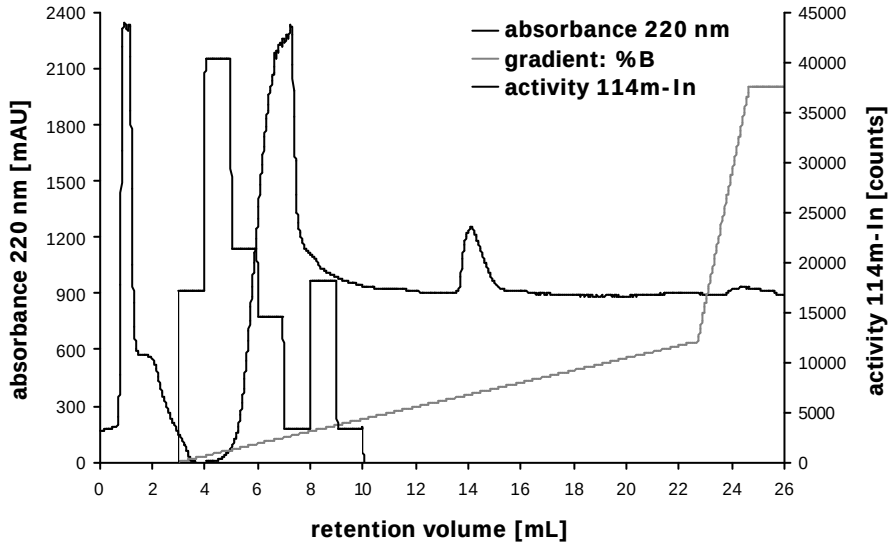

Figure 5.14. Chromatogram of pure [^{114m}In]$InCl_3$ separated on Mono Q anion exchange column and eluted with hepes.

Electrospray mass spectrometry was used to confirm the hypothesis that In^{3+} is complexed by the buffer. A low sample cone voltage was used since the experiments with EDTA showed that at moderate sample cone voltage, considerable in source fragmentation already occurred (for in source fragmentation, see 7.1.1). The sample cone voltage was set to 2 V. Solutions of 15 mM hepes, 1 mM $In(NO_3)_3$ and 15 mM hepes + 1 mM $In(NO_3)_3$ were analysed by infusion full scan MS in negative ion mode (figure 5.15). The spectrum for indium is identical to the one in figure 5.10 (a single peak at *m/z* 363 [$In(NO_3)_4^-$]) and is therefore not shown. Hepes (MM = 238 Da) is observed as the $[M-H]^-$ molecular ion (*m/z* 237) and $[2M-H]^-$ (*m/z* 475). The peak at *m/z* 283 is a result of a formic acid adduct [hepes + $HCOO]^-$. Formic acid was used just before to clean sample cone and syringe. Adding indium to a solution of hepes results in the formation of a complex with *m/z* 300, identified as $[hepes+indium]^{2-}$. Again the peak at *m/z* 346 is due to the formic acid adduct.

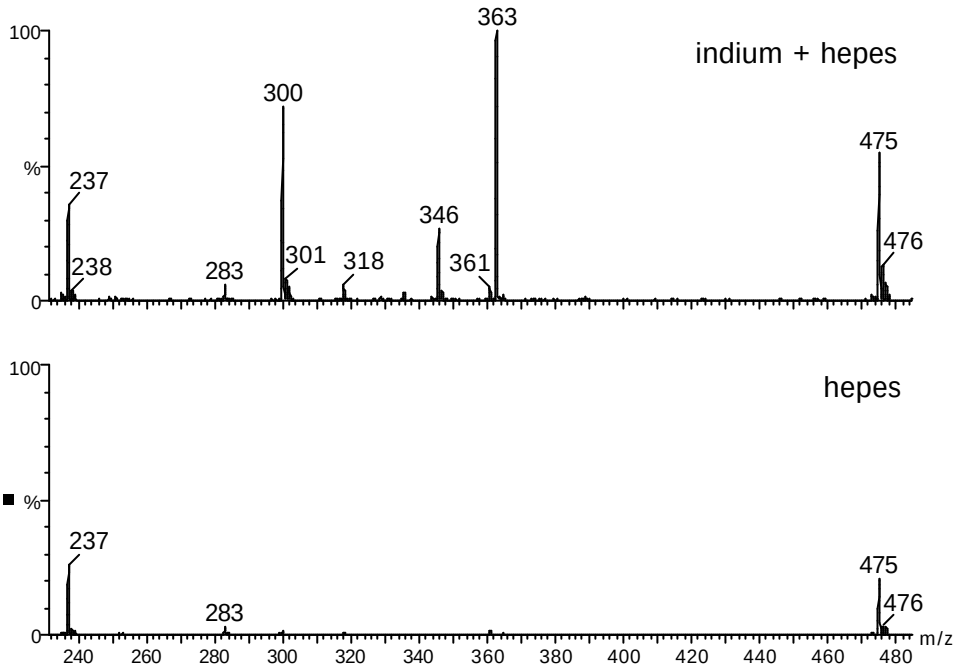

Figure 5.15. ES-MS spectra of $In(NO_3)_3$ + hepes (top) and hepes (bottom) using infusion full scan MS in negative ion mode. Cone voltage was set to 2 V.

5.3.3. Chromatography of indium species in packed cell lysate

Different columns were checked for their suitability in terms of ^{114m}In recovery. Superose 12 HR, Asahipak GS 520 7G, Bio-Gel P2, Bio-Gel P100 and Mono S were examined. Four *in vitro* incubation experiments of packed cell lysate with [^{114m}In]$InCl_3$ and separated on

Asahipak GS 520 7G each time resulted in a mean recovery of 53%. Bio-Gel P2 and P100 yielded quantitative results, but the self-packed Bio-Gel P100 did not give a satisfactory resolution. Figure 5.16 shows the chromatograms of packed cell lysate incubated with [^{114m}In]$InCl_3$ at different pH (2 and 7), separated on Superose 12 HR. Fractions of 0.5 and 1 mL, respectively, were taken and measured for their ^{114m}In content with a NaI(Tl) detector. As in the case of serum, also here the pH of the tracer determines the amount of LMM bound ^{114m}In. Surprisingly the ^{114m}In does not co-elute with haemoglobin. Haemoglobin represents 95% of the total erythrocyte protein content. The ^{114m}In elutes in the transferrin fraction. Transferrin is slightly heavier than haemoglobin (76 kDa versus 64.5 Da).

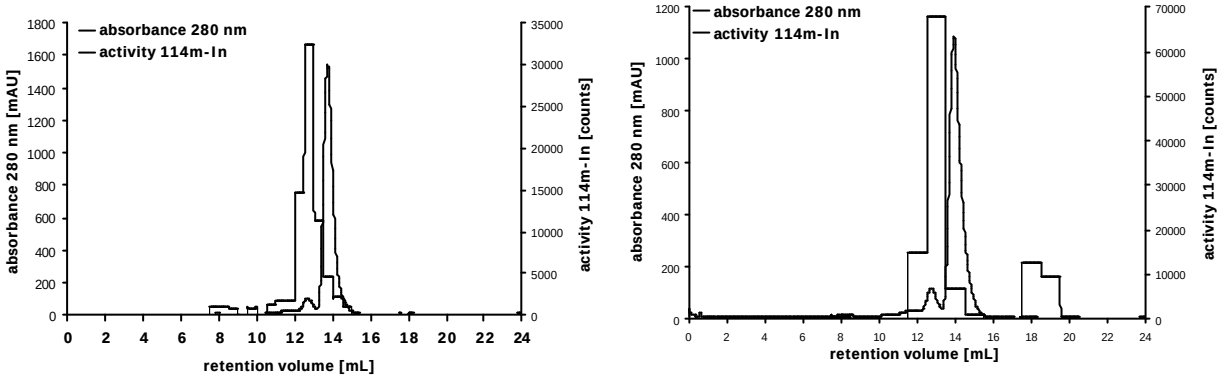

Figure 5.16 Chromatograms of packed cell lysate + [^{114m}In]$InCl_3$ with tracer at pH 2 (left) and at pH 7 (right) separated on Superose 12 HR size exclusion column.

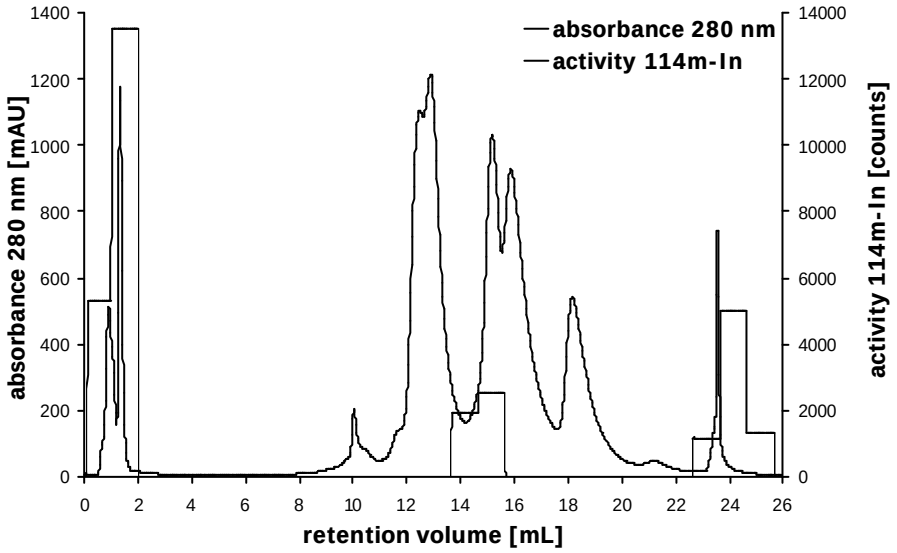

Figure 5.17 Chromatogram of packed cell lysate + ^{114m}In separated on Mono S cation exchange column.

This observation can also be seen when the packed cell lysate + [^{114m}In]$InCl_3$ mixture is eluted on the Bio-Gel P100 column (figure not shown). The fact that indium is not associated with haemoglobin, can be further illustrated by cation exchange chromatography on a Mono S column (figure 5.17). A packed cell lysate + [^{114m}In]$InCl_3$ mixture was chromtographed using 15 mM hepes (buffer A) and 15 mM hepes + 1 M LiCl (buffer B), both at pH 7.0. Recovery of ^{144m}In, however, was only 44%. No further effort was made to improve the quality of the chromatographic separation. It is known that the major share of the indium is associated with the serum fraction rather than with the packed cell fraction.

A list of all columns used throughout this work is given in table 5.5.

References

[Bantan and Milacic, 1998]

Bantan T and Milacic R (1998). *Talanta*, **47**, 929-941.

[Bergdahl *et al.*, 1996]

Bergdahl IA, Schütz A and Grubb A (1996). *J. Anal. At. Spectrom.*, **11**, 735-738.

[Chattopadhyay *et al.*, 1997]

Chattopadhyay S, Das MK, Sarkar BR and Ramamoorthy N (1997). *Appl. Radiat. Isot.*, **48**, 1063-1067.

[Diamond and Whitney, 1966]

Diamond RM and Whitney DC (1966). In *Ion Exchange: a Series of Advances* (ed. Marinsky JA), Marcel Dekker, New York, p 277-351.

[Harris *et al.*, 1994]

Harris WR, Chen Y and Wein K (1994). *Inorg. Chem.*, **33**, 4991-4998.

[Harris *et al.*, 1998]

Harris WR, Cafferty AM, Abdollahi S and Trankler K (1998). *Biochim. Biophys. Acta*, **1383**, 197-210.

[Hosain *et al.*, 1969]

Hosain F, McIntyre PA, Poulouse K, Stern HS and Wagner HN Jr (1969). *Clin. Chim. Acta*, **24**, 69-75.

[Hultkvist *et al.* [1987]

Hultkvist U, Westergren G, Hansson UB and Lewan L (1987). *Res. Exp. Med. Berl.*, **187**, 131-137.

[Kulprathipanja and Hnatowich. 1978]

Kulprathinpanja S and Hnatowich DJ (1978). *Int. J. Nucl. Med. Biol.*, **5**, 140-144.

[Lawson and Kahn, 1957]

Lawson KL and Kahn M (1957). *J. Inorg. Nucl. Chem.*, **5**, 87-92.

[Nitsch *et al.*, 1990]

Nitsch A, Kalcher K and Posch U (1990). *Fres. J. anal. Chem.*, **338**, 618-621.

[Raab and Brätter, 1998]

Raab A and Brätter P (1998). *J. Chromatogr. B*, **707**, 17-24.

[Sanz-Medel, 1995]

Sanz-Medel A (1995). *Analyst*, **120**, 799-807.

[Schweitzer and Coe, 1961]

Schweitzer GK and Coe GR (1961). *Anal. Chim. Acta*, **24**, 311-315.

[Skakun *et al.*, 1975]

Skakun EA, Klyucharev AP, Rakivnenko YN and Romanii IA (1975). *Izv. An. Sssr. Fiz.*, **39**, 24-30.

[Stary, 1963]

Stary J (1963). *Anal. Chim. Acta*, **28**, 132-149.

[Stern *et al.*, 1967]

Stern HS, Goodwin DA, Scheffel U, Wagner HN Jr and Kramer HH (1967). *Nucleonics*, **25**, 62-65,68.

[Taillefert *et al.*, 2000]

Taillefert M, Bono AB and Luther III GW (2000). *Environ. Sci. Technol.*, **34**, 2169-2177.

Table 5.5. Overview of FPLC columns used throughout this work.

	column and stationary phase composition	range [kDa]	resolution (SEC) [plates/m] ionic capacity [µmol/mL]	binding capacity [mg/mL]
SEC	Asahipak GS 520 7G (SD): vinyl alcohol copolymer, 9 µm	< 300	> 32000	
	Bio-Gel P2 (BR): copolymerised acrylamide and N,N'-methylene-bis-acrylamide, 45-90 µm	0.1 – 1.8		
	Bio-Gel P100 (BR): copolymerised acrylamide and N,N'-methylene-bis-acrylamide, 45-90 µm	5 - 100		
	Superose 12 HR (AB): highly cross-linked agarose, 10 ± 2 µm	1 - 300	>40000	
	Superdex Peptide HR (AB): spherical cross-linked agarose and dextran, 13 µm	0.1 - 7	>30000	
	HiPrep Sephacryl S-200 HR (AB): hydrophilic, rigid allyl dextran/bisacrylamide	5 - 250	5000	
AEC	Mono Q HR (AB): spherical monodispersed polystyrene divinylbenzene particles, 10 µm, quaternary ammonium strong anion exchanger	$< 10^4$	320 ± 50 Cl^-	65 (HSA)
	Mini Q HR (AB): non-porous monodispersed hydrophilic polyether, 3 µm, quaternary ammonium strong anion exchanger	$< 10^4$	75 ± 15 Cl^-	< 2 (HSA
	Hi Trap Q FF Sepharose (AB): 6% highly cross-linked agarose, ± 90 µm, quaternary ammonium strong anion exchanger	$< 4x10^3$	215 ± 35 Cl^-	120 (HSA)
AC	Hi Trap Blue Sepharose (AB): 6% highly cross-linked agarose, ± 34 µm, 4 mg cibacron blue 3G-A	$< 4x10^3$		20 (HSA)
CEC	Mono S HR (AB): spherical monodispersed polystyrene divinylbenzene particles, 10 µm, methyl sulfonate strong cation exchanger	$< 10^4$	160 ± 20 Na^+	75 (IgG)

(SD): Showa Denko, (AB): Amersham biosciences, (BR): Bio-Rad, (HSA): human serum albumin, (IgG): immunoglobulin

Chapter 6. Indium: *in vivo* experiments

Three series of *in vivo* experiments with Wistar rats were carried out in the course of this work. Each time five male Wistar rats were used. In a first experiment they were given an intraperitoneal injection of [^{114m}In]$InCl_3$. In a second and third experiment they got [^{114m}In]InAs either subcutaneously or orally. The purpose of the first experiment was to learn the organ distribution and chemical speciation of the indium tracer that is injected directly in the blood stream. InAs was chosen in the other two experiments because it is a frequently used semiconductor material. First the particles were parenterally injected, namely under the skin. The organ distribution and chemical speciation in the body fluids and target organs were examined. Secondly the rats were orally exposed to small particles of InAs. The bioavailability and toxic impact of the orally absorbed InAs particles were checked. The experimental conditions and results of each experiment will be discussed separately.

6.1. *In vivo* distribution and fractionation of indium in Wistar rats after intraperitoneal administration of [^{114m}In]$InCl_3$

6.1.1. Treatment of animals

Five male Wistar rats weighing between 200 and 250 g were maintained in individual polycarbonate cages in an environmentally controlled facility on a 12 h light/dark cycle. Handling of the animals (cleaning of the cages, injections) was done during the active dark period. The animals were allowed to acclimatise for 5 days. Food and water was supplied *ad libitum*. Each rat was given a daily intraperitoneal injection of 500 µL carrier-free 17.5 µCi [^{114m}In]$InCl_3$ on four consecutive days. Consecutive injections were preferred in order to mimic steady state conditions. The indium tracer, which was prepared according to the

procedure described in 5.1, was dissolved in a physiological hepes buffered saline solution. One hour after the last injection the animals were sacrificed. Blood was taken from the arteria carotis. Urine was collected only on the second day. Kidney, liver, spleen, hart, lung, testes, bone, skin, thyroid glands, bladder, stomach and small intestine were removed and washed with 0.9% NaCl solution. All samples were stored at -20°C prior to analysis.

6.1.2. Distribution of indium in the body compartments and in the blood

Depending on the amount of ^{114m}In radio activity and mass of the organ, the total organ or a portion were transferred into counting vials and their radioactivity measured with NaI(Tl) scintillation detection. The results, shown in table 6.1, are listed as % per gram organ (wet mass) and as % per organ (wet mass).

Table 6.1. *In vivo* organ distribution of ^{114m}In in rats (mean and SD of five rats) expressed as % per gram organ of total activity in all measured organs and as % per organ of total activity in all measured organs.

organ	% per g organ	% per organ
liver	16.5 (4.5)	69.2 (7.3)
kidney	17.1 (2.8)	10.8 (2.8)
hart	2.7 (0.5)	0.7 (0.3)
testes	2.8 (0.6)	2.3 (0.6)
thyroid gland	3.7 (0.5)	0.5 (0.1)
lung	4.4 (1.1)	2.0 (0.9)
spleen	21.8 (2.1)	4.2 (0.6)
stomach	6.6 (2.1)	3.0 (1.1)
bladder	13.4 (5.6)	0.9 (0.3)
small intestine	6.1 (2.9)	6.4 (3.1)
bone	4.9 (1.0)	[a]

[a]total bone mass not measured

In both cases the values are denoted as percentage of the total amount of ^{114m}In activity found in all measured organs. The high amount of ^{114m}In in kidney, liver and spleen is consistent with the findings of other studies done by Castronovo and Wagner [1973]. In that study it is stated that the chemical form of the metal largely determines the distribution of indium in body tissues. The kidney extensively accumulates ionic indium while the liver, spleen and the reticulo-endothelial system accumulate colloidal indium oxide. The experiments were done with mice. In the present study ^{114m}In, originally

dissolved in concentrated hydrochloric acid, was adjusted to physiological pH with NaOH and then dissolved in a hepes buffered saline solution. Base induced hydrolysis of In^{3+} solutions causes precipitation at physiological pH. The outcome depends on the nature of the counter-anion and on the particular base and is influenced by temperature and by ageing of the precipitate. If halide ions are present, they are likely to be incorporated in the precipitate ($In_2(OH)_3Cl_3$), but in their absence $In(OH)_3$ (hydrated indium oxide) is formed [Taylor and Brothers, 1993]. Considering that both kidney on the one hand and liver and spleen on the other hand account for a high amount of ^{114m}In activity, it might be supposed that the injected compound has mixed ionic and colloidal properties. Goodwin *et al.* [1966] developed a method for liver scanning using a ^{113m}In colloid. They found that 80% of the injected dose was localised in the liver. I found a value of 69.2 ± 7.3 %.

Table 6.2. Differential centrifugation schedule.

step	centrifugation parameters	outcome
1	300 x g, 10 min, 4°C	removal of intact cells and plasma membrane
2	1000 x g, 10 min, 4°C	precipitation of nuclei, cytoskeleton (A)
3	10000 x g, 20 min, 4°C	precipitation of mitochondria (B)
4	30000 x g, 30 min, 4°C	precipitation of lysosomes, peroxisomes (C)
5	100000 x g, 75 min, 4°C	precipitation of ribosomes and small vesicles (D)

Blood collected in anti-coagulant free vacuum tubes was centrifuged twice at 2000 x g and 4°C for 20 min. The packed cells were washed twice with 0.9% NaCl solution. Both the serum fraction and the packed cell fraction were diluted to the same volume and measured for their ^{114m}In activity with a Ge(Li) detector. The measurement time was set to keep the relative standard deviation below 1%. Serum carries the major share of the ^{114m}In activity in blood. About 90.2 ± 1.8% (mean ± sd, n=4) of total blood ^{114m}In could be found in serum. One rat did not absorb the last injection dose. In that case the amount of ^{114m}In in serum was only 75.0%. This is possibly due to the fact that the clearance of indium from blood cells is slower than the clearance of indium from serum.

Target organs (liver, kidney and spleen) were minced and a 1 + 4 suspension in 0.25 M sucrose solution containing 15 mM hepes at pH 7.4 was lysed in a borosilicate Potter-Elvehjem type homogeniser fitted with a Teflon pestle. For the intracellular fractionation of

^{114m}In in the target organs a five-step differential centrifugation program was used (see table 6.2). By differentially increasing the centrifugal speed, smaller intracellular organelles will be precipitated. After each step, the homogenate and pellet are separated and a next step is carried out on the liquid fraction. The filtrate after step 5 consists of the cytosolic fraction (E) [Chen *et al.*, 1999]. After centrifugation all pellets and homogenates were diluted to the same volume and the ^{114m}In activity was measured with a Ge(Li) detector. The counting time was set variable in order to keep the relative standard deviation below 2%. Table 6.3 shows the results of the *in vivo* intracellular distribution of ^{114m}In in kidney, liver and spleen. In all cases the cytosolic fraction accounts for the highest activity of ^{114m}In, followed by the mitochondrial fraction. Fowler *et al.* found that rats, given a single intraperitoneal injection of $InCl_3$ in doses up to 40 mg/kg, showed an increased number of In-containing autophagic lysosomes [Fowler *et al.*, 1983]. This finding could not be confirmed. However, the difference might be due to the fact that in our study non-toxic tracer doses of In^{3+} were administered.

Table 6.3. *In vivo* intracellular distribution (mean and SD of 5 rats) of ^{114m}In in kidney, liver and spleen. A: pellet of nucleus, B: pellet of mitochondria, C: pellet of lysosomes and peroxisomes, D: pellet of ribosomes and small vesicles, E: homogenate containing cytosol. Results denoted as percentage of total activity within each tissue homogenate.

	kidney	liver	spleen
% in A	9.7 (4.10	6.3 (0.3)	3.4 (1.4)
% in B	22.5 (1.0)	14.1 (2.2)	18.7 (2.9)
% in C	5.7 (2.6)	1.7 (0.5)	7.7 (1.6)
% in D	15.3 (1.0)	4.6 (0.4)	11.8 (1.5)
% in E	46.8 (3.6)	73.3 (3.3)	58.4 (5.3)

6.1.3. Fractionation of indium in body fluids

The chromatographic separations were done with the Äkta Purifier 10 fast protein liquid chromatography system. Before injection into the system, all samples were filtered through 0.22 µm syringe filters. All buffers were also filtered through a 0.22 µm filter and vacuum degassed. Proteins were detected by means of UV/VIS absorption spectrometry at 254, 280 and 410 nm. The detection and quantification of albumin, transferrin, immunoglobulines was done by means of nephelometry.

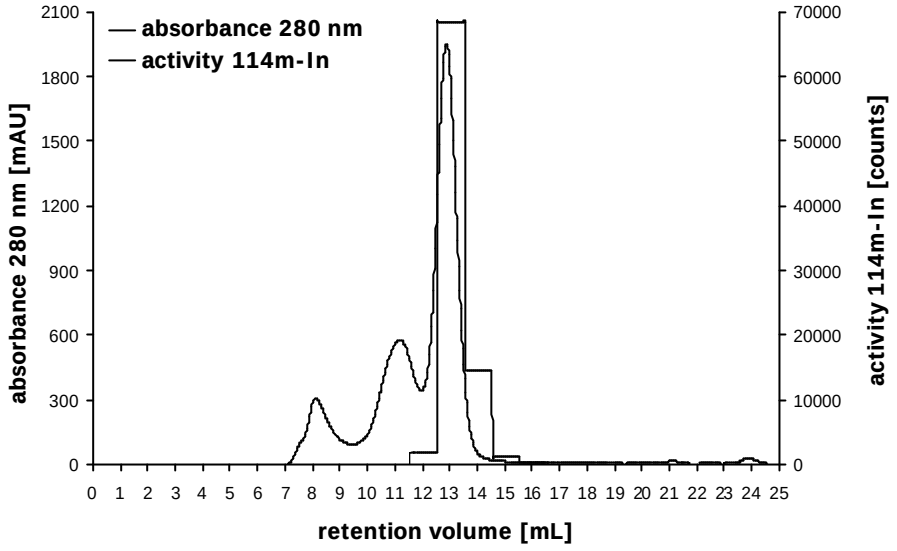

Figure 6.1. Chromatogram of [^{114m}In]$InCl_3$ / rat serum separated on Superose 12 HR size exclusion column.

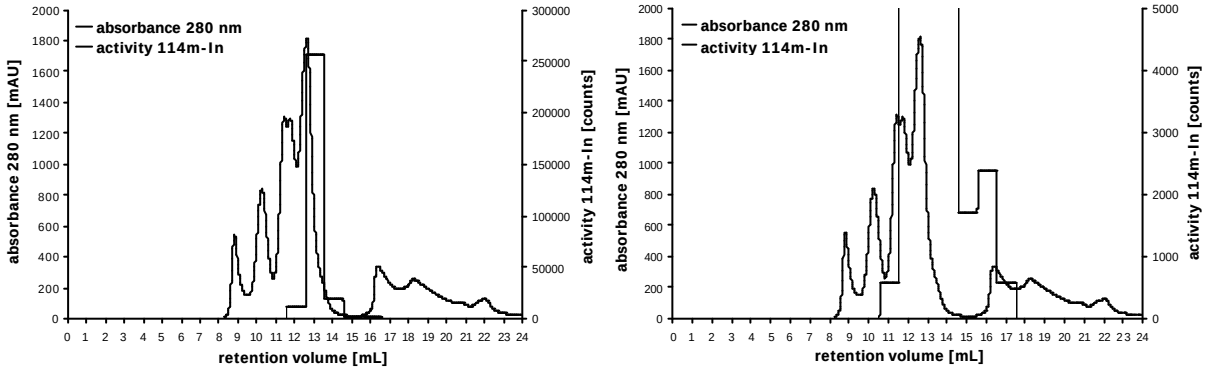

Figure 6.2. Chromatogram of [^{114m}In]$InCl_3$ / rat serum separated on Asahipak 520-GS 7G size exclusion column. Same chromatogram with enlarged scale for the ^{114m}In activity (right).

200 µL of 1+2 diluted rat serum was separated on a Superose 12 HR size exclusion (range 5 - 300 kDa) column and also on an Asahipak 520 GS 7G multi-mode (exclusion limit 300 kDa) column. A 10 mM hepes + 5 mM $NaHCO_3$ + 0.15 M NaCl, pH 7.4 elution buffer was used. Fractions of 0.5 or 1 mL were collected and the ^{114m}In activity was measured by means of NaI(Tl) scintillation counting. The results of the chromatographic separation of rat serum are shown in figures 6.1 (Superose) and 6.2 (Asahipak). One peak at the retention time of transferrin can be observed in the chromatogram of serum separated on the Superose column. A slight increase in the ^{114m}In activity over the albumin fraction can be seen in the case of separation on the Asahipak column. *In vitro*, there is - depending on the pH of $InCl_3$ - a varying amount of indium bound to transferrin and a low molecular

mass compound and a negligible amount of indium is bound to albumin. Also *in vivo* a small amount seems to be bound to albumin. On the other hand *in vivo* indium is not bound to LMM compounds.

500 µL undiluted rat serum was also separated using anion exchange chromatography on a Hi Trap Q anion exchange column. The result can be seen in figure 6.3. The majority of the indium activity is associated with the transferrin fraction although a small fraction can be observed in the albumin fraction and also in the void volume. The amount of ^{114m}In associated with albumin varies between 0.5 and 0.8% (4 sera of 2 rats).

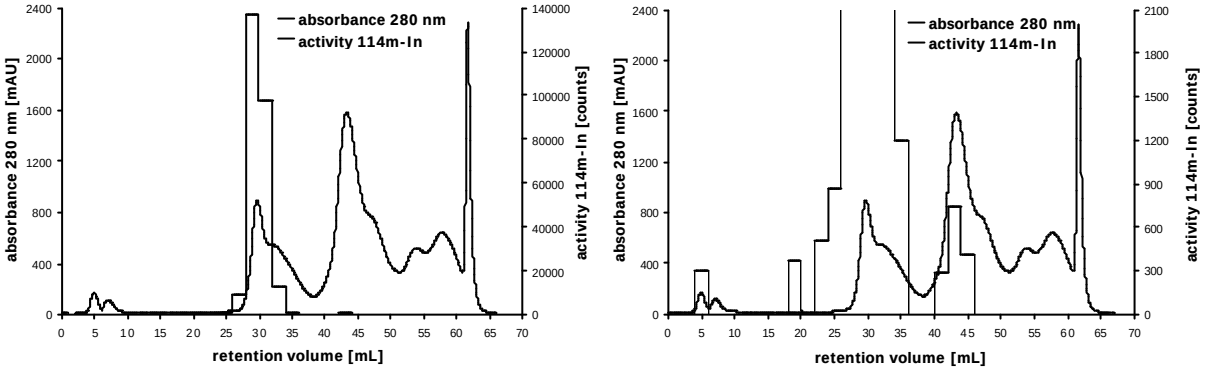

Figure 6.3. Chromatogram of [^{114m}In]$InCl_3$ / rat serum separated on Hi Trap Q anion exchange column. Same chromatogram with detailed activity axis (right).

Prior to chromatographic separation, packed cells were lysed by successive thawing and freezing. Afterwards the partially lysed cells were diluted 1 + 5 in elution buffer and further disrupted in a Potter-Elvehjem homogeniser. Afterwards the homogenate was centrifuged at 13000 x g and 4°C during 40 min to remove remaining cell membranes. No separation was made between red (>99%) and white (<1%) blood cells. A volume of 200 µL was injected on a Superose 12 HR; 1 mL was brought onto a self-packed Sephacryl S-200 HR size exclusion (range 5-250 kDa) column. Fractions of 1 and 2 mL, respectively were measured for their ^{114m}In activity with a NaI(Tl) scintillation detector. Elution was done with a 15 mM hepes + 0.15 M NaCl, pH 7.2 buffer. The chromatogram of the *in vivo* speciation of ^{114m}In in blood cell lysate separated on the Superose 12 HR column is shown in figure 6.4. As was also noted during the *in vitro* experiments ^{114m}In comes slightly ahead of the haemoglobin. In^{3+} is said to influence the haem biosynthesis in red blood cells by inhibiting the enzymatic activity of δ-aminolevulinic acid dehydratase (ALAD) [Conner *et al.*, 1995]. ALAD catalyses the second step of the pathway, *i.e.*, the condensation of aminolevulinic

acid to form the monopyrole, porphobilinogen [Goering *et al.*, 1987]. From the chromatogram it can be seen that there is no major association between indium and the enzyme (*MM* 290 kDa), which elutes at the retention volume 7-9 mL. It could be postulated that the influence of indium on the haem biosynthetic pathway is caused by an indirect interaction, rather than to be due to a direct binding to the enzyme, as has been stated for lead *e.g.*, [Bergdahl and Schütz, 1996]. In the latter case, lead displaces zinc from its SH-mediated binding site, thereby producing an inhibitory effect. In order to confirm the finding about no association between ALAD and indium, the experiments were repeated on a Sephacryl S-200 HR column. The results were the same.

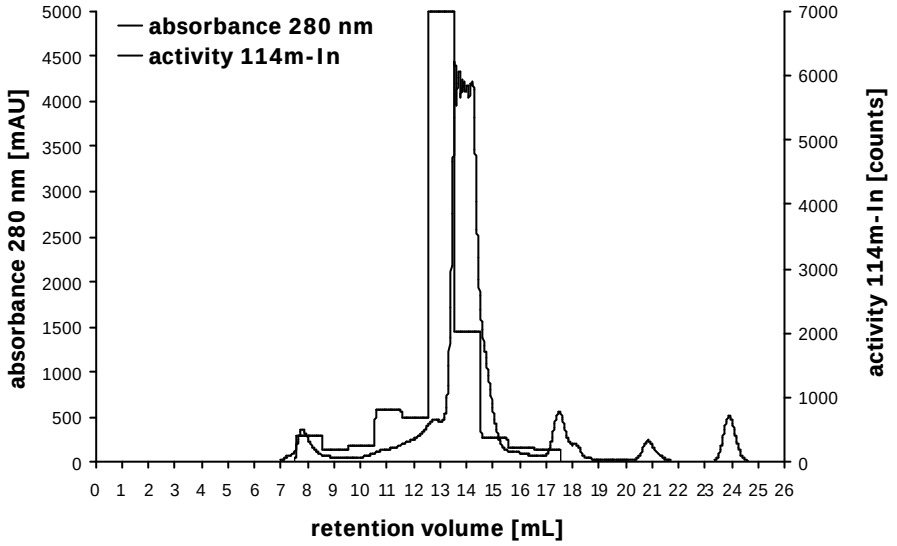

Figure 6.4. Chromatogram of [^{114m}In]$InCl_3$ / rat blood cell lysate separated on Superose 12 HR size exclusion column.

200 µL of undiluted urine was injected on a Superdex Peptide HR size exclusion column. The working range of this column covers the low molecular mass fraction (100 - 7000 Da). Fractions of 1 ml were taken and the activity was measured with a NaI(Tl) scintillation detector. Elution was done with a 15 mM hepes + 0.15 M NaCl, pH 6.5 buffer. The separation of rat urine on size exclusion chromatography is shown in figure 6.5. In urine, indium is mostly bound to the low molecular mass fraction, with a maximum at the retention volume 16.5 - 17.5 mL, corresponding to a molecular mass of 300 - 1000 Da; only a small amount of ^{114m}In can be found in the void volume (> 7000 Da). In chapter 5 where the binding of In^{3+} to the low molecular mass fraction in serum was discussed, we have postulated that indium occurs as $In(OH)_3$, though is possibly complexed by the buffer (hepes and tris:HCl). Taillefert *et al.* [2000] have reported a similar behaviour for soluble

Fe^{3+} solutions complexed to tris:HCl buffer. In urine similar complexation between free In^{3+} and elution buffer might occur.

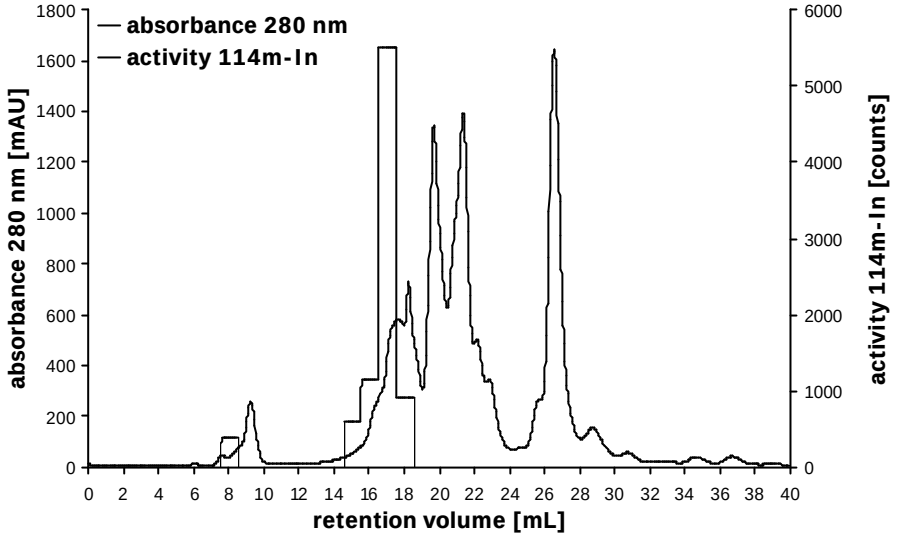

Figure 6.5. Chromatogram of [^{114m}In]$InCl_3$ / rat urine separated on Superdex Peptide size exclusion column.

6.1.4. Fractionation of indium in organs

Liver, kidney, spleen and lung were minced and homogenised as described above and the soluble fraction was obtained after centrifugation at 100000 x g and 4°C for 100 min. A volume of 200 µL 1+1 diluted or undiluted solution was injected on a Superose 12 HR column. Fractions of 0.5 or 1 mL were taken and the activity was measured with a NaI(Tl) scintillation detector. Elution was done with a 15 mM hepes + 0.15 M NaCl, pH 7.2 buffer. The results of the separation of liver, kidney, spleen and lung cytosol with size exclusion chromatography are shown in figure 6.6. In all cases, it appears that indium preferentially binds to the high molecular mass fraction. Small amounts appear in he void and in the total volume of the column in the case of spleen, liver and lung. A considerable amount of ^{114m}In appears in the total volume of the column in case of the kidney. This high amount of ^{114m}In in the HMM fraction might be partly due to serum transferrin still present in the organs after homogenisation. However, the activity peak in both cases is much broader than in the case of rat serum whereas the concentration of the residual transferrin in the organs should be much lower than in serum. Thus, it is expected that another high molecular mass compound is capable of binding indium, leading to an unresolved ^{114m}In activity peak. This

is illustrated in figure 6.7. For serum, and the homogenates of kidney, liver and spleen, an identical chromatographic separation was carried out, but fractions of 500 µL were collected instead of 1 mL. Details of the chromatograms are shown in the figures. It can clearly be seen that the elution profile of ^{114m}In shows a much broader peak shape in case of the organ tissue homogenates compared to that in serum. The fact that In^{3+} binds to more than one HMM compound can also be derived from the anion exchange experiments on the Hi Trap Q column. This is illustrated in figure 6.8.

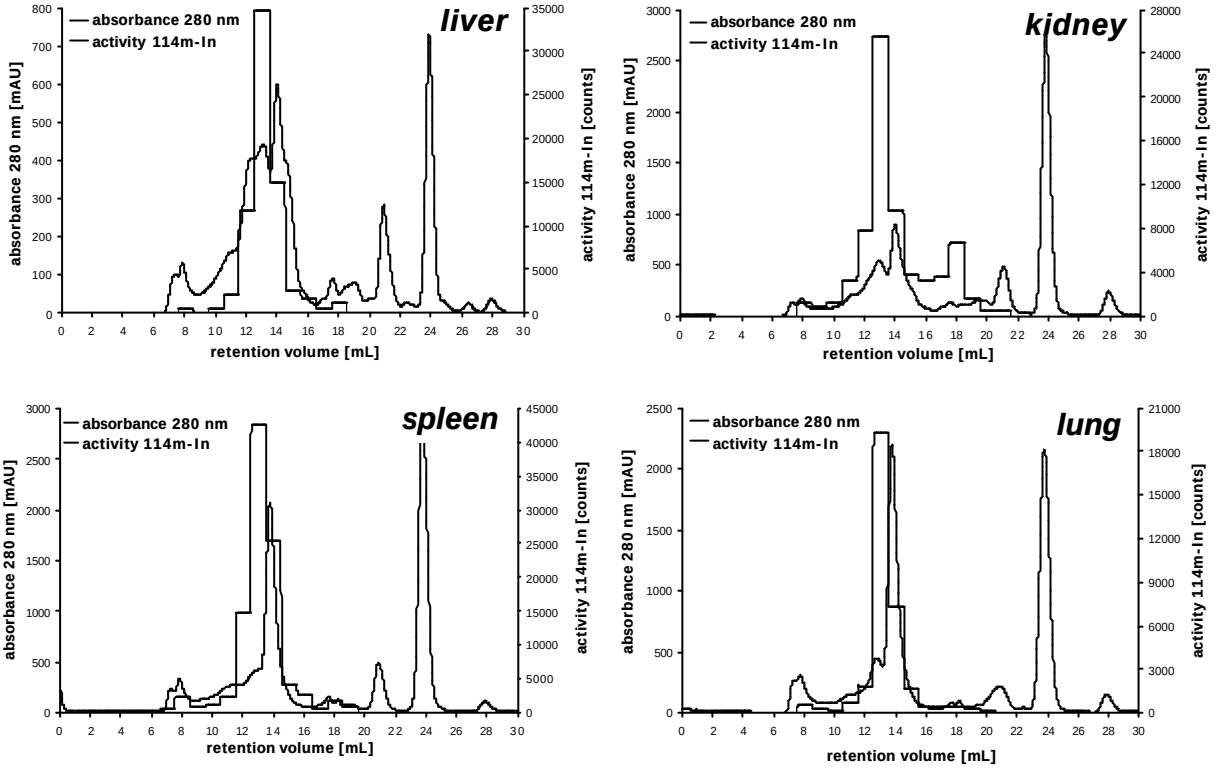

Figure 6.6. Chromatograms of [^{114m}In]$InCl_3$ / rat liver cytosol (top left), [^{114m}In]$InCl_3$ / rat kidney cytosol (top right), [^{114m}In]$InCl_3$ / rat spleen cytosol (bottom left) and [^{114m}In]$InCl_3$ / rat lung cytosol (bottom right) separated on Superose 12 HR size exclusion column.

The activity can be found over different fractions. The ^{114m}In activity found at the retention time around 30 minutes is most probably due to transferrin. In the case of lung cytosol this is clearly illustrated. Removal of blood from this organ was difficult to achieve and this possibly explains the high amount of indium activity recovered from this fraction. All cytosolic fractions show an analogous distribution pattern of ^{114m}In.

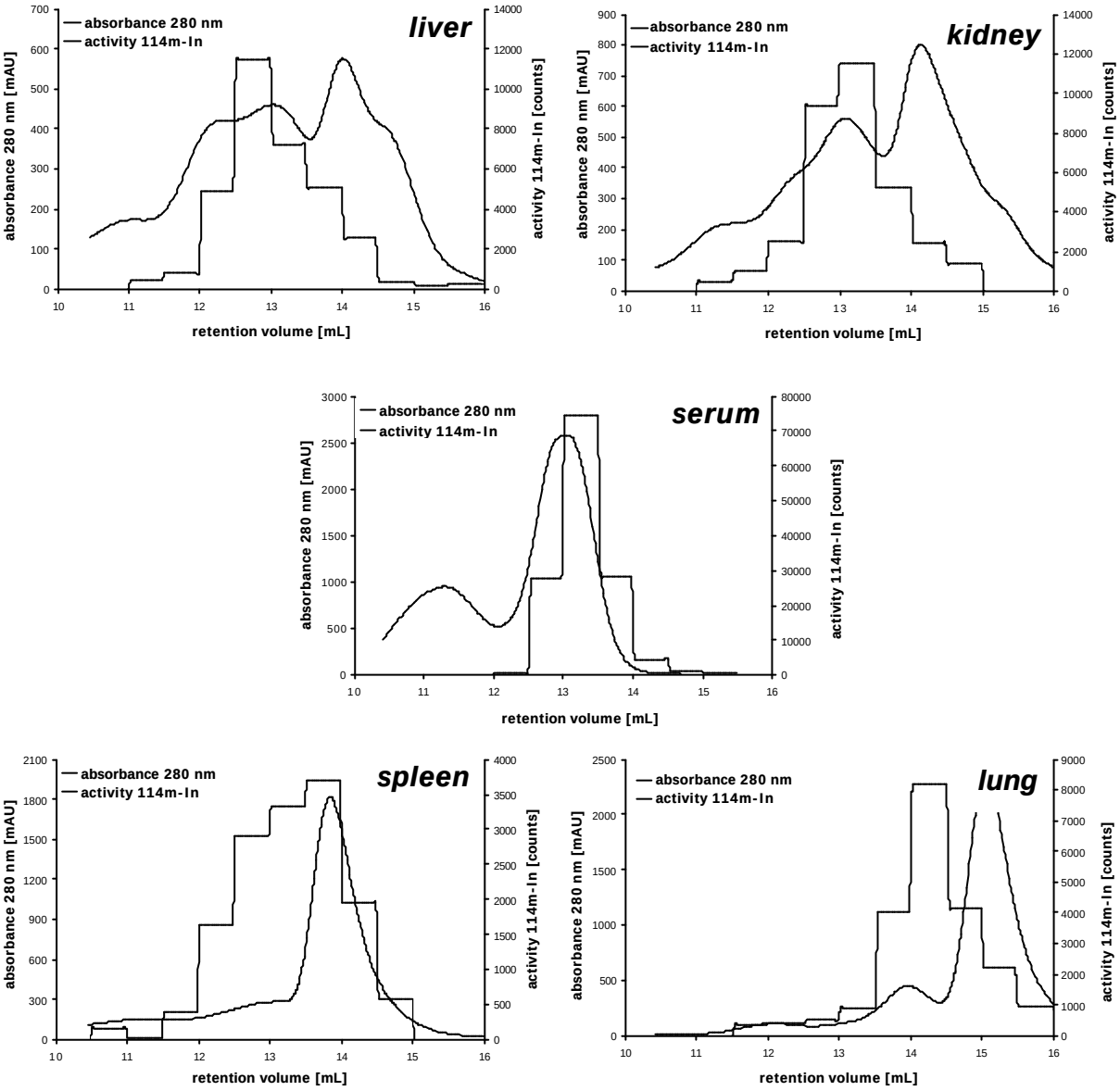

Figure 6.7. Detailed part of chromatogram of [^{114m}In]$InCl_3$ / rat liver cytosol (top left), [^{114m}In]$InCl_3$ / rat kidney cytosol (top right), [^{114m}In]$InCl_3$ / rat serum (middle), [^{114m}In]$InCl_3$ / rat spleen cytosol (bottom left) and [^{114m}In]$InCl_3$ / rat lung cytosol (bottom right) separated on Superose 12 HR size exclusion column.

Only in the case of kidney cytosol does a considerable amount of indium appear in the low molecular mass fraction. In^{3+} influences hepatic and renal ALAD activity *in vitro*; however, In^{3+} inhibits only renal ALAD *in vivo*. [Woods and Fowler, 1982]. These authors postulated that this tissue-specific effect is due to the preferential accumulation of indium by the kidney proximal-tubule cells with selective localisation in the cytosol. Zinc reverses the indium-induced inhibition of renal ALAD *in vitro* and *in vivo*, suggesting that indium acts by binding groups on the enzyme. Although we also found that indium preferentially

accumulated in the cytosolic fraction, the chromatogram shows no direct binding of indium with ALAD and thus replacement of zinc. Therefore the inhibition may be rather due to some other indirect interaction. Again the fact that background levels, far below toxic doses have been used throughout these experiments may be a plausible explanation for the differences between both findings.

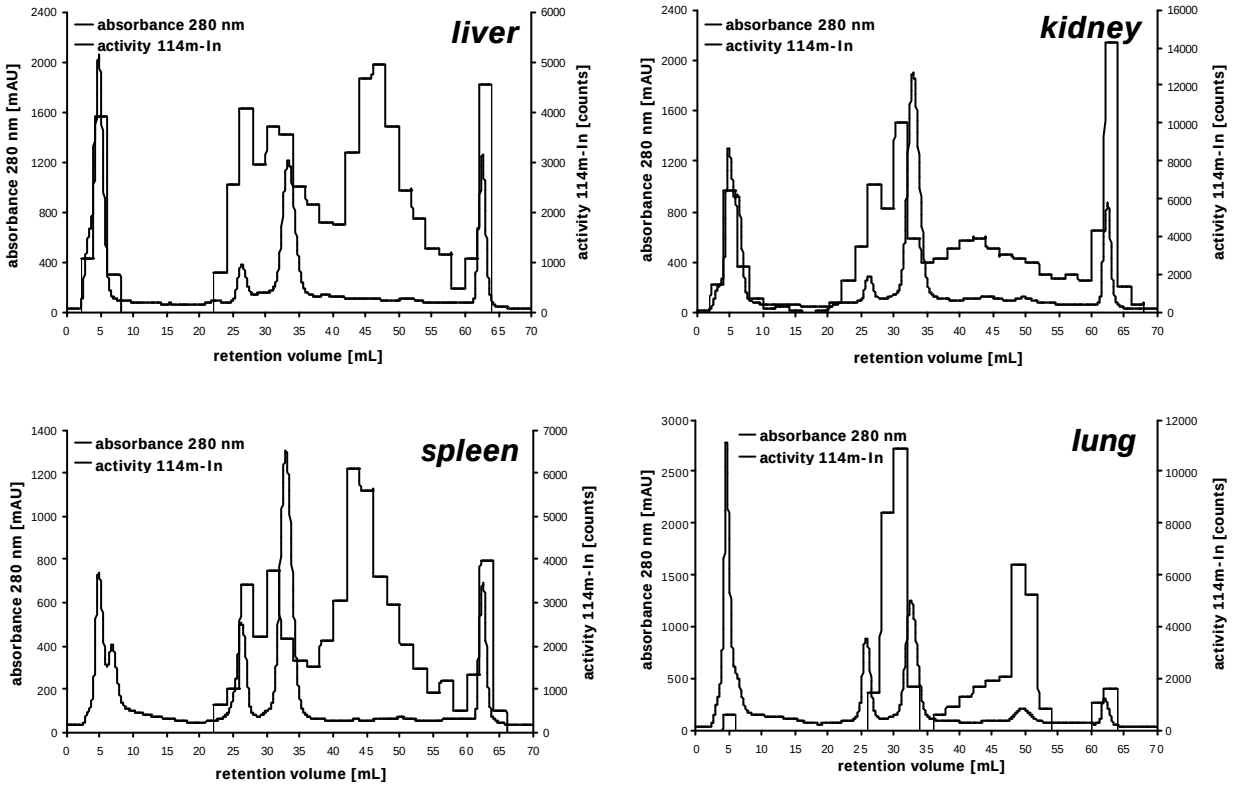

Figure 6.8. Chromatogram of [^{114m}In]$InCl_3$ / rat liver cytosol (top left), [^{114m}In]$InCl_3$ / rat kidney cytosol (top right), [^{114m}In]$InCl_3$ / rat spleen cytosol (bottom left) and [^{114m}In]$InCl_3$ / rat lung cytosol (bottom right) separated on Hi Trap Q anion exchange column.

6.2. *In vivo* distribution and fractionation of indium in Wistar rats after subcutaneous administration of [^{114m}In]InAs

6.2.1. Production of [^{114m}In]InAs

The production of [^{114m}In]InAs can be obtained via two possible routes. In-house produced ^{114m}In (as a hydroxide or a salt) could be used for the manufacturing of InAs by epitaxial layer growth techniques. Alternatively InAs could be irradiated in a nuclear reactor. The first approach could not be considered due to practical limitations. The disadvantage of the second approach would be the extremely long irradiation time. ^{114m}In can be obtained by neutron bombardment of ^{113}In. However, the natural abundance of this isotope is only 4.33%. Given the fact that the thermal neutron flux of the Thetis reactor of our institute is only 1 x 10^{12} $n.s^{-1}.cm^{-2}$, obtaining a substantial amount of ^{114m}In would take several months. Therefore it was decided to use the facilities of the Study Centre for Nuclear Energy (SCK, Mol Belgium). Commercially available InAs was grinded in an agate mortar in order that the main particle size was below 10 µm, as controlled with a microscope. The powder was irradiated for 1 week in the BR-II reactor at the SCK with a neutron flux of $1.5x10^{14}$ $n.s^{-1}.cm^{-2}$. This was 100 times as high as in our institute. [^{114m}In]InAs is formed by the nuclear reaction ^{113}In (n,γ) ^{114m}In ($t_{½}$ 49.5 d). A cooling period of several weeks was respected for radioactive decay of the short living ^{116m}In ($t_{½}$ 54.2 min) and ^{76}As ($t_{½}$ 26.3 h).

6.2.2. Treatment of animals

Five male Wistar rats weighing between 200 and 250 g were maintained in individual polycarbonate cages in an environmentally controlled facility on a 12 h light/dark cycle. The animals were allowed to acclimatise for at least 7 days. Food and water was supplied *ad libitum*. Handling of the animals (cleaning of the cages, injections) was done during the active dark period. Every rat was given two subcutaneous injections of 200 µL containing a suspension of 450 µCi [^{114m}In]InAs each on day 1 and 2. The total amount was equivalent to a dose of 50 mg InAs per kg body mass. The indium tracer was suspended in a physiological hepes buffered saline solution. Two rats were housed in a metabolic cage in order to collect urine and faeces. 15 days after the first injection the animals were sacrificed. Blood was taken from the arteria carotis. Kidney, liver, spleen, hart, lung, testes,

bone, skin and fur, bladder, stomach, small and large intestine were removed and washed with 0.9% NaCl solution. Blood, urine and organs were stored at -20°C prior to analysis.

6.2.3. Distribution of indium in the body compartments

Figure 6.9 shows the clearance of indium by faecal excretion after subcutaneous administration of [^{114m}In]InAs. The highest amount of activity was found at the first collection, two days after the first injection. After 8 days, no further decrease in faecal ^{114m}In activity was noticed. A given amount of ^{114m}In found in the faeces after two days means that *in vivo* dissociation and uptake by the blood must have occurred within this time span. Most of this indium is, however, not stored in the organs and excreted through the faeces. Probably more and more indium is taken up by the organs within the next days to reach an equilibrium between absorbed and unabsorbed indium after 8 days. Only on the second day after the first injection, a detectable amount of ^{114m}In was found in the urine. The major route of excretion is thus faecal.

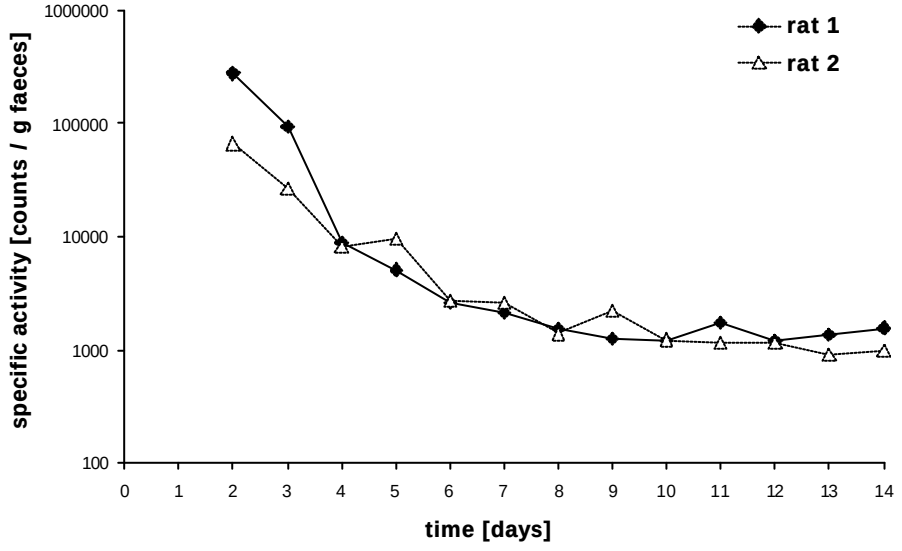

Figure 6.9. Faecal excretion of ^{114m}In in function of time.

Depending on the amount of ^{114m}In and mass of the organ, the total organ or a portion was transferred into polyethylene counting vials and its radioactivity was measured with a NaI(Tl) scintillation detector for 5 min. The *in vivo* distribution of indium over the different organs after sc injection of [^{114m}In]InAs is listed in table 6.4. The results are shown as percentage per gram organ (wet mass) and percentage per organ (wet mass). In both

cases the values are expressed as the percentage of the total amount of ^{114m}In activity found in all measured organs. On a percentage per gram organ base, spleen, kidney and liver account for the majority of the indium activity. On a percentage per organ base, liver is the major target organ. The results are also in close agreement with those obtained after intraperitoneal administration of [^{114m}In]$InCl_3$ (see 6.1.2). This could indicate that InAs behaves similarly to $InCl_3$ *in vivo*. Yamauchi *et al.* [1992] have postulated that InAs is partially dissociated *in vivo* to form inorganic arsenic and indium. Experiments were done with hamsters that were given a single s.c. injection of InAs at a dose of 100 mg/kg body mass. They concluded that InAs dissolves slowly over time with deposits at the site of injection. They also measured the concentrations of indium in liver, kidney, lung and spleen up to 30 days after the administration. The highest concentrations were found in kidney followed by liver. Lower amounts appeared in spleen and lung. For all organs a maximum value was obtained after 30 days. Also in our case a major amount of ^{114m}In activity was deposited at the site of injection and dissolved slowly over time. In this study 15 days was respected between the time of administration and sacrificing.

Table 6.4. *In vivo* organ distribution of ^{114m}In (mean and SD of 5 rats) in rats expressed as % per gram organ (wet mass) and as % per organ of total activity in all measured organs. [a] total bone, skin & fur and tissue mass not measured.

organ	mass [g]	% per g organ	% per organ
large intestine	2.5 (0.5)	2.3 (0.3)	1.6 (0.1)
small intestine	4.2 (0.7)	2.4 (0.5)	2.9 (0.3)
stomach	1.6 (0.2)	2.7 (0.3)	1.3 (0.2)
testes	3.3 (0.3)	3.8 (0.2)	3.7 (0.4)
hart	1.1 (0.1)	3.3 (0.5)	1.0 (0.1)
lung	2.1 (0.3)	3.6 (0.7)	2.2 (0.5)
spleen	0.8 (0.1)	26.8 (4.3)	6.2 (1.5)
kidney	2.6 (0.2)	26.3 (2.6)	20.5 (2.6)
liver	17.2 (1.6)	12.0 (0.8)	60.5 (2.6)
bone	[a]	7.1 (0.5)	[a]
skin & fur	[a]	7.0 (4.7)	[a]
tissue	[a]	2.1 (0.6)	[a]
	[a] total mass not measured		

Organs were minced and a 1 + 4 suspension in 0.25 M sucrose solution containing 15 mM hepes, pH 7.4 and lysed in a mechanical homogeniser. For the intracellular fractionation of ^{114m}In in liver, kidney and spleen the same five-step centrifugation program as described above was used. After centrifugation all pellets and homogenates were diluted to the same

volume and the ^{114m}In activity was measured with a Ge(Li) detector. The counting time was set variable in order to keep the relative standard deviation below 2%.

Table 6.5 shows the results of the *in vivo* intracellular distribution of ^{114m}In in kidney, liver and spleen after sc administration of [^{114m}In]InAs. In all cases the cytosolic fractions account for the highest activity of ^{114m}In. Lower amounts of indium can be found in the mitochondrial fraction of kidney, liver and spleen and in the nuclear fraction of spleen. These results are again in close agreement with those obtained in a previous study, except for the rather high amount of ^{114m}In in the nuclear fraction of spleen found in this experiment. Moreover it was not possible to show an increased amount of indium-containing autophagic lysosomes, as was postulated by Fowler *et al.* [1983].

Table 6.5. *In vivo* intracellular distribution of ^{114m}In (mean and SD of 5 rats) in kidney, liver and spleen. A: pellet of nucleus, B: pellet of mitochondria, C: pellet of lysosomes and peroxisomes, D: pellet of ribosomes and small vesicles, E: homogenate containing cytosol. Results denoted as percentage of total activity within each tissue homogenate.

	liver	spleen	kidney
% in A	2.4 (1.7)	20.1 (9.1)	10.2 (1.1)
% in B	14.2 (5.6)	16.4 (3.7)	19.2 (0.7)
% in C	4.1 (1.4)	12.7 (2.1)	6.2 (1.4)
% in D	8.1 (2.2)	10.6 (0.5)	7.4 (2.0)
% in E	71.2 (5.3)	40.1 (6.7)	57.0 (1.4)

6.2.4. Fractionation of indium in body fluids and organs

Blood was centrifuged twice at 2000 x g and 4°C for 20 min. The packed cells were washed twice with 0.9% NaCl solution. Both the serum fraction and the packed cell fraction were diluted to the same volume and measured for their ^{114m}In activity with a Ge(Li) detector. The measurement time was set to keep the relative standard deviation below 1%. At the end of the experiment 77% of all blood activity was found in serum. This is due to the high affinity for the serum protein transferrin, which transfers many metals, especially trivalent metals, to the target organs.

The chromatographic separations were done in analogy with the experiments described above. A semi-preparative Sephacryl S-200 HR size exclusion (range 5-250 kDa) column

and a self-packed Bio-Gel P2 (range 0.1-1.8 kDa) size exclusion column were used. The low activity present in the samples did not allow the use of analytical columns. Instead semi-preparative columns with a higher sample load capacity, but lower resolution, had to be chosen. 500 µL undiluted rat serum was injected on both columns and eluted with a 10 mM hepes + 5 mM $NaHCO_3$ + 0.15 M NaCl, pH 7.4 elution buffer. Fractions of 1 or 2 mL were collected and the ^{114m}In activity was measured by means of NaI(Tl) scintillation counting. Figures 6.10a shows the chromatogram of the separation of rat serum on the Sephacryl S-200 size exclusion chromatography column. The chromatogram shows that indium is almost exclusively bound to the high molecular mass, namely with a compound eluting at around 57 mL. This is also the retention volume of transferrin. The same conclusion can be drawn from the separation on the Bio-Gel P2 column (figure not shown): the ^{114m}In activity appears in the dead volume of the Bio-Gel P2 column, indicating that indium is associated with the mass fraction above 1.8 kDa. In paragraph 6.1.3 it was shown that in rat serum, after i.p. injection of [^{114m}In]$InCl_3$, indium is associated with transferrin. It seems that indium shows a similar behaviour in serum after injections of InAs or $InCl_3$. The route of exposure appears to be of minor importance. With these columns it is impossible to separate albumin from transferrin. Therefore rat serum was also chromatographed with anion exchange on a Hi Trap Q column with 10 mM hepes + 5 mM $NaHCO_3$, pH 7.4 (buffer A) and 10 mM hepes + 5 mM $NaHCO_3$, pH 7.4 + 1 M NaCl, pH 7.4 (buffer B). The result is shown in figure 6.10b. Except for a small (6.6%) amount of ^{114m}In recovered from the void volume, only one peak eluting at the retention time of transferrin can be seen. No radioactivity is found in the albumin fraction.

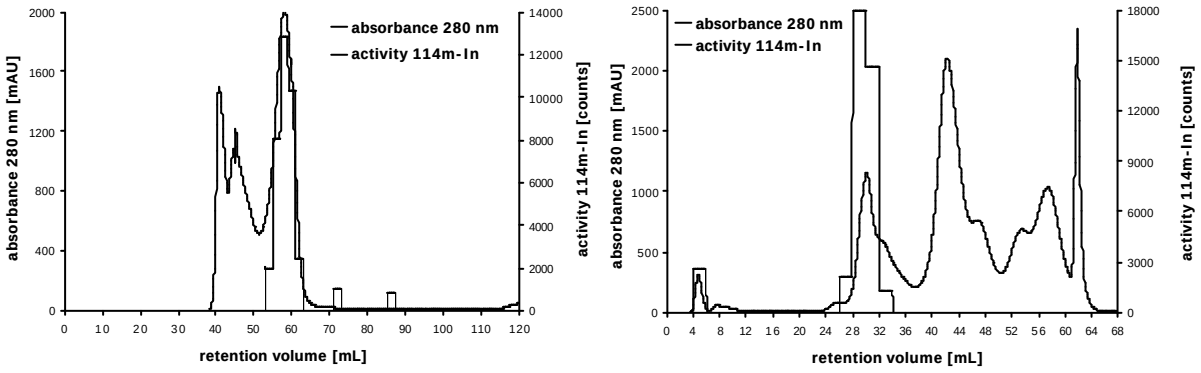

Figure 6.10a. Chromatogram of [^{114m}In]InAs/rat serum separated on Sephacryl S-200 HR size exclusion column (left).

Figure 6.10b. Chromatogram of [^{114m}In]InAs/rat serum separated on Hi Trap Q anion exchange column (right).

Liver, kidney and spleen were minced and homogenised as described above and the soluble fraction was obtained after centrifugation at 100000 x g and 4°C for 100 min. 1 mL was injected on a Sephacryl S200 HR column. Fractions of 2 mL were taken and the activity was measured with a NaI(Tl) scintillation detector. Elution was done with a 15 mM hepes + 0.15 M NaCl, pH 7.2 buffer.

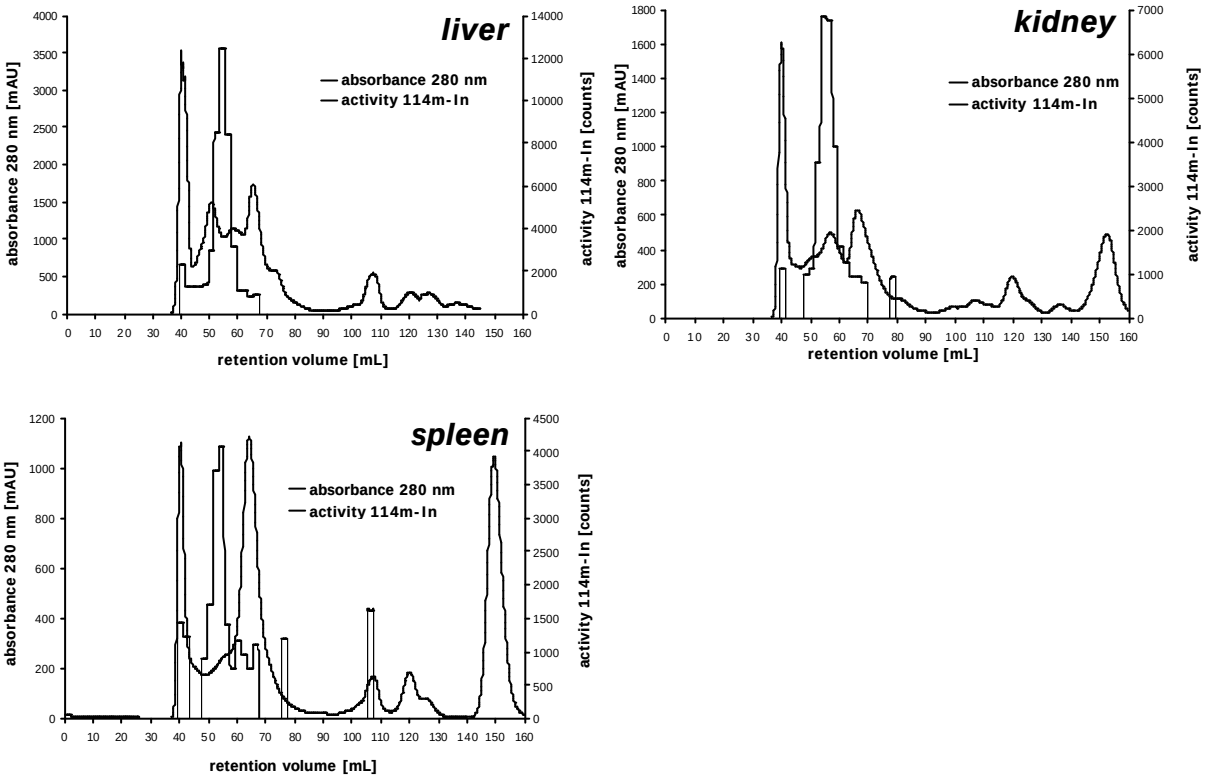

Figure 6.11. Chromatograms of [^{114m}In]InAs/rat liver cytosol (top left), [^{114m}In]InAs/rat kidney cytosol (top right) and [^{114m}In]InAs/rat spleen cytosol (bottom) separated on Sephacryl S-200 HR size exclusion column.

Figure 6.11 shows the chromatograms of the cytosolic fraction of liver, kidney and spleen on the Sephacryl S-200 HR SEC column. Also in this case it is demonstrated that indium is mostly bound to the high molecular mass fraction. The small fraction that elutes in the dead volume of the column might be due to binding of In^{3+} to the haem regulating enzyme δ-aminolevulinic acid (ALAD). Several studies postulate that indium is capable of regulating the haem biosynthesis in kidney, liver and erythrocytes by altering the activity of ALAD [Woods *et al.*, 1979; Woods and Fowler, 1982; Fowler *et al.*, 1983; Goering *et al.*, 1987; Aoki et al., 1990; Conner *et al.*, 1995]. ALAD is the enzyme that catalyses the second step in the biosynthetic pathway, namely the condensation of aminolevulinic acid to form porphobilinogen. The enzyme has a molecular mass of 290 kDa and thus appears in the

dead volume of the column (>250 kDa). In any case ALAD is not the major complexing agent of indium in these matrices. The presence of ^{114m}In in the high molecular mass fraction might be partly due to binding with transferrin. Transferrin is a normal constituent of cells and may also be present as a result of the incomplete removal of blood from the organs. The major share of ^{114m}In elutes, however, at a retention time that is slightly smaller than that of transferrin. So it is expected that other compound(s) are also able to complex indium. Both the results of the *in vivo* distribution among the different organs and of the intracellular distribution in the three target organs are very similar to those obtained after intraperitoneal administration of [^{114m}In]$InCl_3$. Moreover, the chromatograms of serum, and homogenate of spleen, kidneys and liver look very similar to those obtained in the first study. Thus it can be concluded that both $InCl_3$ and InAs act similarly, the route of exposure playing a minor role. The close agreement also suggests that InAs is dissociated *in vivo* after it is dissolved and will have a chemical form which is partly ionic and colloidal.

6.3. *In vivo* distribution and fractionation of indium in Wistar rats after oral administration of [^{114m}In]InAs

6.3.1. *In vitro* solubility of InAs

Prior to this *in vivo* experiment, the *in vitro* solubility of cold InAs in simulated gastric fluid (SGF) and simulated intestinal fluid (SIF) as a function of time was investigated. The purpose of this experiment was to found out more about the degree of solubility, the kinetic aspect by which this happens and thus get an idea about the bioavailability of indium and arsenic. Two solutions containing 36 mg InAs were prepared in 80 mL SGF and SIF, respectively. The final concentration of indium was 272.3 mg/L. SGF and SIF were prepared according to the USP regulations [US Pharmacopeia, 2000]. For the preparation of SGF, 2.0 g NaCl and 3.2 g pepsin (from porcine stomach mucosa, with an activity of 800 to 2500 units per mg of protein) were dissolved in 7 mL HCl and sufficient water to make 1 L. This test solution has a pH of about 1.2. For the preparation of SIF, 6.8 g of KH_2PO_4 was dissolved in 250 mL water, and 77 mL 0.2 M NaOH and 500 mL water was added. After addition of 10.0 g pancreatin (from porcine pancreas, activity at least equivalent to USP specifications), the pH was adjusted to 6.8 with either NaOH or HCl. The solution was finally diluted with water to 1 L. Both solutions were incubated at 37°C in a mechanical shaker during 48 hours. After 0, 15, 30 min, 1, 2, 4, 8, 12, 24, 36 and 48 hours, a 1 mL

sample was pipetted from the solution, filtered through a 0.22 µm filter to remove particles of InAs and diluted 100 times. For the determination of indium in SGF and SIF, graphite furnace atomic absorption spectrometry (GF-AAS) was used. All samples were diluted with 0.2% HNO_3. Two sets of standard series were prepared in both SGF and SIF and diluted to the same extent as the samples. InAs was only slightly soluble in SGF: 3.5 mg/L or 1.3% was dissolved after 48 hours. InAs was not soluble in SIF. InAs shows a solubility behaviour that is different from that of GaAs. The *in vitro* solubility studies of GaAs in physiological buffers and in a hydrochloric acid solution showed that it dissolved to a high extent after 48 hours [Webb *et al.*, 1984].

6.3.2. Treatment of animals

Five male Wistar rats weighing between 200 and 250 g were maintained in individual polycarbonate cages in an environmentally controlled facility on a 12 h light/dark cycle. The experiment started on day 1. The animals were allowed to acclimatise for 19 days. Food and water were supplied ad libitum. Handling of the animals (cleaning of the cages, injections) was done during the active dark period. The last three days of this period the animals were transferred to a metabolic cage. Urine and faeces were collected daily. The animals were weighted each day and the food and water consumption was calculated. On day 20, 23, 26 and 30, the rats were supplied with an equal oral dose of [^{114m}In]InAs. In total the rats were given a dose of 9 mCi. This corresponds to a dose of 40 mg InAs per kg body mass. The production of the radiolabeled indium was identical as in paragraph 6.2.1. However, irradiation time was 3 weeks instead of 1. This explains the higher specific activity and consequently the lower dose per kg body mass. The [^{114m}In]InAs was put on top of the food. Four days after the last administration the animals were sacrificed. Kidney, liver, spleen, hart, lung, testes, pancreas, thyroid gland, thymus, bone, fat, muscle, skin and fur, stomach, small and large intestine were removed and washed with 0.9% NaCl solution. Blood, urine and organs were stored at -20°C prior to analysis.

6.3.3. Excretion of indium

During this experiment four doses were given p.o. to the rats. Virtually all indium activity was each time found in the faeces within the next 72 hours. This is in agreement with the low extent of *in vitro* solubility of InAs in SGF. Only very small amounts of ^{114m}In were

recovered from urine. Figure 6.12 shows the time dependent plot of the amount of ^{114m}In found in the faeces. It is clearly shown that all rats show almost identical behaviour. A maximum amount of activity in the faeces is found between 24 and 48 hours after each oral administration. The slight discrepancies between the rats might be partly due to different eating times. No straightforward conclusion about the kinetics of urinary excretion can be drawn from the results of urinary ^{114m}In versus time (figure not shown). The ^{114m}In activity was multiplied by the volume of the urine to compensate for the differences in urinary behaviour. A maximum ^{114m}In signal was noticed at around 72 hours after each oral administration. A wide variation is seen, partly caused by the different time of eating. The oral administration was not forced. The InAs particles were simply put on top of the food. It seems that urinary excretion is slower and much less important in comparison with faecal excretion. This is due to the very low solubility of InAs in the stomach.

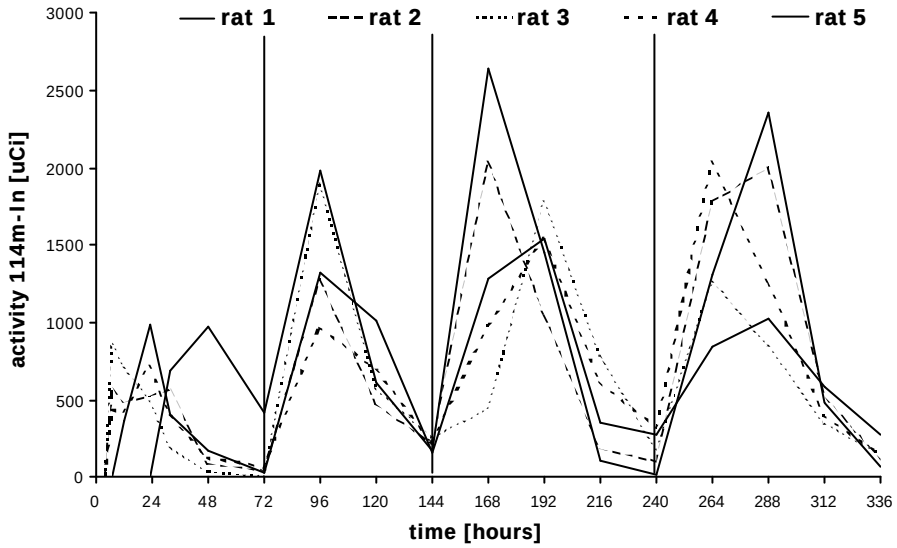

Figure 6.12. Faecal excretion in function of time. The vertical bars indicate the time when the rats were administered an oral dose. Time = 0 at day 20.

Due to the presence of residual ^{114m}In in the organs of the gastrointestinal tract, it was impossible to accurately calculate the *in vivo* distribution of ^{114m}In. Some trends can, however be seen. In contrast to the *in vivo* distribution of ^{114m}In after i.p. and s.c. administration of [^{114m}In]$InCl_3$ and [^{114m}In]InAs respectively, the spleen is not a major target organ. Kidney and liver show only moderate affinity for InAs. Even on a percentage per organ base, kidney is more affected than liver. The lungs seem to be the most important target organ. A reason for the high amount of indium activity found in the lungs of the rats might be that part of the InAs particles that were put on top of the food, was

inhaled. Indeed the InAs particles are very small (<10 μm) and black spots were seen on the nose of the animals. Moreover animals have the habit to sniff at their food before eating. Bone, thymus, thyroid gland, testes, fat, muscle and heart contain only very low amounts of ^{114m}In or none. The organs of the gastrointestinal tract (stomach, small intestine, large intestine) and related organs (pancreas) have the highest amounts of ^{114m}In. A considerable amount of ^{114m}In is found in the fur/skin. These data indicate that uptake of indium is very low. Indium present in liver, kidney and spleen indicates that indium has been taken up by the body. After i.p. injection of a physiological solution of [^{114m}In]$InCl_3$ the indium enters the bloodstream within a few minutes. Kidneys and liver excrete this indium, but it is also taken up by these organs. In case of the subcutaneous administration, InAs slowly dissolves and will be taken up by the blood that flows through the muscles of the site of injection. Excretion occurs in the kidneys and the liver and indium is slowly absorbed and distributed among the different organs. In case of oral administration, however, *in vivo* solubility is too slow compared to the process of ingestion, digestion and excretion. The majority of the InAs particles leave the body unchanged. It can thus be concluded that p.o. administered InAs will not accumulate in the body.

Many of these findings are in agreement with those of Zheng *et al.* [1994]. In that study InP was administered p.o. and i.t. to rats. As a conclusion of their experiments they stated that it seems unlikely that indium will accumulate in the body following InP exposure. As is also described in that study, the moderate amount of ^{114m}In found in skin/fur might be due to contamination and/or skin excretion. In this experiment the rats were housed in metabolic cages and although the cages were regularly cleaned, the animals came continuously into contact with the InAs. To my knowledge this is the first study in which InAs was given orally to test animals. Previous studies dealing with InAs or other indium containing semiconductor compounds were carried out by Omura *et al.* [1996a, 1996b], Conner *et al.* [1995], Tanaka *et al.* [1994, 1996], Morgan *et al.* [1995], Yamauchi *et al.* [1992] and Zheng *et al.* [1994]. All these experiments were done with either i.t. or s.c. instillations to rats or hamsters, except for Zheng *et al.* [1994] who fed rats orally with InP. Not only is the route of administration very important in terms of bioavailability, also very high amounts of InAs were administered in some cases. Subcutaneous, intraperitoneal or intratracheal administration is very useful to find out more about the distribution into the organism, the toxic effects of a compound or binding of the compound to biological components in blood or tissue. These methods of administration give, however, no data about the uptake in the body and thus the degree of toxicity of the compound. Moreover,

the very high amounts of InAs given to the test animals in some studies do not reflect reality. Administered doses of 1 g/kg would be equal to 80 grams of InAs for a person weighing 80 kg. Giving these high amounts of InAs will eventually always lead to toxic effects. In the last study, rats were fed with InAs at a dose of 40 mg per kg body mass, an amount that would be equal to 3.2 grams of InAs for a worker weighing 80 kg. Even in the latter case it is unlikely that a person, working in a workshop where InAs is manufactured or processed, will ingest this amount. It was clear from these studies that s.c. administration is a much more efficient route of exposure compared to p.o. administration. Much higher doses (in terms of specific activity of ^{114m}In) were given in the oral study, but much higher amounts of ^{114m}In were recovered from the body organs and the body fluids in our subcutaneous study.

6.4 Conclusion

After repeated intraperitoneal administration (4 doses in 4 days) of [^{114m}In]$InCl_3$ to male Wistar rats, ^{114m}In is primarily found in liver, kidney and spleen. Within the cells of these organs ^{114m}In is recovered mainly from the cytosolic fraction followed by the mitochondria. In blood ^{114m}In localises mainly in serum. Fractionation analysis shows that in serum In^{3+} is exclusively bound to the HMM fraction. Transferrine is the main complexor. The amount of In^{3+} bound to albumin is less than 1%. In3+ elutes slightly ahead of the haemoglobin fraction. Residual transferrin may be responsible for this binding. Fractionation analysis of the cytosolic fraction of liver, kidney, spleen and lung shows that In^{3+} is mainly found in the HMM fraction, but anion exchange chromatographic analysis shows that transferrin is not the sole complexor.

After duplicate subcutaneous administration of [^{114m}In]InAs to male Wistar rats, major amounts of ^{114m}In were again found in liver, kidney and spleen. Also the intracellular distribution was in good agreement with the one obtained in the first study. In serum, ^{114m}In was found in the transferrine fraction and in the cytosolic fraction of liver, kidney and spleen, ^{114m}In was recovered mainly from the HMM fraction. The similarities between both experiments indicate that InAs dissociates slowly over time and behaves like $InCl_3$.

After oral administration (4 doses in 10 days) of [^{114m}In]InAs to male Wistar rats, more than 99% of the administered InAs was found in the faeces. ^{114m}In was mainly recovered from

the organs of the GI tract. Oral administration does not lead to accumulation of InAs in the body.

References

[Aoki *et al.*, 1990]

Aoki Y, Lipsky MM and Fowler BA (1990). *Toxicol. Appl. Pharmacol.*, **106**, 462-468.

[Bergdahl and Schütz, 1996]

Bergdahl IA and Schütz A (1996). *J. Anal. At. Spectrom.*, **11**, 735-738.

[Castronovo and Wagner, 1973]

Castronovo FP and Wagner HN Jr (1973). *J. Nucl. Med.*, **14**, 677-682.

[Chen *et al.*, 1999]

Chen C, Zhang P, Lu X, Hou X and Chai Z (1999). *Fres. J. Anal. Chem.*, **363**, 512-516.

[Conner *et al.*, 1995]

Conner, Yamauchi H and Fowler BA (1995). *Chem. Biol. Interact.*, **96**, 273-285.

[Fowler *et al.*, 1983]

Fowler BA, Kardish RM and Woods JS (1983). *Lab. Invest.*, **48**, 471-478.

[Goering *et al.*, 1987]

Goering PL, Mistry P and Fowler BA (1987). In *Handbook of Toxicology*, (ed. Haley TJ and Berndt WO), Hemisphere Publishing Corporation, Washington, pp 384-425.

[Goodwin *et al.*, 1966]

Goodwin DA, Stern HS, Wagner HN Jr and Kramer HH (1966). *Nucleonics*, **24**, 65&68.

[Morgan *et al.*, 1995]

Morgan DL, Shines CJ, Jeter SP, Wilson, RE, Elwell, MP, Price, HC, Moskowitz, PD (1995). *Environ. Res.*, **71**, 16-24.

[Omura *et al.*, 1996a]

Omura M, Tanaka A, Hirata M, Zhao M, Makita Y, Inoue N, Gotoh K and Ishinishi N (1996). *Fund. Appl. Toxicol.*, **32**, 72-78.

[Omura *et al.*, 1996b]

Omura M, Hirata M, Tanaka A, Zhao M, Makita Y, Inoue N. Gotoh K and Ishinishi N (1996). *Toxicol. Lett.*, **89**, 123-129.

[Taillefert *et al.*, 2000]

Taillefert M, Bono AB and Luther GW (2000). *Environ. Sci. Technol.*, **34**, 2169-2177.

[Tanaka *et al.*, 1994]

Tanaka A, Hisanaga A, Hirata M, Omura M, Inoue N and Ishinishi N (1994). *Appl. Organomet. Chem.*, **8**, 265-271.

[Tanaka *et al.*, 1996]

Tanaka A, Hisanaga A, Hirata M, Omura M, Makita Y, Inoue N and Ishinishi N (1996). *Fukuoka Acta Medica*, **87**, 108-115.

[Taylor and Brothers, 1993]

Taylor MJ and Brothers PJ (1993). In *Chemistry of Aluminium, Gallium, Indium and Thallium* (ed. Downs AJ), Blackie Academic & Professional, London, pp 111-247.

[US Pharmacopeia, 2000]

US Pharmacopeia XXIV & National Formulary 19 (2000). The United States Pharmacopeial Convention, Rockville, p 2235-2236.

[Webb *et al.*, 1984]

Webb DR, Sipes IG and Carter DE (1984). *Toxicol. Appl. Pharmacol.*, **76**, 96-104.

[Woods and Fowler, 1982]

Woods JS and Fowler BA (1982). *Exp. Molec. Pathol.*, **36**, 306-315.

[Woods *et al.*, 1979]

Woods JS, Carver GT and Fowler BA (1979). *Toxicol. Appl. Pharmacol.*, **49**, 455-461.

[Yamauchi *et al.*, 1992]

Yamauchi H, Takahashi K, Yamamura Y and Fowler BA (1992). *Toxicol. Appl. Pharmacol.*, **116**, 66-70.

[Zheng *et al.*, 1994]

Zheng W, Winter SM, Kattnig MJ, Carter DE, Sipes IG (1994). *J. Toxicol Environ. Health*, **43**, 483-494.

Chapter 7. Arsenic: optimisation of ES-MS/MS and UV-HG-AFS

Hydride generation atomic fluorescence spectrometry (HG-AFS) and electrospray mass spectrometry (ES-MS/MS) were primarily considered for elemental and molecular detection, respectively, of the arsenic species in extracts of algae, urine and serum. HG-AFS was chosen because of its low cost and high sensitivity. Moreover, its small size was advantageous in view of the on-line dual detection. Using this instrumental set-up, elemental and molecular/structural information can be gained at the same time, within the same HPLC run. This may be an interesting feature when searching for unknown arsenic species. Information about an unknown species by ES-MS/MS is gathered at exactly the same time HG-AFS registers a signal for elemental arsenic.

At first the instrumental parameters of both instruments were optimised in order to obtain a good sensitivity for both systems. For evaluation of the sensitivity, the signal intensity is not always a reliable parameter. An increase in signal intensity does not necessarily result in a lower detection limit. Instead a signal to noise (S/N) calculation is preferred. For the determination of the S/N, peak-to-peak was selected, *i.e.*, the greatest height of the peak above the mean noise value is divided by the variance of the selected noise range. Those scans in the noise range whose deviation is greater than one standard deviation are rejected. In case of HPLC-ES-MS/MS and HPLC-HG-AFS, a S/N measurement was preferred. In case of direct infusion ES-MS/MS signal intensities were compared.

Next it was checked whether UV-HG-AFS allowed quantitative on-line photo-oxidation of arsenic species in real-life samples. Furthermore, optimal conditions to perform dual detection were investigated and the capabilities of HPLC-ES-MS/MS were explored using algae samples.

7.1. Optimisation of ES-MS/MS

A Quattro Micro electrospray tandem mass spectrometer (ES-MS/MS) was installed in the laboratory in August 2001. Although ES-MS/MS has been used previously by other researchers in the field of arsenic speciation analysis, the use of this type of mass spectrometer was novel. As it is well known that the sensitivity of ES-MS/MS is species dependent and strongly influenced by the sample matrix (salts, organic solvents, acids, bases…) a thorough optimisation had to be done.

The following instrument parameters were first optimised: capillary voltage, cone voltage, collision energy, desolvation temperature, desolvation gas flow rate, cone gas flow rate, sample flow rate, methanol content in the elution buffer (HPLC) and formic acid content in the sample (infusion). The influence of the type of buffer on the signal intensity of the different arsenic species will be discussed in paragraph 7.4.

7.1.1. Optimisation of voltages and collision energy

In a first stage, instrument parameters such as capillary voltage, sample cone voltage, extraction cone voltage, hexapole RF lens voltage and collision energy were investigated. These parameters are species dependent. The capillary voltage is applied to the stainless steel capillary and supplies an excess of charge to the droplets. In positive ion mode, it optimises at 3.0 kV, although some samples may tune at values above or below this, within the range 2.5 to 4.0 kV. For negative ion operation, a lower capillary voltage is necessary, typically between 2.0 and 3.0 kV. The sample cone voltage assists in drawing the ions into the first vacuum region (first orthogonal spray). A sample cone voltage setting between 25 and 70 V will produce ions for most samples, although solvent ions prefer the lower end and proteins the higher end of this range. The sample cone voltage has the biggest influence on the sensitivity. Increasing the cone voltage will result in ion fragmentation within the source. The extraction cone voltage focuses ions towards the hexapole RF lens and the hexapole RF lens voltage focuses the ions into the centre of the quadrupole. A schematic representation of the electrospray ions source and ion transmission, including the position of the gas flows and voltage positions, is shown in figure 4.4.

Aqueous standards (~1 mg/L As) of the different arsenic species were analysed by infusion ES-MS for optimisation of capillary voltage and sample cone voltage and by infusion ES-MS/MS for optimisation of collision energy. The two most abundant product ions were selected. A list of the optimal parameters and identity of the product ions is shown in table 7.1.

Table 7.1. Instrument settings and identity of product ions for different arsenic species.

	$[M+H]^+$	cap. volt. [kV]	cone volt. [V]	coll. energy [eV]	transition	product ion
As^V	143	2.7	35	25	143 > 109	$AsO(H_2O)^+$
				40	143 > 91	AsO^+
MA	141	3.2	30	25	141 > 91	AsO^+
				25	141 > 93	AsH_2O^+
DMA	139	3.1	30	25	139 > 91	AsO^+
				20	139 > 109	$AsO(H_2O)^+$
TMAO	137	3.5	35	30	137 > 122	$As(O)(CH_3)_2^+$
				25	137 > 107	$As(O)CH_3^+$
TETRA	135	3.3	35	20	135 > 120	$As(CH_3)_3^+$
				25	135 > 105	$As(CH_3)_2^+$
AB	179	3.2	30	25	179 > 120	$As(CH_3)_3^+$
				35	179 > 105	$As(CH_3)_2^+$
AC	165	3.0	30	20	165 > 121	$As(CH_3)_3H^+$
				30	165 > 105	$As(CH_3)_2^+$
DMAE	167	3.3	30	25	167 > 105	$As(CH_3)_2^+$
				20	167 > 123	$As(CH_3)_2H_2O^+$
AsSug-OH	329	3.0	30	20	329 > 97	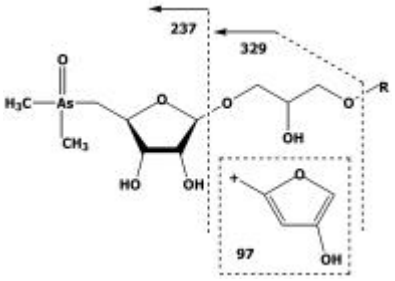
				15	329 > 237	
$AsSug\text{-}PO_4$	483	3.2	45	35	483 > 97	
				25	483 > 237	
$AsSug\text{-}SO_3$	393	3.2	30	30	393 > 97	
				25	393 > 237	
$AsSug\text{-}SO_4$	409	3.2	30	25	409 > 97	
					409 > 237	

The capillary voltage for all species is within the range 2.7 to 3.5 kV. For speciation analysis a mean value of 3.0 was used. The sample cone voltages are within the range 30 to 45 V. The extraction cone voltage and the hexapole RF lens voltage did not differ much and were set to values of 2.0 and 0.2 V, respectively. Product ions with loss of a water molecule were not selected in MRM analysis because they are not selective. Virtually all molecules lose a H_2O unit upon collision with argon.

When the sample cone voltage is increased, in source fragmentation of the analytes occurs. The identity of the fragments is largely the same as those obtained by conventional collision activated dissociation via ES-MS/MS. The disadvantage of in source fragmentation is its non-selective character. All analytes and solvent molecules entering the source can undergo fragmentation. For metal speciation analysis, the advantages are twofold. The isotopic pattern is preserved as long as the fragment in which the element of interest remains is charged. Unfortunately, arsenic is mono-isotopic. Second, it has been observed that a more drastic fragmentation can be induced, often leading to the naked metal ion. Francesconi and co-workers used this approach for the identification of unknown arsenic species in marine samples [Madsen *et al.*, 2000; Francesconi *et al.*, 2000; Francesconi, 2002]. Registration of a signal at *m/z* 75 is, however, no certainty of the presence of arsenic. Other ions can undergo in source fragmentation leading to a fragment with *m/z* 75. The influence of the cone voltage on the signal of the arsenic ion was therefore investigated. For a series of arsenic species it was checked whether an increasing cone voltage resulted in the complete fragmentation to As^+ and at what value of sample cone voltage this happened. Pure standard solutions were infused an analysed in the full scan mode. The result is shown in figure 7.1a and 7.1b.

For complete fragmentation to As^+, a sample cone voltage of minimum 120-130 V is needed for the cationic tetra-alkylated compounds (AC, AB, TETRA). A higher voltage (130-150 V) is needed for the compounds containing an arsenic-oxygen double bond (MA, DMA, TMAO, AsSug-PO_4). This indicates that cleavage of an As-C bond is more readily achieved than cleavage of an As=O bond. The identity of the fragments is given in table 7.2.

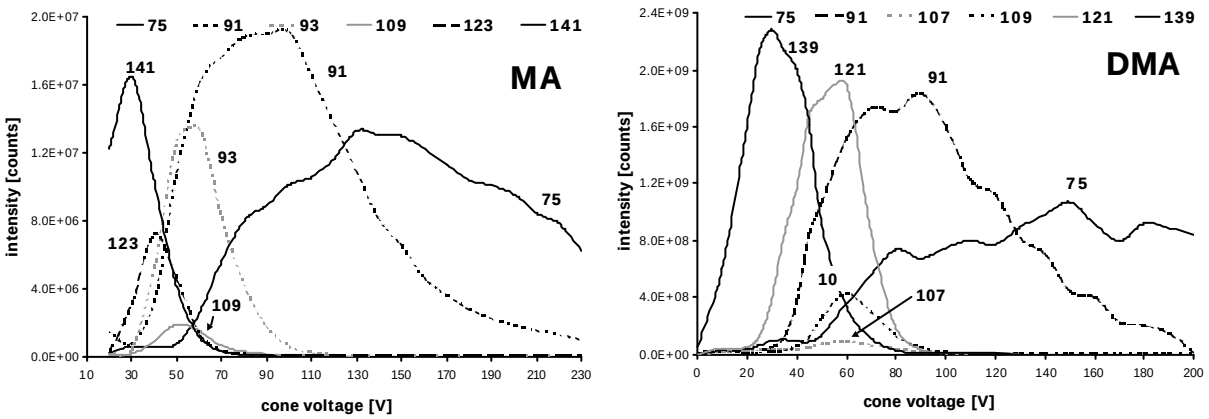

Figure 7.1a. Formation of in source fragments in function of sample cone voltage for MA (left) and DMA (right).

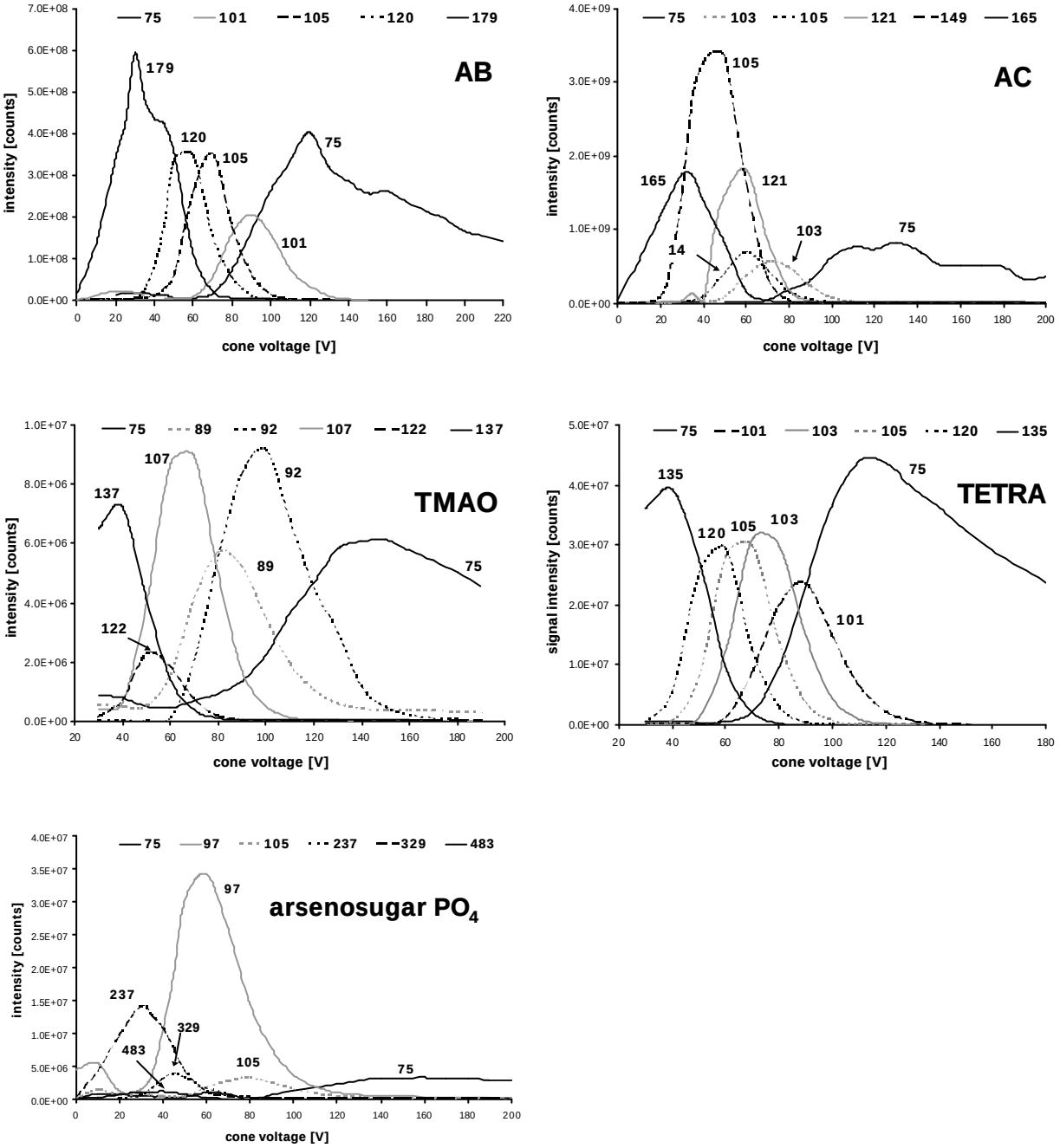

Figure 7.1b. Formation of in source fragments in function of sample cone voltage for AB (top left), AC (top right), TMAO (middle left) and TETRA (middle right) and arsenosugar PO_4 (bottom).

Table 7.2. Mass *(m/z)* and chemical formula of fragments.

m/z	chemical formula	*m/z*	chemical formula
75	As^+	107	AsO_2^+, $(CH_3)AsOH^+$
89	$As(CH_2)^+$	120	$(CH_3)_3As^+$
91	AsO^+, $(CH_3)AsH^+$	121	$(CH_3)_2AsOH^+$
92	$AsOH^+$	122	$(CH_3)_2AsOH^+$
93	$As(H_2O)^+$	123	$(CH_3)As(O)OH^+$
101	$As(CH)_2^+$	135	$(CH_3)_4As^+$
103	$(CH_3)AsCH^+$	149	$(CH_3)_3AsCH_2^+$
105	$(CH_3)_2As^+$	97, 237, 329	see figure 7.1

7.1.2. Optimisation of gas and sample flow rates and of desolvation temperature

Optimum nebulisation for electrospray performance is achieved with a nitrogen flow coaxial to the capillary. A default flow rate of 80 L/h is used. The desolvation gas, also nitrogen, is heated and delivered as a coaxial sheath to the nebulised spray. The optimum desolvation temperature and flow rate is dependent on the mobile phase composition and flow rate. When infusion ES-MS was done a value of 500 L/h was used. Increasing this value up to 700 L/h resulted in a slight increase in signal intensity, but this increase in sensitivity was insufficient to compensate for the higher cost of gas consumption. Only in the case of HPLC-ES-MS/MS this value was increased to 650 L/h to compensate for the increased amount of solvent entering the probe. The cone gas is a reverse flow of nitrogen delivered around the sample cone. The optimum cone gas flow rate is again dependent on the mobile phase composition and flow rate. However, it did not seem to have much influence on the signal intensity within the range 0-100 L/h. The primary use of the cone gas is to prevent contamination of the sample cone. A default value of 50 L/h was used in both infusion and HPLC mode.

The optimal sample flow rate for conventional HPLC columns with a diameter of 4.6 mm is around 1 mL/min. Although the electrospray can accommodate sample flow rates up to 1 mL/min, it is recommended that the sample flow is split post-column to approximately 200 µL/min by means of a T-piece. Higher sample flow rates lead to incomplete ion evaporation in the source and thus a decrease in signal intensity. The split rate is dependent on the inner diameter (i.d.) of the tubing and to a lesser extent on the length. Using two red PEEK tubing of 0.005" i.d. the flow is split with 60% going to the waste. When the waste tubing

is replaced by a yellow PEEK tubing of 0.007" i.d., 75% is directed to the waste. A blue PEEK tubing of 0.01" i.d. leads 85% to the waste. When a sample flow rate of 1 mL/min is used, a flow rate of 400, 250 and 150 µL/min towards the ES source is realised for the red, yellow and blue waste tubing, respectively. It was checked which of these split configurations was best. AB, DMA and MA were chromatographed on a PRP-X100 column with 3 mM ammonium oxalate (pH 6) at different sample flow rates corresponding to the flow rate that would be resulting from a split of a 1 mL/min flow rate by the three different split configurations (*i.e.*, 150, 250 and 400 µL/min). As a consequence, the whole sample was directed to the ES. The results are shown in table 7.3. Increasing the sample flow rate leads to lower signal intensities of the three compounds. This is in correlation with the higher amount of liquid present in the source and thus less efficient ion evaporation. However, when the respective split rates are taken into account, the outcome is totally different (right side of table 7.3). The signal intensities of the three compounds for the three flow rates were multiplied with their respective split ratios (source/total). A split of 85% to the waste implies that only 15% of the original sample is sent to the ES source. Although the lower sample flow rate results in higher signal intensity, the smaller sample amount drastically reduces the overall sensitivity. Thus when a conventional 4.6 mm HPLC column is used, it is advised to use a split ratio that directs more sample to the ion source (*i.e.*, 40% or 400 µL/min to the source).

Table 7.3. Signal intensities for AB, DMA and MA at different sample flow rates.

	signal intensity [counts] 100% injection			**signal intensity [counts]** with split		
total sample flow rate [µL/min]	150	250	400	150	250	400
to waste [%]	0	0	0	85	75	60
to ES source [%]	100	100	100	15	25	40
AB	71122	58683	45579	10668	14671	18232
DMA	145781	101056	67133	21867	25264	26853
MA	24304	17271	12384	3646	4318	4954

Within the same experiment the desolvation temperature was also varied. The desolvation temperature is the temperature of the desolvation gas aiding the solvent evaporation. The optimum temperature is dependent on the mobile phase composition and flow rate, with water-containing mobile phases and high flow rates requiring more heat. Moreover, solvent

cluster ions may form if the temperature is too low. In infusion mode, where flow rates are limited to 10-20 µL/min, a desolvation temperature of 150-200°C is sufficient for drying and desolvation of the aerosol. When doing HPLC-ES-MS(/MS), higher flow rates and consequently higher desolvation temperatures are required. At each flow rate (150, 250 and 400 µL/min), the desolvation temperature was set at 200, 250 and 300°C. For all flow rates the maximum sensitivity was obtained with the highest desolvation temperature (see figure 7.2). The highest relative increase (between 200°C and 300°C) is found for the highest flow rate. All three compounds exhibit almost the same relative increase at each flow rate.

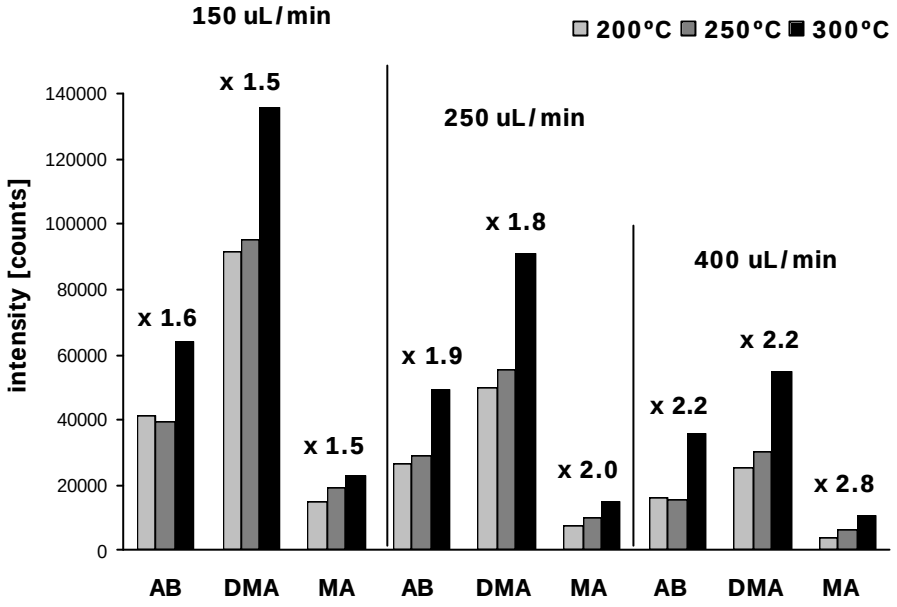

Figure 7.2. Signal intensities for AB, DMA and MA at different sample flow rates and different desolvation temperatures. The relative increases mentioned in the figure are those between a desolvation temperature of 200°C and 300°C.

When a microbore column of 2.1 mm i.d. is used, there is no need for splitting. However, it was again checked at which sample flow rate an optimum ionisation in the ES source was achieved. A more extended experiment was carried out on a standard mixture of AB, AC, TETRA, DMA and MA. This mixture was injected on a PRP-X100 guard column using sample flow rates between 50 and 1000 µL/min. The results are shown in figure 7.3. The maximum sensitivity is reached using a sample flow rate of 100 µL/min. However, a sample flow rate of 200 µL/min (optimal sample flow rate for 2.1 mm microbore columns) does not drastically decrease the signal intensities for the different arsenic species (>85%). The trend is identical to that shown in figure 7.2.

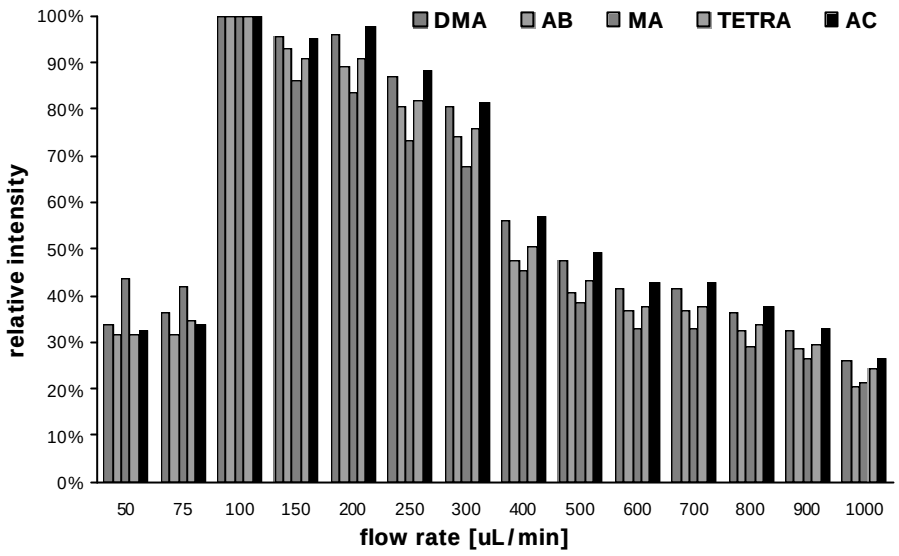

Figure 7.3. Relative signal intensities for DMA, AB, MA, TETRA and AC at different sample flow rates.

7.1.3. Optimisation of MeOH content in the mobile phase and HCOOH content in the sample

In positive ion mode it is advised to add formic acid to the sample. In infusion MS a 50:50 mixture of acetonitrile or methanol and water is a suitable mobile phase for the syringe pump system. Positive ion operation may be enhanced by 0.1 to 1% formic acid in the sample solution. Using a standard mixture of AB, AC, TETRA, MA, DMA and As^{V} (~1 mg/L in As, except As^{V}: 10 mg/L) in water and increasing amounts of formic acid, the influence of the acid on the signal intensity of all compounds was tested. The result is shown in figure 7.4. Increasing the HCOOH content to 1%, leads to a 2.5-3-fold increase in signal intensity in case of the cations AB, AC and TETRA, a 3.5-fold increase in case of DMA, a 10-fold increase in case of MA, and a 100-fold increase for As^{V}. As can be expected the biggest improvement is found for the anions. Surprisingly, further increase of the formic acid content up to 50% drastically improves the signal intensities. The total relative increase is shown in the figure. The cationic species TETRA and AC show an 8-fold increase in signal intensity upon addition of 50% HCOOH. This amounts up to a factor 11 and 13 for AB and DMA, respectively. MA and As^{V} are 40 times and 310 times more when 50% HCOOH is used.

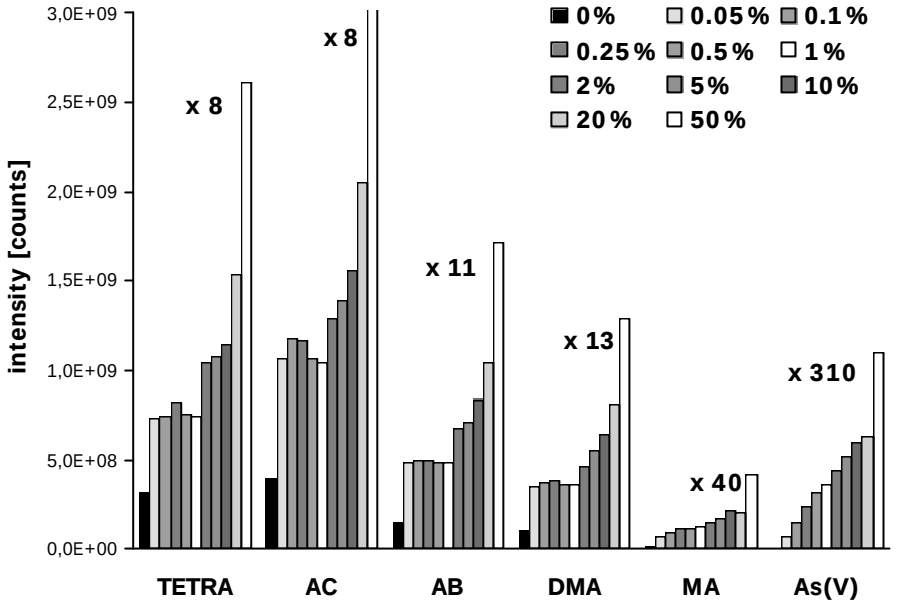

Figure 7.4. Signal intensities for TETRA, AC, AB, DMA, MA and As^V at different formic acid contents. The relative increases mentioned in the figure are those between a HCOOH content of 0% and 50%.

To my knowledge, no reports have yet been published in which a thorough investigation was done of all parameters, which have a profound effect on the signal intensity of arsenic species in HPLC-ESMS/MS analysis. The reason is probably that many of these parameters mutually influence each other and that the influence of these parameters will not be identical for the different arsenic species. Moreover, a different influence is expected between aqueous samples and real-life samples. Add to this that these parameters are probably not easily copied from one instrument to another. A good example is definitely the influence of organic solvents on the sensitivity of the arsenic species in HPLC-ES-MS/MS analysis. It is known that volatile solvents have a positive influence on the signal intensities in ES-MS. Methanol or acetonitrile are more easily evaporated and therefore more analytes will enter the mass spectrometer. In case of infusion ES-MS this is always observed. A sample dissolved in water will have a lower degree of ionisation in the ES source compared to a sample dissolved in 50:50 water/methanol or 50:50 water/acetonitrile. However, in combination with HPLC, the outcome is not that straightforward. The degree of ionisation in the source for a given analyte is dependent on the total amount of molecules in the source. If pyridine is used as a buffer instead of acetate, the sensitivity by which *e.g.*, MA can be detected will be much lower, because of the good ionisation of pyridine in the ES source compared to acetate. In case of HPLC, a compound eluting at a certain retention

time is accompanied by many other analytes, which might influence the degree of ionisation of the compound of interest. Addition of methanol to the mobile phase results in a shift of the retention times. Thus the compound of interest might be accompanied by other analytes, which have another influence on the degree of ionisation. The influence of the varying amounts of methanol on the signal intensities of different arsenic species was investigated with a real-life sample. Both anion exchange and cation exchange buffers were evaluated. An extract of kelp powder was spiked with MA, DMA, TETRA, AB and AC. This mixture was separated on a PRP-X100 anion exchange column with 3 mM ammonium oxalate (pH 6) and on a CS10 cation exchange column with 10 mM pyridine (pH 2.8). To the buffer 0%, 5%, 10% and 20% of MeOH was added. The results are shown in figure 7.5. In anion exchange chromatography, the influence of MeOH on the signal to noise of the different arsenic species is not straightforward. MA and arsenosugar OH are negatively influenced by addition of MeOH. The other arsenosugars are detected more sensitively in the presence of 5% MeOH. AB seems to be not influenced. On the other hand, in cation exchange chromatography, addition of MeOH drastically improves the sensitivity for AC and TETRA. For DMA, arsenosugar OH and AB, the improvement is not that outspoken. There seems to be a correlation between the rate of improvement and the charge of the arsenic species. In the case of cation exchange chromatography, the amount of MeOH has no profound influence on the retention time of the arsenic species, whereas in anion exchange chromatography, the retention times are drastically reduced by addition of MeOH.

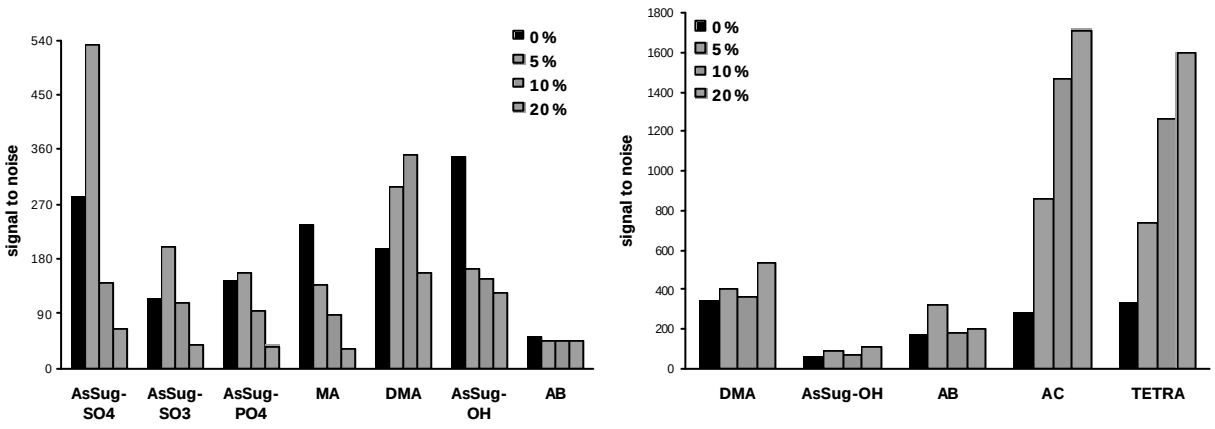

Figure 7.5. Signal intensities for different arsenic species at different methanol contents in anion exchange eluent (left) or cation exchange eluent (right).

The optimised instrumental parameters for infusion and HPLC ES-MS/MS are listed in table 7.4.

Table 7.4. Instrument settings for infusion and HPLC mode ES-MS/MS analysis.

parameter	infusion	HPLC
capillary voltage [kV]	2.8-3.2	3.0
sample cone voltage [V]	30-45	30-45
extraction cone voltage [V]	2	2
hexapole RF lens voltage [V]	0.2	0.2
source temperature [°C]	120	120
desolvation temperature [°C]	200	300
desolvation gas flow [L/h]	500	650
sample cone gas flow [L/h]	50	50

7.2. Optimisation of UV-HG-AFS

In case of conventional hydride generation without UV decomposition step, the experimental conditions prescribed by the manufacturer were used. These are listed in table 7.5. When HG-AFS was preceded by UV decomposition, the following parameters were optimised: $K_2S_2O_8$ and NaOH concentrations, HCl concentration, UV coil type, length and diameter, flow segmentation and reaction coil length.

Table 7.5. Instrument settings for conventional HPLC-HG-AFS analysis.

mobile phase speed	1 mL/min
acid carrier	1.5 M HCl, 1.5 mL/min
reducing agent	1.4% (m/v) $NaBH_4$ in 0.4% (m/v) M NaOH, 1.5 mL/min
carrier gas	argon, 250 mL/min
dryer gas	argon, 2.5 L/min
lamp current	27.5 mA (primary current) and 35.0 mA (boost current)

First a UV decomposition unit supplied by the manufacturer (PSA 10.570) was compared with an old unit that has been previously used in our laboratory, namely a 5 m 0.8 mm i.d. PTFE tube wrapped around a 6 W Philips UV lamp [Zhang *et al.*, 1995 and 1996]. The performance characteristics of the two units were tested with a standard mixture of As^{III}, DMA, MA and As^{V}, using the experimental conditions optimised by Gomez-Ariza *et al.* [1998]. They evaluated HG-AFS with and without photo-oxidation for the measurement of arsenic species and used the following parameters for the UV decomposition: 2% (m/v) $K_2S_2O_8$ in 2% (m/v) NaOH, 8 M HCl and 1.5% (m/v) $NaBH_4$ in 1% (m/v) NaOH. Our unit

provided sharper peaks and consequently better signal to noise ratios. The signal intensities of the peaks for our unit were also higher, indicating a better rate of decomposition. Moreover the signal for DMA proved to be very poor in case of the PSA 10.570 unit. Therefore it was decided not to use the commercial unit. The old Philips unit was afterwards replaced with a 15 W Heraeus TNN 15/35 low pressure Hg lamp (254 nm). A teflon tube was wrapped around it and the lamp was covered with aluminium foil for better light reflection and eye protection.

Next the UV decomposition parameters were further optimised. First it was checked whether decreasing the acidity had a negative influence on the performance characteristics of a measurement of AB in triplicate by flow injection (no column added). In a first step the HCl molarity was decreased from 8 M to 6 and 4 M and in a second step to 6, 5.5 and 5 M. A hydrochloric acid concentration of 5.5 M (decrease of 31.25% of HCl) did not significantly lower the sensitivity. According to Tsalev *et al.* [1998], the concentrations of $K_2S_2O_8$ and NaOH are not critical within the ranges 0.5-4% (m/v) and 1.6-8% (m/v), respectively. Keeping the amount of NaOH constant at 2% (m/v), the influence of varying amounts of $K_2S_2O_8$ on the sensitivity of AB detection was tested. The concentration of persulphate could be lowered to 1.5% (m/v) (decrease of 25% of $K_2S_2O_8$) without a loss in sensitivity. Finally the sodium hydroxide concentration was varied at constant $K_2S_2O_8$ (1.5% m/v) and 2.5% (m/v) NaOH was chosen as an optimal value. The instrumental set-up of HPLC-UV-HG-AFS, shown in figure 4.8 consists of a lot of tubing between the outlet of the column and the detector. This will inevitably result in peak broadening. The *HETP* due to an open tube is decribed by the Golay equation

$$H = \frac{2D_M}{u} + \frac{r^2 u}{24 D_M}$$

with D_M the diffusion coefficient of the solute in the mobile phase, u the linear flow rate and r the radius of the tube. If $u >> D_m/r$ (which will be true for most practical chromatographic systems, then the peak variance (in volume units) is

$$s_V^2 = \frac{p r^4 L}{24 D_M} \cdot Q$$

with Q the flow rate [ml/min] through the tube ($p r^2 u$) and L the length of the tube [http 6].

However, when the flow can be segmented post column with a stream of gas, diffusion will be efficiently reduced. This is proven by the following examples. An equal amount of MA was injected into the system (no column inserted) and analysed in triplicate with and without segmentation. Signal intensity, S/N and FWHM were registered (table 7.6).

Table 7.6. Performance characteristics for AB with and without flow segmentation.

	intensity mean & SD (n = 3)	S/N mean & SD (n = 3)	FWHM [min] mean & SD (n = 3)
without	21908 (1746)	45.66 (3.3)	0.62 (0.4)
with	21824 (567)	129.98 (4.6)	0.17 (0.2)

Whereas the signal intensity of the peak remains the same, the FWHM drastically decreases (factor 3.6). As a consequence, S/N increases (factor 2.8). Similarly a mixture of As^{III}, DMA and MA was separated on a Hamilton PRP-X100 column with and without flow segmentation (figure 7.6). Again better S/N and FWHM values are obtained for all species. The improvement is less outspoken compared to the example of MA analysed without column. By aspirating air through a tube via the same peristaltic pump as the one used for injection of the $K_2S_2O_8$ solution, flow segmentation is realised.

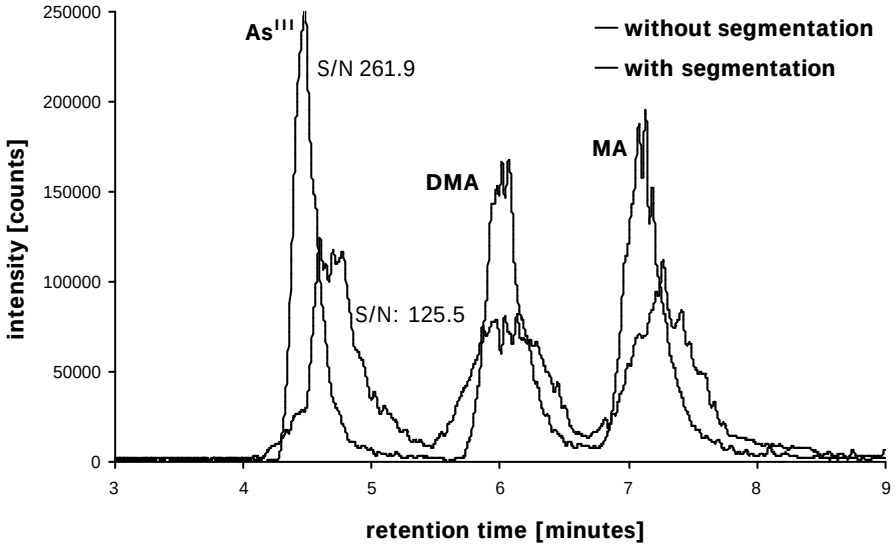

Figure 7.6. Chromatograms of As^{III}, DMA and MA separated on anion exchange column with and without flow segmentation. Detection with HG-AFS.

The type, length and diameter of the teflon tubing were optimised. From the above-mentioned equation it can be derived that peak broadening is proportional to the inner radius of the tube. From this point of view a tube as thin as possible should be used. On the other hand the permeability of teflon for UV light is dependent on the thickness of the walls. Commercially available teflon tubing has a fixed outer diameter of 1.59 mm (1/16 inch). Tubes with smaller inner diameter consequently have a larger wall thickness. Therefore tubing with a larger inner diameter should yield more UV light absorption. Moreover the permeability of teflon for UV light is dependent on the type of teflon material. Conventional PTFE (polytetrafluoroethylene) shows poor permeability for UV light. Other teflon materials such as PFA (perfluoroalkoxy) and FEP (fluorinated ethylene propylene) are less opaque and thus more transparent towards UV light. The transmission for radiation of 250 nm light through a 0.2 mm foil is 86% for PFA and 84% for FEP. PTFE is 20% less transparent [http 7, http 8]. These three types were compared. At first different types of teflon tubing with 0.8 mm internal diameter were tested. Afterwards it was checked whether decreasing the inner radius resulted in an improved peak shape. For each inner diameter, the length was chosen such that it provides an irradiation time long enough for complete conversion of AB into As^{V}. An irradiation time of 70 seconds was selected from literature values [Tsalev *et al.*, 1998]. An equal amount of AB was injected into the UV coil, made of different teflon materials with equal diameter and length. Each time at least 6 replicates were taken. Mean values of signal intensity and signal to noise are reported in table 7.7. The type of teflon and the different transmittance for UV light seems to have no influence on the conversion of AB to As^{V}. When the signal intensities of AB are compared to those of equal amounts of arsenate a conversion of AB to arsenate of more than 94% is achieved for all three materials.

Table 7.7. Performance characteristics for AB using different types of teflon tubing in the UV-coil.

	intensity mean & SD (n > 6)	S/N mean & SD (n > 6)
FEP	30037 (1024)	48.0 (5.5)
PTFE	27946 (1605)	49.7 (10.2)
PFA	30217 (2355)	51.9 (7.3)

A comparison between a UV coil of two different internal diameters of equal volume shows no better FWHM and consequently smaller peak broadening for a 0.5 mm i.d. (7.2 seconds) compared to a 0.8 mm i.d. (7.8 seconds) tubing. It seems that the influence of the inner diameter of the UV coil tubing has no significant influence on the overall peak broadening caused by the column and post column processes. The fact that flow segmentation by argon efficiently reduces peak broadening may be a plausible explanation.

The following conditions for measurement of arsenic by UV-HG-AFS were used (table 7.8):

Table 7.8. Instrument setting for UV-HPLC-HG-AFS analysis.

mobile phase speed	1 mL/min
flow segmentation	air, 0.5 mL/min
oxidant	1.5% (m/v) $K_2S_2O_8$ in 2.5% (m/v) NaOH, 0.5 mL/min
UV unit	15 W Heraeus TNN 15/35 low pressure Hg lamp 0.8 mm i.d. PFA, 3.9 m (volume 2.0 mL)
acid carrier	5.5 M HCl, 1.5 mL/min
reducing agent	1.4% (m/v) $NaBH_4$ in 0.4% (m/v) M NaOH, 1.5 mL/min
carrier gas	argon, 250 mL/min
dryer gas	argon, 2.5 L/min
lamp current	27.5 mA (primary current) and 35.0 mA (boost current)

7.3. Flow injection UV-HG-AFS for analysis of total arsenic

If the UV coil yields quantitative conversion of organoarsenicals to arsenate, it could be tested whether it is possible to directly determine the total arsenic concentration in real-life samples. Individual stock solutions of 1 µg/mL of As^V, MA, DMA, AB, AC, DMAE and arsenosugar PO_4 were prepared. Each of these solutions was diluted (1 + 9) in water, in urine and in 1 + 9 diluted urine. The urine was taken from a volunteer who had not eaten seafood during 3 days. In this urine sample arsenic was detected at a level, which was much lower than the concentration level during this experiment (100 ng/mL As). A volume of 50 µL (water) or 100 µL (urine) was injected in the system. The experimental conditions were as follows: 1.5% (m/v) $K_2S_2O_8$ in 2.5% (m/v) NaOH, 5.5 M HCl, 1.4% (m/v) $NaBH_4$ in 0.4% (m/v) NaOH. The results are shown in table 7.9. The values for the different arsenicals are shown relative to the value obtained for As^V. It can be seen that in water, all arsenicals are completely transformed into As^V. The undiluted urine matrix, on the other hand, exerts a significant influence on the breakdown of arsenic compounds into arsenate. All arsenicals show a lower relative signal intensity than As^V, exception made of MA. Photo-

oxidation converts organo arsenic compounds such as AB and AC to As^V via TETRA, TMAO, DMA and MA. Incomplete breakdown of AB would thus result in a mixture of AB and TETRA, TMAO, DMA, MA and As^V leaving the UV-coil. Some of these compounds have no (AB, TETRA), lower (TMAO, DMA) or higher (MA) sensitivity for hydride formation compared to arsenate. Therefore the incomplete break-down of AB, AC, DMA, DMAE and arsenosugar PO_4 leads to a lower signal compared to As^V, whereas incomplete break-down of MA will result in a higher signal, compared to that of As^V.

Table 7.9. Signal intensities (relative to As^V) for different arsenic species dissolved in water, undiluted urine and 1+9 diluted urine.

	water	undiluted urine	1 + 9 diluted urine
AB	101.6%	56.9%	47.8%
AC	99.8%	53.9%	47.1%
DMA	102.9%	94.3%	76.5%
MA	101.6%	159.6%	104.9%
DMAE	98.0%	59.0%	n.r.
AsSug-PO_4	100.1%	58.3%	n.r.

These findings are in agreement with those described by Tsalev *et al.* [2000]. They also reported that MA yields a higher signal compared to As^V. 1 + 4 diluted urine spiked with different arsenic species revealed lower signals for DMA, AB and AC and higher signals for MA, a pattern that is consistent with the results obtained in this work. Further dilution to 1 + 9 led to an increase in signal intensity of DMA, AB and AC to a level higher than As^V. This probably implies incomplete breakdown of these species to MA. Even at a dilution factor of 1 + 20, the signals of DMA, MA, AB and AC were higher than for arsenate.

In this work, lower values for DMA, AB and AC and higher values for MA were obtained for 1+9 diluted urine. This illustrates again that AB, AC and DMA are not completely broken down and that not much MA was formed yet. The different experimental configurations between this work and that from Tsalev *et al.* [2000] might account for the different outcomes. At the end, it can be concluded that online FI-UV-HG-AFS cannot be used for direct analysis of the total arsenic concentration in urine. Instead a digestion programme with mineral acids ($HClO_4$, H_2SO_4 and HNO_3) and pre-reduction (KI, ascorbic acid) will be used in the continuous flow mode of HG-AFS.

7.4. Selection of suitable buffer for ES-MS and UV-HG-AFS

The sensitivity of both ES-MS and UV-HG-AFS is highly dependent on the type of buffer selected. Whereas volatile buffers and solvents enhance the sensitivity of ES-MS detection, non-volatile buffers should be used with HG-AFS and organic solvents should be avoided. In a study by Le *et al.* [1998] it was shown that the maximal amount of MeOH to be added to the buffer in case of HPLC-HG-AFS was 5%. It has been the intention to simultaneously couple both detectors to the HPLC unit in order to attain both elemental and molecular/structural information at the same time. In order to do so, a buffer had to be found which allows a good separation and detection on both instruments. As both detectors have completely different optimal experimental conditions, a compromise had to be found. The following mobile phases were evaluated: ammonium acetate (20 mM), ammonium formiate (20 mM), ammonium bicarbonate (30 mM), ammonium tartrate (2, 5 and 10 mM), ammonium malonate (2, 5 and 10 mM), ammonium oxalate (2, 5 and 10 mM), sodium phosphate (20 mM) and water. All buffers were adjusted to pH 6 with NH_3 or HCOOH. In a first stage the suitability towards a good separation of arsenite, DMA, MA and arsenate was evaluated using HG-AFS and ES-MS/MS. Concentrations of 5 and 10 mM of the tartrate, malonate and oxalate buffers were too high to allow base-line separation of arsenite, DMA and MA. The concentration of the three buffers was later adjusted from 2 mM to 3 mM. Acetate, bicarbonate and phosphate at this pH and concentration have been used widely and have proved to allow good separation of As^{III}, DMA, MA and As^{V}. Repeated chromatographic separation of the four arsenicals on the Hamilton PRP-X100 column with 20 mM ammonium formiate, however, resulted in gradual degradation of the peak shape and shift of the retention times.

Next individual solutions of As^{V}, MA, DMA, AB and TETRA were eluted with different buffers. No column was used because changing from one buffer to another needs a long equilibration time. Signal to noise ratio (S/N) was used for evaluating the sensitivity. The results are shown in figures 7.7 and 7.8. In the case of UV-HG-AFS water, phosphate, tartrate and oxalate seem to be the best eluents, followed by malonate. Acetate, formiate and bicarbonate gave poor results. It can be seen that the sensitivity is inversely proportional to the buffer volatility. A very high noise level accompanied the poor sensitivity of bicarbonate. This is most probably due to the formation of CO_2 in the UV reaction coil. When UV-HG-AFS is used alone, sodium phosphate is the ideal eluent.

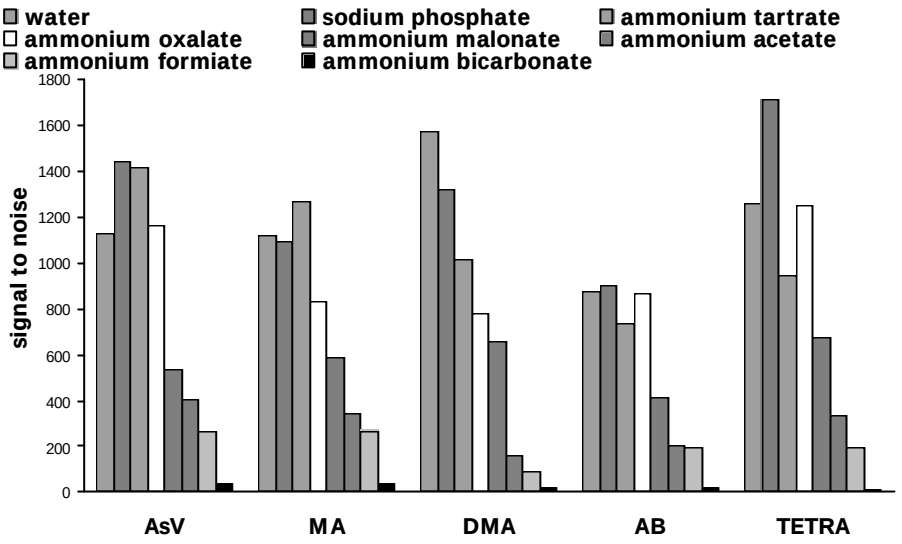

Figure 7.7. Sensitivity of HPLC-UV-HG-AFS for different arsenic species using different mobile phases.

The results for ES-MS are quite different. Note that, because the ionisation efficiency is highly dependent on the identity of the arsenic species, relative signal to noise values were used. Despite the non-volatile character of oxalate, its low concentration allows good detection of all arsenicals. No clogging of the cones is observed with this buffer. Bicarbonate gives good results as well, followed by acetate. Formiate is worse than acetate except for AB. Malonate should be avoided. When both UV-HG-AFS and ES-MS/MS are used, ammonium oxalate is the best compromise between the two detectors.

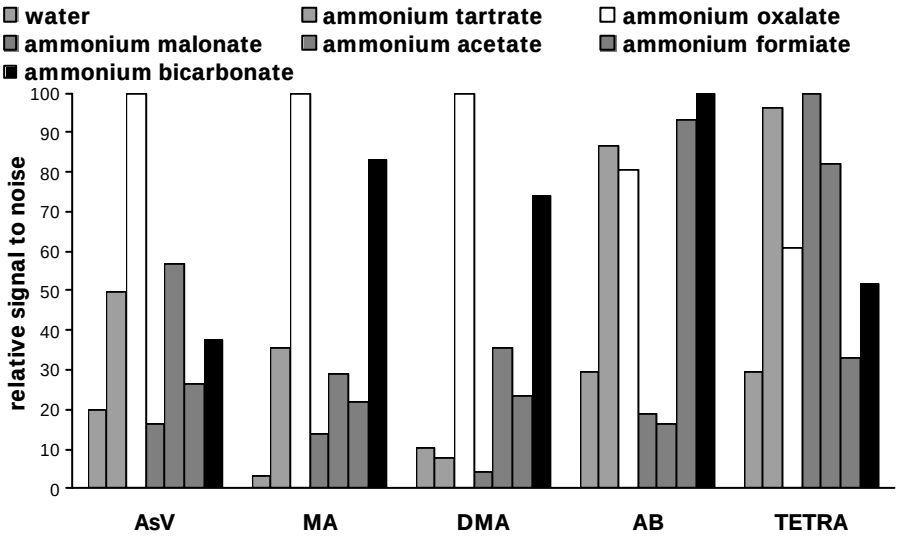

Figure 7.8. Sensitivity of HPLC-ES-MS/MS for different arsenic species using different mobile phases.

7.5. Arsenic speciation in algae

Extracts of algae samples were selected for optimisation of the detection techniques. A commercially available powdered kelp specimen was chosen. Other researchers had analysed it and it contains the four major arsenosugars and DMA. ICP-MS, UV-HG-AFS and ES-MS/MS were used as detectors. A portion of 0.1 g kelp was transferred into a centrifuge tube, extracted with 6 mL 1:1 H_2O/MeOH in an ultrasonic bath for 15 minutes and afterwards centrifuged at 9000 rpm for 15 minutes. The extraction procedure was repeated another 5 times. All filtrates were combined and left to dry overnight at 40°C. The dried residue was dissolved in a minimal amount of water, centrifuged, diluted and filtered through 0.22 µm PVDF filters before analysis. The extracts were separated on a Hamilton PRP-X100 column using different mobile phases. Each of these mobile phases allows a good separation of the four arsenosugars and DMA. It was not the intention to fully examine the quantitative aspects of the arsenic species in the algae samples. This part rather served as an exploration of the capabilities of ES-MS/MS for qualitative research of arsenic species in real-life samples, and a check whether UV-HG-AFS and ICP-MS allowed a good detection of the arsenic species.

7.5.1. Detection via ICP-MS and UV-HG-AFS

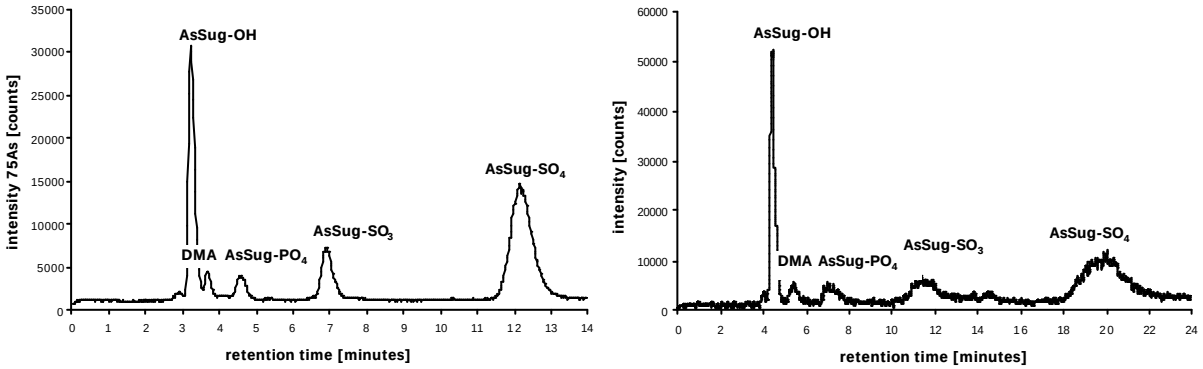

Figure 7.9. Chromatograms of kelp extract separated on PRP-X100 anion exchange column. Detection with ICP-MS (left) and UV-HG-AFS (right).

Two chromatograms of an extract of kelp powder, analysed with HPLC-ICP-MS and HPLC-UV-HG-AFS, respectively, are shown in figure 7.9. The mobile phase was 20 mM $(NH_4)_2HPO_4$ (pH 7) and 3 mM ammonium oxalate (pH 6) for ICP-MS and UV-HG-AFS respectively. The relative abundance of the arsenic peaks was determined and compared

with those obtained by other researchers. The results are given in table 7.10. The results obtained via UV-HGAFS and ICP-MS correlate well, not only mutually, but also with those obtained by other researchers [Wangkarn and Pergantis, 2000; Lai *et al.*, 1997]. The sensitivity of ICP-MS is much better than for UV-HG-AFS, but for marine samples with high amounts of arsenic, UV-HG-AFS proves to be a good and cheap alternative. The good similarity between the measurements with UV-HG-AFS and ICP-MS indicates that the UV cell is capable of completely breaking down the organic arsenicals to arsenate, leading to relative abundances which do not significantly differ from those obtained via ICP-MS. This is in contrast to the analysis of total arsenic in urine samples (paragraph 7.3).

Table 7.10. Relative abundance of arsenic species in kelp powder extract.

reference	detector	AsSug-OH	DMA	AsSug-PO_4	AsSug-SO_3	AsSug-SO_4
[Wangkarn and Pergantis, 2000]	ICP-MS	31.0%	2.6%	4.9%	12.5%	49.0%
[Lai *et al.*, 1997]	ICP-MS	35.2%	n.d.	3.0%	16.4%	45.4%
this work	ICP-MS	29.9%	3.5%	5.0%	12.1%	49.5%
this work	UV-HG-AFS	30.8%	3.2%	6.3%	13.1%	46.6%

7.5.2. Detection via ES-MS(/MS)

The capabilities of HPLC-ES-MS/MS were explored using an extract of kelp powder. The extract was separated on a PRP-X100 anion exchange column with 20 mM NH_4HCO_3 in 20% MeOH (pH 7.7). In paragraph 7.4 it was found that bicarbonate is not the ideal mobile phase for ES-MS/MS, but that experiment was done afterwards. The kelp extract was analysed via different analysis modes: selected ion recording (SIR), multiple reaction monitoring (MRM) and product ion scan. The choice of the product ions was based on infusion experiments. Pure standards of arsenic species were directly introduced in the MS and analysed via a product ion scan. The most abundant product ions were selected.

In SIR mode, the molecular ion *m/z* is selected. As can be seen from figure 7.10, more than one peak appears in each chromatogram, indicating that other compounds in the kelp extract also have the same mass as the compound of interest. In the chromatogram of arsenosugar OH (bottom), a peak at retention time 10.6 minutes co-elutes with a peak in the chromatogram of arsenosugar SO_4 (top). As will be discussed later, arsenosugar SO_4

undergoes in-source fragmentation with loss of the SO_3 group, leading to arsenosugar OH. Because of the high abundance of arsenosugar SO_4 in kelp, this peak also dominates the chromatogram of arsenosugar OH.

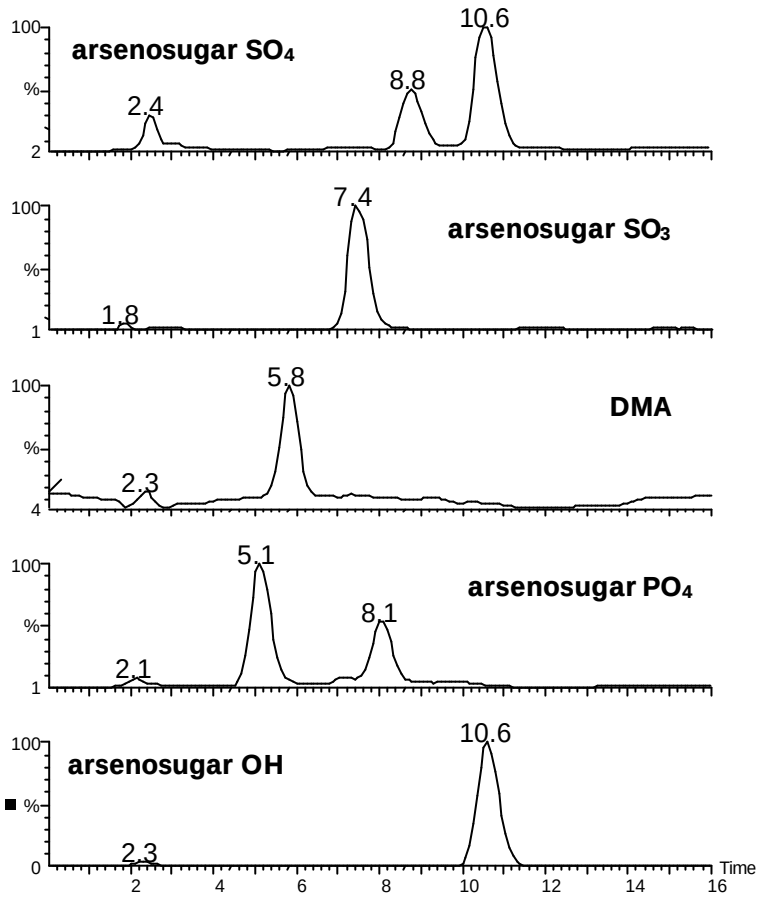

Figure 7.10. Chromatogram of kelp extract separated on a PRP-X100 anion exchange column. Detection with ES-MS (SIR mode): signals (from top to bottom) at *m/z* 409, 393, 139, 483, 329 were monitored. Time is displayed in minutes.

Figure 7.11a shows a series of chromatograms of the same kelp extract analysed in MRM mode. In MRM, Q_1 and Q_2 are set to the molecular ion and a product ion, respectively and the collision cell is filled with argon. Now it can be seen that only one peak appears, except for the arsenosugars that undergo in source fragmentation. In figure 7.11b, the chromatograms of the MRM of AsSug-PO_4 and AsSug-SO_4 are shown again, with a 10 times enhanced y-axis for the retention window 0-8 minutes in the chromatogram of arsenosugar SO_4. It can be seen that in both chromatograms a peak elutes at the same retention time. In fact arsenosugar PO_4 also undergoes in source fragmentation with cleavage of the carbon-phosphodiester bond, as is shown in figure 7.12.

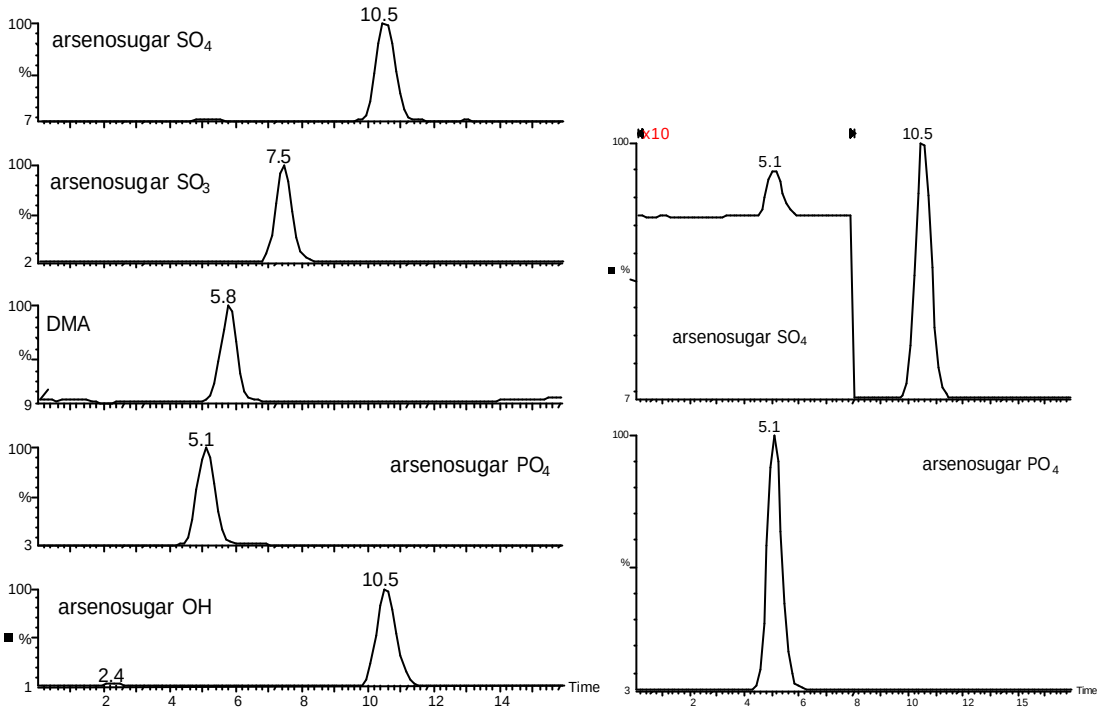

Figure 7.11a (left). Chromatogram of kelp extract separated on a PRP-X100 anion exchange column. Detection with ES-MS/MS (MRM mode): transitions (from top to bottom) at *m/z* 409>97, 393>97, 139>121, 483>97 and 329>97 were monitored. Time is displayed in minutes.

Figure 7.11b (right). Same chromatogram of kelp extract separated on a PRP-X100 anion exchange column. Detection with ES-MS/MS (MRM mode): transitions at *m/z* 409>97 (top) and 483>97 (bottom) were monitored. An enhanced y-axis in a part of the chromatograms of arsenosugar SO_4 indicates in source fragmentation of arsenosugar PO_4. Time is displayed in minutes.

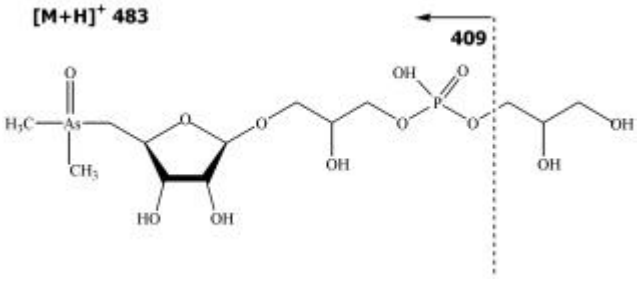

Figure 7.12. In source fragmentation of arsenosugar PO_4.

Figure 7.13 shows a series of HPLC-ES-MS/MS chromatograms analysed in product ion scan mode. Q_1 selects the molecular ion $[M+H]^+$, the collision cell is filled with argon and Q_2 scans the product ions in a given *m/z* range. Figures 7.14 and 7.15 show the product ion spectra of DMA and the 4 arsenosugars from that product ion scan, respectively. The product ion spectra of the pure standards of DMA and the four arsenosugars are found in

figures 7.14 and 7.16, respectively. In figures 7.15 and 7.16, the region between *m/z* 100 and 300 is enlarged five times. The product ion spectra of the 5 arsenic species in the kelp extract are in good agreement with those of the pure standards.

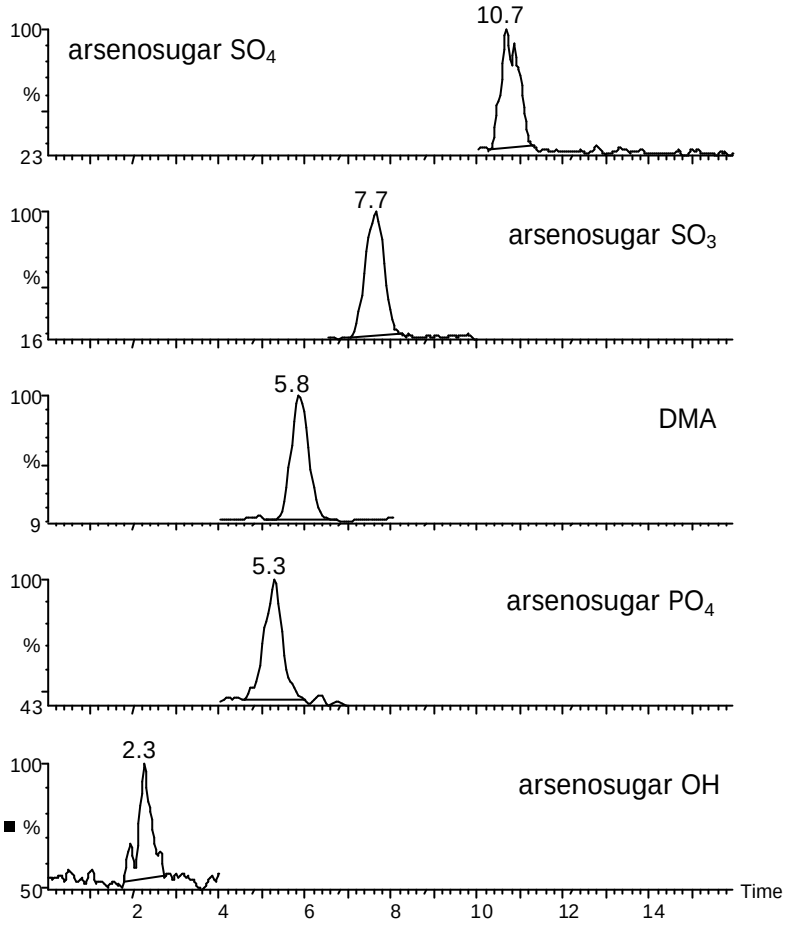

Figure 7.13. Chromatogram of kelp extract separated on a PRP-X100 anion exchange column. Detection with ES-MS/MS (product ion scan mode): product ions of (from top to bottom) *m/z* 409, 393, 139, 483 and 329 were monitored. Time is displayed in minutes.

The type of analysis mode (product ion scan, precursor ion scan, MRM, SIR, neutral loss scan, full scan) has implications for the ion energies in the mass spectrometer region (see also table 4.2). Quadrupoles that perform a scan (Q_2 in product ion scan mode, Q_1 in precursor ion scan mode, Q_1 and Q_2 in neutral loss scan mode, Q_1 in full scan MS1 mode) are set at a lower ion energy than quadrupoles that perform a static analysis (Q_1 and Q_2 in MRM, Q_1 in SIR, Q_1 in product ion scanning and Q_2 in precursor ion scanning), because ions should pass sufficiently slowly to allow a complete scan over a wide m/z range (*e.g.*, 500 Da) within a short time span (1-2 seconds).

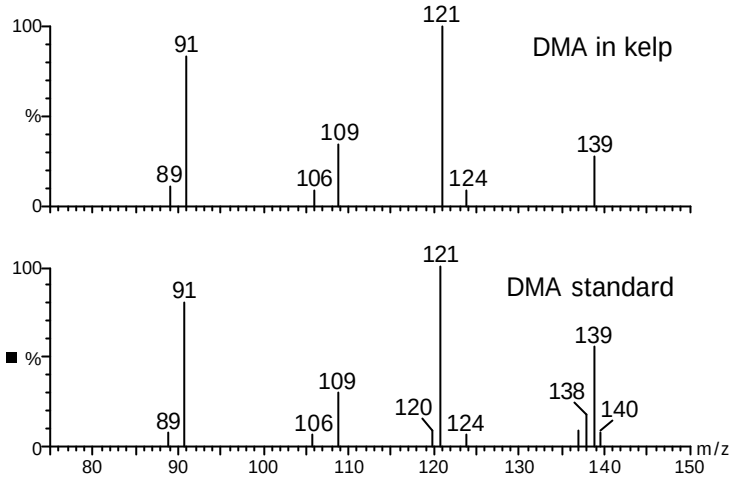

Figure 7.14. Product ion spectra of DMA in kelp (top) and a DMA standard (bottom).

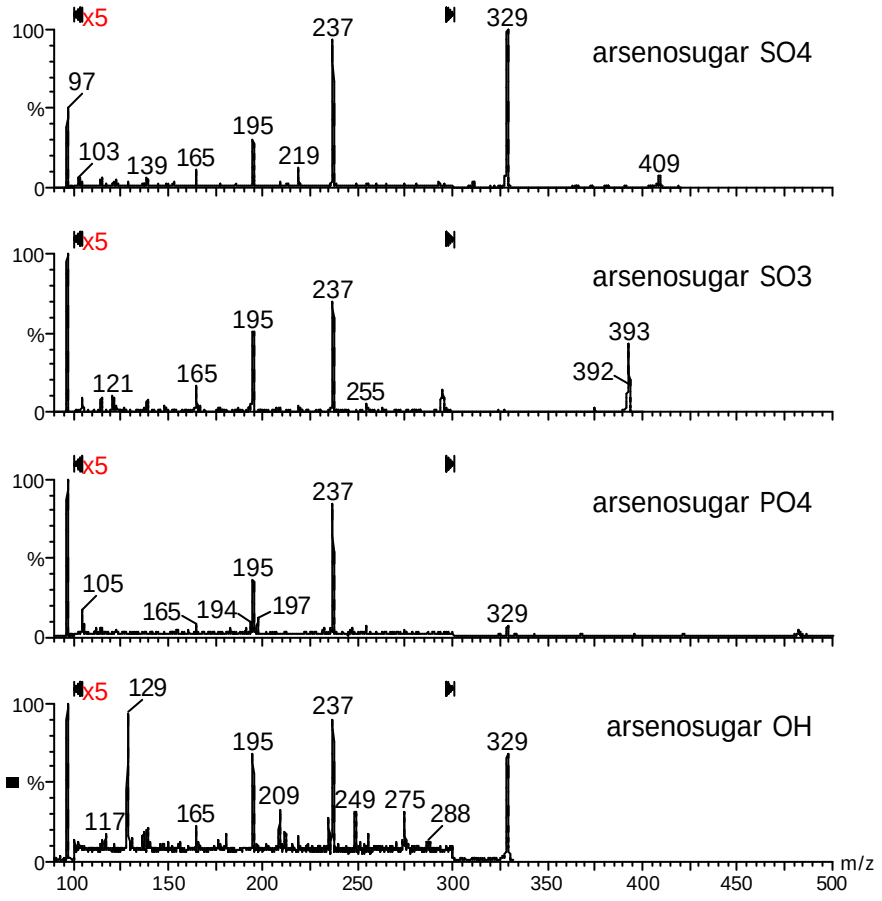

Figure 7.15. Product ion spectra of the 4 arsenosugars in kelp. From top to bottom: AsSug-SO_4, AsSug-SO_3, AsSug-PO_4 and AsSug-OH.

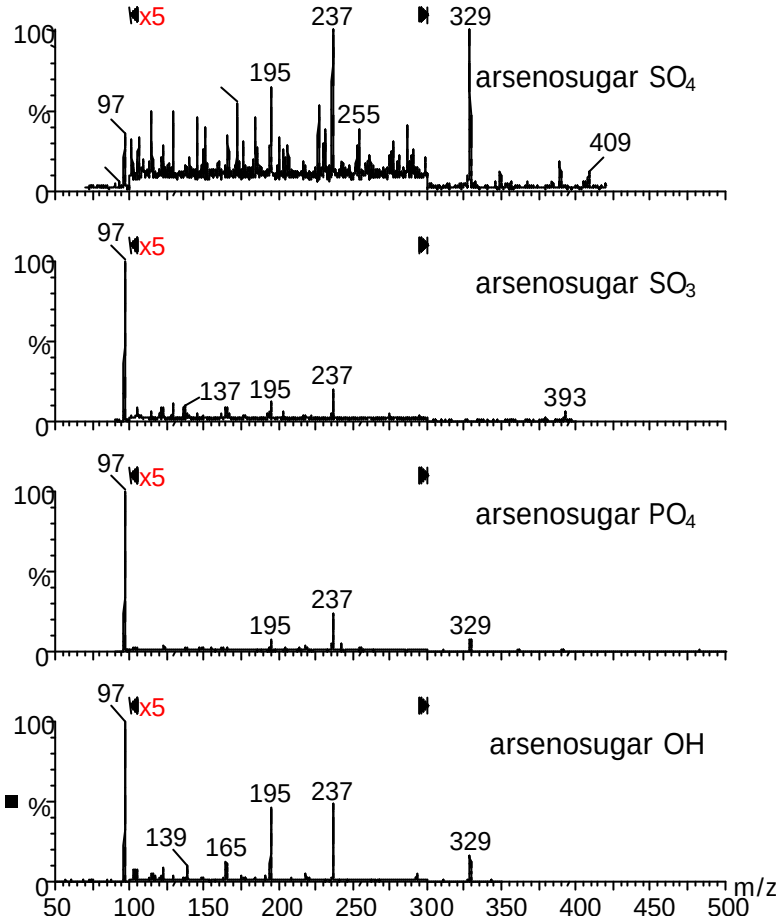

Figure 7.16. Product ion spectra of the 4 arsenosugar standards. From top to bottom: AsSug-SO_4, AsSug-SO_3, AsSug-PO_4 and AsSug-OH.

More details about the identity of the different product ions formed from arsenic species have been compiled in a review of McSheehy and Mester [2003].

7.5.3. Dual detection with UV-HG-AFS and ES-MS/MS.

Figure 7.17 gives an example of the capabilities of dual detection with UV-HG-AFS and ES-MS/MS (MRM mode). An extract of kelp was analysed via anion exchange chromatography with 3 mM ammonium oxalate (pH 6). The fact that both elemental and molecular/structural information is obtained within one run is especially advantageous when searching for unknown arsenic species. When UV-HG-AFS is combined with full scan ES-MS, each signal of elemental arsenic is accompanied by a signal obtained from the full scan spectrum at exactly the same retention time.

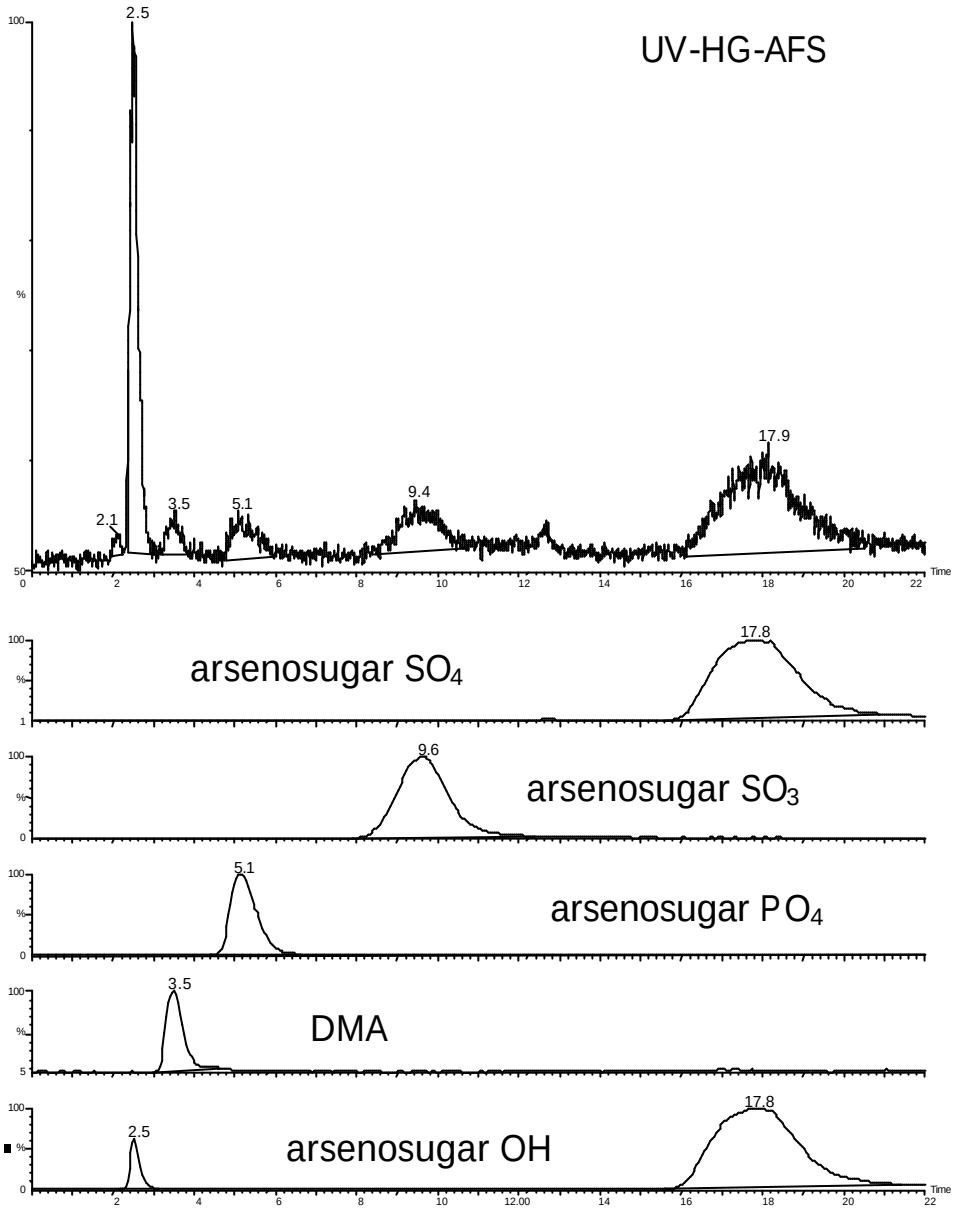

Figure 7.17. Chromatogram of kelp extract separated on PRP-X100 column. Detection with UV-HG-AFS (top) and ES-MS/MS (below) in MRM mode: transitions (from top to bottom) 409 > 97, 393 > 97, 483 > 97, 139 > 91 and 329 > 97. Time is displayed in minutes.

It can, however, be questioned whether UV-HG-AFS is sensitive enough to detect the low amounts of unknown arsenic metabolites in urine. At least for the identification of unknown arsenicals in marine samples, this approach is very promising.

7.5.4. Elemental detection via ES-MS

Madsen *et al.* [2000] have analysed an extract of the alga *Fucus serratus* with HPLC-ICP-MS and HPLC-ES-MS on a single quadrupole MS. They used the approach of in source fragmentation to identify the arsenosugars. Using variable cone voltage values in source fragmentation allows the detection of the molecular ion (low cone voltage), a fragment of the arsenosugars (moderate cone voltage) and at very high voltage the naked $^{75}As^+$ ion.

Figure 7.18 shows a series of chromatograms of an extract of *Fucus*. The top chromatogram is an overlay of 4 MRM transitions (329>97, 483>97, 393>97 and 409>97). The small peaks at the retention time of AsSug-PO_4 and AsSug-SO_4 are the result of in source fragmentation of AsSug-PO_4 to AsSug-SO_4 and AsSug-SO_4 to AsSug-OH, respectively. Below a SIR chromatogram is given in which the signal at *m/z* 75 is recorded using a cone voltage of 150 V. As described in paragraph 7.1.1., a cone voltage of 150 V results in complete fragmentation of the arsenic-oxygen bond. Although the base line severely fluctuates, 4 peaks corresponding to the retention time of the 4 arsenosugars dominate. The bottom chromatogram again clearly proves the high matrix dependence of ES-MS/MS. The drop in baseline in the void volume is a result of the co-elution of many neutral molecules and cations.

When searching for unknown arsenic species, this approach is a good alternative to the dual detection approach. An additional advantage is that no compromise of the experimental conditions for the HPLC separations is needed to fit as well elemental as ES-MS/MS detection. It should, however, be reported that a signal at *m/z* 75 is no proof for the presence of arsenic. Other compounds can also undergo in source fragmentation and lead to a compound with the same mass. It can again be questioned whether this approach will allow the detection of the low amounts of arsenic metabolites in urine. On the other hand, if each peak at *m/z* 75 (As^+) is accompanied by a signal at *m/z* 90, ($MeAs^+$), 91 (AsO^+), 105 (Me_2As^+)... there is convincing proof of the presence of an arsenic containing compound.

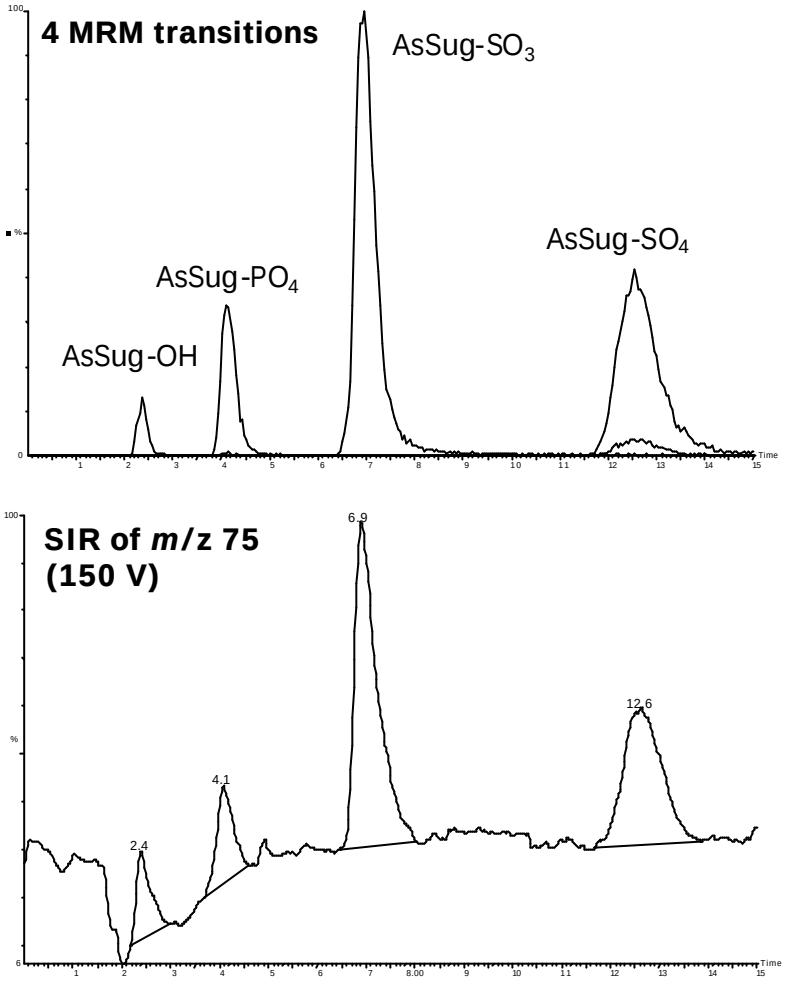

Figure 7.18. Chromatogram of *Fucus* extract separate onPRP-X100 anion exchange column. Detection via MRM (top) of 4 arsenosugars and via SIR of *m/z* 75 (bottom) at high cone voltage. Time is displayed in minutes.

References

[Francesconi *et al.*, 2000]

Francesconi KA, Khokiattiwong S, Goessler W, Pedersen SN and Pavkov M (2000). *Chem. Comm.*, 1083-1084.

[Francesconi, 2002]

Francesconi KA (2002). *Appl. Organomet. Chem.*, **16**, 437-445.

[Gomez-Ariza *et al.*, 1998]

Gomez-Ariza JL, Sanchez-Rodas D, Beltran R, Corns W and Stockwel P (1998). *Appl. Organomet. Chem.*, **12**, 439-447.

[http 6]

http://www.laboratorytalk.com/books/chem/chrom/rs_10/rs_10_18.html

[http 7]

http://www.dupont.com/teflon/af/

[http 8]

http://www.agrenetics.com/page9.html

[Le and Ma, 1998]

Le XC and Ma M (1998). *Anal. Chem.*, **70**, 1926-1933.

[Madsen *et al.*, 2000]

Madsen AD, Goessler W, Pedersen SN and Francesconi KA (2000). *J. Anal. At. Spectrom.*, **15**, 657-662.

[McSheehy and Mester, 2003]

McSheehy S and Mester Z (2003). *Trends Anal. Chem.*, **22**, 210-224.

[Rubio *et al.*, 1993]

Rubio R, Padro A, Alberti J and Rauret G (1993). *Anal. Chim. Acta*, **283**, 160-166.

[Tsalev *et al.*, 1998]

Tsalev DL, Sperling M and Welz B (1998). *Analyst*, **123**, 1703-1710.

[Tsalev *et al.*, 2000]

Tsalev DL, Sperling M and Welz B (2000). *Spectrochim. Acta B*, **55**, 339-353.

[Zhang *et al.*, 1995]

Zhang X, Cornelis R, De Kimpe J, Mees L, Vanderbiesen V and Vanholder R (1995). *Fres. J. Anal. Chem.*, **353**, 143-147.

[Zhang *et al.*, 1996]

Zhang X, Cornelis R, De Kimpe J and Mees L (1996). *Anal. Chim. Acta*, **319**, 177-185.

Chapter 8. Arsenic: measurement of arsenic metabolites from arsenosugars

The main part of the work on arsenic speciation deals with the metabolism of arsenosugars in humans. Arsenosugars appear in marine plants and animals. Algae were chosen as the food source of arsenosugars, because the concentration of the arsenosugars in algae is normally higher than in marine animals and because arsenosugars are, except for some DMA, the main organic arsenicals present in algae. Urine and blood samples were analysed for their total arsenic content and speciation of arsenic compounds. Because low levels of arsenic were expected in urine and blood, ICP-MS was chosen besides UV-HG-AFS, as the element specific detector. The ICP-MS measurements were optimised to obtain a high sensitivity. During the past years, a series of experiments have been carried out in which several volunteers ingested the edible seaweed *Laminaria japonica*. These experiments will be described chronologically.

8.1. Optimisation of ICP-MS

RF power and methanol content are considered the most relevant factors to exert an influence on the sensitivity of the arsenic detection [Larsen and Stürup, 1994]. These were checked, as well as the other instrumental parameters that were optimised daily. Furthermore it was checked whether simple sample dilution would yield quantitative recovery of arsenic notwithstanding the high carbon and salt content in urine.

A solution of DMA (20 ng/mL As) in 1% HNO_3 was measured using RF power settings between 1100 and 1350 W. Signals at *m/z* 75 ($^{75}As^+$), 77 ($^{40}Ar^{37}Cl^+$) and 51 ($^{35}Cl^{16}O^+$) were detected. The signals at *m/z* 77 and 51 served as a measure for the chloride interference.

The results are shown in table 8.1. There is a significant increase in signal intensity for arsenic, which is likely to further increase above 1350 W. In order not to damage the instrument, it was chosen to use a value of 1300 W. At this value different degrees of methanol were added to either a solution of DMA (20 ng/mL As) in 1% HNO_3 or DMA (20 ng/mL As) in 1:50 diluted urine. A urine sample was taken from a volunteer who had not recently eaten arsenic-rich food (table 8.2). In both cases, the highest signal intensity was obtained at a methanol degree of 3%. Changing the RF power from 1100 W to 1300 W and adding 3% MeOH to the solution thus resulted in a six-fold increase in signal intensity. The influence of an increasing amount of MeOH on the signal intensity of As at a normal RF value of 1100 W was less outspoken (data not shown).

Table 8.1. Influence of RF power on signal intensities of $^{75}As^+$, $^{77}[ArCl]^+$ and $^{51}[ClO]^+$ in solution of DMA (20 ng/mL As) in 1% HNO_3.

RF power [W]	$^{75}As^+$ [counts] mean & SD of 10 replicates	$^{77}[ArCl]^+$ [counts] mean & SD of 10 replicates	$^{51}[ClO]^+$ [counts] mean & SD of 10 replicates
1100	35465 (1535)	445 (50)	942 (66)
1150	58131 (1496)	712 (31)	1792 (115)
1200	70603 (1196)	896 (44)	2271 (68)
1250	80243 (712)	1057 (37)	2831 (86)
1300	86457 (645)	1151 (49)	3213 (100)
1350	90029 (969)	1273 (81)	3516 (77)

Table 8.2. Influence of MeOH on signal intensity of $^{75}As^+$ in solution of DMA (20 ng/mL As) in 1% HNO_3 and of DMA (20 ng/mL As) in 1:50 diluted urine.

% MeOH	1% HNO_3 $^{75}As^+$ [counts] mean & SD of 20 replicates	1:50 urine $^{75}As^+$ [counts] mean & SD of 20 replicates
0%	84717 (2272)	83774 (1230)
1%	155319 (6433)	145727 (9359)
3%	207011 (8194)	209827 (5580)
5%	107083 (12512)	136813 (8112)
10%	21816 (3384)	26425 (4101)

The influence of NaCl on the signal intensity of As was investigated in order to derive which dilution factor had to be used in order to overcome a significant polyatomic interference

from $^{75}ArCl^+$. The average urinary chloride concentration is 135 mmol/day with extreme ranges of 80-270 mmol/day. This is equivalent to a maximum of 7.04 g/L chloride, taking into account a mean daily urinary volume of 1.36 L (33 men). These values were obtained from literature data [Geigy, 1981]. First a blank urine and then spiked (DMA, 20 ng/mL As) solutions of 1% HNO_3 and diluted urine (1:50 and 1:100) were analysed. The results are shown in table 8.3. The signal intensity of $^{51}ClO^+$ in the blank and spiked samples increases in the series 1% HNO_3 < 100x diluted urine < 50x diluted urine. This indicates that the amount of NaCl increases in the series 1% HNO_3 < 100x diluted urine < 50x diluted urine. On the other hand, there is no apparent difference between the signal intensities of $^{75}As^+$ for 20 ng/mL As in nitric acid, in 50x diluted urine and in 100x diluted urine, indicating that at these dilution factors, the NaCl does not give rise to a significant spectral interference of $^{75}[ArCl]^+$. Notice that a 1 mg/L NaCl solution does not significantly contribute to a signal at *m/z* $^{75}As^+$ either. It causes an apparent arsenic concentration of 0.7 ng/mL. Notice that the signal for $^{75}As^+$ and $^{77}[ArCl]^+$ in the urine samples is lower than in the 1% HNO_3 solution. This is most probably due to the presence of easy ionisable elements in the urine sample that cause a decrease in the ionisation efficiency of $^{75}As^+$ and $^{77}[ArCl]^+$.

Table 8.3. Influence of salt content on signal intensities of $^{75}As^+$, $^{77}[ArCl]^+$ and $^{51}[ClO]^+$ in blank and spiked solutions of 1% HNO_3, 1:100 diluted urine and 1:50 diluted urine.

sample	$^{75}As^+$ [counts] mean & SD of 30 replicates	$^{77}[ArCl]^+$ [counts] mean & SD of 30 replicates	$^{51}[ClO]^+$ [counts] mean & SD of 30 replicates
blank 1% HNO_3	4435 (150)	1406 (53)	2662 (85)
20 ng/mL As as DMA in 1% HNO_3	83232 (699)	1126 (38)	3020 (116)
blank 100x diluted urine	3707 (148)	1201 (50)	5058 (125)
20 ng/mL As as DMA in 100x diluted urine	82364 (561)	1107 (50)	5130 (126)
blank 50x diluted urine	3943 (108)	1227 (55)	6902 (305)
20 ng/mL As as DMA in 50x diluted urine	82730 (697)	1179 (51)	6907 (232)
1 mg/L NaCl in 1% HNO_3	2719 (136)	1200 (55)	2911 (117)

No methanol was added to these solutions, so the question can be asked whether or not the carbon present in urine influences the signal intensity of arsenic. The total carbon content of urine is around 3.6 g/L, estimated from mean urinary levels of urea (CH_4N_2O,

20.0% (m/m) C, 20.6 g/d), creatine ($C_4H_9N_3O_2$, 36.6% (m/m) C, 85 mg/d), creatinine ($C_4H_7N_3O$, 42.5% (m/m) C, 1.4 g/d) and uric acid ($C_5H_4N_4O_3$, 35.7% (m/m) C, 528 mg/d) and a mean urinary volume of 1.36 L/d [Geigy, 1981]. In 50x diluted urine the total carbon content would be 0.073 C g/L or 0.0073% (m/v) C. This is equivalent to 0.0194% MeOH. Although the influence of a solution of 0.0194% MeOH on the signal intensity of $^{75}As^+$ was not tested, it is unlikely that this low amount of carbon would significantly contribute to an increased signal at *m/z* 75. Moreover when the urine samples will be analysed the amount of carbon in the diluted samples will be negligible compared to the amount of MeOH added.

Table 8.4. Influence of urine matrix on signal intensities of $^{75}As^+$, $^{77}[ArCl]^+$ and $^{51}[ClO]^+$.

sample	$^{75}As^+$ [counts] mean & SD of 10 replicates	$^{77}[ArCl]^+$ [counts] mean & SD of 10 replicates	$^{51}[ClO]^+$ [counts] mean & SD of 10 replicates
20 ng/mL As in 1% HNO_3	59506 (875)	939 (42)	**3002 (39)
20 ng/mL As in 1:100 urine	59608 (569)	947 (31)	**5504 (137)
20 ng/mL As in 1:50 urine	60489 (628)	846 (25)	**7853 (215)
20 ng/mL As in 1:30 urine	59195 (748)	935 (54)	**11004 (386)
20 ng/mL As in 1:10 urine	61340 (802)	*1395 (43)	**25696 (1570)

* significantly different from other $^{77}[ArCl]^+$ values (P = 0.05)
** correlation coefficient R^2 = 0.9994

The influence of the urine matrix was further checked. Solutions of DMA (20 ng/mL As) in 1% HNO_3 and in 1:100, 1:50, 1:30 and 1:10 urine were prepared. The results are shown in table 8.4. There is no significant increase in signal intensity for *m/z* 75 and 77 up to 1:30 diluted urine. The good correlation (R^2 0.9994) of the signal intensity at *m/z* 51 shows the increasing amount of chlorine in the samples. The signal intensity for *m/z* 77 in the 1:10 urine is significantly (P = 0.05) different from the other four values. The increase for the signal at *m/z* 77 for the 1:10 diluted urine sample amounts to 478 counts compared to the other four urine samples. An increase of 478 counts for *m/z* 77 corresponds to an increase of 1495 counts at *m/z* 75, taking into account the isotopic ratio of $^{35}Cl/^{37}Cl$. This increase of 1495 counts is almost identical to the increase noted between the 1:10 diluted urine and the mean of the other samples at *m/z* 75 (difference of 1640). Vanhoe *et al.* [1994] investigated the spectral interferences encountered in the analysis of biological samples by ICP-MS. They calculated that chlorine concentrations of 100 and 500 mg/L (4 and 20 g/L,

respectively, before dilution) gave rise to an apparent arsenic concentration of 1.6 and 7.6 ng/mL, respectively. A linear relationship between chloride concentration and apparent arsenic concentration was found in the interval 1-1000 mg/L chloride. A maximum of 7.04 g/L chloride (176 mg/L after dilution) results in an apparent arsenic level of 2.78 ng/mL. This is well below the expected elevated arsenic levels in urine (up to 100 ng/mL As) found after ingestion of arsenosugar containing food.

8.2. Arsenic speciation in urine and blood

In order to study the metabolites of the arsenosugars after ingestion of the seaweed *Laminaria*, seven trials were designed whereby Belgian and Chinese volunteers ate a given portion of seaweed. In the consecutive trials, new findings of previous trials and new findings of other researchers were checked, and other separation and detection methods were used. Prior to each trial, *Laminaria* was thoroughly cleaned with tap water and rinsed with deionised water. The volunteers ingested a portion of 20-30 g (dry mass) algae, either dried, wetted or boiled within a time span of 30 minutes. The total arsenic content in the *Laminaria* is 43.2 ± 0.4 mg kg^{-1}. A chromatogram of an extract of the *Laminaria*, as ingested, is shown in figure 8.1. It contains AsSug-OH, AsSug-PO_4, AsSug-SO_3 and a small amount of DMA. The volunteers refrained from eating arsenic-rich food (fish, crustaceans, molluscs, mushrooms...) 3 days prior to and during the experiment.

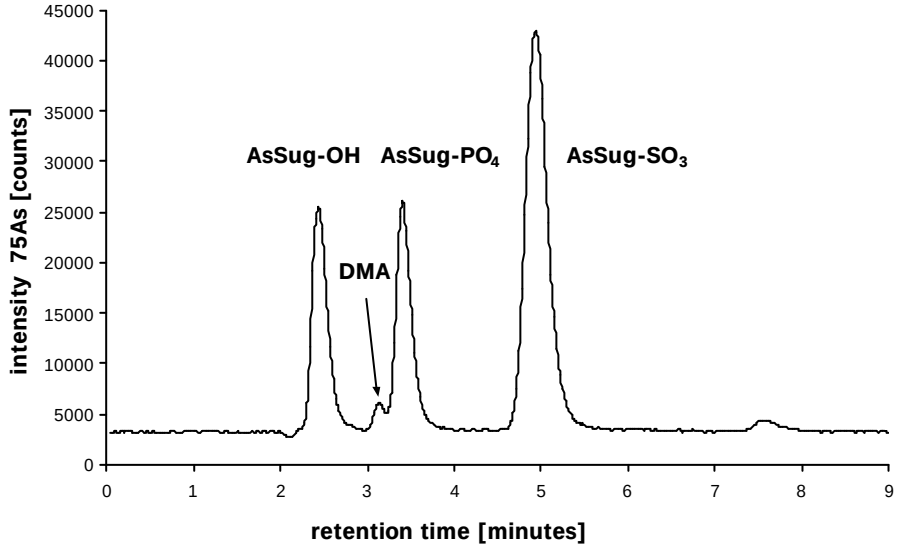

Figure 8.1. Chromatogram of *Laminaria* extract separated on PRP-X100 anion exchange column. Detection with ICP-MS.

8.2.1. First trial

A first experiment was conducted at the Tsinghua University in Beijing, P.R. China in April 2001. Four male Chinese volunteers (aged 21, 24, 28 and 45 y) and myself (age 25 y) ingested a portion of 20 g raw *Laminaria*. Volunteer 1 mixed the seaweed in his soup. Volunteer 2 ate fish two days after ingestion of the seaweed and repeated the experiment two weeks later. Therefore small differences in retention times can be seen between the peaks in the chromatograms of volunteer 2 compared to the others. Urine was collected before and up to 120 hours after uptake. Each of the volunteers was asked to collect as much urine samples as possible. A minimum of four urine samples was collected each day. The urine samples were collected in acid washed polyethylene (PE) beakers and transferred into acid washed PE bottles, or collected directly in the PE bottles. The bottles were stored at 4°C. All urine samples were analysed for their total arsenic (ICP-MS) and creatinine (HPLC-UV) content and selected urine samples of all volunteers were chromatographed (anion exchange HPLC-ICP-MS) for speciation analysis. The objective of this first trial was to get a general idea about the concentration of arsenic in the urine samples and about the amount of urinary arsenic metabolites in a small population who is used to ingest algal food.

For the analysis of the total amount of arsenic in urine, the samples were diluted 40x in 1% HNO_3 to which 3% MeOH was added. Standards were also diluted in 1% HNO_3 to which 3% MeOH was added. All samples and standards were measured by means of ICP-MS on an Elan 6000 (PE Sciex, Toronto, Canada). External calibration using an arsenic standard solution (As^V) was applied. The ICP-MS measurement conditions were optimised on a daily basis. Average values for nebuliser gas flow (1 L/min), RF power (1300 W) and lens voltage (9 V) were obtained. The ion intensities at *m/z* 75 (As^+) and 77 (Se^+, $ArCl^+$) were monitored. Urinary creatinine was determined in order to normalise the different urine samples of each volunteer. The method is based on that of Archari *et al.* [1983]. Reversed phase HPLC with UV detection on a Waters 600 pump and a Waters 486 UV detector (Waters, Milford, USA) was used. A volume of 50 µl of a 50x diluted urine was chromatographed with 50 mM sodium acetate (pH 6.5) in 98+2 water/acetonitrile on a Waters C18 column using a flow rate of 1 mL/min. A plot showing the creatinine adjusted urinary arsenic concentration versus time after ingestion for all volunteers is given in figure 8.2. It can be seen that for the Chinese volunteers a maximum arsenic/creatinine ratio is obtained within 15 to 25 hours after ingestion. Only low concentrations were to be noted

for volunteer 5; a small maximum can be seen at 38 hours. From the figure, it might be concluded that the arsenic metabolism of volunteer 5 differs from that of the other volunteers. However, in terms of non-normalised amounts, the maximum urinary arsenic levels of volunteer 5 are not significantly below the others. The highest value was found in the urine of volunteer 4 (228 ng/mL), followed by volunteer 2 (158 ng/mL), volunteer 3 (141 ng/mL), volunteer 1 (72 ng/mL) and volunteer 5 (70 ng/mL). On the other hand, the mean urinary creatinine value of volunteer 5 was higher than for volunteers 1, 2 and 3. Volunteer 4 showed the highest mean creatinine value. Creatinine is a waste product from meat protein in the diet and from the muscles. The diet and the physical condition/behaviour therefore play an important role. In fact none of the 5 volunteers had problems in digesting the seaweed or felt uncomfortable during the course of the experiment. All concentration levels return to background levels after about 80 h. The different ethnic origin and food culture might explain the different background level of arsenic in urine.

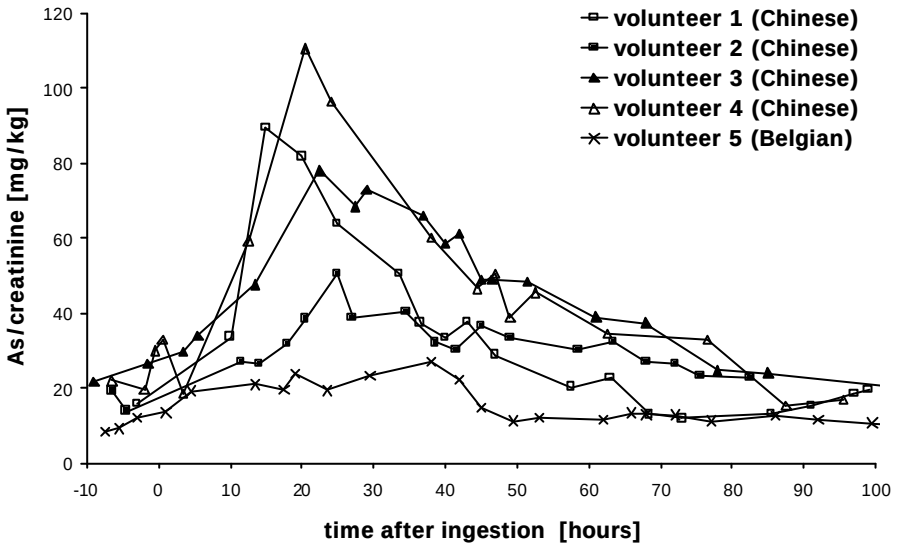

Figure 8.2. Urinary creatinine-normalised arsenic concentrations of five volunteers before and after ingestion of *Laminaria*. Detection with ICP-MS.

The results correlate well with those obtained by Le *et al.* [1994], Ma and Le [1998] and Francesconi *et al.* [2002]. Le *et al.* found that 9 volunteers who ingested 9.5 g of nori showed maximum concentrations 10-60 hours after ingestion. Their values, however, were not normalised versus creatinine. Using non-normalised data we also obtained a broader time span. According to Ma and Le [1998], the highest concentrations in the urine of the 4 volunteers who ingested 9.5 g of nori were found between 22 and 38 hours after ingestion.

In the study by Francesconi *et al.* [2002] one volunteer obtained the maximum normalised arsenic value 27 hours after ingestion of a pure arsenosugar.

Table 8.5. Chromatographic conditions of anion and cation exchange for separation of arsenicals in algal extracts and urine.

technique	anion exchange	cation exchange
column	Hamilton PRP-X100	Dionex Ionpac CS10
dimensions & particle size guard column	25 x 2.3 mm id, 12-20 µm	50 x 4 mm id, 10 µm
dimensions & particle size anal. column	250 x 4.1 mm id, 10 µm	250 x 4 mm id, 10 µm
flow rate [mL/min]	1	1
buffer	20 mM $(NH_4)_2HPO_4$ (pH 7) in 3% MeOH	20 mM pyridine (pH 3) in 3% MeOH

Speciation analysis using anion exchange and cation exchange was done. The experimental conditions for HPLC are listed in table 8.5. For the anion exchange buffer a pH of 7 was chosen on the basis of the separation of the *Laminaria* extract. At pH 6 no base-line separation of arsenosugar OH from DMA can be achieved. Only later it was realised that at pH 7, DMA and MA are not well separated from one another. Figures 8.3 to 8.7 show the anion exchange HPLC-ICP-MS chromatograms of urine samples from all volunteers. In the figures 8.3a to 8.7a the chromatogram of the urine sample containing the highest amount of arsenic is shown for each volunteer. In the insert of each of these chromatograms a detailed area (the retention window 0-5 minutes) of four urine samples obtained at different points of time relative to seaweed intake is shown. In the figures 8.3b to 8.7b a more detailed insert of the urine sample containing the maximum amount of arsenic is shown, also for each of the volunteers. A total of 11 arsenic containing peaks can be observed. Peak identification was done using a blank urine sample spiked with AB, As^{III}, DMA, MA and As^{V}. Peak 1 is unknown. Peaks 2 and 3 co-elute with AB and As^{III}, respectively. Peak 4 is DMA, while peak 5, in the right shoulder of the DMA peak, is MA. Peaks 7 to 11 are unknown. A small peak sometimes appears which co-elutes with the signal of $^{51}ClO^{+}$, indicating the presence of a $^{75}ArCl^{+}$ interference. This peak is denoted as X throughout all chromatograms.

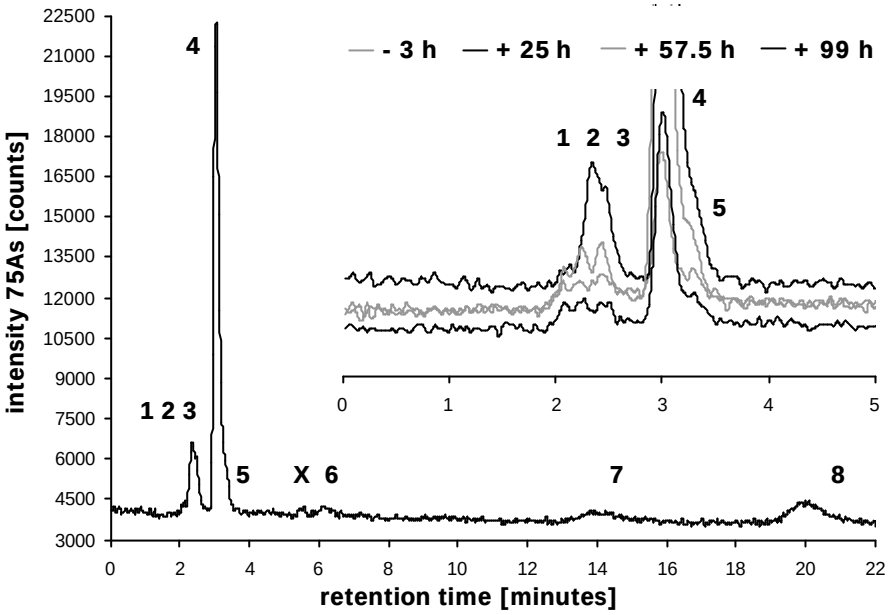

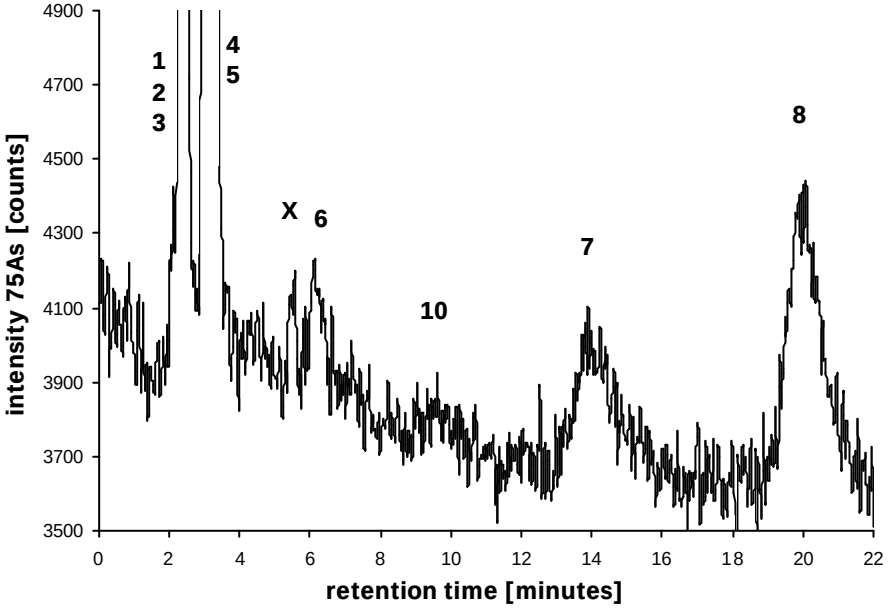

Figure 8.3a (top). Chromatogram of urine sample from volunteer 1. In insert a detailed area of different urine sample. Separation on PRP-X100 anion exchange column, detection with ICP-MS.

Figure 8.3b (bottom). Same chromatogram as in figure 8.3a with enhanced y-axis.

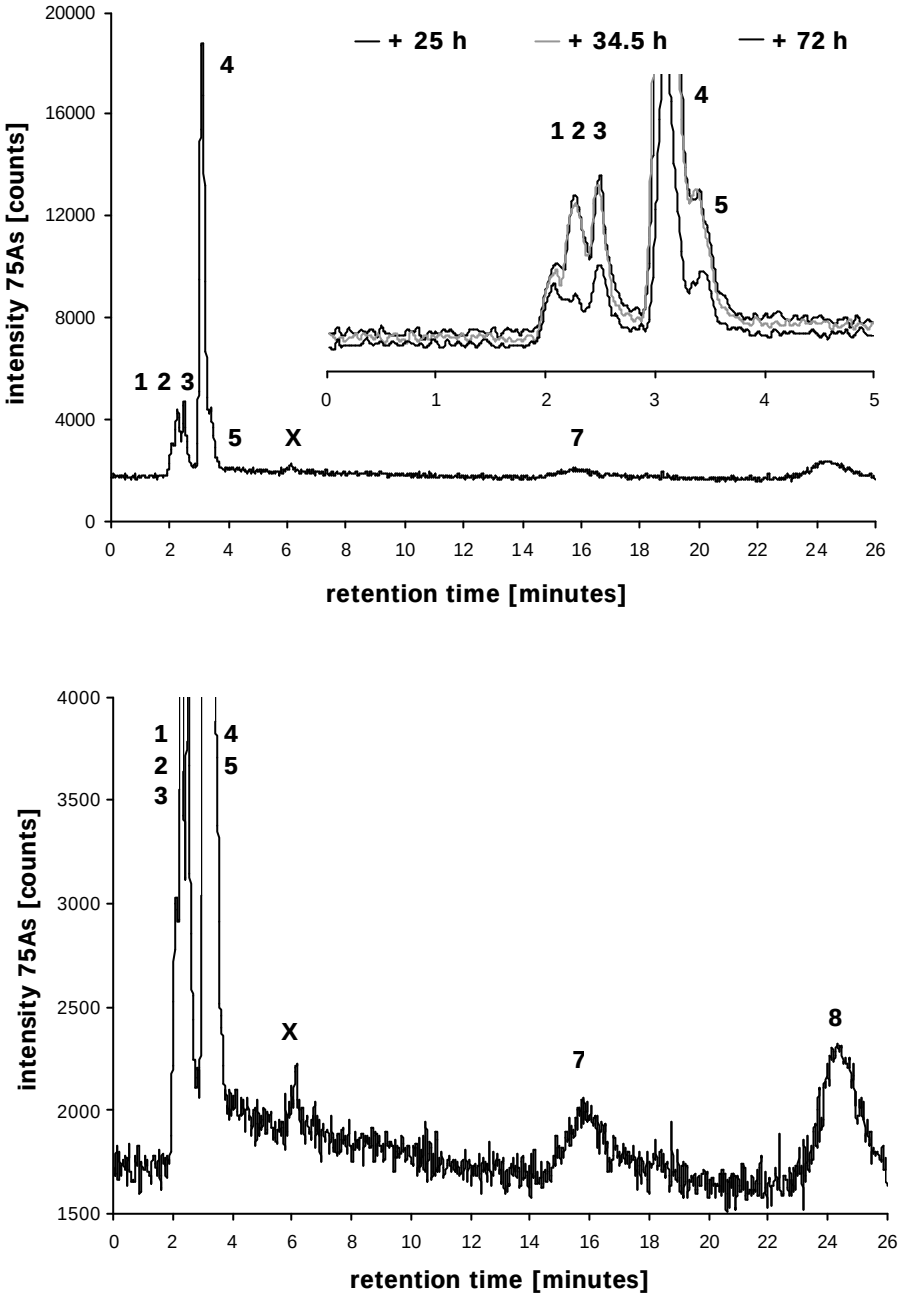

Figure 8.4a (top). Chromatogram of urine sample from volunteer 2. In insert a detailed area of different urine sample. Separation on PRP-X100 anion exchange column, detection with ICP-MS.

Figure 8.4b (bottom). Same chromatogram as in figure 8.4a with enhanced y-axis.

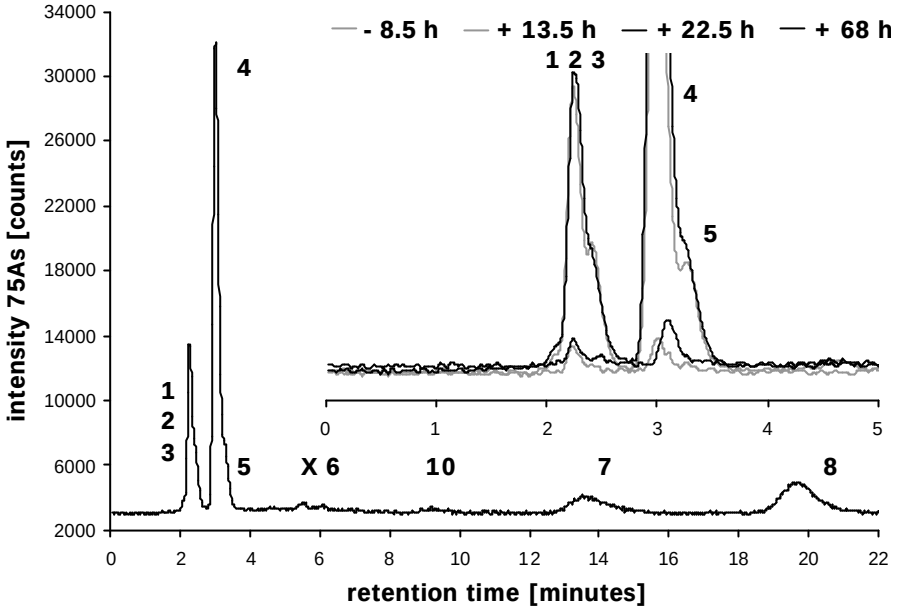

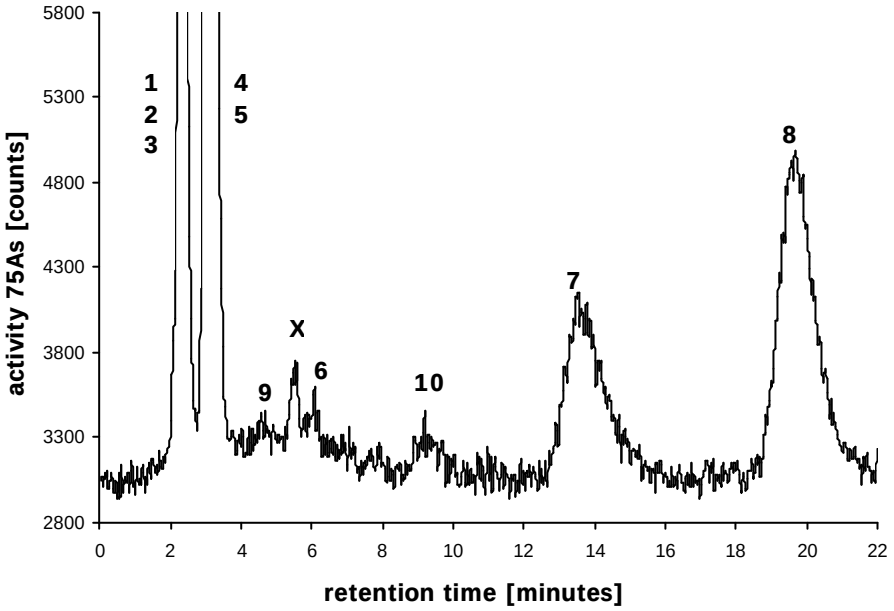

Figure 8.5a (top). Chromatogram of urine sample from volunteer 3. In insert a detailed area of different urine sample. Separation on PRP-X100 anion exchange column, detection with ICP-MS.

Figure 8.5b (bottom). Same chromatogram as in figure 8.5a with enhanced y-axis.

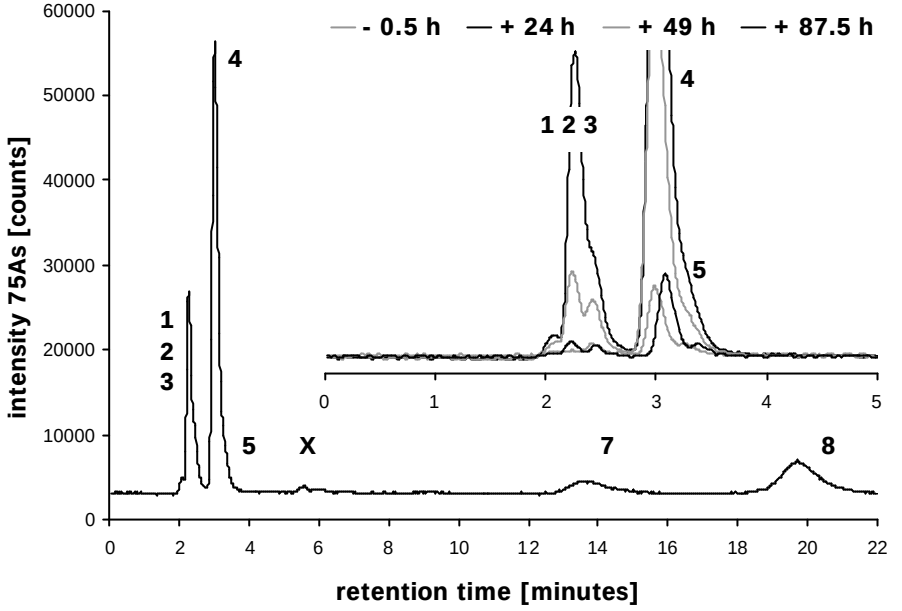

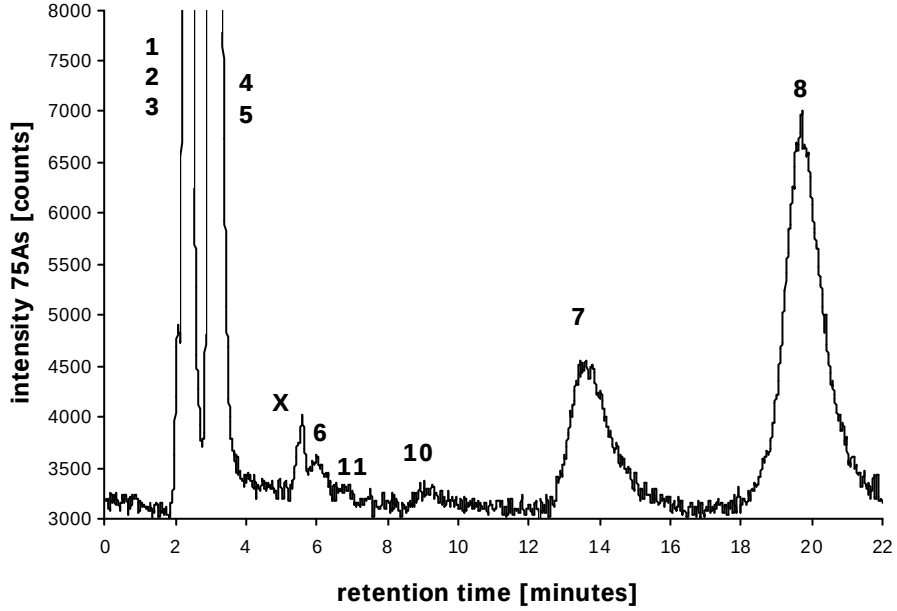

Figure 8.6a (top). Chromatogram of urine sample from volunteer 4. In insert a detailed area of different urine sample. Separation on PRP-X100 anion exchange column, detection with ICP-MS.

Figure 8.6b (bottom). Same chromatogram as in figure 8.6a with enhanced y-axis.

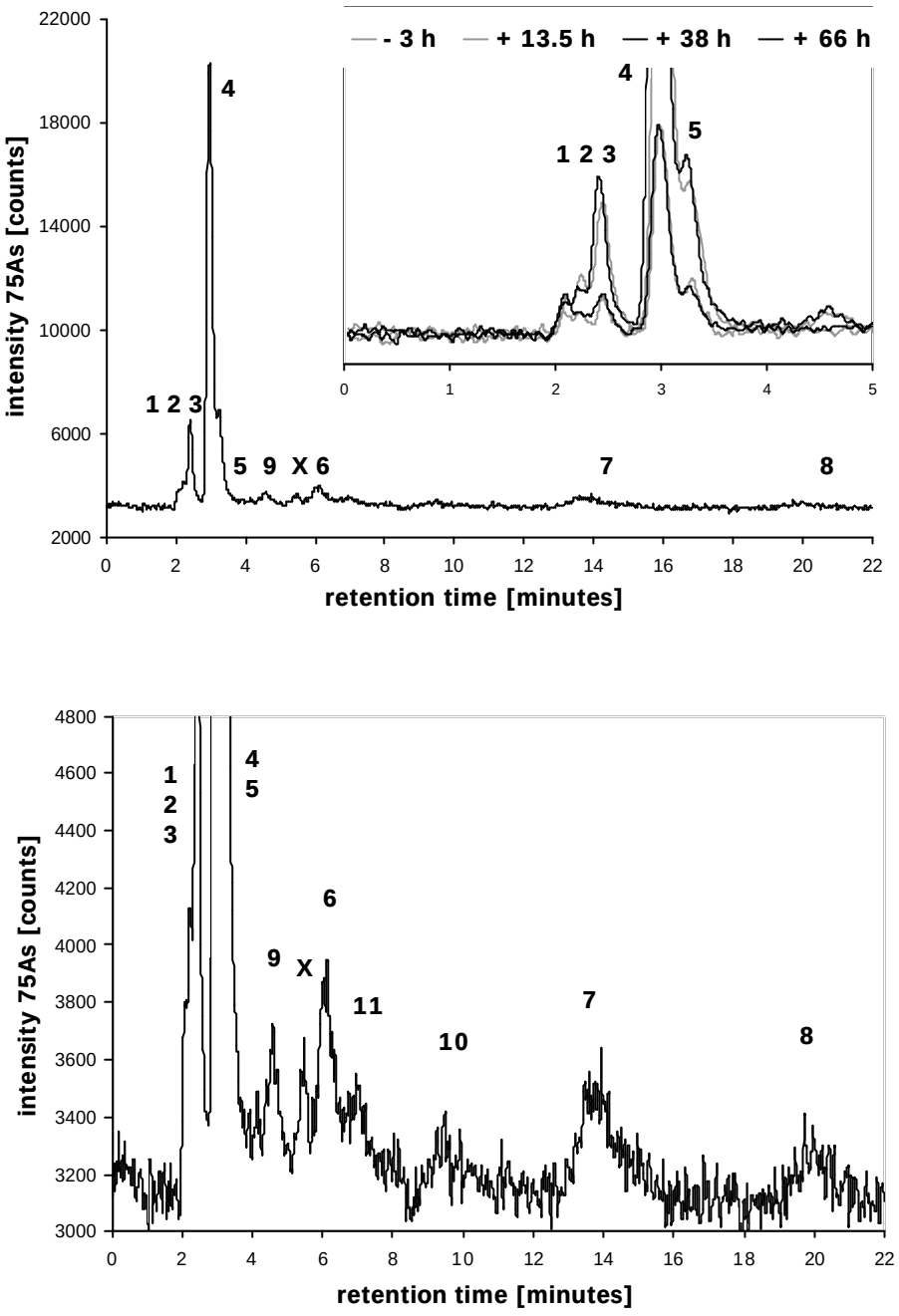

Figure 8.7a (top). Chromatogram of urine sample from volunteer 5. In insert a detailed area of different urine sample. Separation on PRP-X100 anion exchange column, detection with ICP-MS.

Figure 8.7b (bottom). Same chromatogram as in figure 8.7a with enhanced y-axis.

It was noticed that, under the used instrumental parameters, a certain signal for $^{51}ClO^{+}$ is accompanied by a $^{75}ArCl^{+}$ signal that is ten times lower in intensity. Peak 6 is most likely As^{V}. Similar chromatograms were obtained for the other 3 Chinese volunteers. The urine of the European volunteer shows only a very small peak 8. Peak 9 and 10 are absent in the

urine of volunteers 1 and 2, respectively, whereas peak 11 is only present in the urine of volunteers 4 and 5. Peak 6 is only absent in the urine of volunteer 2. Only volunteer 5 does not show a significant increase of peak 2 (see inserts in figures 7.3a to 7.8a). Except for these small discrepancies the chromatograms of the 5 volunteers look very similar. Le *et al.* [1994] and Ma and Le [1998] mentioned that individuals metabolise arsenosugars in different ways. Our findings do not fully confirm this statement. Furthermore the fact that there is no difference between the Chinese volunteer 1 (boiled in soup) and the others (eaten raw) might indicate that mixing the seaweed with soup does not change the chemical composition of the arsenicals. However, to be sure, a more thorough study would be needed. Looking at the five chromatograms, it seems strange that the time-dependent urinary arsenic profile of volunteer 5 is so much different from the others. During conservation of the urine samples at 4°C, a pink precipitation was frequently observed for this volunteer. Pink precipitation was much less often seen for the other volunteers. The presence of this precipitation might have influenced the measurement of total urinary arsenic with ICP-MS. Complete microwave digestion with mineral acids ought to be preferred. Because this equipment was not available on the spot, it could not be considered. On the other hand, it was not the intention to determine very accurately the exact arsenic concentration in all urine samples. The extra work to be spent on sample digestion would not have given us relevant additional information. There is a difference between the two ethnic groups in the increase of peak 2 (AB) for the Chinese volunteers. There is, however, a presumption that the algae were not the only source of arsenicals in the diet of the Chinese volunteers. Although hypothetical, it makes sense to assume that the Chinese people unknowingly to them ingested arsenic-rich food, which may not be the case for the Belgian volunteer. The Chinese cuisine is dominated by rice, food from marine origin, mushrooms, stock prepared from fish... It is therefore more likely to conclude that the presence of AB originates from AB-containing food, rather than from decomposition of arsenosugars. Moreover, AB is absent from algae or at least no reports on the presence of AB in algae are available.

The speciation analysis results correlate well with those obtained by Francesconi *et al.* [2002]. They noted 4 major and 4 minor peaks in the urine of a 47 year old male volunteer, 27 hours after the ingestion of a pure arsenosugar. Differences in the mobile phase composition make a direct comparison difficult, but most probably, at least 3 of the major peaks found in their study match peaks 2, 4 and 8 in our chromatograms. It is

difficult to compare these results with those of Le *et al.* [1994] and Ma and Le [1998] because they used ion pair RPC.

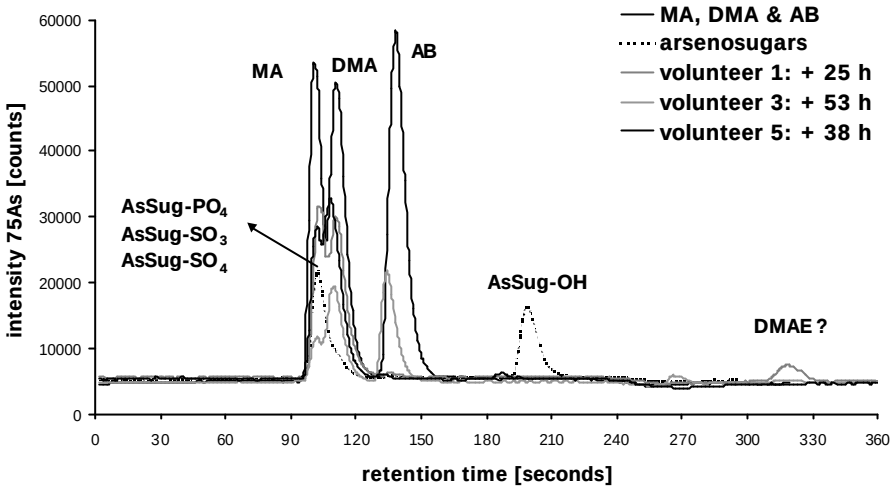

Figure 8.8. Chromatograms of standards and urine samples from 3 volunteers separated on CS10 cation exchange column. Detection with ICP-MS.

None of the peaks in the anion exchange chromatogram of the urine samples, except for those in the void volume, match the original arsenosugars in the seaweed extract. Because arsenosugar OH shows no retention in anion exchange mode, cation exchange chromatography was applied. The chromatograms showing selected standards (MA, DMA and AB: black line; arsenosugars: dotted black line) and urine samples is given in figure 8.8. In none of the urine samples, a peak was found that matched the retention time of arsenosugar OH. On the other hand it can be seen that the increase of the peak in the void volume of a urine sample from a Chinese volunteer is most likely due to AB (grey line). The AB peak in the chromatogram from the urine comes a few seconds ahead of that of a standard mixture. The high salt content in the urine matrix always results in a shorter retention time. Likewise it can be seen that the increase of the peak in the void volume of a urine sample from volunteer 5 is not due to AB (thick black line). From the same figure it can also be seen that in a urine sample from volunteer 1, taken 25 hours after ingestion, a peak at the retention time of 320 seconds appears, but no increase at the retention time of AB is seen (thick grey line). The peak at 320 s might be DMAE. At that time, however, I was not aware of the possible presence of that compound in urine and consequently had no standard available. From the first experiment it can thus be concluded that the arsenosugars are completely transformed into DMA, MA and a series of unknown metabolites. All five volunteers show a fairly similar urinary arsenic pattern. Although three

peaks can be distinguished in the void volume, it is difficult to unambiguously identify them. On the basis of the cation exchange chromatograms, it is tempting to state that the second and third peak in the void volume of the anion exchange chromatograms are AB and As^{III}, respectively. Most probably other neutral and/or cationic species are also present. The presence of arsenite remains an open question.

8.2.2. Second trial

A second experiment was carried out in Ghent in June 2002. A portion of 20 g (dry mass) *Laminaria* was boiled for three minutes and ingested by a Belgian (age 26 y) and a Chinese volunteer (age 28 y), both male. Only selected urine samples (within the first 36 hours) were collected. The urine samples were collected in acid washed PE bottles. The bottles were stored at 4°C. It was the intention to test the possibilities of HPLC-UV-HG-AFS for the detection of arsenic species in the urine samples. It was also checked whether boiling of the algae had an influence on the stability of the arsenosugars.

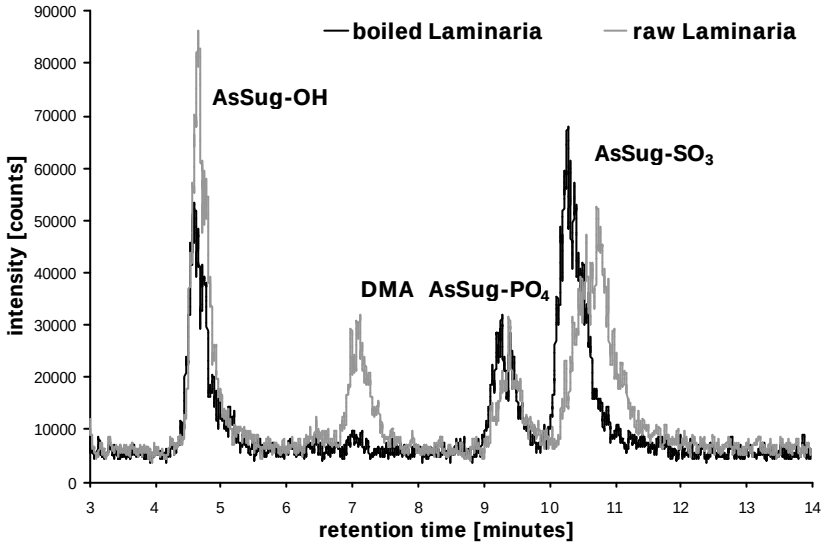

Figure 8.9. Chromatograms of boiled and raw *Laminaria* extract separated on PRP-X100 anion exchange column. Detection with UV-HG-AFS.

A raw and a boiled portion of *Laminaria* were extracted with 50:50 water/methanol as described before (section 7.5). Both portions were extracted under exactly the same conditions. These algae extracts, together with the urine samples were analysed using HPLC-UV-HG-AFS with 20 mM Na_2HPO_4 (pH 6) on a Hamilton PRP-X100 anion exchange column. Figure 8.9 shows the chromatograms of both algae extracts. It can be seen that

boiling of the *Laminaria* efficiently extracts nearly all DMA and a significant amount of arsenosugar OH. The signal intensities for the peaks of arsenosugars PO_4 and SO_3 remain stable. Because of these small changes, it was decided to ingest only raw *Laminaria* in all other experiments.

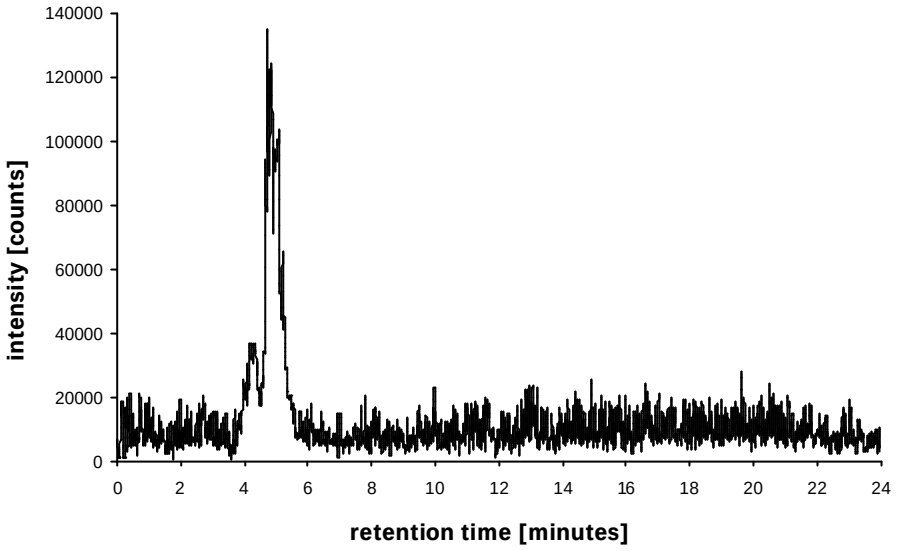

Figure 8.10. Chromatogram of urine separated on PRP-X100 anion exchange column. Detection with UV-HG-AFS.

An example of a urine sample, analysed with HPLC-UV-HG-AFS, is given in figure 8.10. It can be seen that the sensitivity of the AFS detector is much lower compared to that of ICP-MS (figures 8.3 to 8.7). No further efforts were made to improve the sensitivity of UV-HG-AFS. Instead, ICP-MS will be used in all further experiments.

8.2.3. Third trial

A third experiment was conducted in October 2002 in Ghent as well as in Beijing. Two Belgian male volunteers (aged 26 and 22 y) ingested a portion of 20 g raw *Laminaria*. Blood was collected before and within a short time-span after ingestion. The blood was collected in heparin free vacuum tubes. Afterwards serum and packed cells were separated by centrifugation (two times at 3000 rpm, 20 min, 4°C) and both fractions were stored at 4°C. Urine was sampled only between 15 to 48 hours after ingestion. The urine samples were collected in acid washed PE bottles. The bottles were stored at 4°C. Portions of the urine and serum samples were freeze dried and analysed in Beijing by HPLC-ICP-MS. Speciation analysis was carried out on the same ICP-MS instrument as described in section

8.2.1. Samples were chromatographed on a Hamilton PRP-X100 anion exchange column with 30 mM NH_4Oac in 3% (v/v) MeOH (pH 6). The objective of this experiment was to confirm the presence of MA in urine and to check whether DMAE and TMAO were present in urine, as was found by Francesconi *et al.* [2002]. Furthermore a first idea about speciation in serum should hopefully be obtained. Finally the capabilities of HPLC-ES-MS/MS for arsenic speciation analysis were explored.

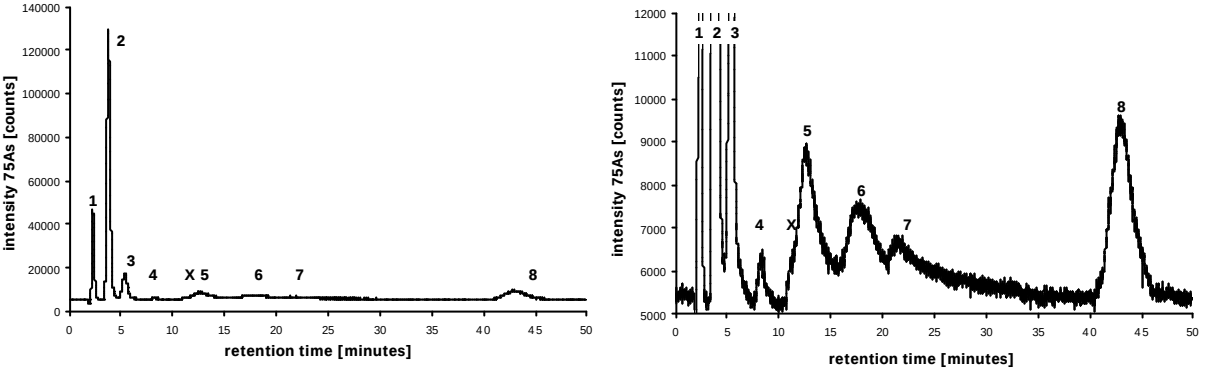

Figure 8.11. Chromatogram of urine (left) separated on PRP-X100 anion exchange column. Same chromatogram with 12x enhanced y-axis (right). Detection with ICP-MS.

Figure 8.11 shows an anion exchange HPLC-ICP-MS chromatogram of urine from volunteer 1 collected 17 hours after ingestion of *Laminaria*. A total of 8 arsenic species can be detected. In contrast to the first experiment, only one peak elutes in the void volume. However, most probably different neutral and positively charged arsenic species may account for this. The peak denoted as X is due to the presence of a $^{75}ArCl^+$ interference. Peak identification by spike addition was done on another urine sample. A urine sample was spiked with a standard mixture of As^{III}, DMA, MA and As^{V}. The chromatograms are shown in figure 8.12. Peaks 2 and 3 are DMA and MA, respectively. Peak 6 is most probably arsenate.

Although no information is given about the mechanism of formation of DMA from arsenosugars, DMA is generally accepted as one of the main metabolites of arsenosugars. [Le *et al.*, 1994; Ma and Le, 1998, Feldmann *et al.*, 2000; Francesconi *et al.*, 2002]. It makes sense to state that DMA is formed by cleavage of the arsinoyl moiety in the arsenosugars.

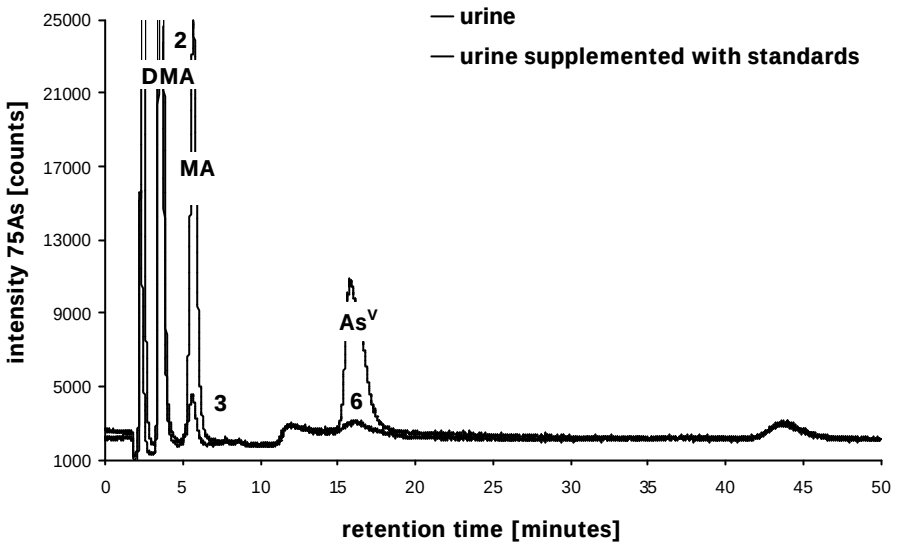

Figure 8.12. Chromatograms of urine and urine supplemented with standards of As^{III}, DMA, MA and As^{V}, separated on PRP-X100 anion exchange column. Detection with ICP-MS.

To my knowledge this is the first report on the presence of MA in urine of people who ingested arsenosugar-containing food. It is unlikely that MA is an intermediate in the formation of DMA, as it is in the metabolism of inorganic arsenic. Therefore the presence of MA indicates a demethylation process. At present, I can give no explanation for the presence of MA. However, arsenosugars seem to be unstable when stored for a long time. A composite chromatogram of an old extract of kelp powder that was stored for more than one year at 4°C, and a standard mixture of As^{III}, DMA, MA and As^{V} is shown in figure 8.13. In comparison with figure 7.9 (left), in which a fresh extract of kelp powder is shown, the percent abundance of DMA increases, and a peak of MA appears, whereas all arsenosugars show a lower relative abundance (see table 8.6). Also old extracts of *Laminaria* give rise to formation of MA (chromatogram not shown). Francesconi *et al.* [2002] could not find MA in the urine of a volunteer who had ingested a pure arsenosugar. On the other hand Feldmann *et al.* [2000] reported on MA as a urinary metabolite in sheep that fed on algae. According to them, the occurrence of MA is assumed to be a precursor of the exposure to inorganic arsenic, since demethylation of dimethylated or trimethylated organoarsenic compounds is not known. In a more recent paper from that research group [Hansen *et al.*, 2003b], however, they make report of DMAA as a metabolite instead of MA. Both compounds elute closely together using anion exchange chromatography.

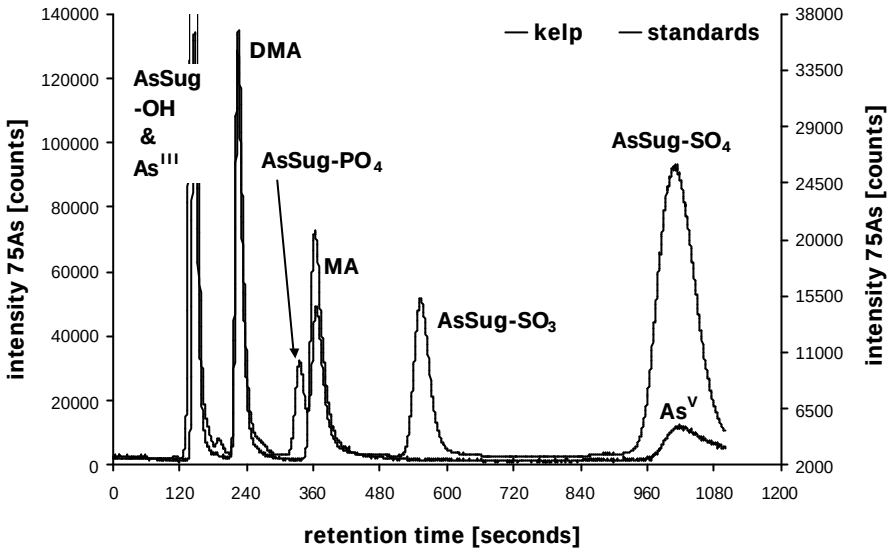

Figure 8.13. Chromatograms of old extract of kelp powder and standards of As^{III}, DMA, MA and As^{V}, separated on PRP-X100 anion exchange column. Detection with ICP-MS.

The similarity with the urine samples of the five volunteers from the first experiment is good. The retention times of the arsenicals are, however, longer because the elution strength of 30 mM NH_4OAc (pH 6) is lower than that of 30 mM $(NH_4)_2HPO_4$ (pH 7).

Table 8.6. Relative abundances of arsenicals in old and fresh extract of kelp powder.

	AsSug-OH	DMA	AsSug-PO_4	MA	AsSug-SO_3	AsSug-SO_4
fresh extract	29.9%	3.5%	5.0%	0.0%	12.1%	49.5%
old extract	28.6%	12.0%	3.2%	7.7%	9.0%	39.5%

The urine samples were also subjected to HPLC-ES-MS/MS using a 30 mM NH_4Oac in 20% (v/v) MeOH (pH 6) buffer. Figure 8.14 shows an HPLC-ES-MS/MS chromatogram with two MRM transitions for DMA. The detection of the molecular ion signal as well as two product ions unambiguously proves the presence of this compound. The peak containing DMA was also collected off-line, freeze-dried and reconstituted in 50:50 water/methanol to which 0.2% HCOOH was added. A product ion scan was done. The resulting mass spectrum is shown in figure 8.15. The presence of fragments with *m/z* 91, 93, 106, 109 and 121 is in close agreement with a standard solution of DMA. ES-MS/MS shows a poor sensitivity for MA and it could thus not be detected.

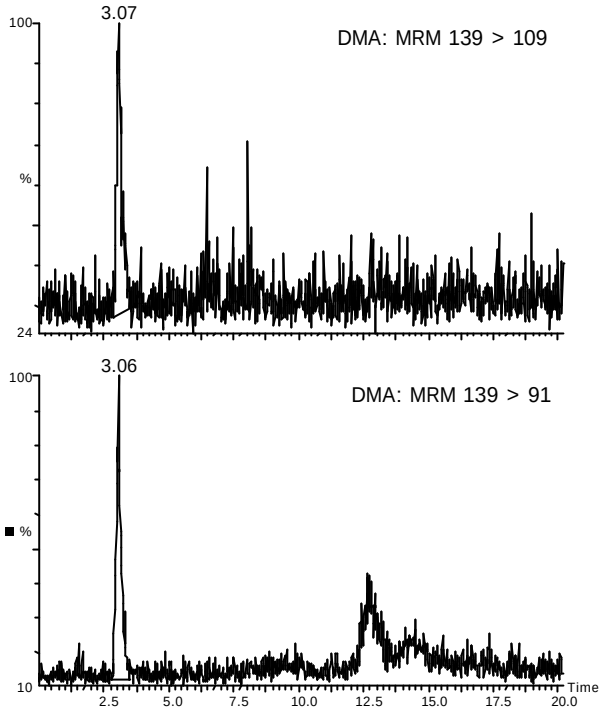

Figure 8.14. Chromatograms of urine, separated on PRP-X100 anion exchange column. Detection of 2 MRM transitions of DMA with ES-MS/MS. Time is displayed in minutes.

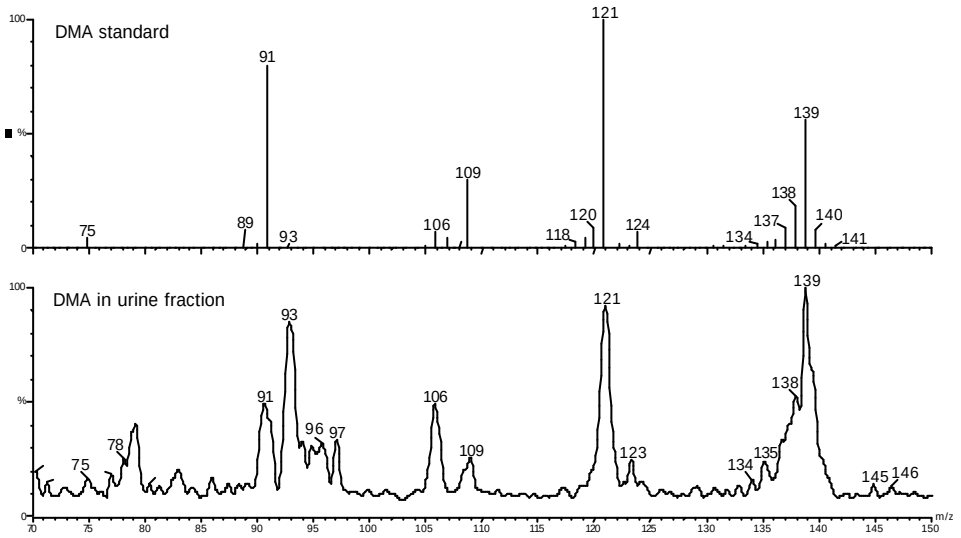

Figure 8.15. Product ion scan spectra of DMA standard (top) and urine HPLC fraction containing DMA (bottom). Detection with ES-MS/MS.

Cation exchange chromatography was also applied on selected urine samples. At that time Francesconi *et al.* [2002] reported on the presence of DMAE in urine. Using both HPLC-ICP-MS as well as HPLC-ES-MS/MS the presence of DMAE could be confirmed. Figure 8.16

shows a detailed area of the chromatograms of a urine sample and a urine sample supplemented with DMAE, separated on a Dionex CS10 cation exchange column with 20 mM pyridine buffer in 3% (v/v) MeOH (pH 2.8).

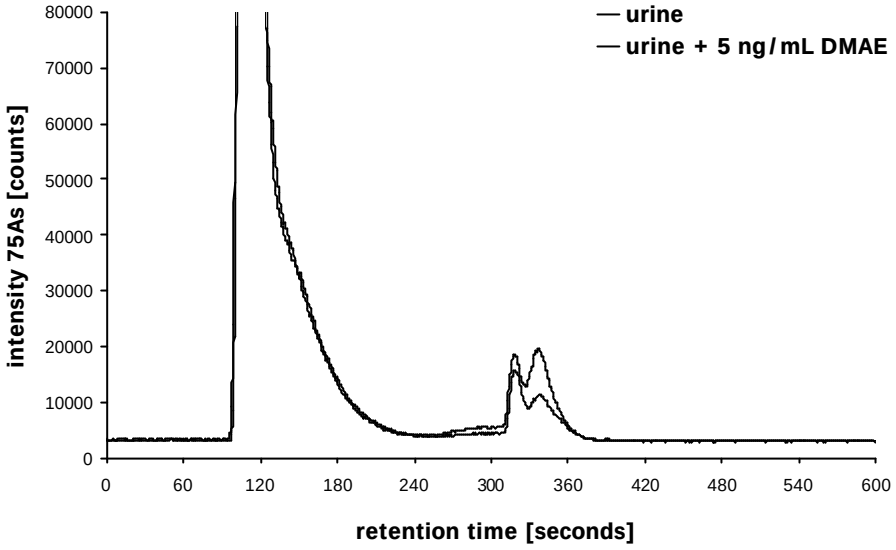

Figure 8.16. Detail of the chromatograms of urine and urine supplemented with DMAE separated on CS10 cation exchange column. Detection with ICP-MS.

In figure 8.17, two MRM transitions of DMAE in a urine sample and one MRM transition of DMAE in that same extract spiked with DMAE are shown. The experimental conditions were identical to those used with ICP-MS except that 10 mM buffer was used instead of 20 mM. This logically results in longer retention times. Francesconi *et al.* [2002] were first to report on the presence of DMAE in urine after ingestion of arsenosugars by means of HPLC-ICP-MS and HPLC-ES-MS on a single quadrupole instrument. In their paper, they postulate that DMAE is likely to be originating from the degradation of the arsenosugars in the gut micro flora, rather than from the addition of the CH_2CH_2OH moiety to DMA. Their hypothesis is supported by experimental evidence [Edmonds *et al.*, 1982].

The peak containing DMAE was also collected off-line, freeze-dried and reconstituted in 50:50 water/methanol to which 0.2% HCOOH was added. A product ion scan was done. The resulting mass spectrum is shown in figure 8.18. The spectrum of the urine fraction shows more peaks than the DMAE standard. The presence of fragments with *m/z* 103, 105, 121 and 149, however, is a good match.

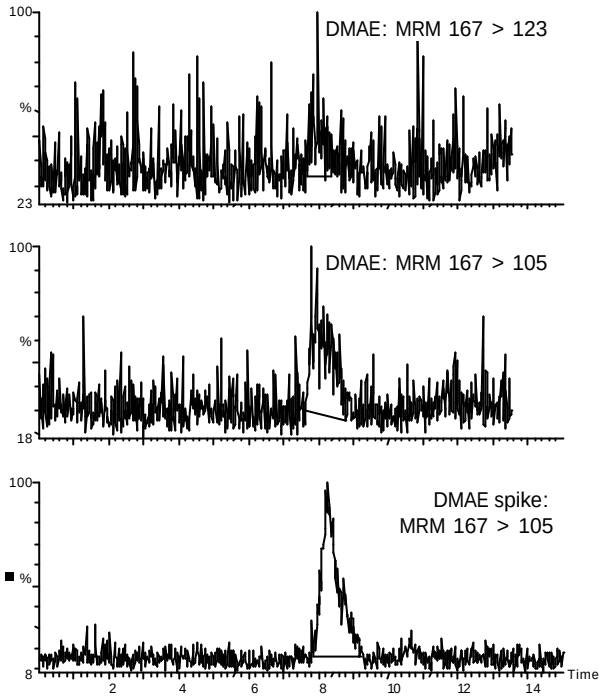

Figure 8.17. Chromatograms of urine and urine supplemented with DMAE, separated on CS10 cation exchange column. Detection of 2 MRM transitions of DMAE (bottom and middle) in urine sample and 1 MRM transition of DMAE (bottom) in supplemented urine sample with ES-MS/MS. Time is displayed in minutes.

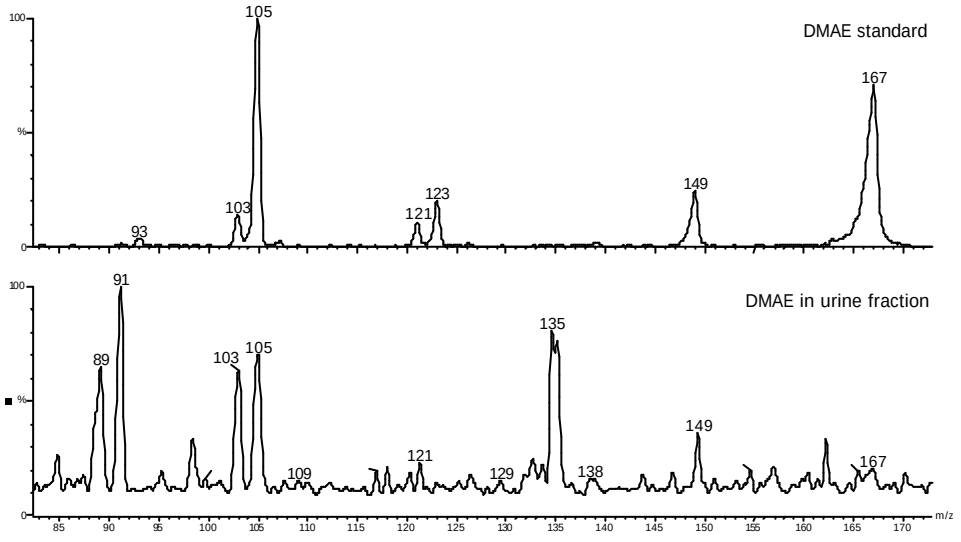

Figure 8.18. Product ion scan spectra of DMAE standard (top) and urine HPLC fraction containing DMAE (bottom). Detection with ES-MS/MS.

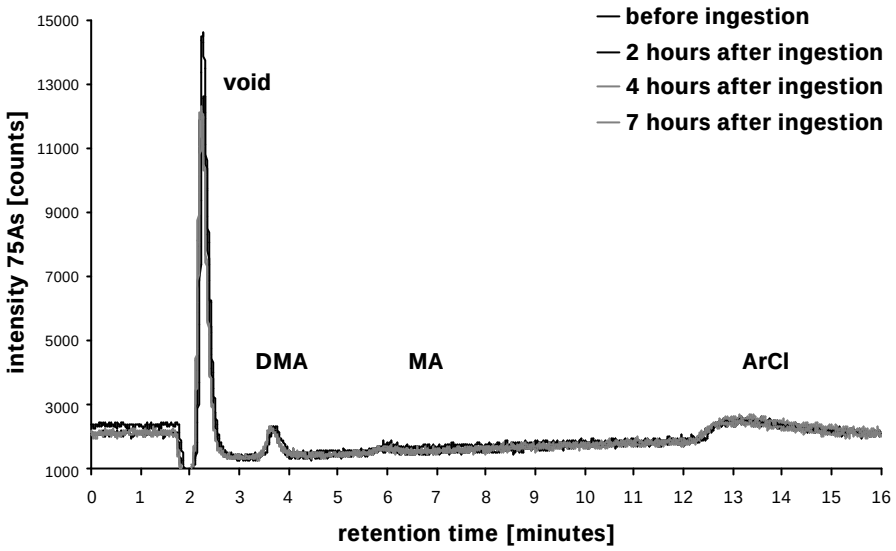

Figure 8.19. Chromatograms of four serum samples from 1 volunteer separated on PRP-X100 anion exchange column. Detection with ICP-MS.

Serum samples of both volunteers were also subjected to speciation analysis. Blood samples were collected before and 2, 4 and 7 hours after ingestion in heparin free vacuum tubes. The blood was centrifuged (20 min, 3000 rpm, 4°C) twice to obtain serum and packed cells. The packed cell fraction was discarded and the serum was freeze-dried. After freeze-drying, all serum samples were reconstituted to their original volume and analysed similarly as the urine samples. Figure 8.19 shows the HPLC-ICP-MS chromatograms of the 4 serum samples from volunteer 2. Surprisingly no change in the arsenic profile can be seen, although the residence time of food in the stomach and small intestines is shorter than 7 hours. Moreover, uptake of dissolved arsenic species in the gastro intestinal tract by blood is believed to be fast and its elimination efficient in case of normal renal function. It is worth mentioning that the peak in the void volume is not due to arsenite, because spiking one of the serum samples with a mixture of As^{III}, DMA and MA shows two closely eluting peaks in the void volume (figure 8.20). Arsenite is the second peak in the void volume.

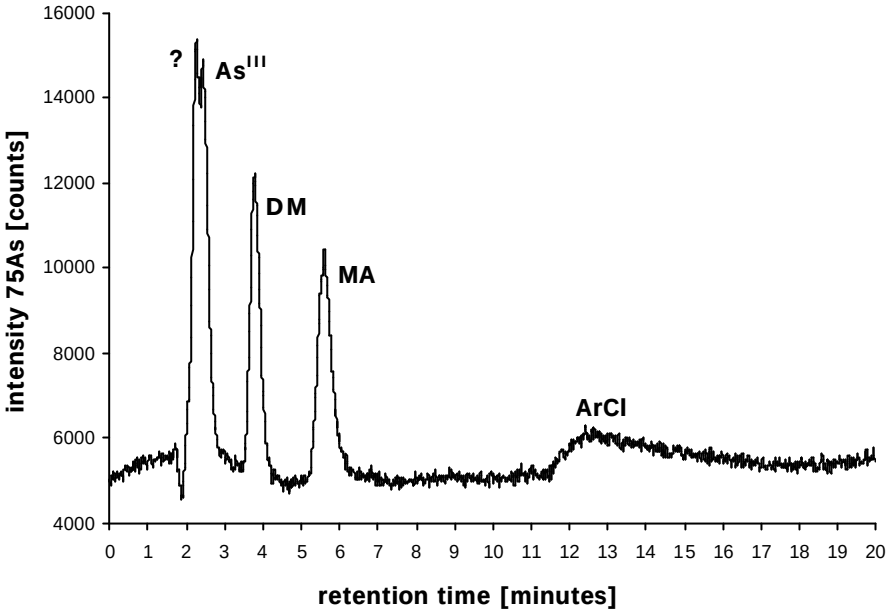

Figure 8.20. Chromatogram of serum sample supplemented with standards of As^{III}, DMA and MA, separated on PRP-X100 anion exchange column. Detection with ICP-MS.

8.2.4. Fourth trial

A fourth experiment was conducted in March 2003 and focussed only on the analysis of total arsenic in blood samples by HG-AFS. To find out whether or not arsenic was taken up by the packed cell fraction, whole blood, serum and packed cells were analysed for their total arsenic content. In this experiment, blood samples were collected from two volunteers (A Belgian aged 27 y and a Chinese aged 25 y) before and 4 and 7 hours after ingestion of 20 g *Laminaria*. The blood was collected in heparin free vacuum tubes. Afterwards serum and packed cells were separated by centrifugation (two times at 3000 rpm, 20 min, 4°C) and both fractions were stored at 4°C. The arsenic content in blood, serum and packed cells was analysed by HG-AFS. All samples were digested in open vessels using a mixture of HNO_3, H_2SO_4 and $HClO_4$ (7:2:1) and a 3-step temperature programme. First the sample was heated at 85°C for 2 hours, followed by a heating step at 130°C (3 hours) and 230°C (3 hours). The length of the digestion programme was also dependent on the amount of sample added to the vessel. On average, 3 mL serum, 2 mL blood and 1 mL packed cells were digested with 10 mL of the acid mixture. The final solution was diluted to 25 mL with 3 M HCl to which 0.1 g L^{-1} KI and 0.02 g L^{-1} ascorbic acid was added in order to reduce all arsenic to its trivalent state. Hydride generation was realised by mixing a flow of the sample at a speed of 9 mL min^{-1} with a stream of 0.7% (m/v) $NaBH_4$ in 0.4% (m/v) NaOH

at 4.5 mL min^{-1}. The accuracy of the measurement was tested by the analysis of a certified reference material, freeze-dried human serum, with a certified value of 19.6 ± 4 ng g^{-1} As [Versieck *et al.*, 1988]. The value obtained with our method was 24.0 ± 1.8 ng g^{-1} As for 3 sub samples, each measured in triplicate. There is no siginificant difference (P = 0.05) between the experimental results and the certified value. The results are shown in table 8.7. In whole blood as well as in serum and packed cells, the concentration of arsenic does not significantly change. Only one sub-sample was available. It was measured in threefold. Volunteer 1 shows higher background levels of arsenic. This might be due to the fact that he is Chinese. Higher urinary background levels for Chinese people were also noticed in experiment one.

Table 8.7. Arsenic concentration in the different blood compartments of two volunteers. Detection with HG-AFS.

		concentration & SD (n = 3) [ng/g]		
		before	after 4 h	after 7 h
volunteer 1	blood	4.4 (0.5)	4.1 (0.5)	5.7 (0.3)
	packed cells	8.5 (1.4)	6.0 (0.7)	9.9 (2.2)
	serum	2.2 (0.3)	2.2 (0.3)	2.4 (0.3)
volunteer 2	blood	1.9 (0.1)	1.8 (0.1)	1.7 (0.2)
	packed cells	2.0 (0.2)	2.5 (0.1)	2.0 (0.1)
	serum	0.8 (0.5)	1.1 (0.6)	2.0 (1.0)

8.2.5. Fifth trial

A fifth experiment was carried out in May 2003 with the same volunteers as in experiment three. Two male Belgians aged 27 y and 23 y ate a portion of 20 g *Laminaria*. The urine samples were collected in acid washed PE bottles. The bottles were stored at 4°C. Only selected urine samples were taken (range 0 to 48 hours after ingestion). Speciation analysis was done with a 3 mM ammonium oxalate buffer in 3% MeOH, pH 6 and detection was realised with ICP-MS. The objective was to get a better insight into the possible presence of reduced methylated species (MA^{III} and DMA^{III}).

The results of the speciation analysis in urine again confirmed those from the previous experiments and a good agreement with the results of Francesconi *et al.* [2002] was again

noticed. Efforts were made to confirm the presence of the reduced DMA, which was proposed by Francesconi *et al.* [2002]. There is much debate about the real identity of the synthesised MA^{III} and DMA^{III}. An easy means of getting the reduced compounds is by the so-called 'Reay and Asher' method: reduction of DMA or MA with an acid solution of $Na_2S_2O_3$ and $Na_2S_2O_5$ leads to DMA^{III} and MA^{III}, respectively [Reay and Asher, 1977]. Reduction of MA leads to two product peaks $MA^{III}{}_1$ and $MA^{III}{}_2$ and a trace of unchanged MA. DMA leads to one product peak and a trace of unchanged DMA (figure 8.21).

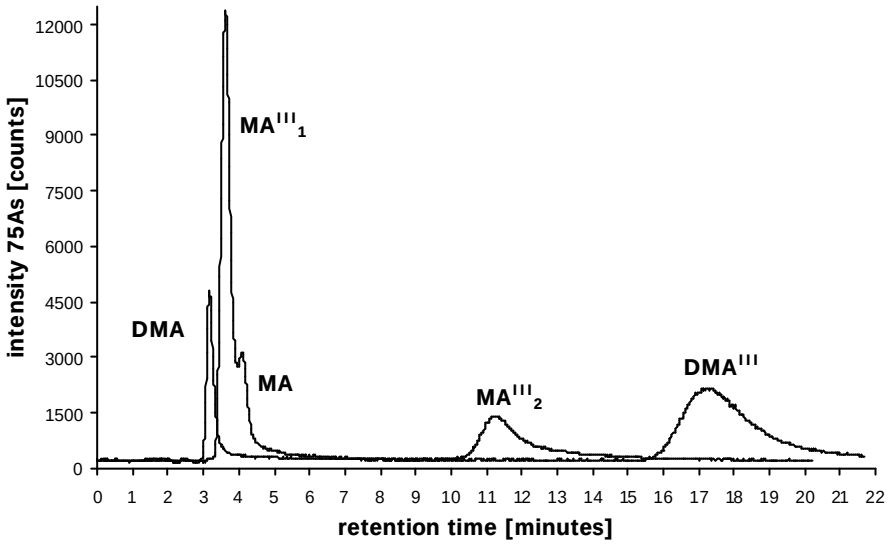

Figure 8.21. Chromatograms of solutions of DMA and MA and their reduced compounds upon reaction with $Na_2S_2O_3$ and $Na_2S_2O_5$ in H_2SO_4. Separation on PRP-X100 anion exchange column, detection with ICP-MS.

The retention time of the first MA^{III} peak is consistent with that reported by others [Francesconi *et al.*, 2002; Gailer *et al.*, 1999] and this is most likely the real $(CH_3)As(OH)_2$. According to Feldmann *et al.* [unpublished data], the reduction of DMA does not lead to DMA^{III}, but to a compound in which the arsenic-oxygen double bond is replaced by an arsenic-sulphur double bond. They also mention that reduction of MA also leads to one, possibly two sulphur-containing arsenicals. The peak of $MA^{III}{}_2$ at t_R 11.4 min and DMA^{III} at t_R 17.4 min are due to these sulphur containing arsenic species. It is noteworthy to mention that both sulphur-containing compounds have a long retention time on the Hamilton PRP-X100 column. Moreover, according to Gailer *et al.* [1999] the retention time of DMA^{III} is invariable with varying buffer pH.

DMA^{III} is an intermediate in the methylation pathway suggested by Challenger [Challenger, 1945]. Although DMA is the end metabolite of inorganic arsenic in humans, some mammals do further methylate DMA to TMAO, via DMA^{III}. I consider it justified to state that DMA is formed from arsenosugars by a mechanism in which TMAO is also involved, because in dimethylarsinoyl arsenosugars, the arsenic is bound to two methyl groups, oxygen and an alkyl substituent. Whether the real DMA^{III} has been detected by Francesconi *et al.* [2002] or not, it makes sense to assume that this species can be present. DMA is the main metabolite of arsenosugars and TMAO has been detected in trace amounts [Francesconi *et al.*, 2002]. This demethylation process goes via DMA^{III}. Because MA has been detected in many of our urine samples, a similar interpretation can be made about the presence of MA^{III}. MA^{III} and DMA^{III} are known to be very unstable and their detection should be realised within a very short time span. But even then speculations can be made whether oxidation should already have occurred *in vivo*, taking into account the residence time of the metabolites in urine in the bladder. On the other hand, the bladder is considered a reducing environment, preventing oxidation to the pentavalent state.

Spiking a urine sample with a solution of reduced DMA shows that it does not co-elute with the unknown peak at the end of the chromatogram. The sulphur-containing DMA^{III} compound has a longer t_R. The chromatogram of the same urine sample to which MA^{III} was added, shows that the peak at t_R 11.4 min co-elutes with a very small but broad peak (figure not shown). However, it is not very clear whether this bump is due to $MA^{III}{}_2$. The urine sample was analysed within a short time span that should allow the detection of MA^{III} according to the findings of Gong *et al.* [2001]. But even if this bump co-elutes with the synthesised $MA^{III}{}_2$, then we may be dealing with the sulphur-containing arsenical and not the real MA^{III}. As told before the issue of reduced methylated species is far from clear. At the moment there are still doubts about the proper method of synthesis. Add to this that convincing analytical methodology is yet lacking. Therefore it is premature to make any further assumptions about the possible presence of these reduced species in urine.

8.2.6. Sixth trial

Experiment six was done in August 2003. Only one volunteer participated (Belgian male, aged 27 y). He ate a portion of 20 g *Laminaria*. The urine samples were collected in acid washed PE bottles. The bottles were stored at 4°C. All urine within the interval of 3 prior to

100 hours after ingestion was collected. Speciation analysis was done with a 3 mM ammonium oxalate buffer in 3% MeOH, pH 6 on a Hamilton PRP-X100 anion exchange column and detection was realised with ICP-MS. The purpose of this experiment was to find out more about the unknown metabolite eluting at the end of the chromatogram and to confirm the presence of MA.

A urine sample was chromatographed with 3 mM ammonium oxalate in 3% (v/v) MeOH (pH 6) on both an analytical and a preparative PRP-X100 column and spiked with MA. In both cases a perfect match was observed (figures not shown).

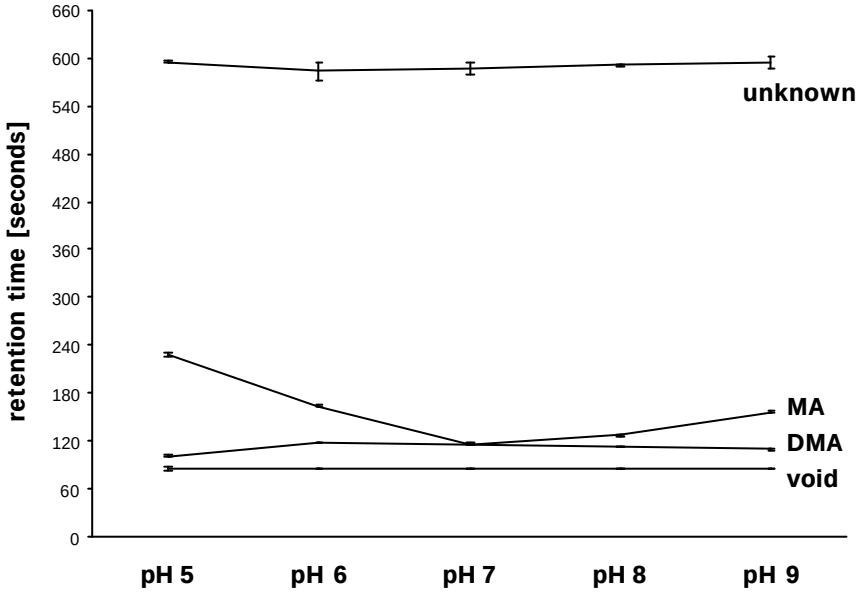

Figure 8.21. Retention time of urinary arsenic metabolites in function of different buffer pH values.

One of the urine samples was chromatographed on a Hamilton PRP-X100 anion exchange column using a 30 mM sodium phosphate with variable pH values (5, 6, 7, 8 and 9). The results are shown in figure 8.21. The retention behaviour of DMA and MA is completely in accordance with the findings of Gailer *et al.* [1994; 1999]. At pH 7, DMA and MA co-elute. The unknown component shows no change in retention behaviour. This might be due to the fact that it is highly negatively charged or that it experiences other than purely ionic interactions. Francesconi *et al.* [2002] have done a similar experiment on a urine sample. They chromatographed a urine sample on the same type of column (though shorter) with a 20 mM NH_4HCO_3 buffer at pH values 8, 9.5, 10 and 10.7. For the strongly retarded unknown metabolite, they observed a great influence of the retention time in function of a

variable pH. They noticed that this behaviour was similar to that of arsenate. In conclusion they stated that both arsenate and the unknown form carbonate complexes in the mobile phase. The difference between both outcomes might be due to the fact that another buffer was used, or that we are dealing with a different compound.

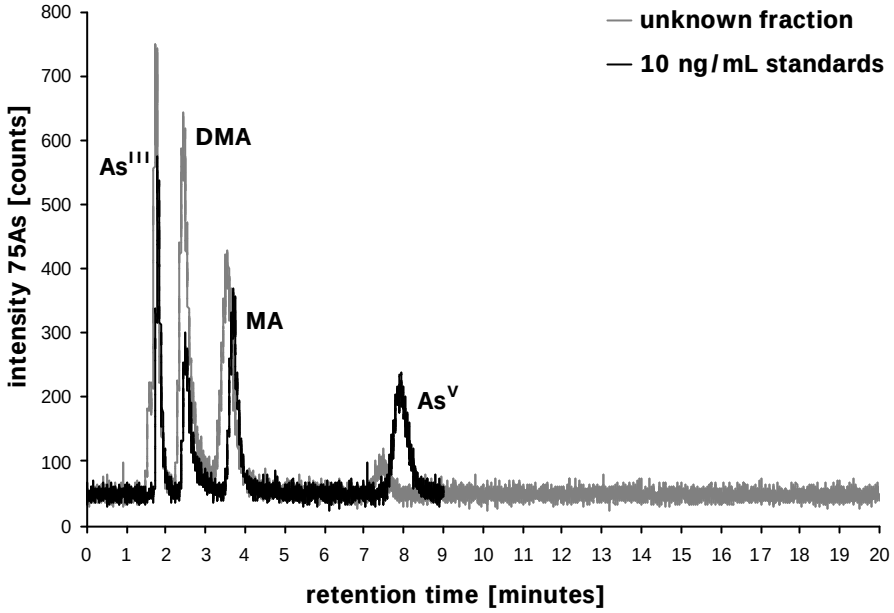

Figure 8.22. Chromatograms of isolated unknown peak in urine and solution of standards of As^{III}, DMA, MA and As^{V}. Separation on PRP-X100 anion exchange column, detection with ICP-MS.

Using a preparative Hamilton PRP-X100 column, this unknown metabolite was isolated, freeze-dried and analysed in Graz during a short stay at the research group of Prof. Dr. Francesconi. In total 16 preparative separations were done using 0.5 mL undiluted urine. The flow rate of 10 mL/min was split to enable 95% to be collected by a fraction collector. 5% was sent to the ICP-MS for determination of the retention time. All fractions were combined and freeze-dried. A total of 45 ng As was isolated. This would allow analysis with infusion ES-MS/MS. First the freeze-dried fraction was reconstituted in a minimal amount of water and separated on a Hamilton PRP-X100 anion exchange column with 20 mM $(NH_4)_2HPO_4$ in 3% (v/v) MeOH, pH 6. The result is shown in figure 8.22. The original fraction completely disappeared. Instead 5 peaks can be observed: two in the void volume, one co-eluting with DMA and two closely eluting near MA and As^{V}, respectively. The high salt content in the fraction can cause this shift in retention time. No further efforts were made to repeat this experiment. Only very recently Hansen *et al.* [2004] reported on the presence of 2-dimethylarsinothioyl acetic acid $(CH_3)_2As(S)CH_2COOH$ in sheep urine. This

compound has a retention time, which is consistent with the one isolated in trial 6. The identity was confirmed by ES-MS, NMR and spiking. On the one hand it is likely that this arsenical is also the compound that appears in the human urine samples throughout all seven trials in this work. On the other hand, Hansen *et al.* reported that when using a mobile phase pH of 5.3, the compound was permanently absorbed on the anion exchange chromatogram. They used an NH_4HCO_3 mobile phase. Also Francesconi *et al.* [2002] used an NH_4HCO_3 mobile phase and observed a strong pH dependency of the strongly retarded component. We have found no pH dependency of the unknown compound, but we used a phosphate buffer. Upon oxidation 2-dimethylarsinothioyl acetic acid forms DMAA, so the peak closely eluting to MA (in figure 8.22) could be DMAA.

8.2.7. Seventh trial

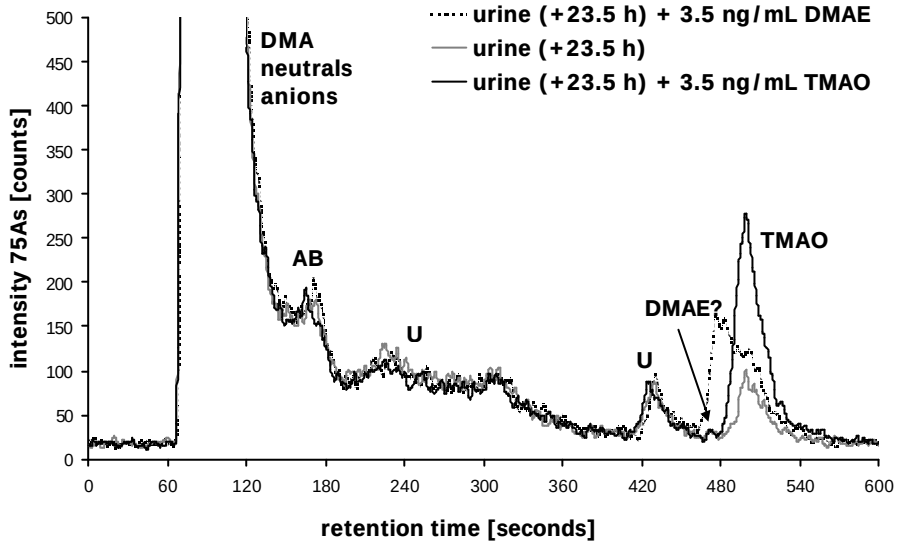

Figure 8.23. Chromatograms of a urine sample and the same urine sample spiked with DMAE and TMAO. Separation on CS10 cation exchange column, detection with ICP-MS.

A last experiment was conducted in November 2003. Again only one volunteer participated (Belgian male, aged 27 y). He ate a portion of 24 g *Laminaria*. The urine samples were collected in acid washed PE bottles. The bottles were stored at 4°C. All urine samples within the interval of 3 prior to 120 hours after ingestion, were collected. The main focus was on the use of cation exchange chromatography, investigation of the chromatographic recovery and of a mass balance of arsenic in urine. At that time, Hansen *et al.* [2003b] had reported on the presence of DMAA and the fact that it closely elutes near MA. Therefore it was checked again whether MA was present in the urine samples.

Cation exchange chromatography was done on a Dionex CS10 column with 10 mM pyridine buffer, in 3% (v/v) MeOH, pH 2.7. Anion exchange chromatography was done using a 3mM ammonium oxalate buffer in 3% (v/v) MeOH, pH 5.2 and 8.2. In both cases, ICP-MS served as the element-selective detector. Total arsenic in urine was done via HG-AFS using the digestion procedure described in section 8.2.4. Figure 8.23 shows the chromatograms of urine taken 23.5 hours after ingestion of the *Laminaria*, and the same urine sample to which individual solutions of TMAO and DMAE, respectively, were added. In contrast to the findings in experiment three, no clear occurrence of DMAE could be stated this time. Instead TMAO could be identified. TMAO was also identified by Francesconi *et al.* [2002] as a trace in the urine of a volunteer who had ingested a pure arsenosugar. Similar spiking with TETRA and AB shows that no TETRA is present in the urine samples and that some AB could be found, possibly because of ingestion of other seafood.

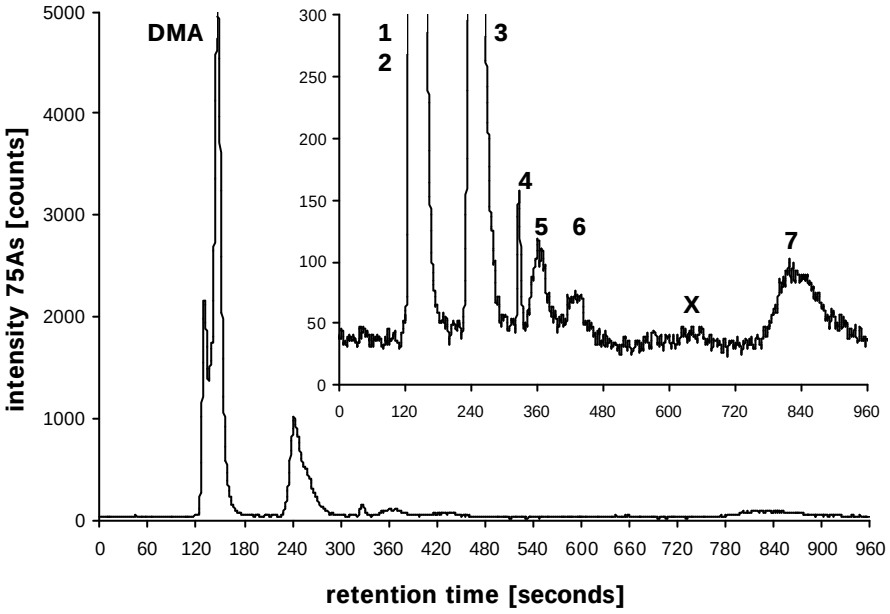

Figure 8.24. Chromatogram of urine sample separated on PRP-X100 anion exchange column. In insert a detailed area of same chromatogram. Detection with ICP-MS.

The anion exchange chromatogram of the urine sample collected 23.5 hours after ingestion is shown in figure 8.24. The oxalate buffer at pH 5.2 was used. Seven peaks and an interference of $^{75}ArCl^{+}$ can be observed. The same urine sample was spiked with individual solutions of DMA (not shown), MA, As^{V} and *Laminaria* extract, respectively. This is shown in figure 8.25. Peaks 3, 4 and 6 co-elute with MA, As^{V} and arsenosugar SO_3, respectively. This is the first time the presence of an arsenosugar is noticed. Arsenosugar SO_3 is the most abundant of the three arsenosugars present in the *Laminaria*.

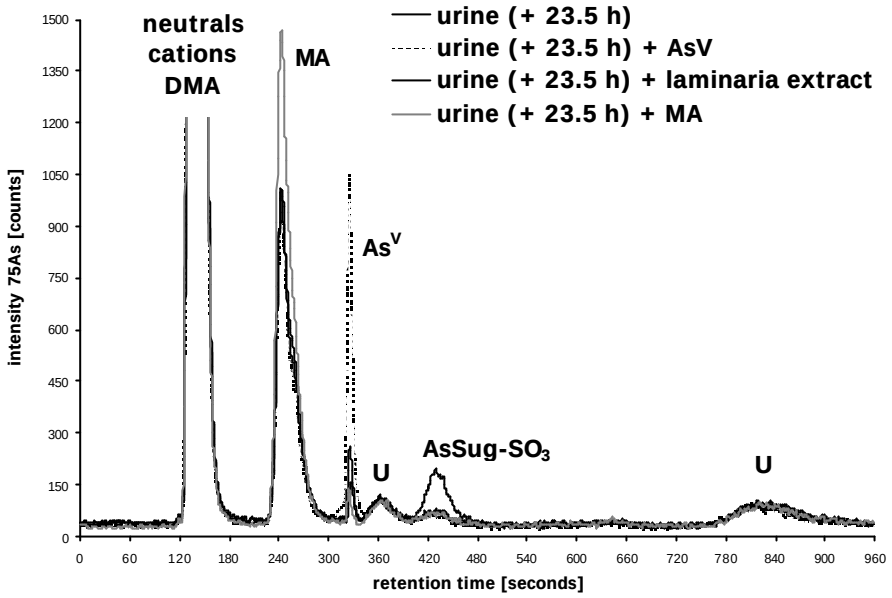

Figure 8.25. Chromatogram of urine sample and the same urine sample spiked with As^V, MA and Laminaria extract. Separation on PRP-X100 anion exchange column, detection with ICP-MS.

Figure 8.26 shows the same urine sample, spiked with a solution of DMAA. A different and more diluted urine sample had to be used, because only a DMAA standard with low concentration was available. DMAA appears at the same retention time as MA when using the oxalate buffer at pH 5.2. Therefore the urine sample was again spiked with both solutions of MA and DMAA and chromatographed using a buffer at pH 8.2 (figure 8.27). Now, it can be clearly seen that DMAA is absent and MA is present. DMAA appears in the right shoulder of the DMA peak. Hansen *et al.* [2003b] also evaluated the retention behaviour of DMAA and DMA on the same column, but with a 30 mM acetic acid buffer at pH 3, 4, 5.3, 6.4 and 8.5. They also observed a decrease in the t_R of DMAA and an increase in the t_R of DMA, respectively, in function of an increasing pH. At pH 8.5, DMA and DMAA eluted closely together. Although oxalate and acetate are not identical, both buffers contain a carboxyl group.

All urine samples were analysed for their total arsenic content using HG-AFS. 2 mL urine was digested using the procedure described in section 8.5. The results are shown in table 8.8. The data are not normalised according to the creatinine content. It can be seen that the maximum amount of arsenic is recovered from the urine sample collected 23.5 hours after ingestion. The arsenic content in the *Laminaria* was measured with NAA and found to be 43.4 mg/kg. The sample was irradiated at a thermal neutron flux of 1.2×10^{12} n cm^{-2} s^{-1}

during 7 h. Iron flux monitors were used to correct for the discrepancies in neutron flux between samples as a result of different positioning versus the reactor core. As_2O_3 was used as a standard. The 559 keV ?-rays emitted by the ^{76}As ($t_{½}$ 26.3 h) isotope were measured with a Ge(Li) detector coupled to a multi channel analyser. Taking into account an amount of 24 g *Laminaria* that was ingested, a total of 22.6% of all ingested arsenic is recovered from the urine. The remainder is still in the algae matrix and excreted via the faeces or is taken up and excreted via another route than renal. Hansen *et al.* [2003a] have estimated the average urinary excretion of arsenic by sheep to be 86%. This assumption was based on the calculation of arsenic excreted in the faeces. However, a big difference might be expected between sheep whose diet is entirely based on algae and a human who does not normally consume seaweed.

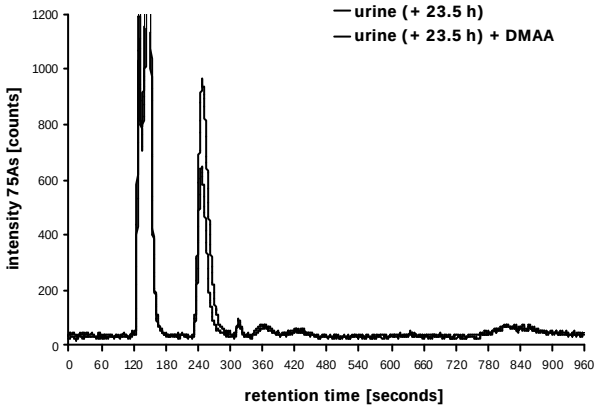

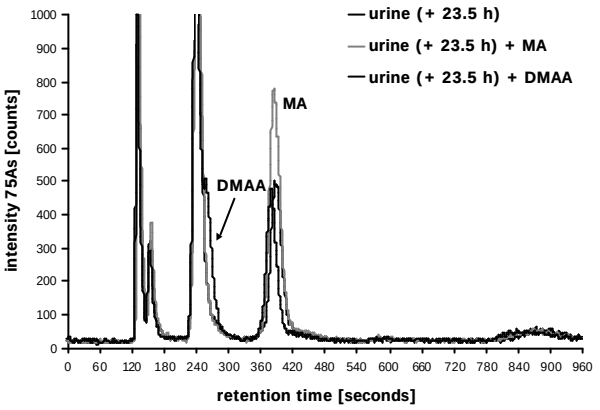

Figure 8.26 (left). Chromatograms of urine sample and the same urine sample spiked with DMAA. Separation on PRP-X100 anion exchange column, detection with ICP-MS. Mobile phase pH 5.2.

Figure 8.27 (right). Chromatograms of urine sample and the same urine sample spiked with DMAA and MA. Separation on PRP-X100 anion exchange column, detection with ICP-MS. Mobile phase pH 8.2.

Quantitative analysis of the urine sample (+ 23.5 h) by HPLC-ICPMS using a calibration curve obtained with standards of DMA shows that the arsenic content is 115.5 ng/mL. This means 65.5% of the arsenic is recovered from the anion exchange column. The remainder is still bound to the stationary phase. Feldmann and co-workers [unpublished data] have reported that recoveries could be extremely low and that flushing the column with ammonia slowly released a large amount of arsenic compounds from the column.

Table 8.8. Arsenic concentrations in urine samples.

sample	mass [g]	relative time [h]	As conc. [ng/mL]	As mass [µg]	As cumulative [µg]
blank urine		- 0.75	11.5		
urine 1	410.9	+ 0.75	2.0	0.8	0.8
urine 2	479.0	+ 2.25	5.3	2.6	3.4
urine 3	211.4	+ 3.25	13.5	2.8	6.2
urine 4	243.5	+ 7.00	82.2	20.0	26.2
urine 5	161.1	+ 9.75	83.2	13.4	39.6
urine 6	204.9	+ 15.25	144.0	29.5	69.1
urine 7	223.1	+ 23.50	176.3	39.3	108.5
urine 8	177.4	+ 27.00	118.1	21.0	129.4
urine 9	164.6	+ 30.75	107.8	17.7	147.2
urine 10	167.4	+ 35.00	88.5	14.8	162.0
urine 11	138.9	+ 39.25	64.7	9.0	171.0
urine 12	249.4	+ 48.00	75.4	18.8	189.8
urine 13	195.3	+ 52.00	42.0	8.2	198.0
urine 14	245.1	+ 54.00	13.0	3.2	201.2
urine 15	167.0	+ 56.25	22.9	3.8	205.0
urine 16	141.7	+ 59.00	24.0	3.4	208.4
urine 17	197.8	+ 61.50	2.0	0.4	208.8
urine 18	426.4	+ 72.00	1.7	0.7	209.5
urine 19	228.3	+ 76.50	29.1	6.6	216.1
urine 20	218.8	+ 82.00	38.5	8.4	224.6
urine 21	194.6	+ 87.00	20.0	3.9	228.5
urine 22	329.8	+ 96.25	19.5	6.4	234.9

8.3 Stability of arsenosugars in SGF and SIF

When algae are consumed, it takes a long pathway before the non-digestible residue is excreted. Mastication breaks down the algae as the salivary glands release enzymes that initiate the chemical digestion of carbohydrates. This mixture then enters the acid environment of the stomach. In the stomach the food is mixed into chyme and proteins are being digested. Afterwards the debris enters the small intestines in which most nutrients are digested and absorbed. At this stage, arsenic compounds in solutions are efficiently taken up by the bloodstream and quickly transported. The arsenic compounds are mostly excreted by the kidneys. A few preliminary *in vitro* incubation experiments were carried out. Algae were incubated in solutions of simulated gastric fluid (SGF) and simulated intestinal fluid (SIF). SGF and SIF were prepared according to the USP regulations [USP, 2000]. The preparation of both SGF and SIF is described in section 6.3.2.

In a first experiment, *Laminaria* seaweed was boiled, chewed and afterwards incubated in SGF. At different time intervals between 1 minute and 4 hours a portion of the masticated algae were taken from the SGF, cleaned and dried. The dried products were cooled with liquid nitrogen before grinding in a dismembrator. The powdered *Laminaria* was analysed for its total arsenic content by NAA as described in section 8.2.7. The accuracy of the measurement was tested by the analysis of a certified reference material, NIST SRM 1571 orchard leaves, which has a certified value of 10 ± 2 mg kg^{-1} As. The value obtained using our method was 12.4 ± 0.4 mg kg^{-1} As (n = 4). The results are shown in table 8.9. Boiling of the algae efficiently extracts a large amount (40%) of arsenic. Surprisingly however, incubation in SGF does not lead to further leaching of arsenicals from the algae matrix.

Table 8.9. Arsenic concentrations in raw, boiled and processed *Laminaria*.

sample	As conc. [mg/kg] (n = 1)	sample	As conc. [mg/kg] (n = 1)
unboiled *Laminaria*	23.9	*Laminaria* after 1 h in SGF	15.0
boiled *laminaria*	14.3	*Laminaria* after 2 h in SGF	15.1
Laminaria after 1 min in SGF	16.1	*Laminaria* after 3 h in SGF	15.4
Laminaria after 30 min in SGF	15.1	*Laminaria* after 4 h in SGF	15.3

The powdered *Laminaria* was extracted according to a method similar to that of Shibata and Morita [1992]. A 0.1 to 0.2 g portion was weighed into 12 ml centrifuge tubes. 10 mL of a 1+1 H_2O/MeOH mixture was added. The suspension was vortex-mixed, ultrasonicated during 15 minutes and centrifuged at 5000 rpm during 15 minutes. The supernatant was transferred into a Petri dish. This procedure was repeated another two times. The collected supernatant fractions were left drying overnight in an oven at 40°C. The residue was diluted with 5 mL deionised water, weighed and stored at 4°C prior to analysis. Triplicate analysis was done using HPLC-ES-MS/MS. For each arsenosugar and DMA, one MRM transition was recorded. The results are shown in figure 8.28. Looking at the right side of figure 8.28, it can indeed be seen that the arsenosugars are efficiently extracted by the 3 minute boiling step. However, incubation in SGF seems to further extract the arsenosugars and DMA from the seaweed matrix. On the other hand, the free arsinoyl riboside (denoted as AsSug-254 in the chromatograms, the molecular mass of this compound) is formed upon incubation in SGF. Gamble *et al.* [2002] have reported on the stability of arsenosugars in

an acid environment and in simulated gastric fluid (SGF). They reported that solutions of arsenosugars are slowly degraded (1.4% per h at 38°C) into a compound with mass 254 Da. Their measurements were done using both HPLC-ICP-MS and HPLC-ES-MS/MS.

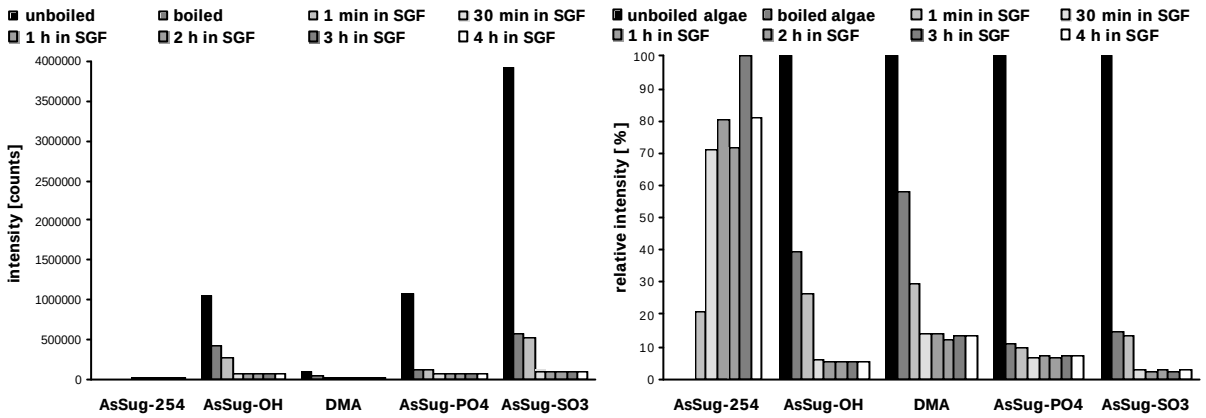

Figure 8.28. Abundance (left) and relative abundance (right) of different arsenic species in *Laminaria* methanol extracts.

The degradation involves an acid hydrolysis of the acetal group at C_1 of the ribose and leads to the free arsenosugar, a compound that is identical to all arsenosugars. Taking into account the fact that the total amount of arsenic does not significantly change, it could be concluded that all arsenosugars are transformed into the free arsenosugar. Looking at absolute intensities (left side of figure 8.28), AsSug-254 accounts only for a minor amount, but this compound might have a very low ionisation efficiency in the ES source. Unfortunately no standard of the free arsenosugar is available. However, it seems unrealistic that this sugar analogue has an ionisation efficiency that low compared to those present in the *Laminaria* sample. Therefore it makes more sense to doubt about the extraction efficiency of boiled algae versus algae that have been incubated in SGF. Because extraction efficiencies were not determined, it is difficult to draw any conclusions about possible transformations of arsenosugars in SGF. The only fact that can be retained is that a certain amount of the free arsenosugar is formed in the acid environment of the stomach.

This experiment was also carried out on raw *Laminaria*. In function of the incubation time in SGF a similar pattern could be observed compared to boiled *Laminaria*, with the exception that the amount of DMA did not significantly change. The same remark can be made as in the first experiment. The free arsenosugar was detected in the algae extracts after incubation in SGF, but quantitative aspects are missing.

Table 8.10. Arsenic concentrations in raw and processed *Laminaria*.

sample	As conc. [mg/kg] (n = 1)	sample	As conc. [mg/kg] (n = 1)
raw *Laminaria*	29.7		
Laminaria in SGF		*Laminaria* 3 h in SGF & in SIF	
15 min in SGF	22.8	15 min in SIF	21.6
30 min in SGF	21.0	30 min in SIF	21.2
60 min in SGF	20.3	45 min in SIF	24.4
120 min in SGF	18.9	60 min in SIF	22.0
180 min in SGF	20.3	120 min in SIF	19.1

The experiment was repeated on raw *Laminaria*, but now measurements were carried out with HPLC-ICP-MS. Again the seaweed was first chewed. The *Laminaria* was divided in two portions for incubation in SGF and in SGF and SIF, respectively. The procedure was exactly the same as described above. The results are shown in table 8.10. Because the algae were not boiled, incubation in SGF extracts about 23% after 15 minutes and 32% between 30 and 180 minutes. This is more or less in agreement with the 22.6% of the total ingested arsenic that was recovered from the urine in the last ingestion experiment. However, it is difficult to compare an *in vitro* incubation experiment in SGF that only partly mimics the action of the stomach and an ingestion experiment in which the total GI tract is involved.

The chromatograms of methanol extracts from algae incubated in SGF for different time periods, are shown in figure 8.29. The amount of AsSug-PO_4 and AsSug-SO_3 decreases and arsenosugar OH co-elutes with the free arsenosugar. The concentration of these arsenicals was determined using a calibration curve of DMA. Thus the efficiency of the methanol extraction can be calculated. In case of the raw *Laminaria* the methanol extraction efficiency is 32.9%. For the *Laminaria* incubated in SGF for different time periods, the mean methanol extraction efficiency is only 8.8% $\pm$ 1.1%. Unfortunately it was not possible to conclude about the methanol extraction efficiency of the individual arsenicals. When, however, the peak intensities are divided by the overall methanol extraction efficiencies for raw and SGF-processed *Laminaria*, around 83% of the sum of the peak intensities is recovered (mainly as compound 254) in the *Laminaria* methanol extract after 15 min incubation in SGF compared to raw *Laminaria* methanol extract.

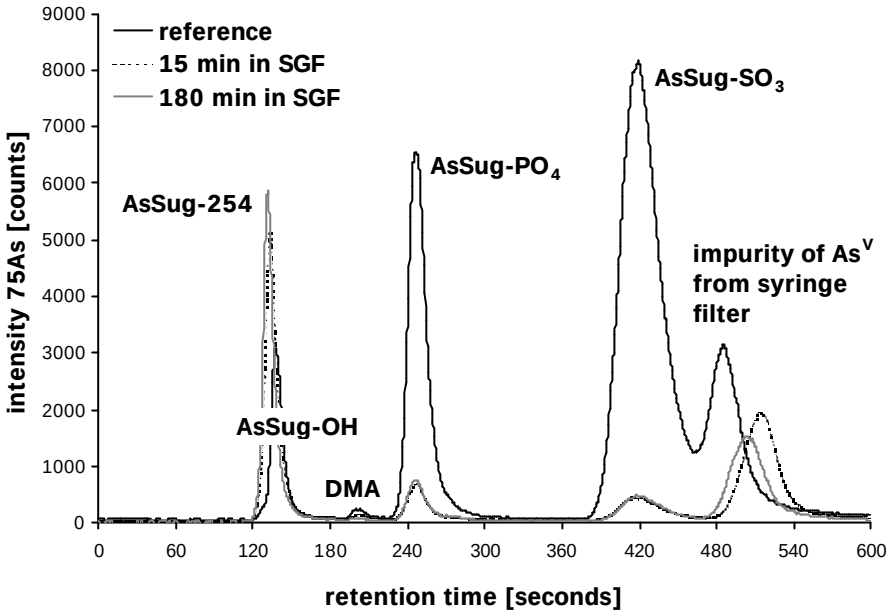

Figure 8.29. Chromatograms of raw *Laminaria* methanol extract and *Laminaria* methanol extracts incubated in SGF. Separation on PRP-X100 anion exchange column, detection with ICP-MS.

Because in anion exchange, free arsenosugar and arsenosugar OH co-elute, cation exchange HPLC-ICP-MS was also used. The same samples were separated on a Dionex CS10 column with 10 mM pyridine in 3% (v/v) MeOH (pH 2.7). Using cation exchange the free arsenosugar is retained by the stationary phase. The chromatograms of the methanol extracts of raw *Laminaria* and *Laminaria* after 180 minutes of incubation in SGF, are shown in figure 8.30. The peak of the free arsenosugar is clearly observed in the incubated *Laminaria* sample. An interesting feature is the presence of TMAO in the same sample. The identity was confirmed on the basis of spiking with a standard of TMAO (figure not shown). The presence of TMAO might indicate that a harsher breakdown than just acid hydrolysis of arsenosugars occurs in SGF. Moreover, it confirms the hypothesis that arsenosugars degrade to DMA via a pathway in which TMAO is involved. The retention time of the free arsenosugar was determined via monitoring of 2 MRM transitions (255>195 and 255>97) and via a product ion scan of the molecular ion with *m/z* 255 with HPLC-ES-MS/MS using the sample of *Laminaria* methanol extract that was incubated in SGF for 180 minutes. Based on anion and cation exchange it can be concluded that the free arsenosugar is formed although quantitative aspects are missing.

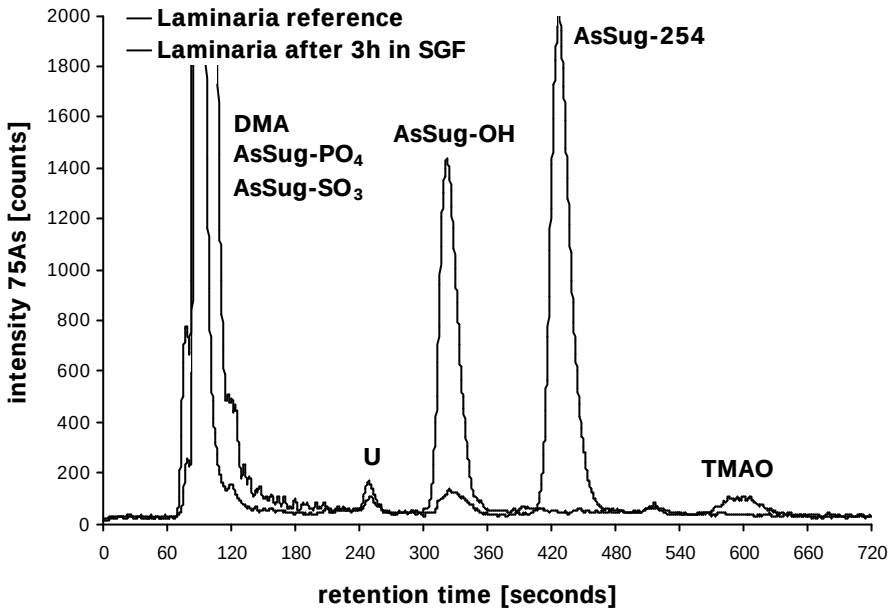

Figure 8.30. Chromatograms of *Laminaria* methanol extract and *Laminaria* methanol extract incubated in SGF for 180 min. Separation on CS10 cation exchange column, detection with ICP-MS.

The SGF was also chromatographed using anion and cation exchange HPLC-ICP-MS. Arsenosugar PO_4 and arsenosugar SO_3 were found in equal relative amounts as in the *Laminaria* itself, meaning that they are extracted into the SGF to the same extent. Speciation analysis of methanol extracts of *Laminaria* that were incubated for 3 hours in SGF and transferred into SIF for further incubation up to two hours shows no significant additional extraction. Only minor amounts of the arsenosugars can be found in the SIF, again in the same ratio as in the raw *Laminaria* methanol extract, indicating that extraction proceeds, be it to a minor degree. Based on the findings of the methanol extracts of *Laminaria* incubated in SIF and the constant extraction efficiency, it is more likely that some residual SGF was mixed into the SIF. Because of the presence of AsSug-254, a larger peak is found in the void volume (AsSug-OH + AsSug-254) of the chromatogram of the SGF and SIF compared to the methanol extract of raw *Laminaria*. Figure 8.31 shows three chromatograms: the SGF after 3h incubation with *Laminaria*, a methanol extract of *Laminaria* after 3 h incubation, and a mixture of both solutions. They were separated using cation exchange chromatography on the Dionex CS10 column. The thick black line represents the SGF after 3 hours of incubation. It can be seen that the free arsenosugar is also extracted from the seaweed matrix and can thus be taken up by the blood. The peak shape of the free arsenosugar and arsenosugar OH are deformed compared to the sample of *Laminaria* after incubation in SGF (thin black line). This is most probably due to the high

acidity of the SGF sample. When *Laminaria* and SGF were mixed and chromatographed the resulting peaks of free arsenosugar and arsenosugar OH (thick grey line) appear in between the peaks of the separate samples. Besides free arsenosugar and TMAO, two other minor unknown arsenic species appear in the SGF-processed *Laminaria* methanol extract. They could, however, not be detected in the SGF itself.

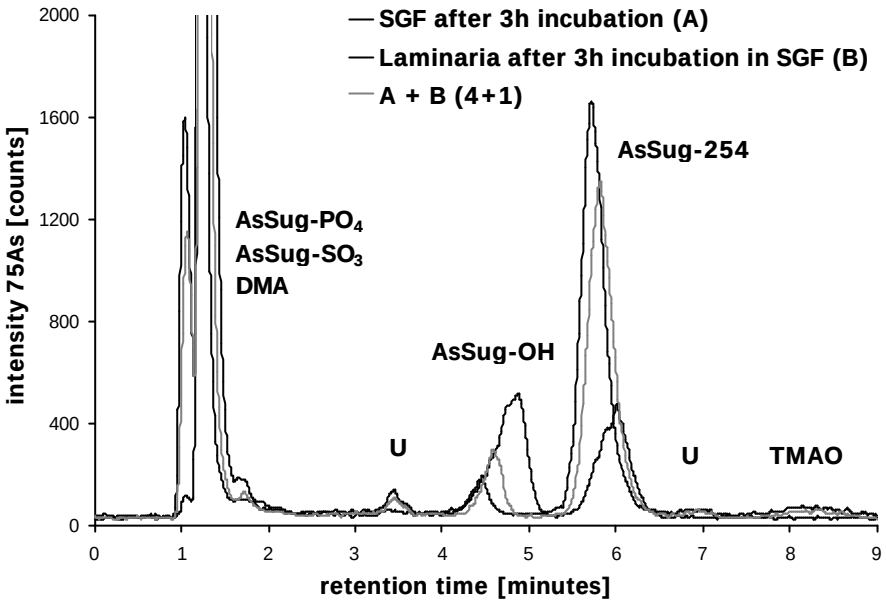

Figure 8.31. Chromatograms of *Laminaria* methanol extract incubated in SGF, SGF after incubation with *Laminaria* and a mixture of both samples. Separation on CS10 cation exchange column, detection with ICP-MS.

Finally it was questioned whether the free arsenosugar is one of the unknown metabolites in the urine of people who had ingested algae. Because the last urine experiment (trial 7) was conducted at the same time, urine samples were compared with incubated algae samples. Figure 8.32 shows the chromatograms of a urine sample and sample of an extract of *Laminaria* after 3 hours incubation in SGF. It can be seen that the free arsenosugar does not appear in the urine but that one of the unknown peaks in the chromatogram of the *Laminaria* extract co-elutes with an unknown urinary arsenic metabolite.

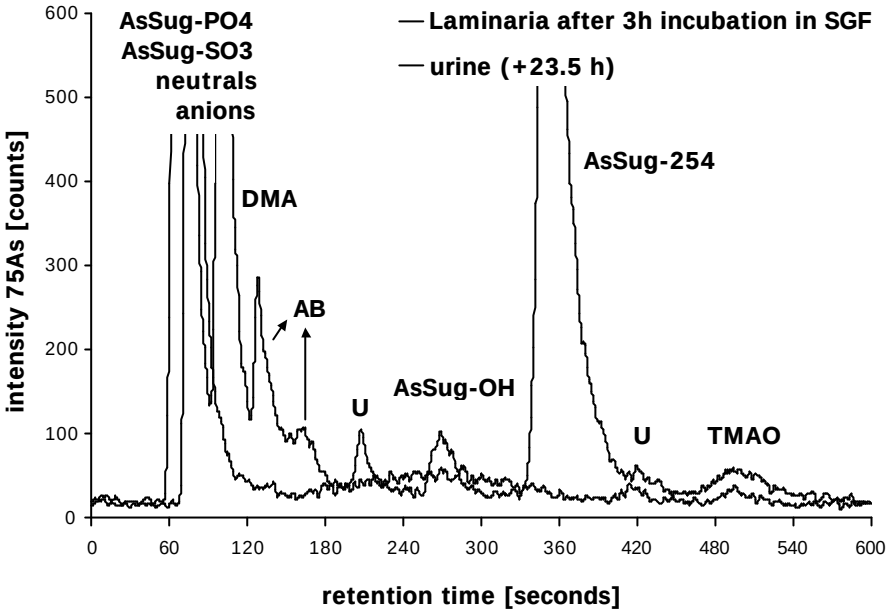

Figure 8.32. Chromatograms of urine sample and *Laminaria* methanol extract incubated in SGF. Separation on PRP-X100 anion exchange column, detection with ICP-MS.

8.4. Conclusion

ICP-MS was optimised for analysis of arsenic in urine. RF power and methanol content are considered the most relevant factors to exert an influence on the sensitivity of the arsenic detection. Furthermore it was checked whether simple sample dilution would yield quantitative recovery of arsenic notwithstanding the high carbon and salt content in urine. Changing the RF power from 1100 W to 1300 W and adding 3% MeOH to the solution resulted in a six-fold increase in signal intensity. At a dilution factor of 1:40, the NaCl in urine does not give rise to a significant spectral interference of $^{40}Ar^{35}Cl^{+}$. Several studies were carried out in which a number of volunteers ingested a portion of the seaweed *Laminaria*. Urine and/or blood were collected and analysed for their total arsenic content and/or arsenic speciation. A maximum As/creatinine in urine appears between 15 and 25 h after ingestion. DMA, MA, TMAO, DMAE, As-Sug-SO_3 and As^{V} were identified as metabolites of arsenosugars by analysis with cation and anaion exchange HPLC-ICPMS. DMA and DMAE were also identified using HPLC-ES-MS/MS. In total 11 different arsenic metabolites were detected. With the exception of a few minor differences, the chromatograms of 5 volunteers look very similar. The total amount of arsenic in the whole blood, serum and packed cell fraction of two volunteers who ate *Laminaria* were analysed. Blood was collected before and 4 and 7 h after ingestion. There seems to be no significant increase in arsenic level at the three intervals. The results for serum are confirmed by speciation

analysis. In one experiment a mass balance was determined showing that 23% of all ingested arsenic was recovered from urine. Chromatographic separation showed a recovery of 66%, indicating that the remainder of the arsenic species could not be eluted from the column. By altering the pH of the mobile phase it was again shown that MA was present and that its presence was not confused with DMAA. In a series of incubation experiments of *Laminaria* in SGF and SIF it was shown that incubation in SGF extracts the arsenicals form the seaweed matrix and that the arsenosugars are partially degraded into the free arsenosugar and into TMAO. This free arsenosugar is also extracted into the SGF. Further incubation into SIF does not lead to a significant extraction. It was investigated whether this free arsenosugar appears in urine. The answer was, however, negative.

References

[Archari *et al.*, 1983]

Archari R, Mayersohn M and Conrad K (1983). *J. Chromatogr. Sci.*, **21**, 278-281.

[Edmonds *et al.*, 1982]

Edmonds JS, Francesconi KA and Hansen JA (1982). *Experientia*, **38**, 643-644.

[Feldmann *et al.*, 2000]

Feldmann J, John K and Pengprecha P (2000). *Fres. J. Anal. Chem.*, **368**, 116-121.

[Francesconi *et al.*, 2002]

Francesconi KA, Tanggaard R, McKenzie CJ and Goessler W (2002). *Clin. Chem.*, **48**, 92-101.

[Gailer and Irgolic, 1994]

Gailer J and Irgolic KJ (1994). *Appl. Organomet. Chem.*, **8**, 129-140.

[Gailer *et al.*, 1999]

Gailer J, Madden S, Cullen WR and Denton MB (1999). *Appl. Organomet. Chem.*, **13**, 837-843.

[Gamble *et al.*, 2002]

Gamble BM, Gallagher PA, Shoemaker JA, Wei X, Schwegel CA and Creed JT (2002). *J. Anal. At. Spectrom.*,**17**, 781-785.

[Geigy, 1981]

Geigy Scientific Tables, Volume 1: Units of Measurement, Body Fluids, Composition of the body, Nutrition (ed. Lentner C). Ciba-Geigy, Basle, 1981, pp 53-100.

[Gong *et al.*, 2001]

Gong Z, Lu, X, Cullen WR and Le XC (2001). *J. Anal. At. Spectrom.*, **16**, 1409-1413.

[Hansen *et al.*, 2003a]

Hansen HR, Raab A, Francesconi KA and Feldmann J (2003). *Environ. Sci. Technol.*, **37**, 845-851.

[Hansen *et al.*, 2003b]

Hansen HR, Raab A and Feldmann J (2003). *J. Anal. At. Spectrom.*, **18**, 474-479.

[Hansen *et al.*, 2004]

Hansen HR, Pickford R, Thomas-Oates J Jaspars M and Feldmann J (2004). *Angew. Chem. Int. Ed.*, **43**, 337-340.

[Lai *et al.*, 1997]

Lai VW-M, Cullen WR, Harrington CF and Reimer KJ (1997). *Appl. Organomet. Chem.*, **11**, 797-803.

[Larsen and Stürup, 1994]

Larsen EH and Stürup S (1994). *J. Anal. At. Spectrom.*, **9**, 1099-1105.

[Le *et al.*, 1994]

Le XC, Cullen WR and Reimer KJ (1994). *Clin. Chem.*, **40**, 617-624.

[Ma and Le, 1998]

Ma M and Le XC (1997). *Clin. Chem.*, **44**, 539-550.

[Reay and Asher, 1977]

Reay PF and Asher CJ (1977). *Anal. Biochem.*, **78**, 561-568.

[Shibata and Morita, 1992]

Shibata Y and Morita M (1992). *Appl. Organomet. Chem.*, **6**, 343-349.

[USP, 2000]

U.S.Pharmacopeia XXIV & National Formulary 19 (2000). The United States Pharmacopeial Convention, Rockville, pp 2235-2236.

[Vanhoe *et al.*, 1994]

Vanhoe H, Goossens J, Moens L and Dams R (1994). *J. Anal. At. Spectrom.*, **9**, 177-185.

[Versieck et al., 1988]

Versieck J, Vanballenberghe L, De Kesel A, Hoste J, Wallaeys B, Vandenhaute J, Baeck N, Steyaert H, Byrne AR and Sunderman FR (1988). *Anal. Chim. Acta*, **204**, 63-75.

[Wangkarn and Pergantis, 2000]

Wangkarn S and Pergantis SA (2000). *J. Anal. At. Spectrom.*, **15**, 627-633.

Chapter 9. Summary, conclusion and future work

9.1. Indium

Indium is widely used in the micro-electronic industry as a component in III-V semiconductor materials. InAs, InP, $CuInSe_2$ are used in photovoltaic cells, light emitting diodes, laser diodes, high frequency microwave devices, millimetre wave telecommunications and ultra fast supercomputers. The superior performance characteristics of III-V indium containing semiconductors will further increase the use and production of this element. Indium is also incorporated in several alloys, solders, thermometers, infrared detectors etc. Indium is considered to be toxic to mammals with, depending on the physicochemical form in which it is administered, the kidneys and the liver being the major target organs. *In vivo* experiments on animals have proved indium to cause teratogenic and embryopathic effects. The testicular toxicity of several indium-containing compounds has been recognized. Indium is capable of altering the haem biosynthetic pathway in liver, kidney and erythrocytes. Indium induces apoptosis in rat thymocytes at low doses and causes necrosis at higher doses. Indium is also responsible for severe damage to the lungs of animals. For the reasons described above indium has become an element of interest in clinical, toxicological and analytical studies. These studies have focused mainly on pathological, morphological, kinetic and biochemical aspects, whereas fractionation and speciation techniques have only been used rarely. It is well known that toxicity, bioavailability and metabolism are highly dependent on the chemical form in which the metal is present. As a result speciation experiments are becoming increasingly important. Method development and optimisation of the separation techniques was done using radioisotopes of indium. ^{114m}In was chosen because of its favourable nuclear properties. ^{114m}In was produced by irradiation of a cadmium target with protons. Afterwards a suitable separation procedure was developed to isolate the indium from the

cadmium matrix. The separation method was done using solvent extraction (oxine in chloroform) and liquid chromatography (HBr and HCl on a Dowex 50wx4 cation exchange resin). The suitability of a chromatographic buffer for fractionation experiments was checked with batch ultrafiltration experiments. Ultrafiltration is a convenient means of studying the behaviour of trace elements in clinical samples and the influence of different parameters on this behaviour. Ultrafiltration experiments were conducted in which serum, packed cells and solutions of transferrin, albumin and haemoglobin were incubated with [^{114m}In]$InCl_3$ and ultrafiltered on a 10 kDa cut-off filter. The activity in the ultrafiltrate was measured and compared with a reference sample of the same incubated mixture. Thus a value of the amount of radio indium bound to the high molecular mass (HMM) and low molecular mass (LMM) fraction could be determined. Compared to the amount of In^{3+} bound to the HMM fraction of the undiluted serum sample (93%), dilution in the hepes and tris:HCl buffer systems does not drastically alter the binding characteristics of indium. Moreover, hydrolysis of In^{3+} is not responsible for the high amount of indium in the HMM fraction. The binding of $InCl_3$ to transferrin and albumin was also checked. In the case of transferrin, binding was quantitative in the presence of bicarbonate. When hepes and tris:HCl were used without bicarbonate, they themselves bind to the protein and inhibit binding between metal and protein. Also in the case of albumin, the binding was dependent on the ligands in solution. Similar to serum, the effect of different buffers on the binding between [^{114m}In]$InCl_3$ and packed cell proteins was tested. There is no difference in % HMM bound ^{114m}In in case of 0.9% NaCl, tris:HCl and hepes buffer. A solution of haemoglobin was also incubated with [^{114m}In]$InCl_3$ and ultrafiltered. However, only 40% of the ^{114m}In was found in the haemoglobin fraction. It can thus be expected that other proteins of the erythrocytes are capable of forming a complex with In^{3+}. Different chromatographic columns were tested for their suitability for indium speciation. The suitability of the chromatographic procedure was tested with *in vitro* experiments. *In vitro* incubation experiments were carried out with human serum and packed cells. Separation on a gel filtration column showed that most of the activity is found within the elution volume that also contains transferrin. Some activity is spread out over the fraction containing albumin and a third peak containing 9.3% of all ^{114m}In is found within the low molecular mass (LMM) fraction. This was also confirmed by anion exchange chromatography. The outcome is, however, dependent on the pH. A higher pH leads to hydrolysis of the In^{3+} with a decrease in the transferrin-bound fraction. The LMM compound of indium is most probably a complex of $InCl_3$ with the elution buffer as experiments with gel filtration and electrospray mass spectrometry do presume.

Fractionation of packed cell lysate shows that In^{3+} does not bind to haemoglobin. 40% of all [^{114m}In]$InCl_3$ is found in the HMM fraction of a pure haemoglobin solution. In packed cell lysate the ^{114m}In activity peak comes slightly ahead of the haemoglobin peak. In cation exchange chromatography, only a small amount of ^{114m}In can be found in the haemoglobin fraction.

During this work three *in vivo* experiments were carried out on male Wistar rats. In a first experiment five rats were given an intraperitoneal injection of [^{114m}In]$InCl_3$ during four consecutive days. One hour after the last injection the rats were sacrificed. The *in vivo* distribution of ^{114m}In was studied in blood and in different organs. Differential centrifugation was used to study the distribution in liver, kidney and spleen homogenate. Rat serum, packed cell lysate, urine and the cytosol of liver, kidney and spleen homogenate were examined by size exclusion fast protein liquid chromatography. The results show that serum accounts for 90% of the indium activity in whole blood. Indium is preferentially accumulated within liver, spleen and kidney, the highest amount of ^{114m}In being localised in the cytosolic fraction followed by the mitochondria. Size exclusion experiments show that in rat serum In^{3+} is bound to transferrin and a minor fraction to albumin. The present experiments also showed that $InCl_3$ is not bound to haemoglobin in packed cell lysate. Indium is associated to the high molecular mass fraction in liver, kidney and spleen cytosol; only in the case of kidney, small amounts of ^{114m}In can be found in the low molecular mass fraction. In a second experiment five rats were given two subcutaneous injections of [^{114m}In]InAs. Major target organs were again spleen, liver and kidney. The results were similar to those obtained after intraperitoneal injection of [^{114m}In]$InCl_3$, indicating that *in vivo* dissociation has occurred. The intracellular distribution of indium was examined by differential centrifugation. The cytosolic fraction contained most of the indium activity followed by the mitochondrial fraction, in close agreement with the previous experiment. Chromatographic separations on a preparative size exclusion column were carried out. It was shown that indium was mostly bound to high molecular mass compounds in serum and in the cytosolic fraction of spleen, liver and kidney. In a third experiment five rats were given four oral doses of [^{114m}In]InAs over a short period. Prior to this experiment the *in vitro* solubility in simulated gastric fluid and simulated intestinal fluid was determined. In case of the SGF only 1.3% of an InAs suspension dissolved after 48 hours incubation at 37ºC. InAs was not soluble in SIF. Uptake of InAs after oral administration was minimal (<1%). Due to incomplete removal of traces of [^{114m}In]InAs from the gastrointestinal tract, it was impossible to calculate accurately the *in vivo* distribution over the different organs.

As the uptake and consequently the radioactivity in the organs were very low, no further chromatographic separations could be carried out. Considering this very low uptake, the toxic impact of InAs after oral administration should not be overemphasized.

9.2. Arsenic

The study of the speciation of arsenic in the marine environment is very complex. In seawater arsenic occurs as inorganic arsenite and arsenate at about 2 ng/mL. Algae take up this arsenate, possibly because they cannot distinguish it from phosphate. They accumulate it and transform it into a series of arsenofuranoside derivatives, denoted as arsenosugars. Although a total of 16 different arsenosugars have been identified, 4 are predominant. Algae can reach levels of 200 mg As /kg (dry mass), a factor 100000 higher than in seawater, but the average concentration amounts around 30-40 mg/kg. Arsenosugars are also present in crustaceans and molluscs, as a consequence of the presence of symbiotic unicellular algae. Most probably arsenosugars are the precursors of arsenobetaine. Arsenobetaine is the main arsenic species in fish, crustaceans and molluscs and is considered as the end metabolite in the marine geocycle. Because of their omnipresence in marine foodstuffs, arsenosugars enter the human food chain. In contrast to the metabolism of inorganic arsenic and of arsenobetaine, little is known about the impact of arsenosugars on humans. As a consequence no toxicity data are available. Biological monitoring of acute arsenic exposure is done by urine analysis. However, total arsenic determination in urine is not relevant. Instead, speciation analysis should be carried out. By using a combination of a separation technique and powerful detection systems, better insight into the different arsenic species will be obtained. The problem was addressed from this point of view.

Hydride generation atomic fluorescence spectrometry and electrospray mass spectrometry were primarily considered for elemental and molecular detection, respectively, of the arsenic species in extracts of algae, urine and serum. At first the instrumental parameters of both instruments were optimised in order to obtain a good sensitivity for both systems. Because it is well known that the sensitivity of ES-MS/MS is species dependent and strongly influenced by the sample matrix (salts, organic solvents, acids, bases...) a lot of optimisation work had to be done. In a first stage instrument parameters such as capillary voltage, sample cone voltage, extraction cone voltage, hexapole RF lens voltage and collision energy were investigated. These parameters are species dependent. The capillary

voltage for all species is within the range 2.7 to 3.5 kV. For speciation analysis a mean value of 3.0 was used. The sample cone voltages are within the range 30 to 45 V. The extraction cone voltage and the hexapole RF lens voltage did not differ much and were set to values of 2.0 and 0.2 V, respectively. When the sample cone voltage is increased, in source fragmentation of the analytes occurs, leading to the naked As^+ ion at high values. This approach is valuable when searching for unknown compounds. For complete fragmentation to As^+, a sample cone voltage of minimum 120-130 V is needed for the cationic trimethylated compounds. A higher sample cone voltage is needed for the compounds containing an arsenic-oxygen double bond (130-150 V). This indicates that cleavage of an As-C bond is more readily achieved than cleavage of an As=O bond. When conventional 4.6 mm i.d. columns are used with a flow rate of 1 mL/min, the best sensitivity is reached when the sample is split with 60% going to the waste. A desolvation temperature of 300°C proves to best. With microbore 2.1 mm columns, 200 µL /min flow rate directly to the source gives almost optimum sensitivity. Addition of formic acid to the sample up to 50% leads to a 10-fold (cationic species and DMA), 40-fold (MA) or 300-fold (As^V) increase in sensitivity for infusion experiments. Addition of MeOH to the mobile phase does not necessarily improve the sensitivity. In the case of cation exchange, the sensitivity is improved by addition of 20% MeOH, whereas in anion exchange chromatography the outcome is dependent on the identity of the arsenical. UV-HG-AFS was also optimised. Inner diameter and type of teflon tubing did not seem to have much influence on the photo-oxidation properties of the UV-cell. Segmentation of the flow by addition of a stream of air efficiently reduces post-column peak broadening. Despite the quantitative breakdown of the organoarsenicals in the UV-cell, this approach cannot be used for determining the total amount of arsenic in real-life samples. The complex urine matrix prevents complete breakdown to arsenate. Sodium phosphate proves to be the best buffer for HPLC-UV-HG-AFS detection, whereas ammonium bicarbonate and ammonium oxalate are best for HPLC-ES-MS/MS. For dual detection purposes, ammonium oxalate seems to be the best compromise. The capabilities of HPLC-ES-MS/MS were explored using extracts of kelp powder. AsSug-SO_4 and AsSug-PO_4 undergo in source fragmentation. HPLC-ES-MS/MS via MRM analysis mode allows unambiguous detection of known arsenic species. The approaches of dual detection and increased sample cone voltage work fine in case of algae samples, but it is questioned whether these approaches will be able to detect the low amounts of unknown arsenic species in urine samples.

Several studies were carried out in which a number of volunteers ingested a portion of the seaweed *Laminaria*. Urine and/or blood were collected and analysed for their total arsenic content and/or arsenic speciation. First ICP-MS was optimised for analysis of arsenic in urine. RF power and methanol content are considered the most relevant factors to exert an influence on the sensitivity of the arsenic detection. Furthermore it was checked whether simple sample dilution would yield quantitative recovery of arsenic notwithstanding the high carbon and salt content in urine. Changing the RF power from 1100 W to 1300 W and adding 3% MeOH to the solution resulted in a six-fold increase in signal intensity. At a dilution factor of 1:40, the NaCl in urine does not give rise to a significant spectral interference of $^{75}ArCl^{+}$. In a first experiment four Chinese and one Belgian volunteer ate 20 g of *Laminaria*. The total amount of arsenic was determined via ICP-MS. A maximum As/creatinine in urine appears between 15 and 25 h after ingestion. The urine samples were also analysed via HPLC-ICP-MS. DMA and MA were identified. In total 11 different arsenic metabolites were detected. With the exception of a few minor differences, the chromatograms of the 5 volunteers look very similar. In a second experiment the sensitivity of UV-HG-AFS was tested. This technique was, however, inappropriate to detect the very low amounts of arsenic species in urine. It was also observed that boiling of the Laminaria resulted in partial degradation of the arsenosugars. A third experiment was conducted in Belgium and in China. Two Belgian volunteers ate 20 g of *Laminaria*. Urine was collected before and up to 40 h after ingestion. Blood was taken before and 2, 4 en 7 h after ingestion. Via HPLC-ICP-MS a similar urinary arsenic profile was observed as in experiment 1. DMA and MA were identified by spiking with standards. Via HPLC-ES-MS/MS in MRM mode the presence of DMA and DMAE could be proved. The presence of MA in urine cannot be explained. After analysis of a kelp powder extract, that was stored at 4°C during one and a half year, it appears that the arsenosugars are partially degraded into DMA and MA. The different serum samples were separated via anion exchange HPLC-ICP-MS. No differences can be observed in the chromatograms of the serum samples taken before and 2, 4 and 7 h after ingestion. In a fourth experiment only the total amount of arsenic in the whole blood, serum and packed cell fraction of a Belgian and a Chinese volunteer who ate 20 g *Laminaria* were analysed. Blood was collected before and 4 and 7 h after ingestion. The arsenic concentration was determined via HG-AFS after mineralisation. There seems to be no significant increase in arsenic level at the three intervals. A fifth experiment was carried out on two volunteers who ate 20 g of *Laminaria*. Attention was given to the possible presence of MA^{III} and DMA^{III}. Measurements with HPLC-ICP-MS again showed a good similarity with the previous experiments. MA^{III} and DMA^{III} were produced from MA

and DMA and spiked in the urine samples. DMA^{III} is not present in urine. It could not be unambiguously shown that MA^{III} was present. Because of the controversy around the real identity of the reduction products of MA and DMA, the instability of MA^{III} and DMA^{III} in urine and the difficulties by which these species are detected, no further attention was given. A sixth experiment was done on 1 volunteer. The purpose was to get more information about one of the unknown metabolites. This compound was purified by preparative chromatography. After freeze-drying, this compound appeared to be degraded into a mixture of DMA, MA, As^{V} and possibly also As^{III}. On the other hand, the behaviour of this compound showed to be independent on the pH of the mobile phase by which it is eluted from the anion exchange column. Possibly we are dealing with a polymeric compound that shows affinity to the stationary phase by hydrophobic interactions rather than ionic. A last experiment was conducted with one volunteer. A mass balance was determined showing that 23% of all ingested arsenic was recovered from urine. Chromatographic separation showed a recovery of 66%, indicating that the remainder of the arsenic species could not be eluted from the column. By altering the pH of the mobile phase it was again shown that MA was present and that its presence was not confused with DMAA. Via cation exchange HPLC-ICP-MS the presence of TMAO was shown, whereas the presence of DMAE could not be confirmed. In a series of incubation experiments of *Laminaria* in SGF and SIF it was shown that incubation in SGF extracts the arsenicals form the seaweed matrix and that the arsenosugars are partially degraded into the free arsenosugar and into TMAO. This free arsenosugar is also extracted into the SGF. Further incubation into SIF does not lead to a significant extraction. It was investigated whether this free arsenosugar appears in urine. The answer was, however, negative.

9.3. Future work

As has been shown throughout this work, the investigation of the metabolism of arsenosugars in humans is important from different points of view. First, the fact that arsenosugars are partly transformed into dimethylarsinic acid (DMA) raises questions about the possible toxicity of arsenosugars. The LD_{50} value of DMA, which is also the main metabolite in humans after being exposed to inorganic arsenic, is much higher than of inorganic arsenic, but presumably much lower than that of arsenosugars. Unfortunately, no LD_{50} values for arsenosugars are currently available. DMA has been said to be a potent co-carcinogen. From a toxicological point of view it is thus important to know exactly what kind of metabolites are formed from these arsenosugars and what impact these compounds

pose on human health. Besides DMA, at least ten other metabolites have been registered about which hardly anything is known. Next and closely related to the first statement is the legislative aspect. In view of health standards it is important to know what kind of arsenic species are present in a foodstuff. Limits that are based on total arsenic values do not achieve their aim. In the case of marine foodstuffs more than 90% of the total amount of arsenic is considered innoxious. A revision of arsenic in food standards is highly recommended. In the case of algae, of which the arsenic burden is mainly due to arsenosugars, a similar reasoning prevails, the more so as crustaceans, molluscs and even algae gain popularity in the Western kitchen. Add to this that algae are more and more used in medication, as food additives and cosmetics and as fertilisers. The fundamental scientific aspects of arsenic speciation urgently need a better understanding. The geocylce of arsenic is a complex area in which numerous oxidation, reduction (de)methylation, (de)alkylation, glycosidation and other reactions occur, some of them mediated by microorganisms. Recent insights have shown that the lipid fraction of algae and mammalian tissue also contains high amounts of arsenic. The high affinity of arsenic for sulphur has lead to numerous speculations about the presence of arsenic-sulphur compounds. By getting better insights into these complex processes, other questions about arsenic transformation in other media or environmental compartments may be solved. For these reasons it is important that this research is to be continued.

For the next years I have applied for a post-doc fellowship. The objectives of the project are two-fold. On the one hand research will focus on the analysis of blood and urine samples of a population of volunteers, which have ingested an amount of seaweed. On the one hand urine and blood samples will be analysed. Biological monitoring of acute arsenic exposure is best done using urine samples. Soluble arsenic species are efficiently taken up by the gastro-intestinal tract, quickly transported by the blood and excreted in the urine via the kidneys. Urine samples will be analysed with ion exchange and reversed phase chromatography coupled to both ICP-MS and to ES-MS/MS. Urine analysis must reveal how much metabolites are formed and what their identity is. The population study should also show whether or not the presence of these metabolites is true for a group of people or are more individually determined. Moreover quantitative data and kinetic aspects about the metabolites will be collected. It is necessary to calculate the recovery of a separation. This serves as a quality control for sample preparation and separation and guarantees that hidden species are not overlooked. The amount of absorbed arsenosugars is dependent on the amount of algae ingested. With the *Laminaria* seaweed, the total amount of

arsenosugars is limited to 1.2 mg. A population of 10 men and 10 women will ingest this alga. Besides this population study, it is the intention to carry out similar experiments on a number of volunteers who will ingest larger amounts of arsenosugars. These studies should increase the rate of success for identifying unknown compounds with ES-MS/MS. There are two possible routes for obtaining arsenosugars in large amounts: by organic synthesis or isolation form natural sources. Because of the fast transport of arsenic species by the blood, the analysis of serum and packed cells should focus on those samples taken within a few hours after ingestion. The analysis of serum and packed cells can reveal information about early transformations and how the arsenosugars or their metabolites are transported. The same methodology as for urine samples will be used, complemented with gel filtration chromatography in order to find out whether the arsenic species are protein bound. It is the objective to develop a full methodology in order to quantify all arsenosugar metabolites, identify as many as possible and examine the variability of these metabolites among a given population. A second aspect deals with *in vitro* incubation experiments in which the transformations of arsenosugars in simulated gastric fluid and simulated intestinal fluid will be further examined. Arsenosugars are known to undergo hydrolysis in acid environment and to be broken down by microorganisms. *In vitro* experiments will be carried out in which algae samples will be incubated in simulated gastric fluid and simulated intestinal fluid. The extraction efficiency of these media for the arsenosugars will be determined. It will also be studied whether the microorganisms can further transform the arsenosugars or their hydrolysis products. The experiments will be done in an incubator in which the conditions of stomach and gut (CO_2, microbial activity) will be mimicked as closely as possible.

Chapter 10. Samenvatting, conclusie en toekomstig onderzoek

10.1. Indium

Indium wordt voornamelijk gebruikt in de micro-elektronica industrie, als component in III-V halfgeleiders (InAs, InP...). Aangezien indium toxisch is, houdt blootstelling in de werkplaats gevaren in voor de gezondheid van de arbeider. De chemische speciatie van indium in het menselijk lichaam is tot op heden weinig bestudeerd. Het onderzoek in de jaren '60 en '70 beperkte zich voornamelijk tot toxiciteitstudies van de verschillende indiumverbindingen, studies betreffende de binding van deze elementen met transferrine en experimenten met betrekking tot hun toepassing in de medische diagnostiek en therapie. In de jaren '80 en '90 werden, samen met de snelle evolutie van de productie van de III-V halfgeleiders, eveneens toxiciteitstudies verricht naar de effecten van halfgeleidercomponenten zoals InAs bij proefdieren. Indium wordt beschouwd als een toxisch element, met de nieren of de lever het doelwitorgaan, dit afhankelijk van de chemische vorm van het element. *In vivo* experimenten op proefdieren hebben aangetoond dat indium teratogene en embryopatische eigenschappen heeft. De testiculaire toxiciteit van verschillende indium-bevattende verbindingen werd aangetoond. Indium is in staat de heembiosynthese in lever, nieren en rode bloedcellen te verstoren. Indium induceert apoptose in rat thymocyten bij lage doses en veroorzaakt necrose bij hogere dosissen. Indium is tevens verantwoordelijk voor ernstige schade aan de longen van proefdieren. In deze toxiciteitstudies zijn chromatografische scheidingen weinig of niet aan bod gekomen. Nochtans kan via deze techniek nuttige informatie bekomen worden omtrent de chemisch actieve species van indium in lichaamsvochten en weefsels. Deze techniek biedt de mogelijkheid om het gedrag van indium, zowel *in vitro* als *in vivo*, beter te doorgronden.

Vooreerst werden via *in vitro* experimenten de scheidingsmethoden ontwikkeld en geoptimaliseerd. Daarna werden een reeks *in vivo* experimenten uitgevoerd op ratten.

Voor de *in vitro* en *in vivo* experimenten met indium werd gebruik gemaakt van radioactief ^{114m}In. Deze nuclide werd dragervrij geproduceerd door bestraling van Cd met protonen in het cyclotron. Na een koelingperiode van 30 dagen, nodig voor het verval van kortlevende indiumisotopen diende de isotoop afgescheiden te worden van de oorspronkelijke cadmiummatrix. Hiervoor werd gebruik gemaakt van solvent extractie (oxine in chloroform) en vloeistof chromatografie (HBr en HCl op Dowex 50Wx4). De kwaliteit en het rendement van deze scheidingen werden geoptimaliseerd met behulp van "batch" experimenten met reactor geproduceerde isotopen: ^{116m}In, ^{115}Cd. Om de binding tussen $InCl_3$ en diverse serumproteïnen te onderzoeken, werd onverdund serum geïncubeerd met [^{114m}In]$InCl_3$ (pH 2,3) bij 37°C en na 2 uur ge-ultrafiltreerd (cut-off 10 kDa). De activiteit in het ultrafiltraat werd gemeten via NaI-scintillatietelling. De activiteit werd vergeleken met een standaard, om te corrigeren voor het verschil in doorlaatbaarheid van de filters. Uit de resultaten bleek dat In^{3+} voor 93% geassocieerd was met de HMM fractie. Vervolgens werd het effect van verschillende buffers op de bindingseigenschappen van In^{3+} in serum bestudeerd. Daartoe werd onverdund serum en serum 1 + 9 verdund in 5 verschillende buffers geïncubeerd met [^{114m}In]$InCl_3$ en na 2 uur onderworpen aan ultrafiltratie uitgevoerd zoals hierboven beschreven. Uit de resultaten bleek dat verdunnen in tris:HCl + $NaHCO_3$ en in hepes + $NaHCO_3$ buffer geen weerslag heeft op de verdeling van In^{3+} in serum. De waarden komen nagenoeg overeen met de referentiewaarde van het onverdunde serum. De hydrolyse van indium $[In(OH)_n(H_2O)_{6-n}]^{3-n}$ (n= 0-4) bij neutrale pH is niet de oorzaak voor de aanwezigheid van ^{114m}In in de HMM fractie. Analoge ultrafiltratie experimenten toonden aan dat de binding van $InCl_3$ met transferrine sterk afhankelijk is van de liganden in oplossing. Fosfaat en hepes binden zelf op transferrine en inhiberen hierdoor de binding tussen metaal en eiwit. Waterstofcarbonaat is vereist als ligand voor efficiënte binding tussen In^{3+} en transferrine. Daarom dient $NaHCO_3$ aan de buffers toegevoegd te worden. Analoog als bij transferrine werd onderzocht of indium geassocieerd is met albumine. In een fysiologische oplossing van $NaHCO_3$, fosfaat, citroenzuur en NaCl werd 91% van het In^{3+} teruggevonden in de HMM fractie. In een oplossing van hepes of tris:HCl is de associatie metaal eiwit minder uitgesproken. $InCl_3$ bindt efficiënt met de HMM eiwitten in rode bloedcellen al is hemoglobine waarschijnlijk hiervoor niet verantwoordelijk. *In vitro* incubatie experimenten van [^{114m}In]$InCl_3$ in serum en scheiding op verschillende kolommen toonden aan dat In^{3+} voornamelijk geassocieerd is met transferrine, met een laag

moleculaire component en in geringe mate met albumine. Het resultaat is niettemin afhankelijk van de pH van de [^{114m}In]$InCl_3$ tracer. Bij pH 4 is In^{3+} reeds partieel gehydrolyseerd tot $In(OH)^{2+}$. Deze component bindt veel minder efficiënt met transferrine en komt gedeeltelijk voor als LMM component. Wanneer serum geïncubeerd wordt met indiumtracer die op pH 1 gebracht is, komt indium voor als In^{3+} en bindt het volledig op transferrine. Informatie over de LMM component van In^{3+} werd gevonden via gelfiltratie en electrospray massa spectrometrie. Citraat is niet verantwoordelijk voor binding van In^{3+}. Er wordt vermoedt dat de buffers (hepes en tris:HCl) het $InCl_3$ complexeren. Gelijkaardige patronen werden reeds gerapporteerd voor Fe^{3+} oplossingen in tris:HCl buffer. *In vitro* incubatie van [^{114m}In]$InCl_3$ in het lysaat van rode bloedcellen toonde aan dat In^{3+} niet geassocieerd is met Hb. Geschikte kolommen met kwantitatieve opbrengst voor ^{114m}In zijn Asahipak GS-520 7G, Superose 12 HR, Bio-Gel P2, Sephacryl S-200 HR, Superdex Peptide voor gelfiltratie, en Mini Q, Mono Q, Hi Trap Q FF Sepharose voor anion uitwisselings-chromatografie in serum.

Drie *in vivo* experimenten werden uitgevoerd op 3 groepen van 5 mannelijke Wistar ratten: na intraperitoneale administratie van [^{114m}In]$InCl_3$ en na onderhuidse en orale administratie van [^{114m}In]InAs. Bij het eerste experiment waren de resultaten de volgende. De grootste hoeveelheden ^{114m}In komen voor in nier, lever en milt. Voor elk van deze organen werd de belangrijkste hoeveelheid ^{114m}In teruggevonden in het cytosol, gevolgd door de mitochondriën. Zowat 90% van de totale hoeveelheid ^{114m}In in bloed werd teruggevonden in het serum 2 uur na de laatste injectie. In tegenstelling tot de *in vitro* speciatie van [^{114m}In]$InCl_3$ in serum is $InCl_3$ bijna uitsluitend op transferrine gebonden, met een minieme hoeveelheid op albumine. Chromatografische scheiding van rode bloedcellysaat toonde aan dat ^{114m}In net voor de hemoglobinepiek elueert. In urine is In^{3+} voornamelijk gebonden op een laagmoleculaire massacomponent. Lever, nier en milt werden gehomogeniseerd en het cytosol werd gescheiden via gelfiltratie. In alle gevallen bleek dat In^{3+} voornamelijk (nier) of uitsluitend (lever en milt) geassocieerd is met de HMM fractie. Niettegenstaande sporen transferrine hiervoor verantwoordelijk zijn, was de ^{114m}In piekvorm te breed en de concentratie van transferrine te laag. Verwacht wordt dat een andere component(en) $InCl_3$ bindt.

In de tweede reeks werd een suspensie van [^{114m}In]InAs eenmalig onderhuids geïnjecteerd. De activiteit in de feces bereikte een maximum na 2 dagen en nam daarna steeds maar af. Het ^{114m}In in de urine bereikte eveneens een maximum na 2 dagen. In het geval van urine

was echter na 3 dagen geen significante hoeveelheid ^{114m}In meer te meten. Analoog als bij experiment 1 kon vastgesteld worden dat ^{114m}In zich voornamelijk opstapelt in milt, nier en lever. Wat betreft de subcellulaire verdeling in lever, nier en miltcellen waren de grootste hoeveelheden ^{114m}In terug te vinden in het cytosol, gevolgd door de mitochondriën. Dit was opnieuw analoog als bij de intraperitoneale injectie van [^{114m}In]$InCl_3$. Fractionatie experimenten in serum en cytosol van nier, lever en milt werden eveneens uitgevoerd. De resultaten waren analoog als die bij experiment 1. Indium is voornamelijk geassocieerd met de HMM fractie.

Voorafgaand aan de derde reeks werd de *in vitro* oplosbaarheid van InAs in gesimuleerd maagsap en gesimuleerd intestinaal sap bepaald. InAs bleek slechts beperkt oplosbaar in maagsap (pH 1) te zijn en was onoplosbaar in intestinaal sap (pH 7). 4 dosissen [^{114m}In]InAs werden oraal toegediend binnen een termijn van 11 dagen. Meer dan 99% van alle toegediende activiteit werd de volgende 72 uur teruggevonden in de feces. Slechts minieme hoeveelheden waren terug te vinden in de urine. Door de aanwezigheid van ^{114m}In in het darmstelsel was het moeilijk de *in vivo* verdeling over de organen accuraat te bestuderen. Enkele trends konden hoe dan ook vastgesteld worden. In tegenstelling tot intraperitoneale en onderhuidse administratie was de milt geen doelwitorgaan. Nieren en lever bevatten slechts weinig ^{114m}In. De long bevatte een hoge hoeveelheid ^{114m}In. De oorzaak is te wijten aan het feit dat ratten aan hun eten ruiken en zo een deel van het [^{114m}In]InAs inhaleerden. Maag, pancreas, dunne en dikke darm, niet toevallig de gastro-intestinale organen vertoonden de hoogste hoeveelheid activiteit. De conclusie is dat de toxiciteit van InAs na orale opname niet overschat mag worden. Niettegenstaande de morfologische en biochemische gevolgen van InAs intoxicatie gekend zijn, blijkt dat de opname via ingestie zeer beperkt is.

10.2. Arseen

De speciatie van arseen in de mariene omgeving is een complex gebeuren. De concentratie van arseen in zeewater bedraagt ongeveer 2 ng/mL. Het arseen in het zeewater komt voor als anorganisch arsenaat en arseniet. Algen nemen dit arsenaat op, waarschijnlijk omdat ze het niet kunnen onderscheiden van het isosterische fosfaat. Algen accumuleren dit anorganisch arseen en transformeren het tot een aantal arsenofuranoside (arseensuikers) derivaten. Het gehalte aan arseensuikers in algen kan tot 230 mg As /kg (droge massa) bedragen, een factor 100000 hoger dan in zeewater, maar bedraagt gemiddeld 30-40

mg/kg voor bruinwieren. Arseensuikers komen ook voor in schaal- en weekdieren, dit als gevolg van de aanwezigheid van de symbiotische unicellulaire algen. Men vermoedt dat deze arseensuikers de precursors zijn van arsenobetaïne. Arsenobetaïne is het belangrijkste arseen species in vissen en in schaal- en weekdieren en wordt beschouwd als het eindmetaboliet in de mariene geocyclus. Deze arseenspecies manifesteren zich uiteraard in de voedselketen. In tegenstelling tot het metabolisme van anorganisch arseen en dat van arsenobetaïne, is weinig bekend over de impact van arseensuikers op de mens. Men heeft dan ook geen informatie omtrent de toxiciteit van deze verbindingen. Normaliter wordt arseen in urine bepaald om een idee te verkrijgen over de blootstelling aan dit element. Het totale gehalte aan arseen is echter geen maatstaf voor acute toxiciteit. Men dient speciatie analyse uit te voeren. Met behulp van een scheidingsmethode gekoppeld aan een detector kan men een beter beeld verkrijgen omtrent de verschillende chemische species in een monster. Vanuit deze analytische benadering werd dan ook het onderzoek gevoerd. Anion en kation uitwisselingschromatografie werd aangewend voor de scheiding van de arseen species. HG-AFS en ICP-MS enerzijds en ES-MS/MS anderzijds werden gebruikt als elementselectieve en moleculair-structureel selectieve detectors, respectievelijk. Deze toestellen werden eerst geoptimaliseerd.

ES-MS/MS is sterk afhankelijk van de matrix waarin het analiet is opgelost en de gevoeligheid is verschillend naargelang de aard van de arseenverbinding. Methanol toevoegen aan de mobiele fase heeft niet noodzakelijkerwijze een positieve invloed op de gevoeligheid van ES-MS/MS. Enkel bij kationuitwisseling blijkt een stijgende hoeveelheid MeOH (20%) een positieve invloed te hebben op de gevoeligheid. Daarna werd HG-AFS geoptimaliseerd. Omdat organische arseenverbindingen niet rechtstreeks hydriden vormen werd een foto-oxidatie stap ingevoerd. De parameters voor een kwantitatieve conversie van organo-arseenverbindingen naar arsenaat werden geoptimaliseerd. De invloed van verschillende buffers op de gevoeligheid van beide detectors werd bestudeerd. Natrium fosfaat is de beste buffer wanneer enkel HG-AFS detectie gebruikt wordt. In het geval van ES-MS/MS zijn ammonium waterstofcarbonaat en ammonium oxalaat de beste opties. Indien duale detectie met beide systemen dient te gebeuren, blijkt ammonium oxalaat het beste compromis te zijn. De verschillende analyse modes bij ES-MS/MS werden getest aan de hand van extracten van algen. Arseensuikers SO_4 en PO_4 ondergaan reeds fragmentatie in de ES bron. De benadering van verhoogde bronspanning kan gebruikt worden om de arseenverbindingen compleet te fragmenteren tot het arseen ion. Dit principe biedt een alternatief voor de element selectieve detectors, al is detectie van een signaal bij *m/z* 75

geen garantie voor de aanwezigheid van arseen. Andere analieten kunnen in de bron gefragmenteerd worden tot een component met *m/z* 75. Duale detectie (UV-HG-AFS en ES-MS/MS) en verhoogde bronspanning bij ES-MS/MS kunnen gebruikt worden om onbekende arseenverbindingen te identificeren. De vraag dient echter gesteld te worden of beide toepassingen gevoelig genoeg zijn om de lage gehaltes van onbekende arseenverbindingen in urine op te sporen.

Verschillende klinische studies werden uitgevoerd waarin Chinese en Belgische vrijwilligers een portie *Laminaria* opaten. Urine en/of bloed werden gecollecteerd en geanalyseerd op hun totale hoeveelheid arseen en/of de verschillende arseen species. Vooreerst werd echter ICP-MS geoptimaliseerd voor de bepaling van de zeer lage hoeveelheden arseen in bloed en urine. Voor de bepaling van totaal arseen in urine bleek een verdunningsfactor van 1:40 voldoende om een spectrale interferentie met $^{40}Ar^{35}Cl^{+}$ te vermijden. Toevoegen van 3% methanol en verhogen van het RF vermogen tot 1300 W leidde tot optimale gevoeligheid. Een eerste experiment gebeurde in China. Vier mannelijke Chinezen en een Belg namen hieraan deel. Het verloop van de concentratie van arseen in de urine werd onderzocht en speciatie experimenten werden uitgevoerd. 20 g (droge massa) *Laminaria* wordt gegeten. Arseenbevattende voeding werd vermeden tijdens en drie dagen voor het experiment. Urine wordt gecollecteerd voor en tot 100 uur na de start van het experiment. De totale hoeveelheid arseen in de urinestalen werd bepaald via ICP-MS. Een maximum As/creatinine in de urine treedt op tussen 15 en 25 uur na opname. De urinestalen worden tevens gescheiden via anion- en kationuitwisselingschromatografie en detectie via ICP-MS. In de chromatogrammen is een duidelijke toename te zien in de hoeveelheid DMA en MA. In totaal werden 11 verschillende arseenverbindingen gedetecteerd. Op een paar kleine verschillen na, waren de chromatogrammen van de 5 vrijwilligers zeer analoog. In één tweede experiment werd de gevoeligheid van UV-HG-AFS getest. Deze bleek echter onvoldoende voor de detectie van de arseen species in urine. Er werd tevens vastgesteld dat koken van het zeewier gedurende enkele minuten een invloed heeft op de stabiliteit van enkele arseensuikers. De hoeveelheid arseensuiker PO_4 neemt af en arseensuiker OH en DMA nemen toe. Er werd besloten het zeewier niet meer te koken. Een derde experiment werd uitgevoerd in België en China. Twee Belgische vrijwilligers aten *Laminaria* (20 g). Urine werd gecollecteerd voor en tot 40 uur na opname. Bloed werd afgenomen voor en 2, 4 en 7 uur na opname. Via HPLC-ICP-MS werden opnieuw een groot aantal onbekende arseenverbindingen vastgesteld. DMA en MA konden geïdentificeerd worden via spiking met standaarden. Via HPLC-ES-MS/MS in MRM mode kon de aanwezigheid van DMA

en DMAE aangetoond worden. De aanwezigheid van MA in urine kan voorlopig niet verklaard worden. Na analyse van een extract van zeewier dat anderhalf jaar in de koelkast werd bewaard, bleek echter dat de arseensuikers partieel degradeerden met vorming van DMA en MA. De verschillende serummonsters werd gescheiden via anionuitwisseling HPLC-ICP-MS. Zowel voor als 2, 4 en 7 uur na eten van zeewier is geen verandering in het arseenprofiel te zien. In een vierde experiment werd enkel de totale hoeveelheid arseen in bloed geanalyseerd. Twee vrijwilligers aten een portie *Laminaria*. Bloed werd gecollecteerd voor en 4 en 7 uur na opname. Arseen in bloed, gepakte cellen en serum werd bepaald via HG-AFS na mineralisatie. Ook hier bleek geen significante stijging van de arseengehalten op te treden. Een vijfde experiment werd uitgevoerd met twee vrijwilligers. De aandacht ging voornamelijk uit naar de mogelijke aanwezigheid van MA^{III} en DMA^{III}. HPLC-ICP-MS metingen toonden opnieuw aan dat de resultaten analoog zijn aan die van voorgaande experimenten. MA^{III} en DMA^{III} werden bereid uit MA en DMA en gespiket in de urinemonsters. DMA^{III} is niet in urine aanwezig. Er kon ook niet met zekerheid gezegd worden dat MA^{III} aanwezig is. Omwille van de controverse omtrent de ware identiteit van de reductieproducten van MA en DMA, hun onstabiel karakter in urine en de moeilijkheid waarmee ze kunnen gedetecteerd worden, werd niet verder ingegaan op dit onderwerp. Een zesde experiment werd uitgevoerd met 1 vrijwilliger en had als doel meer informatie te verkrijgen over 1 bepaalde onbekende arseenverbinding die telkens voorkomt in de urine. Deze component werd via preparatieve chromatografie gecollecteerd en opgezuiverd. Na vriesdrogen bleek echter dat deze component volledig omgezet werd in een mengsel van DMA, MA, arsenaat en mogelijks ook arseniet. Scheiding van de urine waarin deze component voorkomt met een fosfaat buffer bij verschillende pH, toonde echter aan dat de retentietijd onveranderd bleef. Mogelijks gaat het om een polymere component die via hydrofobe, en niet via ionaire, interacties interageert met de stationaire fase. Een laatste experiment werd uitgevoerd met 1 vrijwilliger. Er werd een massabalans opgesteld waaruit bleek dat 23% van alle opgenomen arseen teruggevonden werd in de urinemonsters van de vrijwilliger. Verder werd berekend dat het rendement van een scheiding op de kolom 66% bedraagt. Dit betekent dat de resterende hoeveelheid niet geëlueerd kan worden op de kolom. Er werd nagegaan bij verschillende pH waarden van de mobiele fase of de aanwezigheid van MA niet verward werd met die van DMAA. Doch de aanwezigheid van MA bleek gerechtvaardigd. Via kationuitwisseling HPLC-ICP-MS werd de aanwezigheid van TMAO aangetoond. De aanwezigheid van DMAE kon niet bevestigd worden.

Via een reeks incubatie experimenten van *Laminaria* in SGF en SIF werd aangetoond dat SGF de arseenverbindingen uit de algen extraheert en dat ze omgezet worden in de vrije arseensuiker en in TMAO. Deze vrije arseensuiker wordt tevens mee geëxtraheerd in het SGF. SIF zorgt niet voor een significante extractie. Er werd nagegaan of deze vrije arseensuiker tevens in de urine voorkomt, doch het antwoord was negatief.

10.3. Toekomstig onderzoek

Verder onderzoek naar het metabolisme van arseensuikers in de mens is belangrijk vanuit verschillende standpunten. Ten eerste is reeds vastgesteld dat arseensuikers hoofdzakelijk omgezet worden in dimethylarseenzuur (DMA). Dimethylarseenzuur wordt eveneens gevormd als detoxificatiemetaboliet van anorganisch arseen in zoogdieren. Het vermoeden rijst dat DMA co-carcinogene eigenschappen heeft. Vanuit toxicologisch standpunt is het dus belangrijk te weten welke metabolieten gevormd worden uit deze arseensuikers en welke impact ze hebben op de gezondheid. Naast DMA komen nog een tiental verbindingen in urine voor, waarover niets bekend is. Vervolgens en hiermee geassocieerd is er het wetgevende aspect. Naar voedingsnormen toe is het heel belangrijk te weten welke arseenspecies schadelijk zijn en welke niet. Normen voor maximaal toelaatbare waarden die gebaseerd zijn op totale arseengehalten missen hun effect volledig. In het geval voedingsproducten van mariene oorsprong zijn, blijkt meer dan 90% van de arseenspecies in vissen niet toxisch. Een herinterpretatie van deze normen op basis van chemische speciatie dringt zich op. Voor algen, waarvan het arseengehalte nagenoeg uitsluitend uit arseensuikers bestaat, geldt een analoge redenering. Schaal- en weekdieren en zelfs zeewieren winnen veld in de Westerse keuken. Bovendien worden algen steeds meer gebruikt in geneesmiddelen, voedseladditieven en cosmetische producten en als meststof. Het fundamenteel wetenschappelijk aspect van de arseenspeciatie dient dringend aangepast. De geocyclus van arseen is een complex gebeuren van oxidaties, reducties, (de)methylaties, (de)alkylaties, glycosidaties en andere reacties, al of niet microbieel gemedieerd. Het ontrafelen van het mechanisme van het arseensuikermetabolisme in de mens kan meer inzicht bieden in dit complex gebeuren en antwoorden geven op de vele vragen die nog rijzen over arseen transformaties in andere compartimenten.

Voor de komende jaren heb ik een voorstel voor verder onderzoek aangevraagd. De aanpak van dit onderzoek is tweeledig. Enerzijds zal het onderzoek zich toespitsen op het analyseren van bloed- en urinestalen van een populatie vrijwilligers die een hoeveelheid

zeewier hebben gegeten. Urinestalen zullen geanalyseerd worden met behulp van ionuitwisselings- en omkeerfasechromatografie gekoppeld aan zowel ICP-MS als aan ES-MS/MS. Het doel van het analyseren van de urinestalen is nagaan welke en hoeveel metabolieten gevormd worden. De vraag stelt zich eveneens of dezelfde verbindingen voorkomen in een ganse populatie of eerder individueel bepaald zijn, en welke de gehalten en de kinetische aspecten van deze verbindingen zijn. Het opstellen van een massabalans vermijdt dat sommige verbindingen over het hoofd gezien worden. De hoeveelheid ingenomen arseensuikers is afhankelijk van hun gehalten in zeewieren. Een portie van 30 g gedroogd *Laminaria* komt overeen met een hoeveelheid van 1,2 mg As. Voor deze studies wordt gedacht aan een populatie van 10 mannen en 10 vrouwen. Naast deze populatiestudies zullen experimenten uitgevoerd worden waarbij vrijwilligers een grotere hoeveelheid eten, dit om de analyses met behulp van ES-MS/MS meer kans op slagen te bieden. Voor de isolatie van deze grotere hoeveelheden arseensuikers zijn er twee opties: organische synthese en isolatie uit natuurlijke bronnen. Omwille van het snelle transport van arseen door het bloed, zal bloedonderzoek zich toespitsen op de eerste uren na blootstelling. Het analyseren van serum en gepakte cellen laat toe na te gaan in welk stadium de arseensuikers reeds afgebroken worden. Dit zal tevens gebeuren met de hierboven vermelde technieken alsook met gelfiltratie chromatografie om na te gaan in welke mate de arseenverbindingen eiwitgebonden zijn. Via een systematische, interdisciplinaire aanpak, gericht op internationale samenwerking, is het de bedoeling een volledige methodologie ontwikkeld te hebben om kwantitatief alle metabolieten van arseensuikers in kaart te brengen, ze te identificeren en na te gaan in welke mate het metabolisme van arseensuikers systematisch voorkomt of individueel bepaald is. Anderzijds zal met behulp van *in vitro* incubatie experimenten getracht worden de transformaties in gesimuleerd maag- en darmsap te onderzoeken. Het is bekend dat arseensuikers hydrolyse ondergaan in zuur milieu en dat ze door micro-organismen afgebroken kunnen worden. *In vitro* experimenten zullen verder uitgevoerd worden waarbij algen geïncubeerd worden in gesimuleerd maag- en darmsap. Er zal nagegaan worden hoe efficiënt de arseensuikers uit de algen geëxtraheerd. Verder zal onderzocht worden in welke mate maagsap een efficiënt extractant is en of de micro-organismen in staat zijn de arseensuikers of derivaten hiervan verder af te breken. De experimenten zullen uitgevoerd worden in een broedstoof om de condities (CO_2 gehalte, microbiële activiteit) in beide media zo goed mogelijk te imiteren.